INFORMATION TO USERS

This manuscript has been reproduced from the microfilm master. UMI films the text directly from the original or copy submitted. Thus, some thesis and dissertation copies are in typewriter face, while others may be from any type of computer printer.

The quality of this reproduction is dependent upon the quality of the copy submitted. Broken or indistinct print, colored or poor quality illustrations and photographs, print bleedthrough, substandard margins, and improper alignment can adversely affect reproduction.

In the unlikely event that the author did not send UMI a complete manuscript and there are missing pages, these will be noted. Also, if unauthorized copyright material had to be removed, a note will indicate the deletion.

Oversize materials (e.g., maps, drawings, charts) are reproduced by sectioning the original, beginning at the upper left-hand corner and continuing from left to right in equal sections with small overlaps.

Photographs included in the original manuscript have been reproduced xerographically in this copy. Higher quality 6" x 9" black and white photographic prints are available for any photographs or illustrations appearing in this copy for an additional charge. Contact UMI directly to order.

ProQuest Information and Learning
300 North Zeeb Road, Ann Arbor, MI 48106-1346 USA
800-521-0600

PREPARATION AND CHARACTERIZATION OF PORE-FILLED CATION-EXCHANGE MEMBRANES

By

WENYI JIANG, B. Sc., M. Sc.

A Thesis

Submitted to the School of Graduate Studies

in Partial Fulfillment of the Requirements

for the Degree

Doctor of Philosophy

McMaster University

To Jie and Alice

PREPARATION AND CHARACTERIZATION OF PORE-FILLED CATION-EXCHANGE MEMBRANES

DOCTOR OF PHYLOSOPHY (1999) McMaster University
Department of Chemistry Hamilton, Ontario

TITLE: Preparation and characterization of pore-filled cation-exchange membranes

AUTHOR: Wenyi Jiang, B. Sc. (Nanchang University)
M. Sc. (Laurentian University)

SUPERVISORS: Professor Ronald F. Childs

NUMBER OF PAGES: xix, 230

ABSTRACT

Pore-filled cation-exchange membranes containing poly(styrene-sulfonic acid) have been prepared by thermally induced free radical polymerization of polystyrene and divinylbenzene (DVB) in the pores of a polyethylene (PE) microporous membrane followed by sulfonation of the incorporated poly(styrene-DVB).

The mass increase of poly(styrene-DVB) incorporated in the PE substrate membrane can be controlled from 0 to approximately 600%. The degree of sulfonation ranges from 45% to 85% of the theoretical value calculated based on the mono-sulfonation of the incorporated poly(styrene-DVB). The formation of sulfones was been detected by Fourier transform infrared (FTIR). The Energy dispersive X-ray (EDX) spectroscopy, scanning electron microscope (SEM), and FTIR spectra show that the poly(styrene-sulfonic acid) incorporated is evenly distributed in the pores throughout the membranes. The membrane dimensions were examined during various manipulations, such as temperature and solvent, degree of incorporation of poly(styrene-DVB).

These pore-filled membranes were characterized including ion-exchange capacity, ion-exchange concentration, water content, thickness, area electrical resistance, and transport number. These membranes have high water contents (up to 75%), ion-exchange capacities (up to 5.60 meq/g), and ion-exchange concentrations (up to 7.3 eq/kg of water).

The electrical resistance of the membranes were found to be lower than 1.0 ohm·cm^2. The counter-ion (Na^+) transport numbers were determined by an electromotive force (EMF) method and were found to range from 0.80 to 0.96.

The cation-exchange membranes have been tested for the separation of sodium hydroxide and salts by diffusion dialysis. The membranes were capable of separating the base and salts in diffusion dialysis. The results have been discussed in terms of the different transport processes for sodium hydroxide and the salt.

The membranes are capable of rejecting sodium chloride and separating NaCl/$MgCl_2$ mixed solute solutions in pressure-driven processes. It was found that their rejections to NaCl were high but their fluxes were low. The effects of salt concentration on fluxes and rejections were determined. Negative rejections of sodium ions were observed for NaCl/$MgCl_2$ mixed solute solutions. The negative cation rejection can be understood in terms of the combination effect of Donnan exclusion of the cation-exchange membranes and the diffusivity of the mobile ionic species in the pressure-driven processes.

The results obtained in this work are consistent with the recent studies at McMaster University. It clearly demonstrated that gel polymer concentration within the pores is a crucial factor on membrane permeability. The findings of this work verified the pore-filled model developed at McMaster University. The work conducted in this thesis extends the understanding of properties and performance of polyelectrolyte-filled membranes for nanofiltration applications.

ACKNOWLEDGMENT

I would like to extend sincere gratitude to a number of people. Professor R. F. Childs appears to be at the top of the list. His pleasant attitude and constant unwavering faith have allowed me to accomplish goals. Without his mentorship, guidance, help, and knowledge, this would not be possible.

Many thanks should go to my supervisory committee members, Professors J. M. Dickson, B.E. McCarry, and H.D.H. Stöver, for their guidance throughout this thesis. They provided me a lot of valuable and productive suggestions which helped me to accomplish the goals that have culminated in this thesis.

I would like to thank Dr. Alicja Mika for her valuable suggestions and great help during my years at McMaster. I have benefited from her knowledge and experience of membrane preparation and characterization. I would like to thank Mr. Brad Trushinski for his help and friendship. I would like to thank other members of the McMaster Membrane Research Group (Ashok, Brendan, Chris, Dave, Ella, Li, Jesus, Jijun, Junfan, Marcus, Richard) for their friendship.

I would like to thank NSERC, OCMR, and 3M Canada for the financial support.

Finally, I would especially like to thank my wife ***Jie*** for her love and patience. This thesis is dedicated to my lovely daughter ***Alice*** who brings joy to my life every day without exception.

TABLE OF CONTENTS

TABLE OF FIGURES

LIST OF TABLES

CHAPTER ONE

INTRODUCTION

Separation processes are critical and expensive processes in the chemical, pharmaceutical, environmental, and food industries. With increasing demand for more effective separations, new materials and technologies have been investigated and developed. In recent years, membrane separation techniques have grown from simple laboratory research scale up to large scale industrial processes that have considerable, technical and commercial impact [1]. The world market of membrane and membrane based technology is now estimated to be more than US $4.6 billion sales with an annual growth of 10 percent [2].

Membrane systems are used on a large scale to produce drinking water from sea water and to clean industrial effluents by reverse osmosis, to recover valuable constituents by electrodialysis, to separate alcohol from alcohol-water mixtures by pervaporation, to remove toxins from the blood stream in an artificial kidney by diffusion dialysis [3,4], and in emission free automobiles by using fuel cells [5]. In Canada, Zenon Environmental Systems Inc. (Burlington, Ontario) manufactured membrane based water purification systems to produce drinking water for the UN peacekeeping operation in Bosnia. Another Canadian company, Ballard Power Systems Inc. (Burnaby, British Columbia) has developed a proprietary zero-emission engine the heart of which is a fuel

cell. Ballard has been providing fuel cells for electrical power supply used in cars, mini-vans and buses since 1995. Membranes are the heart of these various systems. The key feature of membranes is that they control the transport of species across them.

1.1. OVERVIEW OF MEMBRANE PROCESSES

The driving force for the transport of a species across membrane can be a difference in concentration, pressure, electrical potential, or temperature [6,7]. Table 1.1 summarizes membrane separation processes with the separation phases, membrane porosity, type of driving force, and separation mechanisms.

This thesis is concerned with pressure-driven "liquid‖liquid" phase separation processes. The following section discusses the principles of membrane separations, and the materials and structures of membranes used for pressure drive separations.

1.1.1. Pressure Driven Processes

As can be seen in Table 1.1, pressure driven, "liquid‖liquid" phase separation processes include: microfiltration (MF), ultrafiltration (UF), nanofiltration (NF), and reverse osmosis (RO). These pressure driven processes are often distinguished by the membrane pore size (or particle size) and applied pressure (Table 1.2). For example, MF membranes are capable of removing micron particles, such as pollen, starch and bacteria with sizes greater than 1 μm, while NF and RO membranes are typically able to separate

Table 1.1. Membrane separation processes.

Process		Phase [a]	Membrane porosity	Driving force [b]	Separation mechanism
DD	Diffusion dialysis	L‖ L	Dense	ΔC	Diffusion
MF	Microfiltration	L‖ L	Porous	ΔP	Sieving
UF	Ultrafiltration	L‖ L	Porous	ΔP	Sieving
NF	Nanofiltration	L‖ L	Dense	ΔP	Sieving/Solubility
RO	Reverse osmosis	L‖ L	Dense	ΔP	Sieving/Solubility
ED	Electrodialysis	L‖ L	Porous	ΔE	Electrical charge
PV	Pervaporation	L‖ V	Dense	ΔP	Solubility/diffusion
MD	Membrane distillation	L‖ V / L	Dense	ΔP	Solubility/diffusion
GS	Gas separation	G‖ G	Porous	ΔP	Solubility/diffusion
VP	Vapor permeation	V‖ V	Dense	ΔP	Solubility/diffusion

a. ‖ stands for membrane. L is liquid, V is vapor, and G is gas.

b. ΔC, ΔP, and ΔE stand for differences in concentration, pressure, and electrical potential, respectively.

Table 1.2. Membrane pore size, applications and applied pressures for MF, UF, NF, and RO membrane processes [1].

Membrane process	Membrane pore size (nm)	Molecular weight cut-off	Applications (i.e., Removal of particles)	Typical Applied pressure kPa (*psi*)
MF	10^5	Small particles	Pollen	<100 (*15*)
			Starch	
	10^4	microparticles	Blood cells	
			Typical bacteria	
	10^3	10^5	Smallest bacteria	700 (*100*)
			DNA, viruses	
UF	10^2	10^4	Albumin	1300 (*200*)
			Vitamin B_{12}	
NF	10	10^3	Sucrose	3000 (*430*)
	1		Glucose	
			Electrolytes	
RO	0.1	$<10^2$	Electrolytes	8000(*1200*)

various solutes, for example, the sugars and ions with particle sizes less than 10 nm. On the other hand, filtration processes can be distinguished by the applied pressure with that used in RO > NF > UF > MF. For example, the pressure used in NF and RO is typically between 3000 and 8000 kPa, significantly higher than that used in the MF processes with pressure normally less than 700 kPa.

1.1.2. Cost of Separation Processes

In a separation process, the total cost and efficiency are the critical issues. The total cost of a membrane separation process is the sum of the fixed charges associated with amortization of the plant capital costs which include the equipment with the active membrane and operating costs [8]. The membranes represent approximately a third of the total cost. Thus, the lifetime of the membrane is critical since an increase in membrane costs increases the costs of these membrane processes dramatically.

The total cost of a membrane separation process also depends upon the membrane efficiency. The efficiency of separation processes is strongly related to the concentration of the solution being treated. For example, the comparison of the cost of desalination using the traditional desalination methods (distillation and ion-exchange resins) with ED and RO processes as a function of feed salt (NaCl) solution concentration is shown in Fig. 1.1. RO is the best choice for desalination of solutions containing 10 - 100 g/L of NaCl while ED is good for treating a feed of 2 - 10 g/L of NaCl solutions. When the

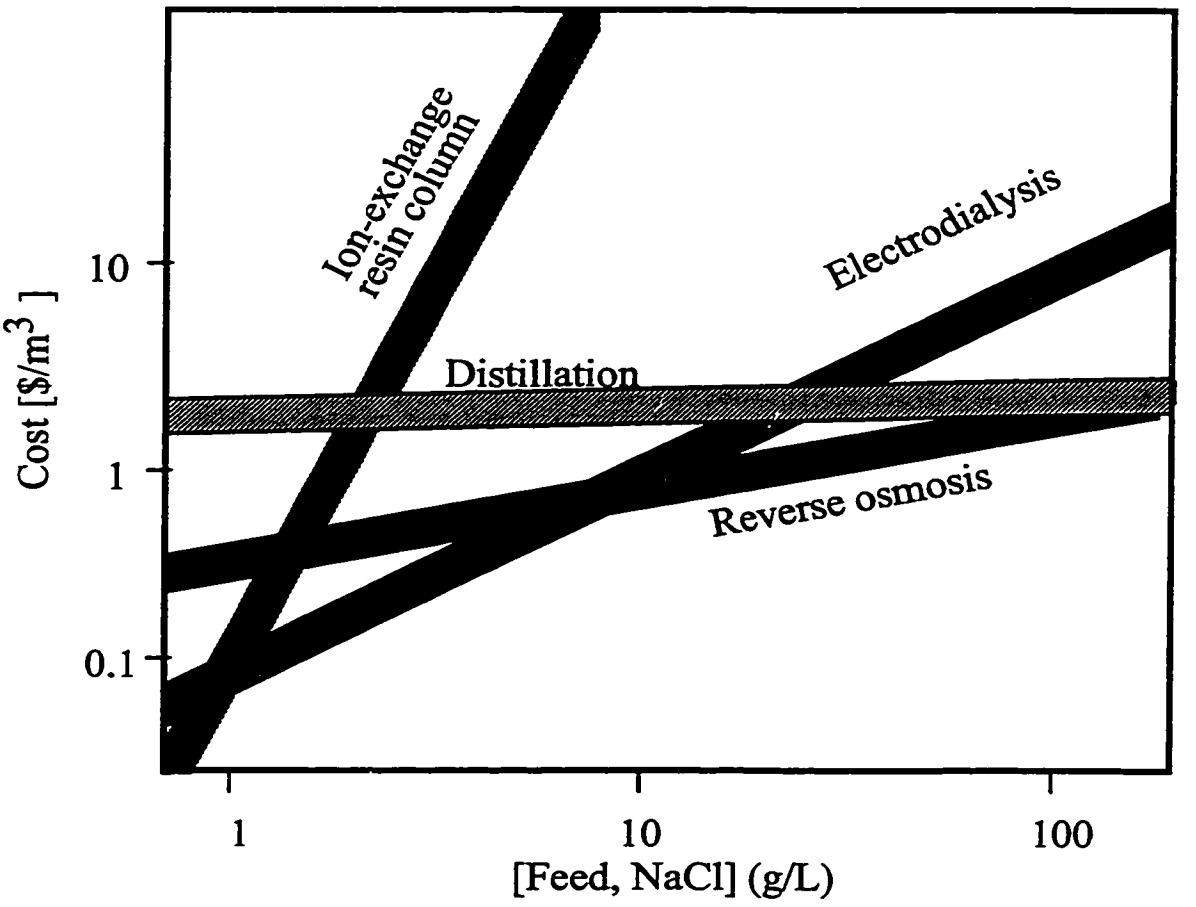

Fig. 1.1. Cost of various desalination processes as a function of feed concentration [8].

concentration is out of this range (2-100 g/L), ion-exchange resin bed processes (< 1 g/L) and distillation (> 100 g/L) have a cost advantage over the membrane processes (ED and RO).

1.2. ION-EXCHANGE MEMBRANES

1.2.1. Definitions of Ion-Exchange Membranes

An ion-exchange membrane consists of a barrier or thin layer, which contains ionogenic (ion exchangeable) groups that restrict the transport of various ionic species. A schematic diagram of a cation-exchange membrane is shown in Fig. 1.2 [9]. This membrane consists of a crosslinked polymeric matrix with the fixed negative charges. The fixed negative charges attract positively charged mobile ions and rejects negatively charged mobile ions.

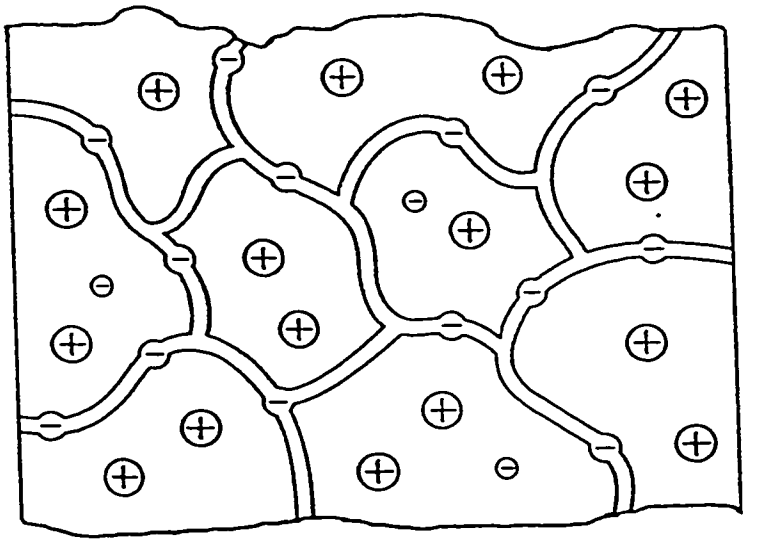

Fig. 1.2. Schematic structure of a cation-exchange membrane.

In terms of the charge of ion-exchangers, there are basically two types of ion-exchange membranes, cation-exchange and anion-exchange membranes which contain fixed negative and positive charges, respectively. A bipolar membrane is a combination of cation-exchange and anion-exchange membranes used as one membrane. For example, bipolar membranes can be formed by simply laminating cation- and anion-exchange membranes [8].

Ion-exchange membranes can be homogeneous or heterogeneous in structure. Homogeneous membranes are coherent ion-exchange gels in the shape of disks, ribbons, foils, etc. Heterogeneous membranes consist of colloidal ion-exchange particles or polyelectrolyte gels embedded in an inert binder (or support), such as polysulfone, polypropylene (PP), polyethylene (PE), polystyrene, wax, etc [10].

An ion-exchange material has fixed positive or negative charges which associate with ions of the opposite charge. These ions are called counter-ions. Ions that have the same sign as the fixed charges of the ion-exchange material are called co-ions. For example, in Fig. 1.2, the positively charged mobile ions are counter-ions and the mobile anions are co-ions.

In the schematic structure shown in Fig. 1.2, the interstices in the membrane network are pores. The pores are filled with counter-ions, co-ions and the solvent. The pores, regardless of their actual geometric forms or diameters, are often assumed to be uniform and identical. Thus, pores in an ion-exchange resin or membrane can be simply described as identical channels or capillaries throughout the cross section [1].

The pores can be occupied by both solute and solvent which can enter the pores when the ion-exchange material is in contact with a solution. The uptake of solvent can result in an expansion of the dimensions of polymer matrix in a resin or membrane. This expansion is termed swelling. The uptake of solutes is called sorption.

Ion-exchange is a diffusion process. At the ion-exchange equilibrium, the concentration ratios of the competing ionic species in the ion-exchange material and in the solution are not the same. The difference in concentration between ionic species in the ion-exchange material is called selectivity. The selectivity coefficient can be calculated from the following equation [10]:

$$E_A^B = \frac{[A^+][\overline{R} - B]}{[B^+][\overline{R} - A]} \qquad \textbf{(1. 1)}$$

where $[A^+]$ and $[B^+]$ are the concentrations of mobile ions A^+ and B^+ in solution at equilibrium, and $[\overline{R}\text{-A}]$ and $[\overline{R}\text{-B}]$ are the concentrations of the ion-exchangers containing A and B at equilibrium, respectively.

The selectivity of an ion-exchange membrane depends on Donnan exclusion which is related to the concentration of fixed charge in the membrane. The two key parameters of membrane are ion-exchange capacity and ion-exchange concentration. The counter-ion content of ion-exchange membrane is called ion-exchange capacity (IEC). IEC is determined solely by the magnitude of the matrix charge and independent of the nature of counter-ion. It has been shown that the IEC is constant with various counter-, or co-ions, or mixed ions [11].

The concentration of fixed ionic groups (ion-exchange concentration), can be expressed either as milliequivalents of fixed ions per gram of the solvent (water) in the resin/membrane (meq/g solvent). It reflects the swelling ability of the resin or membrane in the solvent (water). As a rule, the value of the ion-exchange concentration (fixed charged concentration) changes as the ion-exchange material swells with different ion concentrations and different ion systems.

1.2.2. Applications

Currently, the major uses of ion-exchange membranes are often electrochemical applications, such as ion recovery/separations by electrodialysis (ED) [11]. Other applications are ion-selective devices used in analytical chemistry [12], high temperature process control and metal refining [6,7], in pervaporation (PV) processes to separate alcohol and water [13], in chlor-alkali production, electro-reduction and separation of uranium for nuclear power plants, and fuel cells [1,14,15], etc. Ion-exchange membranes are also used in separation ions by diffusion dialysis (DD) and in medical and biological applications, such as artificial human kidneys, etc. A new class of ion-exchange membrane, pore-filled ion-exchange membranes, produced by the McMaster Membrane Research Group have shown good separation performance of water softening in pressure driven applications [16].

1.2.3. Transport in Ion-Exchange Membranes

Unlike neutral membranes, the sorption and mass transport of ion species in an ion-exchange membrane are affected by the presence of the fixed charges. These interactions can be understood of two key concepts, namely Donnan exclusion and the Donnan potential.

1.2.3.1. Donnan Exclusion

An ion-exchange material in contact with ionic species electrostatically attracts counter-ions and repels co-ions as result of the interactions between ionic species in solution and the fixed charges in the ion-exchange material (Fig. 1.3) [17,18]. The fixed

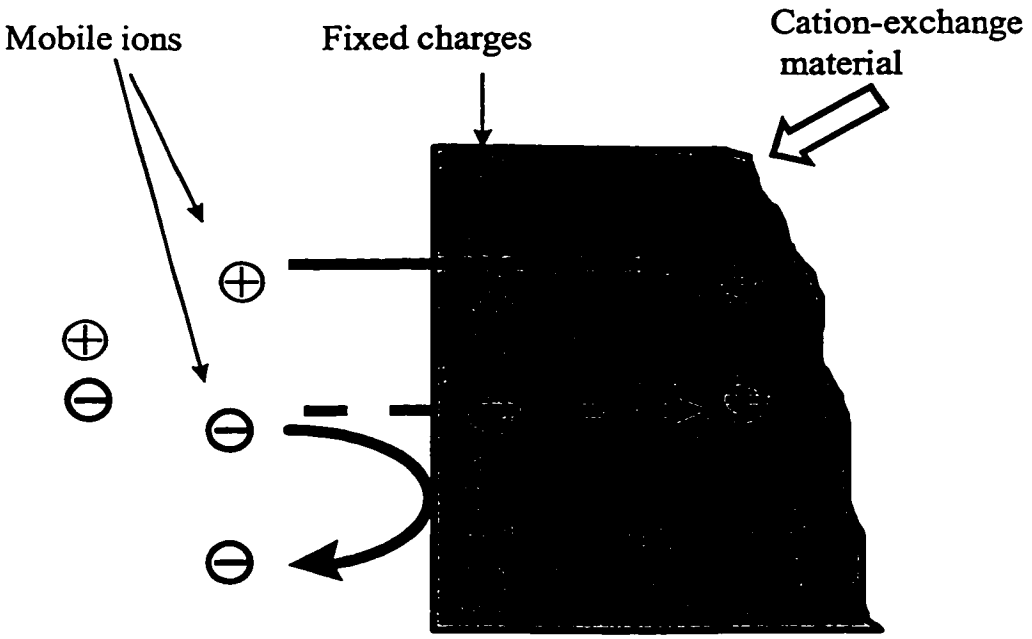

Fig. 1.3. Donnan exclusion in a cation-exchange material.

charges in a cation-exchange membrane absorb the mobile counter-ions (cations) but reject co-ions (anions). This exclusion of the co-ions from an ion-exchange material is known as Donnan exclusion [19]. Charged membranes used in pressure driven processes reject salts by a Donnan exclusion mechanism [20].

1.2.3.2. Donnan Potential

As stated above, ion-exchange membranes reject co-ions. The co-ions in solution attract the counter-ions back into the solution in order to maintain charge neutrality. As a result, counter-ions accumulate in the vicinity of membrane-solution interface in solution as is shown in Fig. 1.4 for a cation-exchange membrane. This accumulation of counter-ions (cations) in solution close to the membrane surface results in an increase in electrical potential of the counter-ion (cations). This potential is called the Donnan potential [22]. The Donnan potential effectively draws the cations into the membrane but the anions into the solution. Kesting assumed that the mobility of ions across a charged membrane was determined by the Donnan potential [22].

The magnitude of the Donnan potential can be calculated. Assume that an ion-exchange membrane is in contact with an ionic solution and an equilibrium is reached. The chemical potentials an ionic component in solution (μ_i) and in membrane (μ_i^m) can be calculated by:

$$\mu_i = \mu_i^\circ + RT\ln a_i + z_i F \psi \qquad \textbf{(1. 2)}$$

$$\mu_i^m = \mu_i^{\circ m} + RT\ln a_i^m + z_i F \psi^m \qquad \textbf{(1. 3)}$$

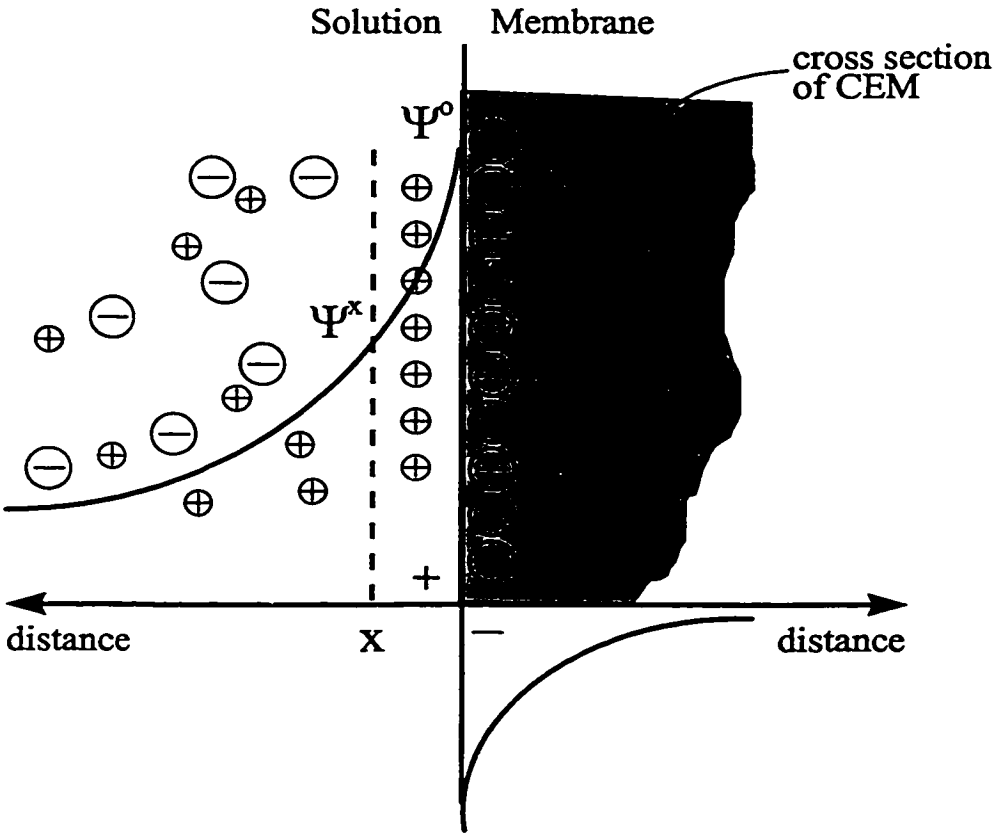

Fig. 1.4. Schematic diagram of the distribution of ions in the vicinity of solution-CEM (cation-exchange membrane) interface [21]; Ψ^0 and Ψ^x are the electrical potentials of the counter-ions from the 0 and x distance from the membrane, respectively.

where μ_i°, a_i , z_i , and ψ are the standard chemical potential, activity, ionic valence, and electrical potential of the ionic component i in solution, respectively. R, T, and F are the gas constant, absolute temperature, and Faraday constant, respectively. The parameters with supercript m are the corresponding parameters in membrane.

At equilibrium, the electrochemical potentials in solution and membrane are equal, $\mu_i = \mu_i^m$. Thus, the Donnan potential, E_{Donnan} can be calculated as follows in combination of Eq. 1.2 and Eq. 1.3:

$$E_{Donnan} \equiv \psi^m - \psi = \frac{RT}{z_i F} \ln\left(\frac{a_i^m}{a_i}\right) \quad \textbf{(1. 4)}$$

For a given mono-valent ionic species at activity ratio (a_i^m/a_i) of 1:10, The Donnan potential is: $E_{Donnan} = [(8.314 \times 298) / 96500] \times \ln(1/10) = -59$ mV.

1.2.3.3. Nernst-Planck Equation

The driving force for ion transport through ion-exchange membranes is a combination of the difference in concentration and electrical potential. The ionic flux due to diffusion ($J_{i,diff}$) of the ionic component i is described by [23]:

$$J_{i,diff} = -D_i \frac{dC_i}{dx} \quad \textbf{(1. 5)}$$

where D_i, C_i and x are the diffusion coefficient, concentration of the ionic species, and membrane thickness, respectively. The flux ($J_{i,elec}$) of the ionic component i due to the electrical potential difference is described by:

$$J_{i,elec} = -u_i C_i \frac{dE_i}{dx} \quad \textbf{(1. 6)}$$

where u_i and E_i are the electrochemical mobility and the electrical potential of the ionic species i, respectively. The term u_i is calculated by Nernst-Einstein equation: $u_i = D_iF/RT$.

The resulting equation is known as Nernst-Planck equation [10]:

$$J_i = J_{i,diff} + J_{i,elec} = - D_i \frac{dC_i}{dx} + \frac{z_i F C_i D_i}{RT} \frac{dE_i}{dx} \qquad (1.7)$$

1.2.3.4. Extended Nernst-Planck equation

In cases of where ions are transported across a charged membrane without an electro-potential difference, such as NF, RO or "dense" UF membranes, a convective term has to be included and the ion flux J_i is now determined by three terms:

$$J_i = J_{i,diff} + J_{i,elec} + J_{i,conv} \qquad (1.8)$$

where the convective term, $J_{i,conv} = C_i J_v$, and J_v is the volume flux. Eq. 1.7 which is called the extended Nernst-Planck equation, can be written as follows:

$$J_i = - D_i \frac{dC_i}{dx} + \frac{z_i F C_i D_i}{RT} \frac{dE_i}{dx} + C_i J_v \qquad (1.9)$$

This extended Nernst-Planck equation can be used to study mass transport of ion species in charged or ion-exchange membranes in which the driving forces are differences in concentration and electrical potential. This equation has been extensively used to model mass transport.

1.2.4. Preparation of Ion-Exchange Membranes

An ion-exchange membrane can be made by attaching charges to a polymer matrix. Casting is one of the classic methods for membrane preparation. An ion-exchange

membrane can be obtained by casting a polyelectrolyte solution followed by drying (to remove the solvent). For example, Gryte and Gregor [24] prepared cation-exchange membranes by casting poly(styrene-sulfonic acid) and poly(vinylidene fluoride) using dimethylformamide and hexamethylphosphoramide as the solvent. Wycist and Pintauro [25] prepared a cation-exchange membrane by casting the sulfonated polyphosphazenes from organic solvents. The major disadvantage of casting methods is that the preparation conditions and membrane parameters are difficult to control.

Ion-exchange membranes can also be produced by extruding ion-exchange beads with melting polymers. These membranes are easy to make and cost effective. The major disadvantage of extruding methods is that the stability of the membranes is poor since the beads are easily washed away after swelling and de-swelling of the membranes.

These problems can be overcome by anchoring the functionality onto to a neutral substrate membrane *via* either covalent bonds between the functional groups and the substrate or the physical entanglement of the chains of the incorporated polymers and the substrate polymers. It should be noted that, recently, the McMaster Membrane Research Group [16] prepared a new class of ion-exchange membranes, namely "pore-filled" ion-exchange membranes based on the "pore-filling" concept. These pore-filled ion-exchange membranes are robust, chemically and physically stable, and potentially cheap. The following section discusses the "pore-filling" concept and the pore-filled ion-exchange membranes.

1.3. PORE-FILLED MEMBRANES

1.3.1. Pore-Filling Concept

Many materials, such as liquid organic complexing agents, polymer hydrogels, hydrogels and polyelectrolytes, could be effective separation materials but lack the mechanical strength necessary to make a membrane. One solution is to anchor these materials into the pores of a suitable framework (or host) as is shown in Fig. 1.5. Such membranes are often termed "pore-filled" membranes [16].

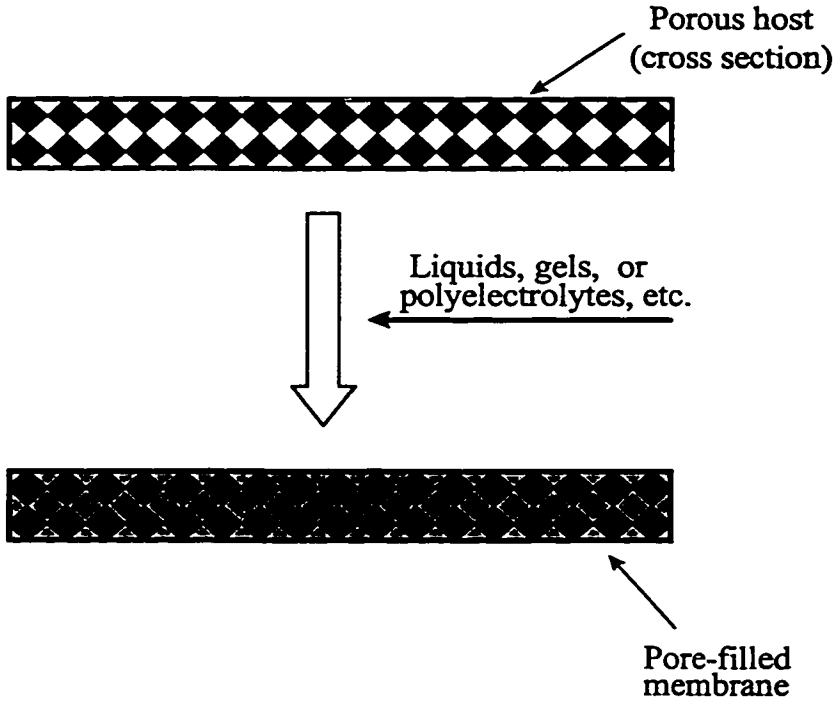

Fig. 1.5. A pore-filling approach to membrane preparation.

A "pore-filled" membrane consists of two key components, a substrate membrane (host) and the pore-filling material. The function of the substrate is to provide physical (mechanical) stability to the membrane and to act as a host (support) to hold the pore-filling material. An ideal substrate is physically and chemically stable, relatively thin with a high porosity and defined pore size. On the other hand, the function of the pore-filling materials is to provide the appropriate chemical and physical interactions required for separation of various solutes. For example, for the separation of ionic species, typical pore-filling materials can be organic complexing compounds [26-28], polymer gels, especially hydrogels [29], or polyelectrolytes [30].

The anchoring of pore-filling materials in substrate membranes is a key issue in preparation of pore-filled membranes. Different methods have been used to "lock" pore-filling materials within the substrate membrane. These are reviewed in the following section [31].

1.3.2. Methods of Anchoring

The different types of anchoring that have been used to prepare pore-filled membranes are physical adsorption, thin layer protection, covalent attachment (grafting), and polymer chain crosslinking and entanglement.

1.3.2.1. Physical Adsorption

Absorbing materials into the pores of a host membrane is one of the simplest "anchoring" methods. The filling materials are held in the host membrane simply by van

der Waals forces between the host and the inserted filling materials. For example, a supported liquid membrane (SLM) can be made by absorbing a solution containing an organic complexing material and an appropriate solvent into a microporous host membrane [32]. Typically van der Waals forces are weak and as a result, SLM's are not stable due to the loss of the pore-filling liquids during use.

The stability of SLM's can be improved by increasing the molecular weight of the pore-filling materials. This approach is effective when the filling materials are polymer gels or hydrogels. For example, Hiratsuka and Yagnuma [33] reported the preparation of "gel-filled membranes" by inserting a solution containing polyacrylamide gels into a non-woven fabric. Kim and Anderson [34] prepared pore-filled membranes by inserting poly(styrene sulfonic acid) in porous mica. While membranes containing polymeric pore-filling materials were found to be more stable than simple SLM's, they still lack long term stability.

1.3.2.2. Thin Layer Protection

The stability of the membranes discussed above (1.3.2.1) can also be improved by applying thin protective layers to one or both sides of the host membrane. The thin layers prevent or reduce the diffusion of the pore-filling material from the pores of the host. For example, the thin layers can contain charged groups which reject charged organic complexing compounds or polyelectrolytes inserted as pore fillings. An example of this approach has been recently reported by Strathmann and coworkers [26], where a 5-nonylsalicyladoxime oxime (a copper carrier) was held in a porous PP membrane (host)

by sandwiching this membrane between two thin sulfonated poly(ether ether ketone) layers.

1.3.2.3. Covalent Attachment (Grafting)

Pore-filling materials can be anchored in the substrates by covalently attaching the pore-filling materials to the host membrane. This can most conveniently be accomplished by graft polymerizing monomers within the pores of the host membrane. The grafting reaction can occur both on the membrane surfaces as well as on the interior surfaces in the pores [35-40].

Yamaguchi et al. [36] reported the preparation of pore-filled cation-exchange membranes by grafting poly(acrylic acid) (PAA) to a PP substrate membrane *via in situ* polymerization (Eq. 1.10). Similarly, Winnik et al. [37], Ulbricht [38], and Thunhorst et al. [39] prepared pore-filled cation-exchange membranes by photografting PAA to PP substrate membranes (Eq. 1.10). Poly(methyl methacrylic acid) and its salt can also be grafted to a substrate membrane [40].

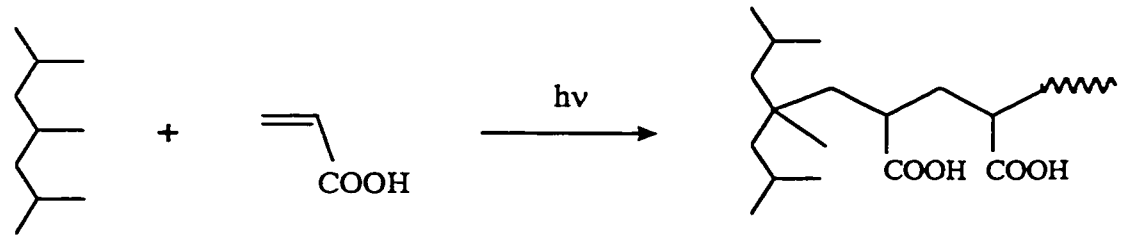

(1. 10)

PP substrate membrane | acrylic acid | PAA-grafted cation-exchange membrane

The McMaster Membrane Research Group [16] has also prepared a series of pore-filled membranes containing poly(4-vinylpyridine) (PVP) and poly(4-vinylpyridium salts) (PVP salts) *via* grafting methods. For example, these grafting reactions can be carried out by inserting monomers, such as 4-vinylpyridine (4VP), and a photo initiator (benzoin ethyl ether, BEE) within the pores of a PP or PE membrane followed by UV-initiated polymerization (Eq. 1.11). The poly(4-vinylpyridine) (PVP) grafted to the substrate membrane can be protonated or alkylated and thus, weak or strong base anion-exchange membranes are produced (Eq. 1.11). Simons and Dickson [41] have made PVP-filled membranes by photografting PVP to a PP substrate membrane. However, these workers did not examine the effect of converting the grafted PVP to its protonated or alkylated forms (the salt forms).

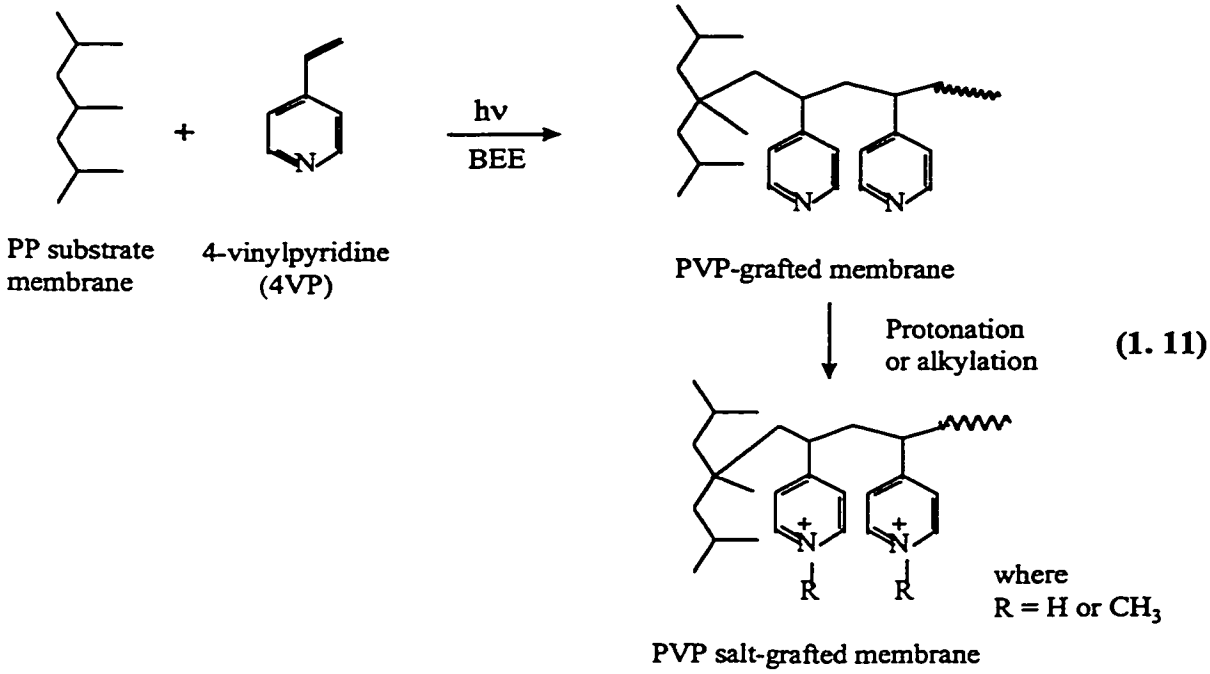

(1. 11)

The general route to produce grafted pore-filled membranes is an *in situ* polymerization. The formation of a strong C-C covalent bonds makes these grafted pore-filled membranes much more stable than those where the pore-filling is simply held in place by physical absorption (1.3.2.1 and 1.3.2.2).

1.3.2.4. Crosslinking and Entanglement

Mika et al. [16,44,52] found that more robust and durable PVP salt-filled membranes were produced by introducing a crosslinking agent to 4-vinylpyridine during an *in situ* polymerization route to form pore-filled membranes. The reactions were carried out as shown in Eq. 1.12. It is likely that grafting is still occurring in these reactions. The crosslinked PVP incorporated can be also be converted into its salt form.

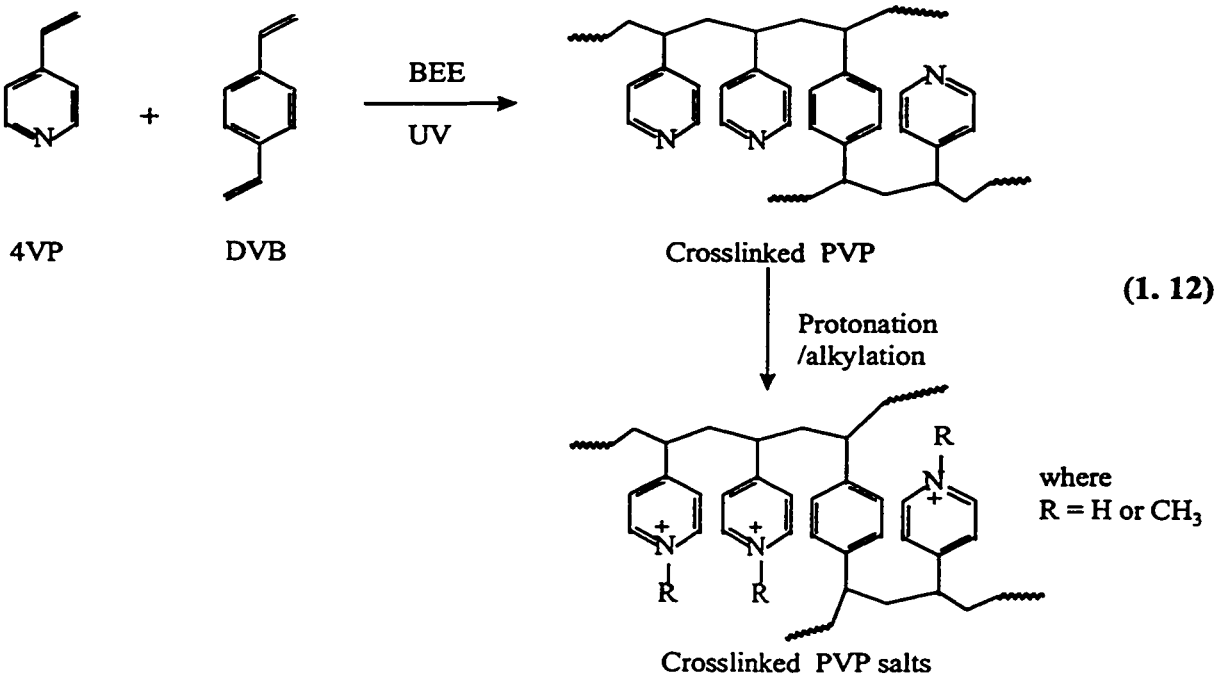

(1. 12)

However, Anderson and coworkers [42] pointed out in 1996 that grafting was not required and that a crosslinked polyacrylamide hydrogel formed within the pores of a poly(vinylidene fluoride) membrane was anchored in place by physical entanglement of the gel polymer materials with the host. In fact, Cussler et al. [43] had earlier reported that pore-filled membranes could be produced by crosslinking pre-formed linear polymers such as polyvinyl alcohol (PVA) in the pores of a substrate membrane, Eq. 1.13.

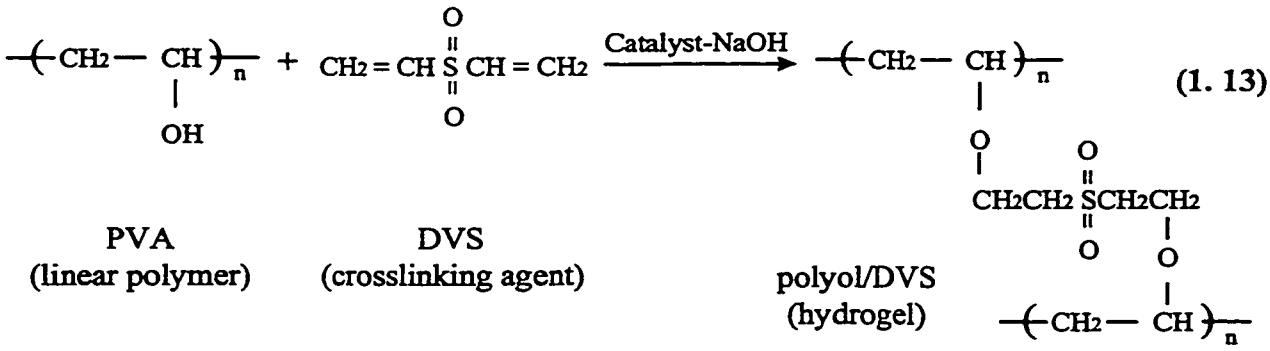

(1. 13)

The McMaster Membrane Group has also recently shown that stable pore-filled membranes can be produced by crosslinking a pre-formed polymer. This crosslinking reaction entangles and "locks" the guest polymers within the pores of the substrate membrane provided that the degree of crosslinking is above a threshold value (ie., 3%). For example, Pandey et al. [44] have made stable, pore-filled anion-exchange membranes by crosslinking, linear poly(vinylbenzyl chloride) (PVBCl) in PP substrate membranes. Crosslinking reagents used included piperazine (PIP) and 1,4-diazabicyclo[2,2,2]octane (DABCO), Eq. 1.14. This crosslinking of a polymer within the pores of a host membrane does not involve any grafting (covalent attachment) of the guest polymer to the host.

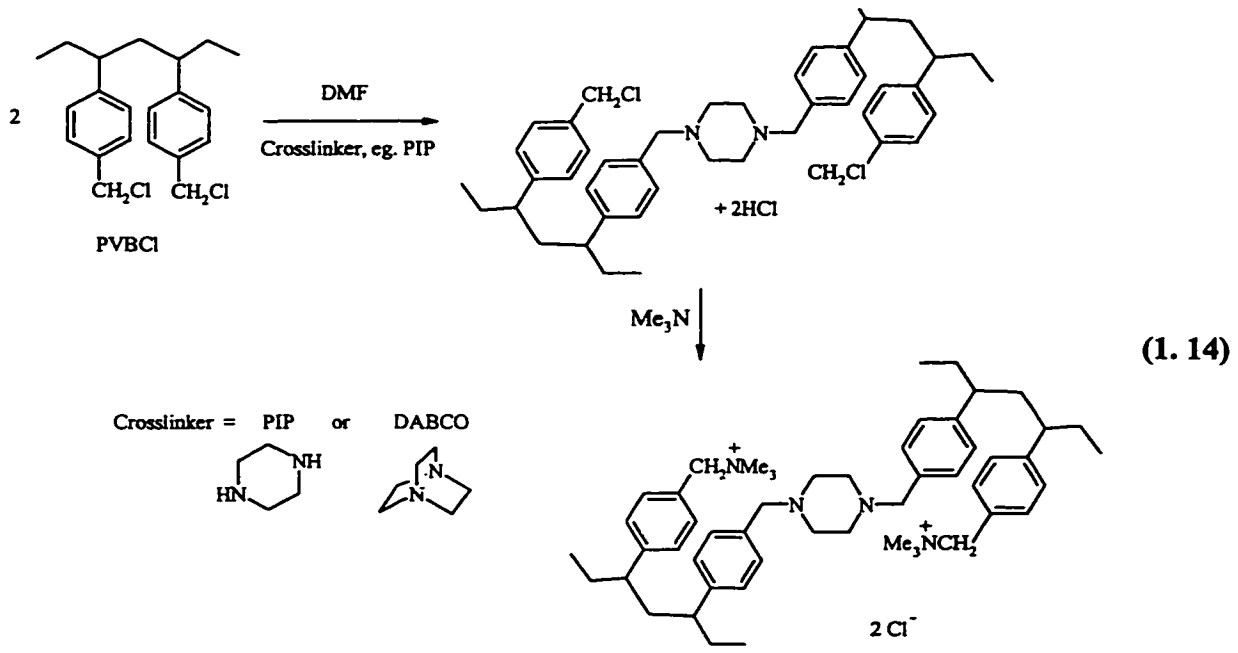

(1. 14)

It should be noted that, at the outset of the work described in this thesis, the *in situ* crosslinking methods had not been developed and the only route to type of pore-filled membrane involved *in situ* polymerization.

1.3.3. Properties of Pore-Filled Ion-Exchange Membranes

A variety of materials can be used as filling agents in pore-filled membranes, including liquids, polymer gels, hydrogels, and polyelectrolytes. When the filling materials are polyelectrolytes, ion-exchange membranes are produced. As this thesis is concerned with ion-exchange membranes, this section focuses on polyelectrolyte-filled membranes. Most of the work with polyelectrolyte-filled membranes has been conducted at McMaster University.

1.3.3.1. The Role of Polyelectrolyte and Substrate Membrane

The properties of pore-filled ion-exchange membranes are determined by the nature of both the anchored polyelectrolyte and the host membrane.

The materials of host membranes are typically hydrophobic but polyelectrolytes are typically water soluble polymers. As crosslinking is introduced into a polymer, its solubility is decreased. Thus, a crosslinked polyelectrolyte typically swells but does not dissolve when contacting with water. The degree of swelling depends inversely upon the degree of crosslinking. With relatively low degrees of crosslinking, soft gels are formed. These gels become less swollen and more physically robust as the degree of crosslinking is increased [45].

1.3.3.2. Gel Polymer Concentration and Ion-Exchange Concentration

The gel polymer concentration and ion-exchange concentration are the critical parameters in terms of understanding the properties of polyelectrolyte-filled membranes. The gel polymer concentration can be defined as the mass (g) of the polymer anchored in the pore volume (mL) of the host membrane (Eq. 1.15) [62,63]. The ion-exchange concentration can be defined as the number of moles of the ion-exchange groups per kilogram of the incorporated water (Eq. 1.16).

$$\text{Gel Polymer Concentration (g / mL)} = \frac{\text{mass of polymer incorported (g)}}{\text{pore volume (mL)}} \qquad \textbf{(1. 15)}$$

$$\text{Ion Exchange Concentration (eq / kg)} = \frac{\text{mole of ion exchange groups (eq)}}{\text{mass of water (kg)}} \qquad \textbf{(1. 16)}$$

The ion-exchange concentration is related to the gel polymer concentration since polyelectrolytes typically have one ion-exchange group in each repeating unit. The ion-exchange concentration of an ion-exchange membrane is important since its interaction with ionic species mainly depends on the Donnan potential [17,18].

Ideally, a membrane should be dimensionally stable, ie., the length, width and thickness should not change significantly. In the present case, the pores of the host membrane contain a water swollen polyelectrolyte. The host membrane provides a constraint on the swelling of the polyelectrolyte gel. Clearly, there will be a balance between the swelling pressure (osmotic pressure) of the polyelectrolytes and the energy required to change the dimension of the host membrane. Typically, host membranes with a high porosity are more prone to dimensional changes than ones with a lower porosity. Thus, Mika [46] found that, for the PVP salt-filled membranes made by *in situ* crosslinking, no change in membrane dimension was observed with a PP substrate membrane of 60% porosity while with a PP substrate membrane of 80% porosity, the thickness increased with the pore-filling. Pandey et al. [44] had similar observations for the PVBA salt-filled membranes (made by *in situ* crosslinking) and found that, with the higher porosity PP substrate membrane (80% porosity), the thickness of pore-filled membranes started to increase when the mass loading was greater than 150%.

Typically, pore-filled membranes prepared by *in situ* polymerization show considerable thickness increase on introduction of the polyelectrolyte [16,37,44,47,48]. It has been suggested that this is likely due to the formation of interpenetrating network between the pore-filling material and the substrate membranes [49]. The thickness

increase of the membranes made by *in situ* polymerization makes comparison of their properties to those of the membranes produced by *in situ* crosslinking.

A polyelectrolyte-filled membrane also contains water. The pore volume of the host membrane is occupied by the gel polymer and the incorporated water. Since the pore volume is fixed, the water content decreases with increasing amount of the gel polymer. This behavior has been observed by the McMaster Membrane Research Group for dimensionally stable membranes, eg., the membranes made by the *in situ* crosslinking routes [44,49,51]. However, for the membranes made by the *in situ* polymerization routes, the water contents typically remain fairly constant with lightly crosslinked polyelectrolyte gels incorporated into the pores due to the changes in dimensions [16,52].

As stated earlier, the degree of swelling of a polyelectrolyte is typically inversely related to the degree of crosslinking introduced [53]. Recently, Stachera et al. [54] found that, for PVP salt-filled ion-exchange membranes with constant mass loadings, the water content decreased with increasing the degree of crosslinking, Fig. 1.6. As a result, the ion-exchange concentration (the fixed charge concentration) increased with increasing crosslinking. The data suggest that the degree of crosslinking can have a good control over the water content.

1.3.3.3. Role of Incorporated Water

Water is an important component of polyelectrolyte-filled membranes. The nature of water in ion-exchange materials, in general, is complex. Terms, such as "bound", "non-

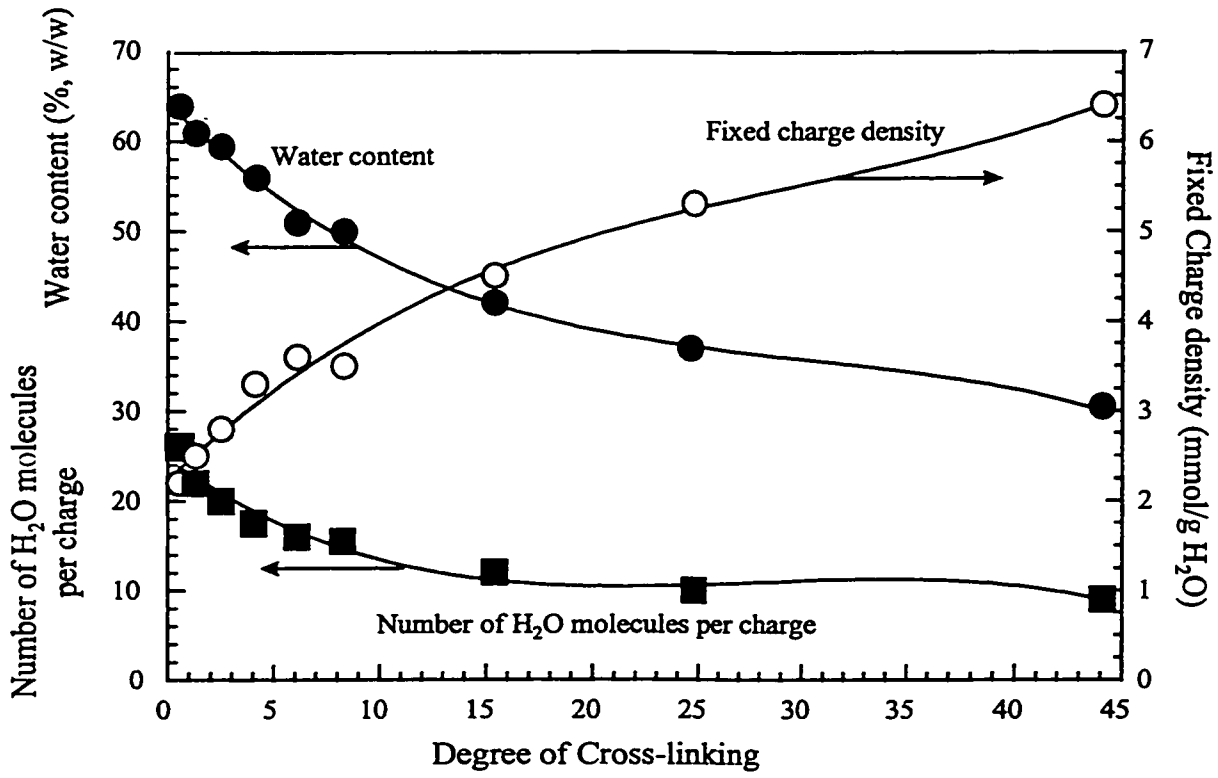

Fig. 1.6. Water content, number of H_2O molecules per charge and charge density of the PVP salt-filled anion-exchange membranes as a function of degree of crosslinking. Membranes studied had the constant mass loading.

freezable", or "associated" water and "free" "freezable", or "bulk-like" water are commonly used in the literature [55,56]. These terms are used as it would appear that there can be two types of water in an ion-exchange membrane. The "free" water resembles bulk water with the major interactions being intermolecular hydrogen bonds between neighboring water molecules. The "bound" water molecule is specifically associated with the charged sites of a polyelectrolyte. The strength of the bonding between bound water molecules and the polyelectrolytes is greater than that of hydrogen

bonding in the free water. Thus, the free water is bulk-like and freezable but the bound water solvating the polyelectrolyte typically does not freeze. The relative proportions of the different water types can be determined by differential scanning calorimeter (DSC), NMR, infrared, and other methods [57]. The total water content of an ion-exchange membrane includes both the free and bound water.

1.3.3.4. Conformations of Gel Polymer in Membranes

It is generally assumed that pressure-driven or diffusive flow through a pore-filled membrane depends on the gel structure. Typically, three conformations of the polymer chains making up the gel in pore-filled membrane have been considered. These are polymer molecular brush (Fig. 1.7 A), extended brush with chain-end overlap (Fig. 1.7 B), and entangled and crosslinked polymer gels (Fig. 1.7 C).

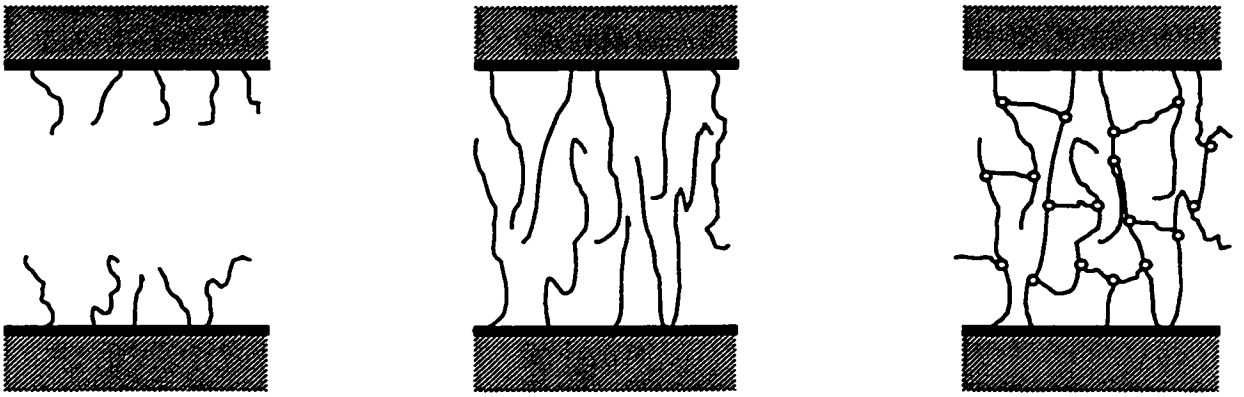

(A) Molecular brush

(B) Extended brush

(C) Crosslinked and entangled gel

Fig. 1.7. The Structures of polymer chains in pore-filled membranes.
∘ stands for the crosslinking agent.

The molecular brush model (Fig. 1.7 A) is the simplest model. The guest polymer is grafted or adsorbed to the host polymer to form "short" polymer brushes. A pressure-driven flow through a membrane with molecular brushes depends upon the external flow (the flow outside the polymer layer) which primarily depends upon the distance between the grafted chain ends (the distance between the solid polymer and the flowing liquid interface [58].

It becomes more complicated when the grafted/adsorbed, non-crosslinked extended molecular brushes overlap (Fig. 1.7 B). In this situation, a homogeneous gel is formed in the pores of the host membrane. Harden et al. [59] reported that extended polyelectrolyte brushes deformed in strong flow through these extended brushes. Anderson and coworkers [60,61] pointed out that the diffusive flow through the "fiber-matrix" pores of "polymer-lined" membrane depended primarily upon the hydrodynamic thickness of the "lined" polymer brushes which was related to nature of the polymer gel.

At McMaster University, Mika et al. [16,46] observed a large effect of "pH valve" for PVP-grafted membranes with gel structures likely involving both Fig. 1.7A and B. This is because the charged chains repel each other and extend into the pores (and block the pores) while a decrease in charge reduces the polymer-lined layer (and finally allows the polymer gel to collapse toward the pore wall). Levie [62] successfully developed a mathematical model for the pH-valve shown by PVP salt-filled anion-exchange membranes. Recently, Mika et al. [44] reported that the models based on the chain structures described in Fig. 1.7A and B can predict the performance of the PVP-grafted membranes under pressure-driven conditions.

Recently, Anderson and co-workers [63] considered flow through the third case (Fig. 1.7C), the crosslinked/entangled polymer gel. The structure of the polymer gel is schematically illustrated in Fig. 1.7C. The gel may or may not have covalent bonds to the host membrane. In their study, the membrane performance was described by the Darcy permeability. According to Darcy permeability, it can be assumed that the permeability depended primarily upon the (hydraulic) radius and the host porosity [59].

Recently, at McMaster University, Mika et al. [44,64,65] have proposed a new model (the pore-filled model) to predict the performance for pore-filled membranes. In this model, the anchored gel (Fig. 1.7C) is assumed to be equivalent to a semi-dilute polymer solution of the identical concentration. This assumption allows one to calculate the gel mesh radius as a function of the gel polymer concentration and polymer statistics. These two fundamental parameters (gel mesh radius and gel polymer concentration) allow the gel hydrodynamic permeability to be calculated [44]. In this model, the permeability through the gel membrane is related to the porosity of the substrate membrane and the pore toruosity [65].

1.3.3.5. Pressure-Driven Permeability and Separation

The use of ion-exchange membranes in RO/NF entirely disappeared when Leob and Sourirajan in 1960s succeeded in preparing high performance asymmetric cellulose acetate membranes [66,67]. Currently, thin film composite (TFC) membranes are dominant in pressure-driven applications.

Recently, Childs et al. [44,49-53,64,65,68] have reported that McMaster pore-filled ion-exchange membranes have shown high permeability and good rejections for ionic species. In fact, these membranes function effectively at ultra low pressures. Table 1.3 lists the results of low pressure water softening using pore-filled anion-exchange membranes containing PVBA salts and PVP salts.

It can be seen from the data in Table 1.3 that the McMaster pore-filled ion-exchange membranes outperform the commercial thin film composite (TFC) membrane, ie., Desal-51 (Osmonics), in low pressure water softening. For example, at 100 kPa, both flux and rejection of membranes I, II and V are higher than those of the commercial membranes (Desal-51, BQO1 and TFV-7450). The flux and rejection of membrane III are in the same range of Desal-51. Membrane V has a better performance in flux without losing ion rejection significantly.

It is known that the separation of ionic species using an ion-exchange membrane depends upon the Donnan effect [44]. For example, the charges incorporated reject co-ions but allow counter-ions to transport through. Mika et al. [68] found that PVP salt-filled membranes separated ionic species very well but allowed neutral species, such as sucrose, to transport through the membranes. The pore-filled membranes have relatively high ion-exchange concentrations and thus the rejections are high.

It should be noted that these pore-filled membranes have thick separating layers (ranging from 50 to 150 μm). The thickness of the effective layer of commercial TFC NF membranes is typically approximately 1 μm. The high flux of these pore-filled membranes is due to the low gel polymer and a high water concentrations. In fact, recent

Table 1.3. Comparison of the results of low pressure water softening[a] using McMaster Pore-filled membranes with commercial nanofiltration membranes.

Membrane	Pressure (kPa)	Crosslinking (%)	Mass gain (%)	Flux (kg/m^2h)	Rejection (%)[a] Na^+	Mg^{2+}	Ca^{2+}
McMaster Pore-Filled Membranes[b]							
Membrane I	100	5	42	12	35	79	80
Membrane II	100	20	38	28	30	58	44
Membrane III	100	9	53	7	24	78	62
Membrane IV	100	20	36	26	17	42	28
Membrane V	100	10	66	8	30	84	81
Membrane V	500	10	66	31	49	82	74
Commercial NF membrane[c]							
Desal 51(Osmonics)	100			7	21	71	54
Desal 51(Osmonics)	500			36	41	87	81
BQO 1 (Osmonics)	500			33	19	26	31
TFV-7450 (Hydranautics)	500			14	33	65	68

a. Feed: Municipal tap water in Hamilton Area (Ontario) contains: 24 ppm of Na^+, 22 ppm of Mg^{2+}, 86 ppm of Ca^{2+}, and other cations (less than 5 ppm).
b. Membrane I: PVBA salt -filled, crosslinking agent PIP [48].
Membrane II: PVBA salt -filled, crosslinking agent PIP [48].
Membrane III: PVBA salt-filled, crosslinking agent DABCO [48].
Membrane IV: PVP salt-filled, crosslinking agent dibromoxylene [44,50].
Membrane V: PVP-salt-filled, crosslinking agent dibromoxylene [50].
c. Ref. [58].

estimates of the "pore-size" of a polyelectrolyte filled membrane give values in the range of 3 - 8 nm [46-48]. Thus, a polyelectrolyte-filled membrane has a high "pore density" and a large "pore size" while the solutes and water are transported through the highly swollen polyelectrolyte gel incorporated.

1.4. PLAN OF RESEARCH

1.4.1. Statement of Problem

The pore-filled membranes made at McMaster University represent a new approach to ion-exchange membranes. As shown above, these membranes have the intriguing properties and the potential of being tuned, eg., the important parameters (water content, gel polymer concentration and ion-exchange concentration).

The preparation and characterization of the PVP salt-filled anion-exchange membranes have been extensively studied [16,46-54] but little work has been done on pore-filled cation-exchange membranes. Some preliminary work has been reported with poly(acrylic acid)-filled cation-exchange membranes, formed using an UV-initiated *in situ* polymerization [37]. Cation-exchange membranes are important in their own right. However, they could also be efficient in water softening applications. Anion-exchange membranes were assumed to be unsuitable in treating natural water containing multi-valent inorganic anions (SO_4^{2-} and PO_4^{3-}) and large, (partially) negatively charged organic compounds, such as humic acids [69,70]. The multi-valent inorganic anions are assumed

to be eventually washed but humic acids and other negatively charged, macro-organic compounds will strongly interact with the fixed positive charges on the membranes and cannot be removed easily. This reduces the permeability and selectively of the anion-exchange membranes.

In contrast, cation-exchange membranes appear to have advantages over anion-exchange membranes in the treatment of natural water and in biological applications since the negatively charged macro-organic compounds will be repelled and rejected effectively by the negative charges in the cation-exchange membranes. Even though multivalent cations (Ca^{2+} and Mg^{2+}) would also interact with the fixed negative charges, these cations can be washed.

1.4.2. Objectives

The general goal of this work is to investigate the preparation and characterization of "pore-filled" cation-exchange membranes. Poly(styrene-sulfonic acid) was chosen as the polyelectrolyte to be incorporated in this work because it is a strong acid and stable in strong acid and base environments [71]. At the outset of this project, the McMaster Membrane Research Group had encountered difficulties in incorporating poly(styrene-sulfonic acid) either directly or indirectly into microporous PP or PE substrate membranes [72]. PE microporous membranes were selected as the host substrate since they were found to be stable while PP membranes were cracked and broken in the chlorosulfonation reactions.

Specifically, the objective of the research of this thesis was to prepare and characterize pore-filled cation-exchange membranes derived from poly(styrene-sulfonic acid). The detailed objectives are:

1. To develop a method to anchor high amount of poly(styrene-DVB) copolymers into polyethylene microfiltration membranes and to chlorosulfonate the incorporated poly(styrene-divinylbenzene). The factors affecting the mass increase and sulfonation yields are to be determined (Chapter 2);
2. To characterize the properties of the cation-exchange membranes, including their electrical resistance, transport numbers, ion-exchange capacity and ion-exchange concentration, water content, thickness, and to examine the uniformity of pore-filling of these membranes (Chapter 3);
3. To examine the performance of the pore-filled cation-exchange membranes in the separation of base and salt by diffusion dialysis (Chapter 4);
4. To test the pore-filled cation-exchange membranes under pressure driven conditions to separation inorganic salt solutions (Chapter 5);
5. To compare the performance with other pore-filled membranes and to draw conclusions (Chapter 6).

CHAPTER TWO

MEMBRANE PREPARATION

The main purpose of this project is the development and evaluation of poly(styrene-sulfonic acid)-filled cation-exchange membranes. The first step in the entire project is to incorporate poly(styrene-DVB) into the pores of a PE substrate membrane. The next step of the project is to introduce strong acid functionality into the membranes. This can be achieved by sulfonation of the incorporated poly(styrene-DVB) to produce strong acid groups in the resulting membranes. The chemistry of the copolymerization and sulfonation reactions, the materials and apparatus used, the experimental procedures, and the results and discussion are described in this chapter.

2.1. CHEMISTRY OF POLYMERIZATION AND SULFONATION

2.1.1. Copolymerization of Styrene and DVB

A thermally induced free radical polymerization was used to copolymerize styrene and DVB. This reaction is described in Eq. 2.1.

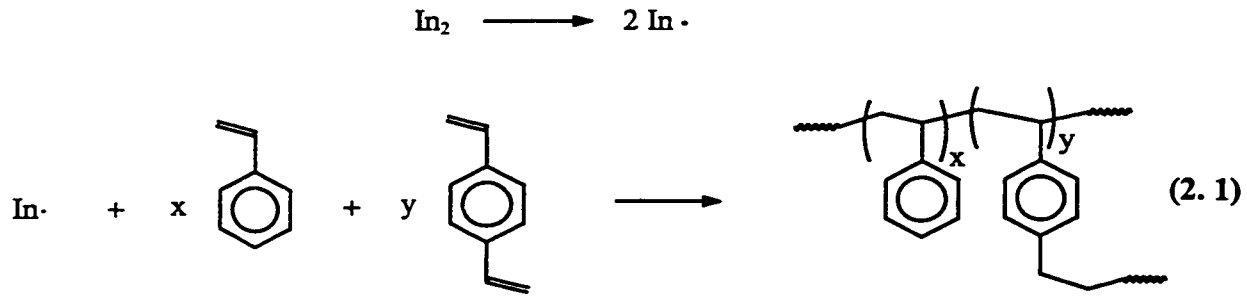

(2. 1)

The initiator (In_2), for example, benzoyl peroxide (BPO), decomposes to give two free radicals (In•). These can initiate the copolymerization of styrene and DVB incorporated in the pores of a substrate membrane. BPO was selected as the initiator in this work since it is known to be a good initiator for polymerization of styrene when heated to approximately 80°C [73]. This initiator (BPO) has been used in the preparation of ion-exchange membranes [74].

2.1.2. Sulfonation of Poly(Styrene-DVB)

Sulfonation of aromatic rings is a complicated reaction with competing side-reactions that give various by-products [75,76]. Early work on sulfonation of polystyrene was reported by Pepper et al. [77,78] in the 1940s. These workers used concentrated sulfuric acid, ie., temperature above 90°C. Since that time, the sulfonation of polystyrene have been extensively studied [75,75,79-82,89] and a number of patents have been issued [83-86]. A range of sulfonating reagents can be used, including concentrated sulfuric acid [87], fuming sulfuric acid [88], sulfur trioxide [25], sulfuryl chloride [90], and chlorosulfonic acid [91]. In this work, chlorosulfonic acid was selected as sulfonating

reagent since the chlorosulfonation procedures seem to be among the best methods [19,92].

The chlorosulfonation reaction of polystyrene is described in Eq. 2.2. In this study, the sulfonation was carried out by reacting poly(styrene-DVB) with 15% (v/v) chlorosulfonic acid in 1,2-dichloroethane at either 0°C or 40°C. This step was followed by hydrolysis with a 20% (w/w) aqueous sodium hydroxide solution.

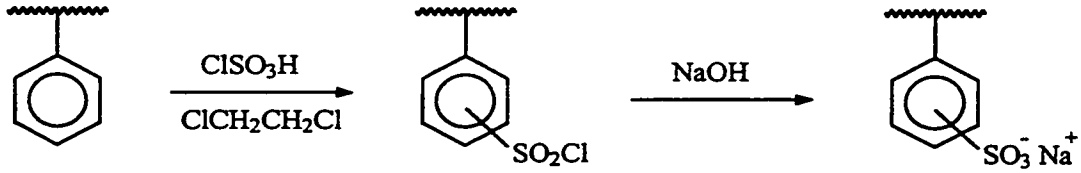

(2. 2)

2.2. EXPERIMENTAL

2.2.1. Materials

The porous substrate membrane used in this study was PE microfiltration membranes (provided by the 3M Canada Company). Table 2.1 summarizes the physical properties of this membrane.

Table 2.1. Physical properties of the microfiltration PE substrate membrane

Membrane material	Product I. D. Number	Thickness [a] (μm)	Porosity [a] (%)	Pore size [a] (μm)	Water permeability [b] (kg/m^2kPa)
Polyethylene	PE-1 #533-10	45	78	0.19	1.45

a. Data provided by 3M.
b. Measured at 100 kPa (*14.3 p.s.i.*)

Styrene and DVB (Aldrich) were purified by vacuum distillation to remove inhibitors. The purity of the distilled DVB was found to be approximately 52.5% by 200 MHz ^{1}H NMR spectroscopy (AC 200, Bruker). In this study, the degree of crosslinking introduced by DVB refers to the percentage of pure DVB which was used. The initiator (BPO), chlorosulfonic acid, 1,2-dichloroethane and chloroform (Aldrich) were used without further purification. Water used in this work was carbon filtered and deionized using the Barnstead/Thermolyne system (D 8904 and D 8901). The conductivity of the deionized water was approximately 2.0 μs/cm.

2.2.2. Experimental Procedure

2.2.2.1. Polymerization of Styrene and DVB

The method for polymerization of styrene and DVB was described elsewhere [93]. The *in situ* polymerization was carried out in a reaction vessel as shown in Fig. 2.1. The procedure for making a pore-filled ion-exchange membrane *via in situ* polymerization was similar to that described by Mika et al. [16] using 4-vinylpyridine.

The PE substrate membrane was cut into rectangular pieces, 12.7 cm (*5.0 inches*) × 10.5 cm (*4.1 inches*), pre-soaked in acetone for at least 16 h, vacuum dried, and weighed. The membrane was placed on the inner wall of the reaction vessel (Fig. 2.1). Approximately 2.0 g of a reaction mixture containing 92~98% of styrene, 1~7% of DVB and 1% of BPO (w/w) was poured into the bottom of the reaction vessel. The vessel was stoppered and the contents were frozen in an acetone-dry ice bath. The vessel with the

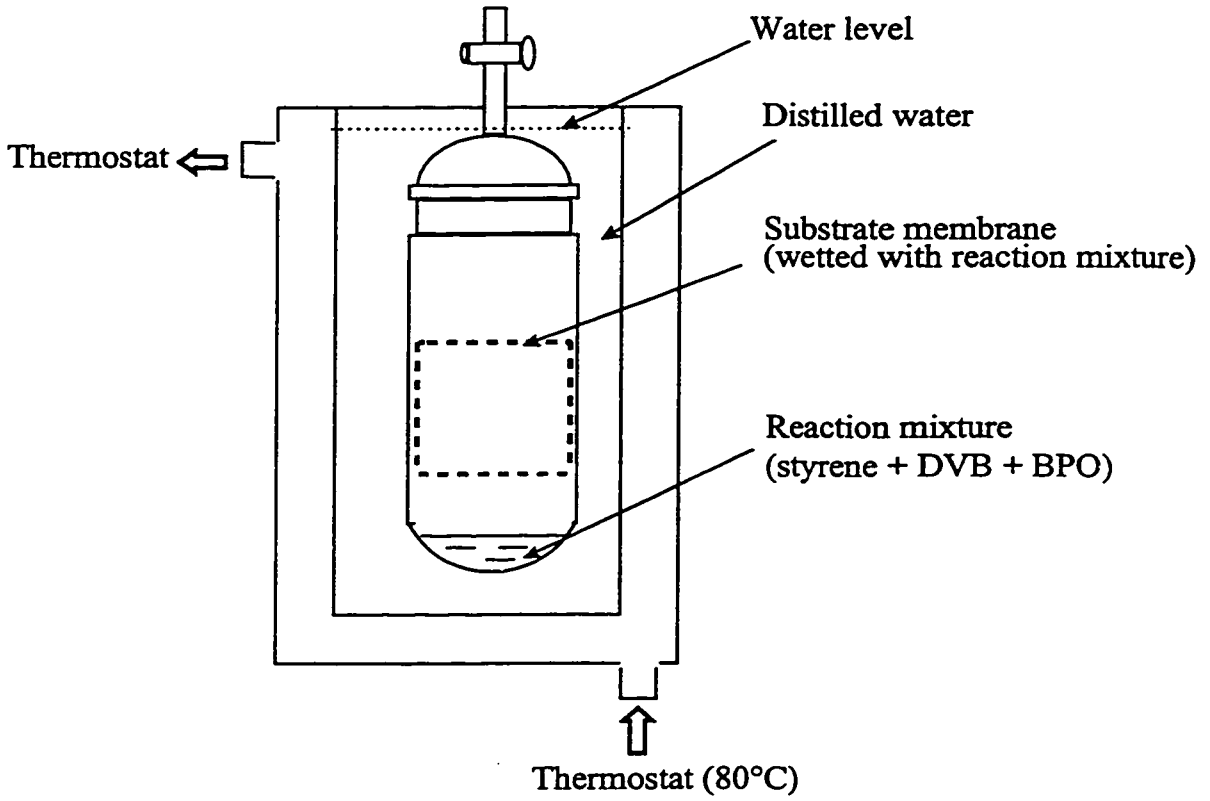

Fig. 2.1. Apparatus used in polymerization of styrene and DVB [16].

frozen contents was placed under vacuum and re-filled with dry nitrogen. The samples in the vessel were allowed to thaw. Three freeze-pump-thaw cycles were used. In the last cycle, the reaction vessel remained under vacuum was allowed to warm to room temperature. The membrane was wetted evenly with the reaction mixture. The radical polymerization reaction was induced by submerging the whole reaction vessel into a temperature-controlled water bath at 80 ± 0.5°C (Fig. 2.1). The polymerization time was varied from 0.5 to 10 h. The detailed conditions of membranes preparation in this work are presented together with the properties of the resulting membranes in Section 2.3 (Results and Discussion).

2.2.2.2. Extraction

After polymerization, the resulting membrane was removed from the reaction vessel and extracted (Soxhlet) with chloroform to remove non-anchored homopolymers. The extraction was carried out until no change in mass of the resulting dried membrane (approximately 72 h) was detected. The resulting membrane was vacuum dried for at least 48 h and weighed.

The mass increase (or mass gain) of the poly(styrene-DVB) copolymers anchored in the PE substrate membrane was calculated by the following equation:

$$\text{Mass increase (\%)} = \frac{m_{PS+PE} - m_{PE}}{m_{PE}} \times 100 \qquad \textbf{(2. 1)}$$

where m_{PE} and m_{PS+PE} were the masses of the PE substrate membrane and chloroform-extracted and dried membrane incorporated with poly(styrene-DVB) in the PE substrate membrane, respectively.

2.2.2.3. SEM

The procedure for the scanning electron microscopic (SEM) examination has been described by Mika et al. [16]. Membrane samples for the SEM examination were vacuum dried for at least 48 h. Cross sections were obtained by cracking the samples in liquid nitrogen. The membrane samples (both surface and cross section) were coated with gold to give approximately an 8 - 12 nm thick layer. The membrane samples were examined by SEM (ISI, DS130) at 15 kV.

2.2.2.4. Fourier Transform Infrared (FTIR) Spectroscopy

The substrate PE microfiltration membrane was opaque but became transparent when compressed at 1000 p.s.i. for 1 min. The resulting membranes containing poly(styrene-DVB) were vacuum dried (for at least 48 h) and examined using an infrared spectrometer (Bio-Rad FTS-40) without further treatment. Transmission FTIR spectra were obtained by scanning from 4000 to 400 cm^{-1}. The FTIR spectra were recorded using a minimum of 16 scans and at a resolution of 0.5 cm^{-1}.

2.2.2.5. Sulfonation

The method for chlorosulfonation of poly(styrene-DVB) was similar to that described by Pozniak and Trochimczuk [91]. The sulfonation was carried out with 15% (v/v) chlorosulfonic acid in 1,2-dichloroethane at either 0°C or 40°C. A poly(styrene-DVB) incorporated membrane (approximately 0.50 g) was placed in 200 mL of 1,2-dichloroethane for approximately 10 min. Then, 35 mL of chlorosulfonic acid was carefully added to the 1,2-dichloroethane with stirring at either 0°C or 40°C for 1 - 4 h. After the reaction, the membrane was dark brown. The membrane was removed from the solution and washed with chloroform (3 × 100 mL) to remove the unreacted chlorosulfonic acid. The membrane was placed in a stirred aqueous solution of 20% (w/w) NaOH at room temperature for 24 h. The resulting membrane was washed with deionized water, and conditioned by repeated alternating treatments with 1 M HCl (30 min), deionized water (30 min) and 1 M NaOH (30 min). The membranes were stored in deionized water at room temperature.

2.2.2.6. Ion-Exchange Capacity (IEC)

The method for measuring the IEC's has been described by Mika et al. [16]. The sulfonated membranes obtained above were converted into their sodium salt forms by treatment with 0.5 M NaOH solution (50 mL). The membranes were washed thoroughly with deionized water till the washing water was neutral. Each of the membranes was placed in an HCl solution of known volume (50.00 mL) and concentration (~ 0.0500 M) for at least 16 h. The membrane was removed and washed thoroughly with deionized water till the washing water was neutral. The washing water and the residual solution were combined and diluted to 250.00 mL. The concentration of Na^+ in the solution was determined in triplicate analyses by ion chromatography (Dionex, DX-100). The IEC obtained by ion chromatography, $(IEC)_{IC}$, was calculated by the following equation:

$$(IEC)_{IC}\ (meq / g) = \frac{1}{22.99} \cdot \frac{[Na,\ ppm]}{m_{PS + PE}} \qquad (2.4)$$

where [Na, ppm] was the concentration of sodium ion (Na^+) in ppm as determined by ion chromatography, and 22.99 the atomic weight of sodium.

The concentration of HCl in the solution was also determined by titrating 50.00 mL of the solution with a standard NaOH solution (~ 0.0500 M), using methyl red as an indicator. The $(IEC)_{titration}$ was calculated from the following equation:

$$(IEC)_{titration}\ (meq / g) = \frac{M_{HCl} V_{HCl} - M_{NaOH} V_{NaOH}}{m_{PS + PE}} \qquad (2.5)$$

where M_{HCl} and V_{HCl} were the concentration (M) and volume (mL) of the HCl solution, M_{NaOH} and V_{NaOH} the concentration (M) and volume (mL) of the standard NaOH solution, respectively. The IEC value for each membrane was taken as the average of values determined by both methods.

2.2.2.7. Sulfonation Yield

The sulfonation yield in this work refers to the ratio of the IEC measured above, $(IEC)_{exp}$, to that of the $(IEC)_{cal}$ calculated based on mono-sulfonation of the aromatic rings of poly(styrene-DVB). The sulfonation yield was calculated by the following equation:

$$\text{Sulfonation yield (\%)} = \frac{(IEC)_{exp}}{(IEC)_{cal}} \times 100 \qquad \textbf{(2. 6)}$$

2.2.2.8. Energy Dispersive X-ray (EDX) Analysis

The EDX analysis is an important method to determine elemental distribution across the membrane thickness [16,38]. The analytical procedure of EDX analysis has been described by Ulbricht [38]. A sulfonated membrane was converted into its acid form by treatment with an HCl solution (0.5 M, 50 mL) for 30 min. The membrane was washed with deionized water and placed in an Erlenmeyer flask containing a $Ca(OH)_2$ solution (0.2% w/w, 250 mL). The flask was stoppered and the solution was stirred overnight. The resulting membrane was carefully washed with deionized water till the washing water was neutral. The membrane was vacuum dried. The membrane cross

section specimens were obtained by freezing and cracking the membrane in liquid nitrogen. The amounts of sulfur and calcium on the membrane cross sections were determined by the EDX analysis (JEOL 1200 EX TEMSCAN).

2.2.2.9. Elemental Analysis

The amounts of carbon (C), hydrogen (H), and sulfur (S) in the sulfonated membranes were determined using a combustion method (ASTM D5373/ASTM D5291 for C and H, and ASTM D4239/D1552 for S).

The membranes prepared above were treated with an HCl solution (0.5 M, 100 mL) for 30 min, washed thoroughly with deionized water, immersed in an NaOH solution (0.5 M, 100 mL) for 30 min, and washed thoroughly with deionized water. This procedure was repeated twice to remove the multivalent ions in the membranes, such as Mg^{2+}, Ca^{2+} and SO_4^{2-}. Finally, the membranes which were in the Na^{+}-salt form were thoroughly washed with deionized water until the washing water was neutral. The wet membrane samples were sealed in a plastic bag and sent to Galbraith Laboratories (Tennessee, USA) where C/H/S analyses were performed. The wet membrane samples were vacuum dried for a minimum 8 h at room temperature before it was analyzed.

2.3. RESULTS AND DISCUSSION

2.3.1. Polymerization of Polystyrene and DVB

The *in situ* polymerization of styrene and DVB was carried out in pores of a PE substrate membrane initiated by BPO at 80°C. The pores of the substrate membranes were filled with styrene and DVB at the start of the reaction. The extra styrene and DVB mixture which was at the bottom of the reaction vessel were condensed on the film to continue the *in situ* copolymerization. The appearance of the resulting membranes was slightly brownish yellow. The color varied with the mass increase of poly(styrene-DVB). Membranes with high masses of poly(styrene-DVB) incorporated (>150%) became translucent and more brittle.

2.3.1.1. Mass Increase

The mass increase of incorporated poly(styrene-DVB) was found to be dependent on the polymerization reaction time. The relationship between mass increase and reaction time is shown in Fig. 2.2. For both sets of data (DVB% = 1.0% and 2.5%), the mass of incorporated poly(styrene-DVB) increases slowly at the beginning of the polymerization but increases dramatically afterwards. In the final stage (after approximately 3 - 4 h), little further mass increase occurs.

The S-shaped curve relating mass increase with time is similar to those reported for conversion of monomers in radical polymerization processes [94]. At the beginning of

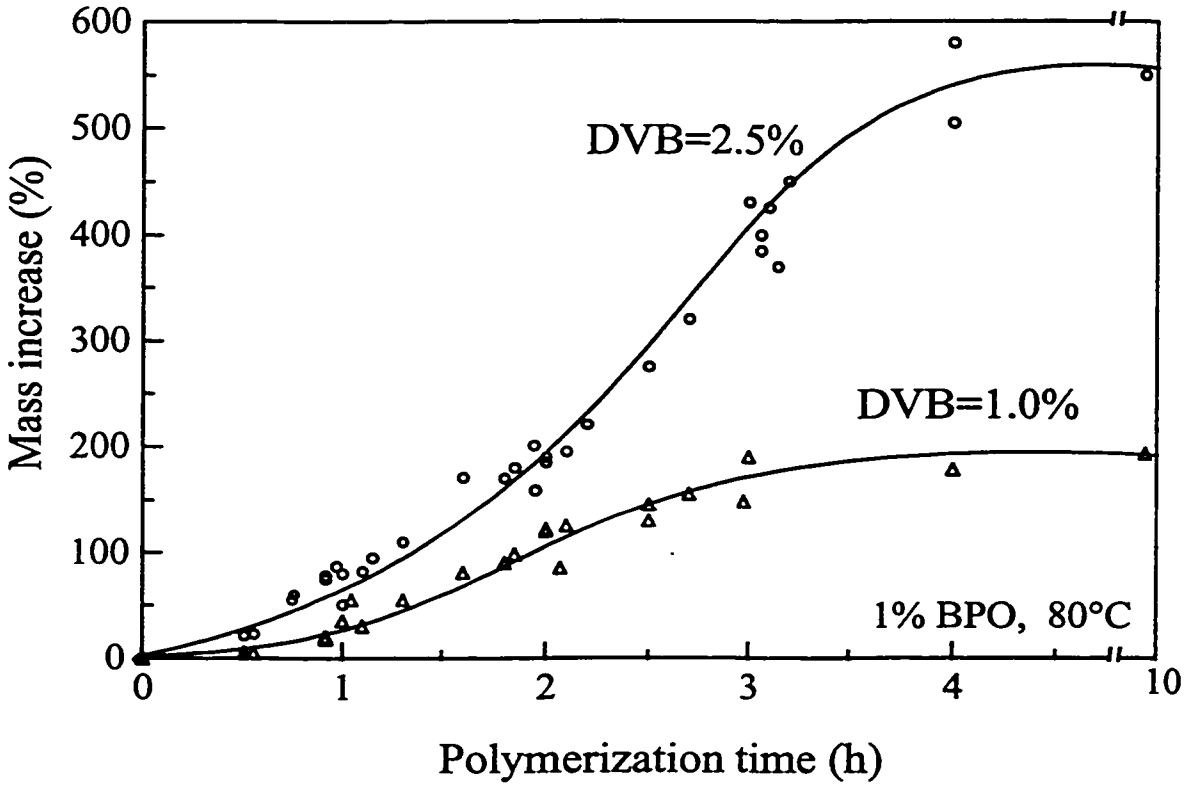

Fig. 2.2. Mass increase as a function of polymerization time.

the polymerization, there is an induction period possibly due to the small amount of oxygen and other inhibitors which consume radicals produced by decomposition of the initiator. When the inhibitors are consumed, the rate of mass increase of the incorporated poly(styrene-DVB) increases dramatically. In the final stages, the reaction rate becomes low due to the high viscosity of the incorporated copolymers which slow down the chain movement and reduce the reaction opportunity between the radicals and the monomers. This effect is called the Trommsdorff effect [95].

The porosity of the PE substrate membrane is 78% (Table 2.1). This means that the maximum incorporation of poly(styrene-DVB) would be approximately 350% if the pores of the PE substrate membrane are filled fully with the styrene-DVB copolymers and no significant change in structure of the PE substrate membrane occurred during the thermally initiated *in situ* polymerization*. The observed mass increase ranging up to approximately 600% (DVB% = 2.5%) indicates either (i) that a change in structure of the substrate membrane occurs, due to the thermally induced polymerization of styrene and DVB, or (ii) that the incorporated poly(styrene-DVB) is located not only within the pores but also on the surfaces of the PE substrate membrane, or (iii) both of above.

The relationship between mass increase and degree of crosslinking is shown in Fig. 2.3. All the experiments were conducted for identical times (3 h). The mass increase of poly(styrene-DVB) incorporated was found to strongly depend upon the degree of crosslinking. For example, as can be seen from Fig. 2.3, no poly(styrene-DVB) was incorporated when no crosslinking reagent was present. This suggests that when DVB is used, the incorporated poly(styrene-DVB) copolymers are not grafted to the substrate membrane but crosslinked and entangled (and "locked") in the pores of the PE substrate membrane. As can be seen from the data in Fig. 2.3, the mass gain of incorporated poly(styrene-DVB) increases dramatically with increasing DVB. Again, a typical S-shaped relationship was found. When the amount of DVB is low, the slightly crosslinked

---

* It should be noted that pore contractions of the PE substrate membrane are observed due to the thermal treatment (see Chapter 3 for detail).

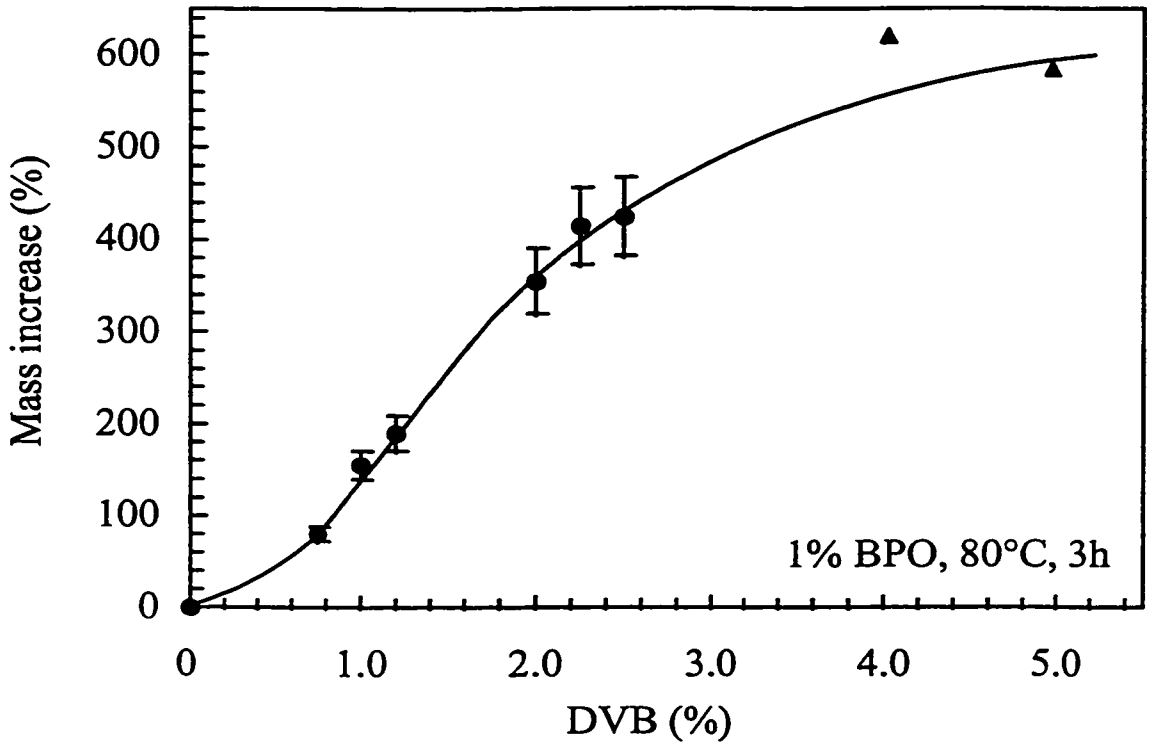

Fig. 2.3. Mass increase as a function of degree of crosslinking. The data points marked as (•) are the average of at least three experiments. The points marked as (▲) are the data from single measurements. The experimental errors (standard deviation) of the measurements are *ca.* ± 10%.

poly(styrene-DVB) seems not to be stable and apparently can be removed easily by the Soxhlet extraction. When the more DVB is used, the more of the poly(styrene-DVB) are incorporated and the resulting membrane is more robust [96]. In the final stage, the mass increase reaches the maximum due to the Trommsdorff effect.

2.3.1.2. Morphology

SEM images of the micro-structure of the PE substrate membrane and the poly(styrene-DVB)-filled membranes are shown in Fig. 2.4. The PE substrate membrane has two surface layers and a sponge-like porous region in-between.

Images of the cross section and surface of the membrane with a mass increase of 150% (2.5% degree of crosslinking) are shown in Fig. 2.5. As can be seen by comparison of Figs. 2.4 and 2.5, the dried resulting membrane is still porous after the incorporation of the poly(styrene-DVB). The cross section of the resulting membrane is similar to that of the substrate membrane. After the copolymerization, a porous center region is still evident. This indicates that the structure of the PE substrate membrane does not change significantly during the copolymerization. Fig. 2.5 shows that there are some changes in the appearance of the surface and in the center sponge region. This suggests that the poly(styrene-DVB) incorporated forms both on the surfaces and in the pores of the PE substrate membrane. This observation is consistent with the results of Mika et al. [16] who observed, from the SEM images of the surface and cross section of PVP-filled membranes, that the structure of substrate membranes did not change significantly after the *in situ* polymerization of 4-vinylpyridine. Ulbricht [38] reported that the structure of the substrate membrane was basically preserved while the grafted poly(acrylic acid) (PAA) was found to cover the fibrous substrate PP matrix.

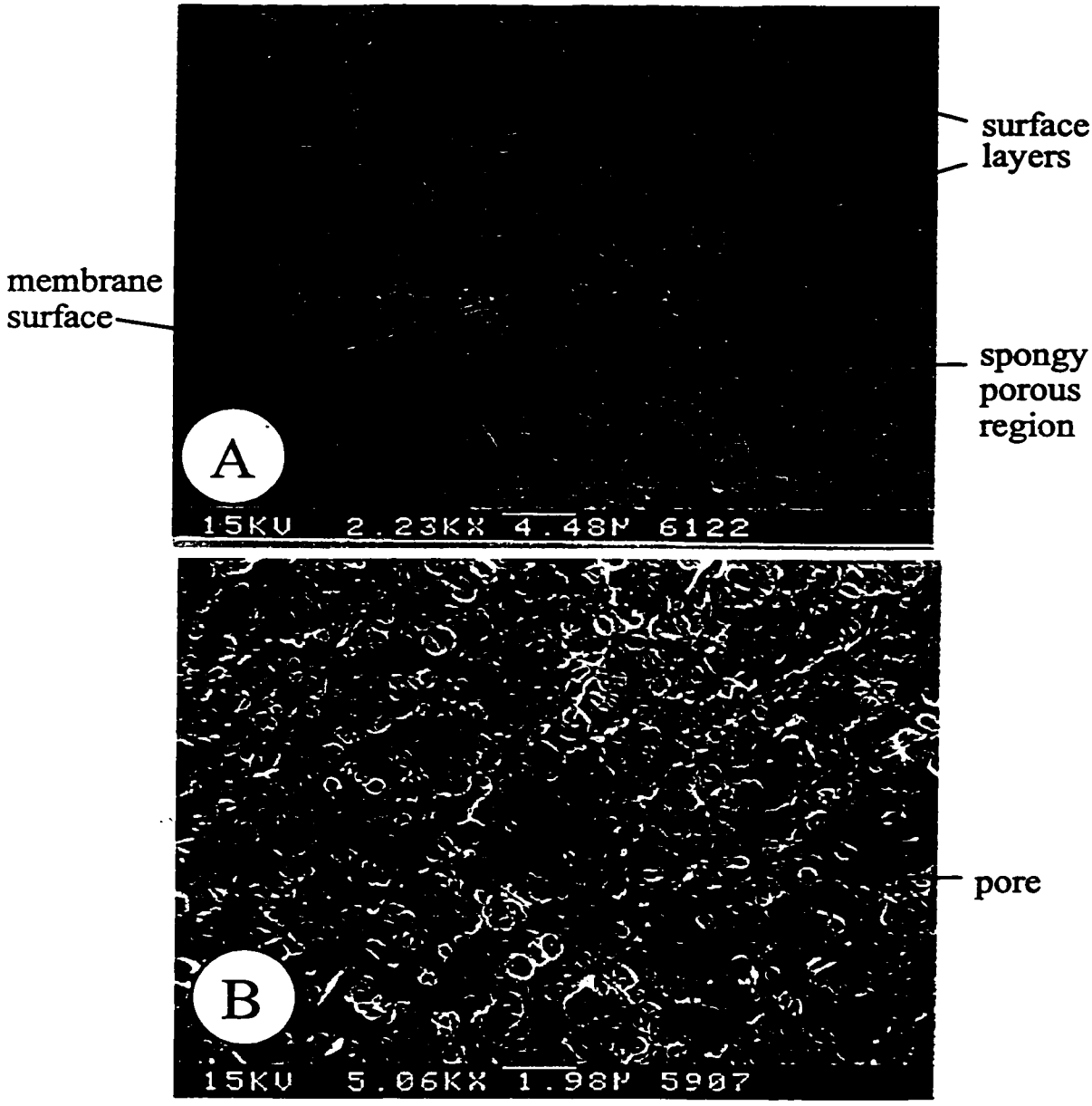

Fig. 2.4. SEM's of the PE substrate membrane:
(A) cross section and (B) surface.

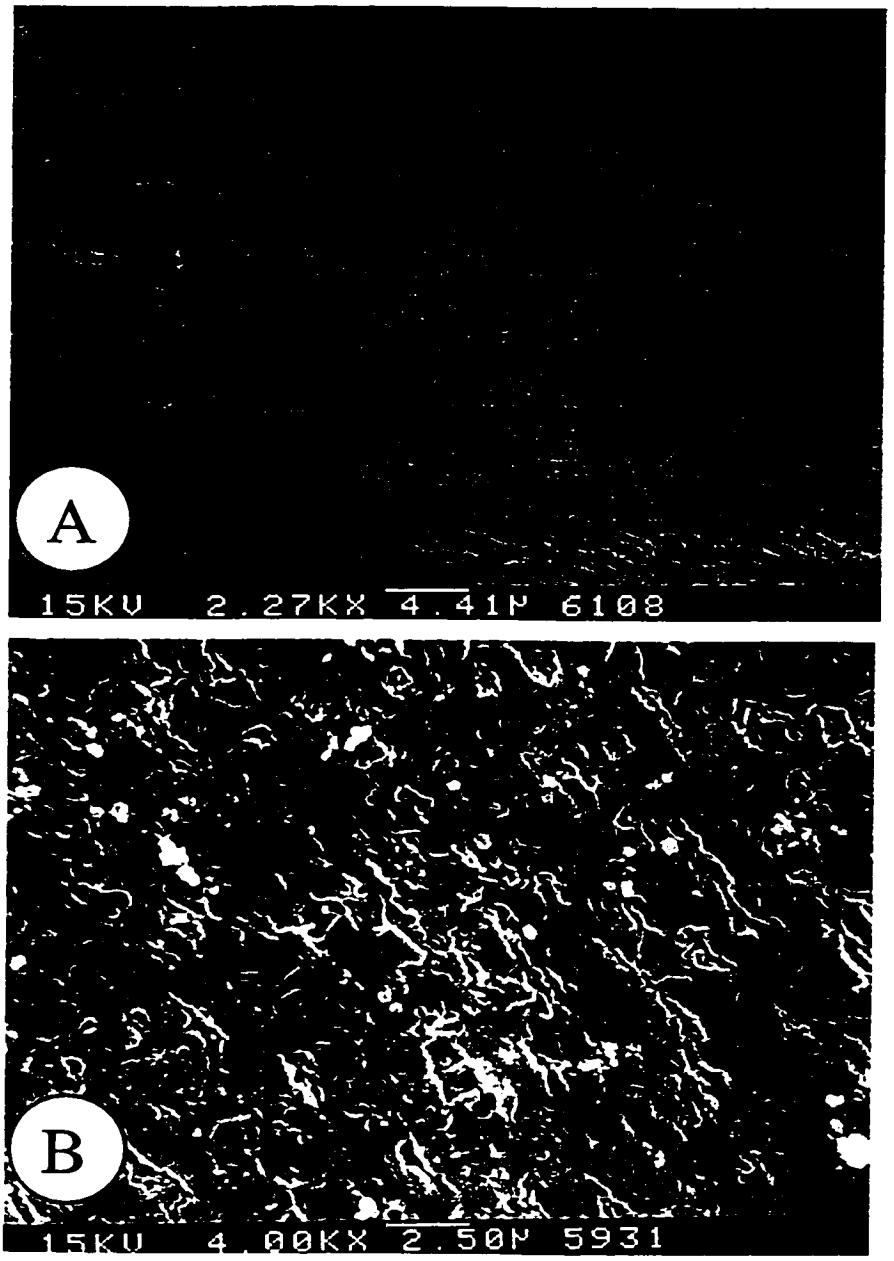

Fig. 2.5. SEM's of (A) cross section and (B) surface of poly(styrene-DVB) incorporated in the PE substrate membrane (mass increase = 150%, DVB = 2.5%).

2.3.1.3. Spatial Distribution of Poly(Styrene-DVB)

The spatial distribution (or evenness) of the pore-filling styrene-DVB copolymers across the length/breadth of a membrane was determined by measuring the amounts of PS and PE from the FTIR spectra of the resulting membranes. Ihm and Ihm [97] have reported using FTIR to monitor the amount of polystyrene grafted onto porous poly(vinyldene fluoride) films. A comparable method was used in this work which allows profiling of chemical composition across the membrane.

The FTIR spectra of the PE substrate membrane, the poly(styrene-DVB) incorporated membranes with various mass increases, and polystyrene (PS) are shown in Fig. 2.6. The peaks at 1493 and 1473 cm^{-1} correspond to the C-H bending vibrations of PS and PE, respectively [98]. The peaks are well separated and can be used to give a relative measure of the ratio of PS to PE. It can be seen that the sizes of the PS peaks (1493 and 1452 cm^{-1}) increase with increasing mass of incorporated poly(styrene-DVB).

The reproducibility of repeated measurements (of relatively ratio of polystyrene/ PE) using the FTIR instrument is within ± 5%. This suggests that the PE substrate membrane is only roughly even. While this technique gives an estimation of the amount of incorporation, it is not particularly sensitive, especially if the peaks overlap when the mass increase is too high or too low due to the overlap of the peaks. However, it gives an indication of the distribution of the incorporation of the copolymers.

A pore-filled membrane containing 118% of poly(styrene-DVB) with a degree of crosslinking of 2.5% was analyzed by FTIR at 12 points over the area of the membrane. The ratio of the absorbances at 1493 and 1473 cm^{-1} was determined at each point and the

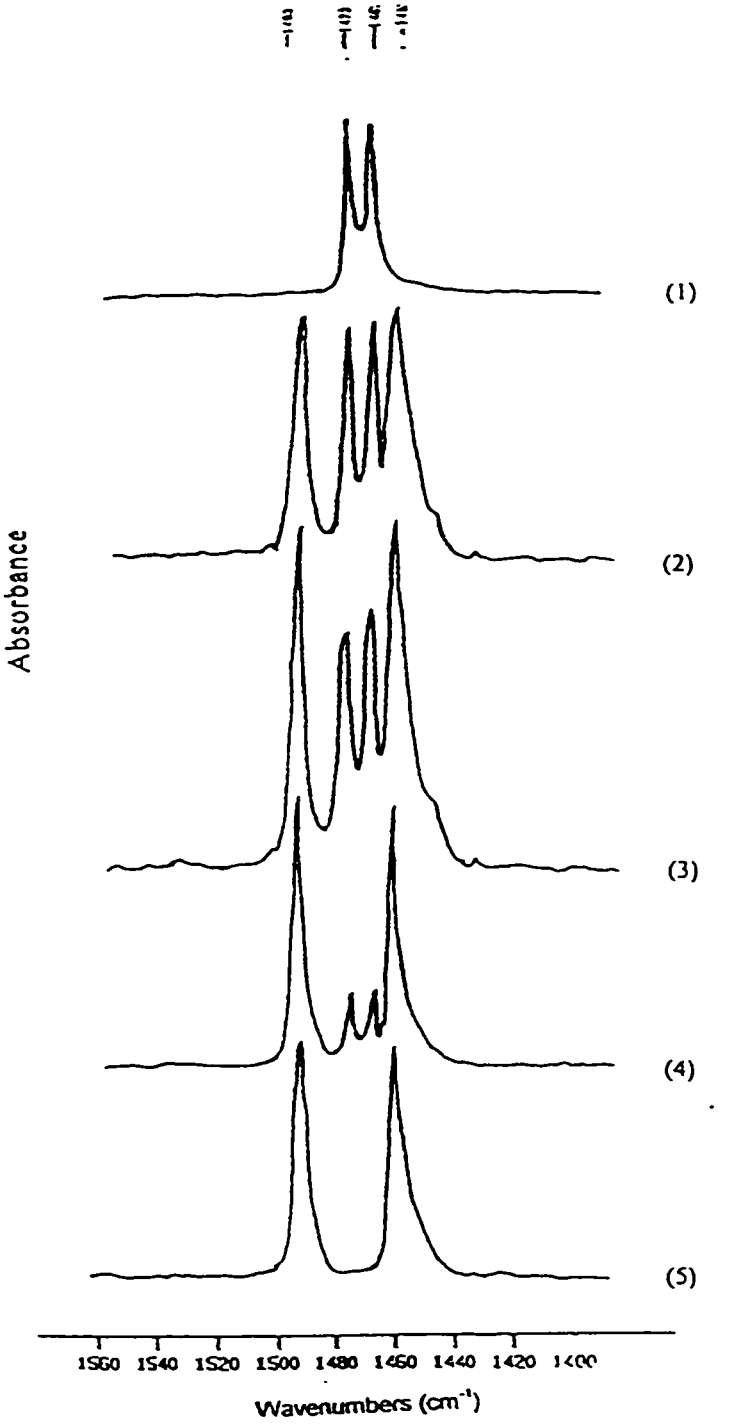

Fig. 2.6. FTIR spectra from 1520 to 1420 cm^{-1} of the membranes.
(1) PE substrate membrane
(2) poly(styrene-DVB) incorporated in the PE membrane, mass increase 78%
(3) poly(styrene-DVB) incorporated in the PE membrane, mass increase 150%
(4) poly(styrene-DVB) incorporated in the PE membrane, mass increase 291%
(5) poly(styrene-DVB)

data are shown in Fig. 2.7. The heights of the bars (absorbance ratios), Fig. 2.7, are nearly identical. It should be noted that the differences between the absorbance ratios (heights of the bars) are within ±7% which is similar to the variation of ±5% in absorbances of the substrate membrane. This indicates that the distribution of the poly(styrene-DVB) copolymers is relatively even across the length and breadth of the PE membrane.

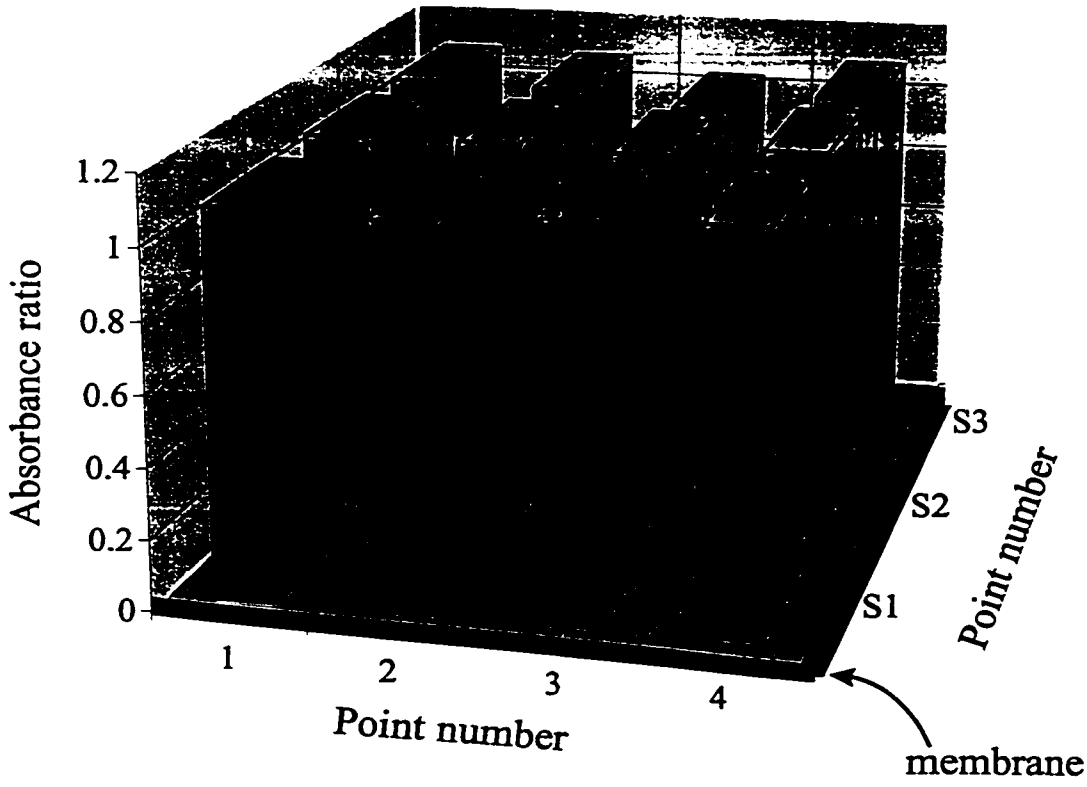

Fig. 2.7. FTIR absorbances ratios of a poly(styrene-DVB) incorporated membrane (mass increase 118%, DVB=2.5%).

2.3.2. Sulfonation

The membranes containing poly(styrene-DVB) obtained after the *in situ* polymerization were chlorosulfonated with 15% chlorosulfonic acid in dichloroethane.

This reaction was followed by hydrolysis with a 20% (w/w) aqueous sodium hydroxide solution to give the sodium salt of the poly(styrene-DVB sulfonic acid). This section describes the characterization of these sulfonated membranes.

2.3.2.1. Morphology

The morphology of the resulting cation-exchange membranes was examined by SEM. Micrographs of the cross sections of a membrane in its protonated and sodium salt forms are presented in Fig. 2.8.

A comparison of the SEM images of the sulfonated membrane with the substrate PE microfiltration membrane, Fig. 2.4(A), and the poly(styrene-DVB) incorporated membrane, Fig. 2.5(A), shows that the structure of the membrane does not seem to change significantly in the sulfonation reaction. The sulfonated membrane still has thin surface layers and a porous region in-between, just as did the PE substrate membrane and the poly(styrene-DVB) pore-filled membrane. The structure of the membrane surface and cross section appear to change when the counter-ion changes from Na^+ to H^+ (Fig. 2.8) suggesting that the sulfonated styrene-DVB copolymers are both on the surface and through the cross section of the membrane. This is consistent with the observation in Fig. 2.5 that the poly(styrene-DVB) incorporated was observed on the surfaces and in the

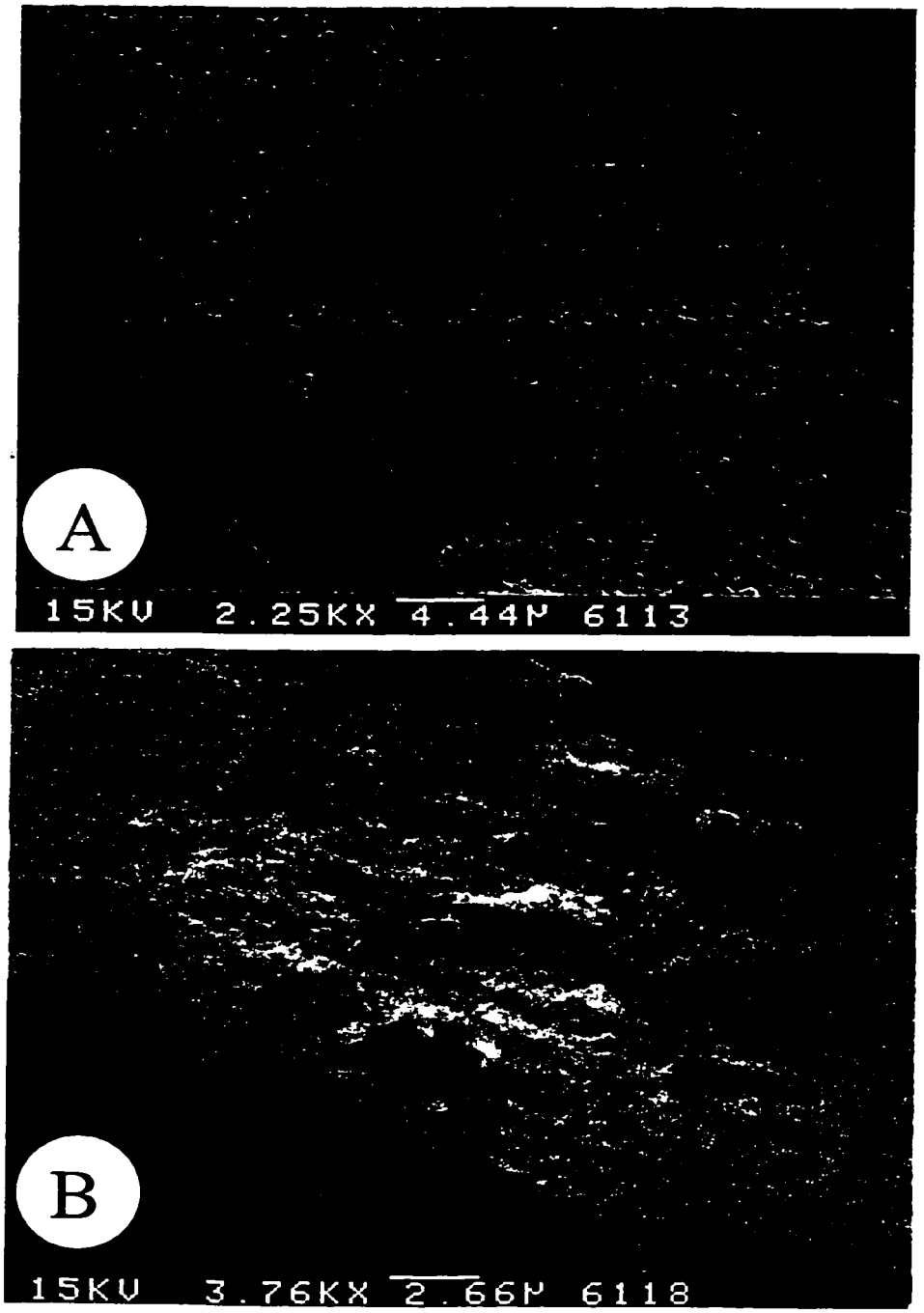

Fig. 2.8. SEMs of cross sections of a sulfonated poly(styrene-DVB)-incorporated in the PE membranes: (A) in Na^+ salt form, and (B) in H^+ form.

pores. The images seem to show that a change in counter-ion from Na^+ to H^+ leads to a change in conformation of the polyelectrolyte gel. It should be noted that these membranes were vacuum dried. These images might not truly reflect the conformation of the wet, swollen gels. Since poly(styrene sulfonc acid) is a strong acid and is difficult to dry, the difference between the two images should also be affected by the difference in water present in the two membranes.

2.3.2.2. EDX Analyses

A pore-filled cation-exchange membrane with a mass increase of 150%, DVB = 2.5%, and IEC = 3.5 meq/g was selected for analysis by energy dispersive X-ray spectroscopy (EDX). The sulfur (S) and calcium (Ca) contents of the membrane were determined as functions of membrane thickness. The calcium ion was chosen as the counter-ion rather than the sodium ion since calcium is more readily detectable than sodium in EDX analyses.

The membrane was slowly air dried at room temperature in order to maintain the micro-structure of the membrane. The sulfur (S) and calcium (Ca) contents on the membrane cross section were determined by EDX. Six different locations on cross sections of the membrane were examined. The sulfur and calcium signals were at 2.310 and 3.693 keV, respectively. The sulfur and calcium contents were calculated from the corresponding areas of the signals. The error of the measurements was within 10%.

The measured sulfur and calcium contents through the thickness of the membrane (the cross section) are shown in Fig. 2.9. The analyses of top surface, shown in dark grey,

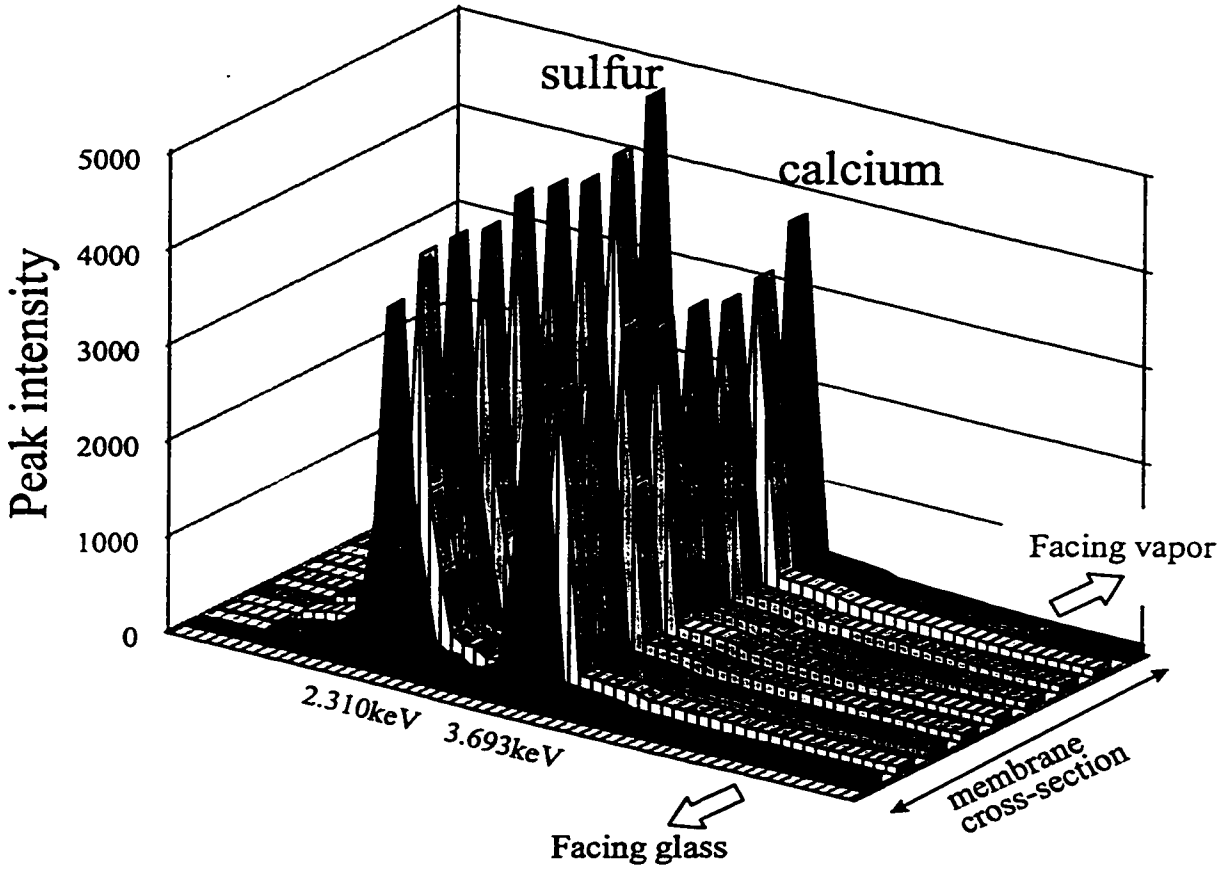

Fig. 2.9. EDX analysis of sulfur and calcium on the membrane surfaces and cross section; membrane: mass increase = 150%, DVB = 2.5%, IEC = 3.5 meq/g.

were measured on either side of the membrane. The lighter grey points were determined from the X-ray cross section analysis. It can be seen that, through the membrane cross section, the heights (and areas) of the sulfur (S) and calcium (Ca) peaks (marked in lighter grey color) do not change significantly within experimental error. However, the heights on the surfaces (marked in the dark color) are different. The surface facing the monomer vapor has high S and Ca contents than the surface facing the glass of the

reaction vessel (Fig. 2.1). However, this difference was not observed from the SEM's. The results indicate that the incorporation of poly(styrene-DVB sulfonic acid) is even across the membrane cross section.

Ulbricht [38] prepared pore-filled membranes by one-step grafting PAA onto the microporous PP host membranes in which the incorporated contents were found to be evenly distributed. Momose et al. [99] reported that quaternary ammonium salts were evenly incorporated throughout the cross section of the host membranes. Mika et al. [16], have reported the similar findings with PVP salt-filed membrane. The EDX results obtained in this work mean that the styrene-DVB copolymers are incorporated evenly in the substrate membrane during the thermally induced radical polymerization and the sulfonation gives an even distribution of poly(styrene-DVB sulfonic acid within the substrate membrane.

2.3.2.3. IEC and Sulfonation Yield

The ion-exchange capacity (IEC) is one of the most important parameters of ion-exchange membranes. The IEC's of the resulting membranes were measured by both acid-base titration and ion chromatography methods. The differences in measured IEC's between the two methods were less than 1% due to small amount of other metal ions other than Na^+ in the NaOH solution which were ignored in the ion chromatographic measurements. The IEC values reported in this study is the average value of the IEC's obtained from the titration and ion chromatography methods.

The IEC's of the membranes as a function of mass increase of poly(styrene-DVB) are shown in Fig. 2.10. The degree of crosslinking of these membranes was 2.5% and the sulfonation time was 4 h. As can be seen, the membranes with high mass increases have very high IEC's, up to 5.60 meq/g. The IEC increases with increasing the mass increase of the incorporated poly(styrene-DVB) for both the 0°C and the 40°C sulfonations. The higher sulfonation temperature (40°C) leads to a higher IEC for membranes with the identical mass gains. These IEC's measured are lower than the calculated IEC's.

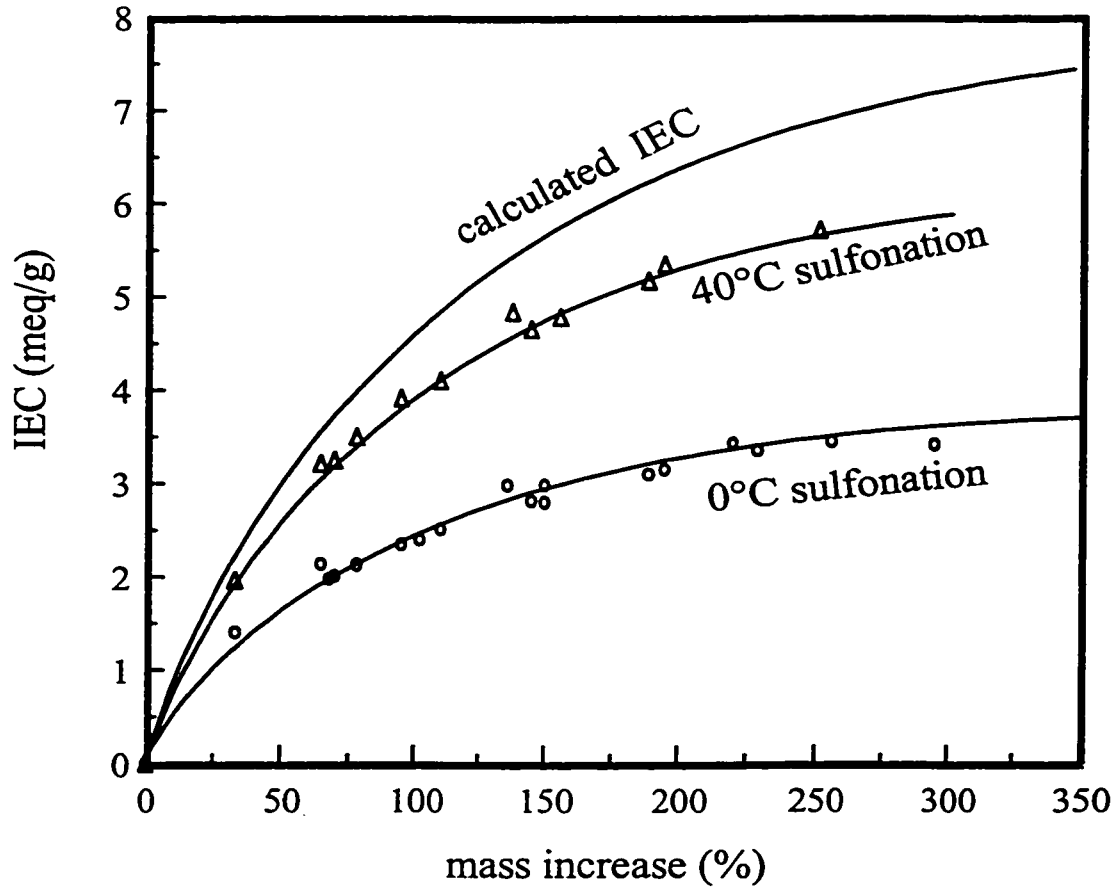

Fig. 2.10. Ion-exchange capacity (IEC) as a function of mass increase of poly(styrene- DVB) (DVB = 2.5%, sulfonation time = 4h).

The calculated IEC is the number of moles of sulfonic acid groups (meq) in the membrane (g). The number of moles of sulfonic acid groups is based on the mass of incorporated poly(styrene-DVB), assuming that 100% of mono-sulfonation of the aromatic rings takes place. The relationship between the sulfonation yield and the mass increase of the incorporated poly(styrene-DVB) for both 0 and 40°C sulfonations is shown in Fig. 2.11. As can be seen from the data shown in Fig. 2.11, for 40°C sulfonation

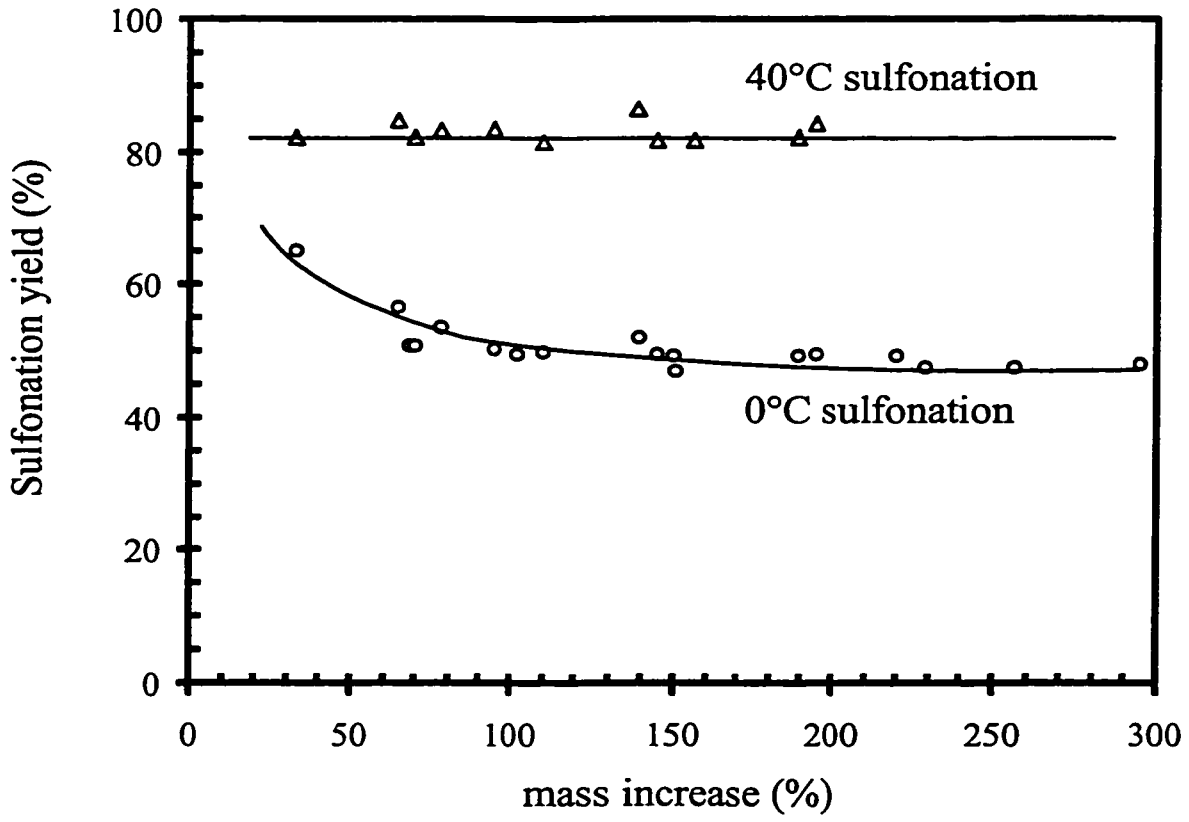

Fig. 2.11. Sulfonation yield as a function of mass increase of poly(styrene-DVB); sulfonation time: 4 h, and DVB = 2.5%.

reactions, the sulfonation yields remain constant at approximately 81%. The sulfonation yield for 0°C sulfonation reactions decreases with increasing the mass increase For the 0°C sulfonations, the sulfonation yields decrease and level off at approximately 50%.

The effect of crosslinking on sulfonation yield is shown in Fig. 2.12. It was observed that sulfonation yields (0°C) decreased with increasing degree of crosslinking

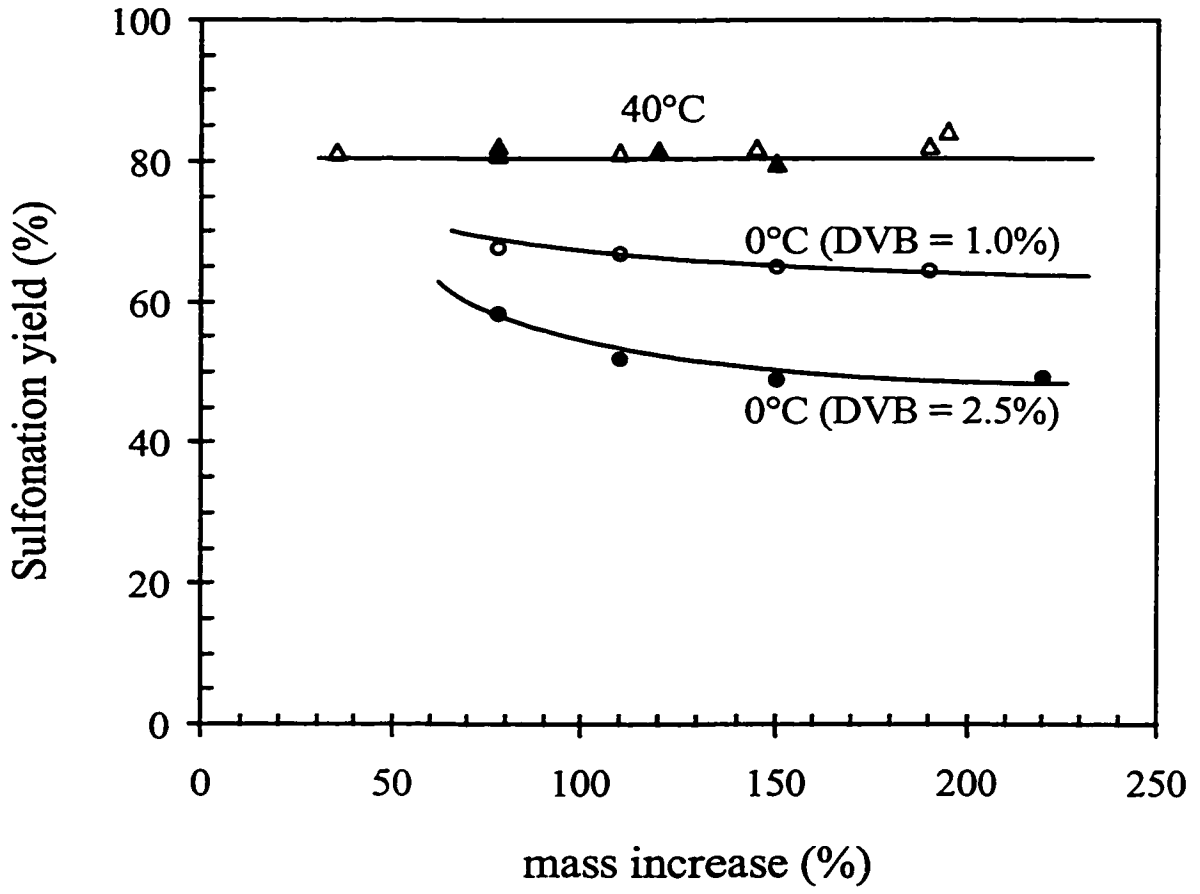

Fig. 2.12. Effect of degree of crosslinking on sulfonation yield.

o - 0°C, DVB = 2.5%, • - 0°C, DVB = 1.0%,
Δ - 40°C, DVB = 2.5%, ▲ - 40°C, DVB = 1.0%.

while at 40°C no significant difference was observed. Specifically, at 0°C, with constant mass increases (150%), the sulfonation yield was 66% and 49% when DVB was 1.0% and 2.5%, respectively.

It is also evident in this work that the reaction temperature is a significant factor on the sulfonation step. Sulfonation yields for the reactions carried out at 40°C were found to be approximately 80%, significantly higher than the reactions carried out at 0°C (45%, DVB = 2.5%, mass increase = 76%).

The results are consistent with the findings of Trochimczuk et al. [91,100], who reported the preparation of poly(styrene-DVB sulfonic acid) membranes made by extruding poly(styrene-DVB)/PE melt. The authors found that, for the same reaction system (chlorosulfonation of poly(styrene-DVB)) at another temperature (23°C) for various reaction times, the sulfonation yield decreased with increasing the DVB% (degree of crosslinking). For the same reaction carried out at 23°C, Gozdz and Trochimczuk [100] observed the sulfonation yield of 55% for chlorosulfonation of the membranes containing 78% of poly(styrene-DVB) with degree of crosslinking of 3%.

The effects of reaction time on sulfonation yields was also examined (Table 2.2). At 0°C, the sulfonation yield increases from approximately 44% to 50% when the sulfonation time increases from 2 h to 4 h. A second 4 h sulfonation was carried out on the membranes that had already been sulfonated for 4 h at 0°C. The membranes were hydrolyzed with NaOH and their IECs measured prior to the second sulfonation. The sulfonation yields were found to increase from 50% to 60% after the second sulfonation.

Table 2.2. Sulfonation yields of the membranes which were prepared in sulfonation reactions in 15% chlorosulfonic acid (v/v) of various time at 0 and 40°C.

Membrane		Sulfonation Yield (%) [a]			
Mass increase	DVB	Total sulfonation time			
(%)	(%)	1.5h	2h	4h	8h
			0°C		
76	2.5	-	45	-	-
78	2.5	-	43	-	-
80	2.5	-	-	50	61 [b]
83	2.5	-	-	49	57 [b]
91	1.0	-	-	66	-
135	1.0	-	-	65	-
			40°C		
117	2.5	81	-	-	-
138	2.5	78	-	-	-
131	2.5	-	-	82	-
132	2.5	-	-	82	-
135	1.0	-		84	-
135	1.0	-	83	-	-
139	1.0	-	83	-	-

a. Error less than ±1%.

b. Second sulfonation membranes. These membranes were sulfonated twice. These membranes were sulfonated and measured IECs, and re-sulfonated under the same conditions.

This is consistent with the findings of Byun et al. [79], who observed the sulfonation yield increased with increasing reaction temperature when sulfuric acid was used as the sulfonating reagent. However, for the 40°C sulfonations, sulfonation yields were found to be constant at about 78 - 84% at reaction times of 1.5 h, 2 h, and 4 h.

2.3.2.4. "Layer-by-Layer" Sulfonating Process

This sulfonation can be understood in terms of the "layer-by-layer" sulfonating process [101], illustrated in Fig. 2.13. When a polymer is contacted with the sulfonating reagent, sulfonation occurs at the surface of the polymer. Once the surface of the polymer has been sulfonated, this layer becomes a barrier which slows down the diffusion rate of the sulfonating reagents into the interior regions of the polymer gels. As more of the polymer is sulfonated, this sulfonated layer becomes thicker and the rate of sulfonation becomes slower due to more difficult diffusion of the sulfonating reagent. Longer time and higher temperature should lead to an increase in sulfonation yield.

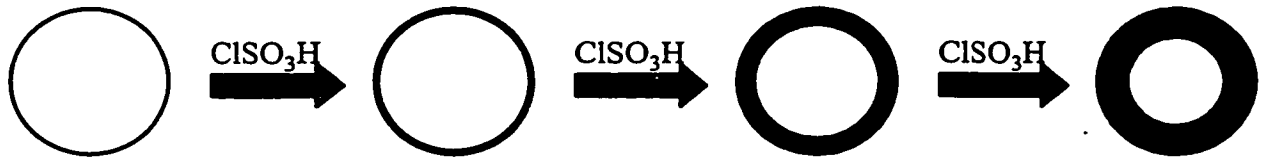

Fig. 2.13. The "layer-by-layer" sulfonating process.

2.3.2.5. Mechanism of sulfonation

Sulfonation reactions with aromatic rings occur by an electrophilic substitution. The mechanisms of sulfonations using SO_3 and H_2SO_4 as sulfonating reagents have been reviewed [102]. It is known that the formation of a cationic σ-complex is the rate-determining step.

The mechanism of chlorosulfonation is illustrated in Fig. 2.14. The sulfonating reagent, chlorosulfonic acid (1), is in equilibrium with (3), (4) and (5) in the solvent (1,2-dichloroethane). Species (3) is a good electrophile which can react with polystyrene (2) *via* electrophilic substitution preferentially at either the *ortho* or *para*-position on an aromatic ring to give a cationic σ-complex (6) which can lose a proton to produce poly(styrene-sulfonic acid) (7). It is known that when one sulfonic acid is introduced on an aromatic ring, the introduction of a second sulfonic acid on the same ring is more difficult due to the deactivating effect of the initial sulfonic acid group [103].

The chlorosulfonation reaction was carried out in an excess of chlorosulfonic acid so that the aromatic sulfonic acid group (7) can either react with another aromatic sulfonic acid group (7) to yield the sulfonic anhydride (8), or react with sulfur trioxide (5) to produce or pyrosulfonic acid (9), or be protonated to yield (10) which can lose a water molecule to produce (11). The cation (11) can be converted into the sulfonyl chloride (12) by reacting with a chloride ion. Finally, species (8), (9) and (12) can be hydrolyzed into poly(styrene-sulfonate) sodium salts (13) in a 20% NaOH aqueous solution.

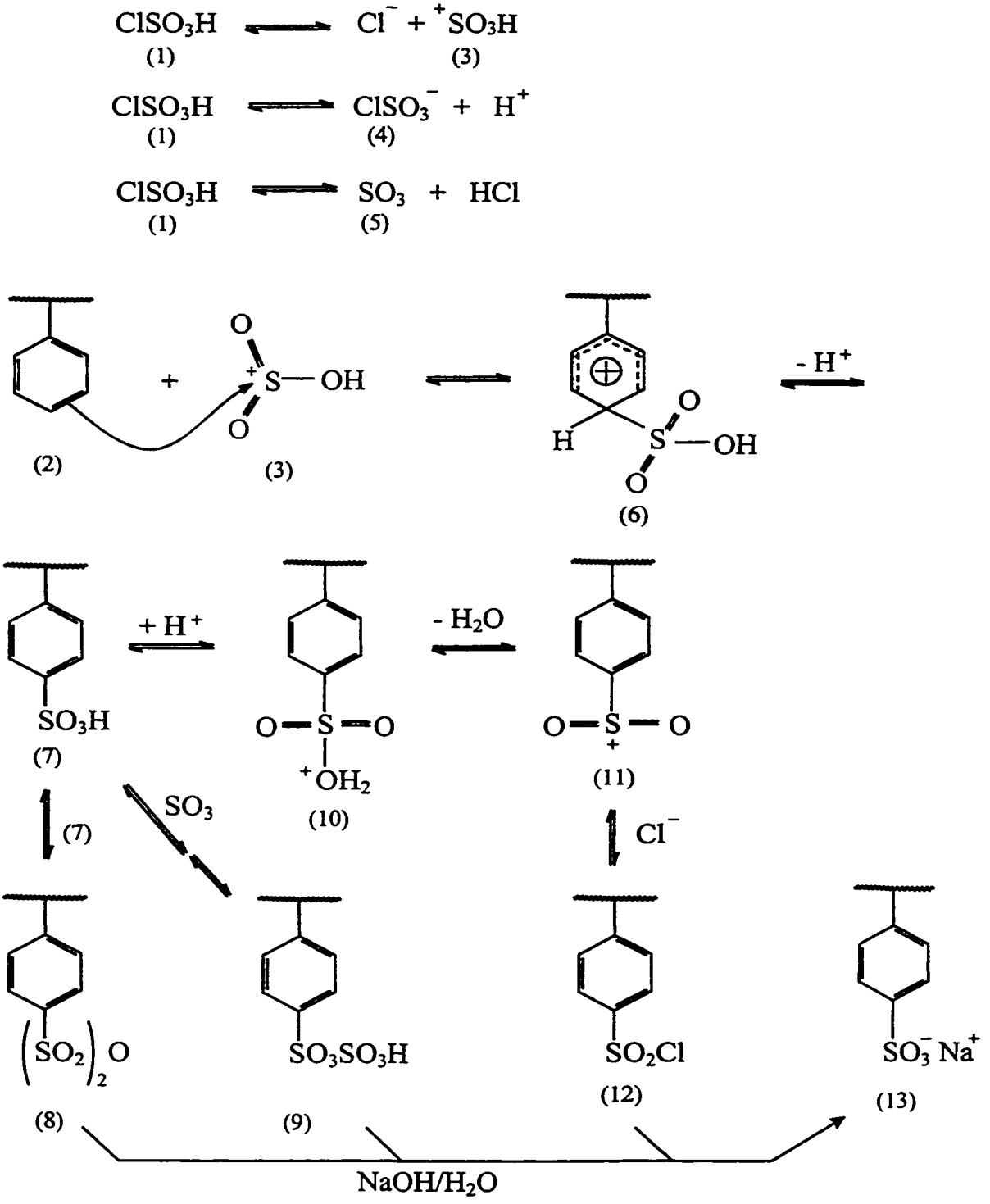

Fig. 2.14. Reaction mechanism of chlorosulfonation.

2.3.2.6. Sulfone formation

One would expect the sulfonation yield in the reactions to exceed 100%. In the other words, each aromatic ring has a sulfonic acid group. In the literature, the sulfonation yield were found to more than 100% using concentrated sulfuric acid [77,78]. However, it was found in this work that the highest sulfonation yield was 84% with the 40°C sulfonations. A question arises as to why a maximum sulfonation yield of approximately 84% is reached. One possible explanation is that a side reaction to form sulfones is occurring. Such reactions are known to occur particularly when chlorosulfonic acid is used as the sulfonating reagent [75,76,78] due to formation of the sulfonyl chloride which is readily to converted into sulfone. Another possible reason is that not all the sulfonic acid groups can be measured since part of sulfonic acid groups are formed in the central region of the crosslinked polymers and are not ion-exchangeable. In other words, these sulfonic acid groups cannot be measured by the methods discussed in the previous section.

In order to examine the possibility of sulfone formation, FTIR and elemental analysis methods were used to examine whether sulfones were being formed. Two sulfonated membranes were examined by FTIR: membrane #73 with 78% of mass increase which was sulfonated at 0°C and membrane #83 with 80% of poly(styrene-DVB) which was sulfonated at 40°C. Both membranes had an identical degree of crosslinking (2.5%). The FTIR spectra of the two membranes (in their Na^+ salt forms) were obtained. As can be seen, the FTIR spectra are nearly identical, Fig. 2.15(A) and (B). In addition, as

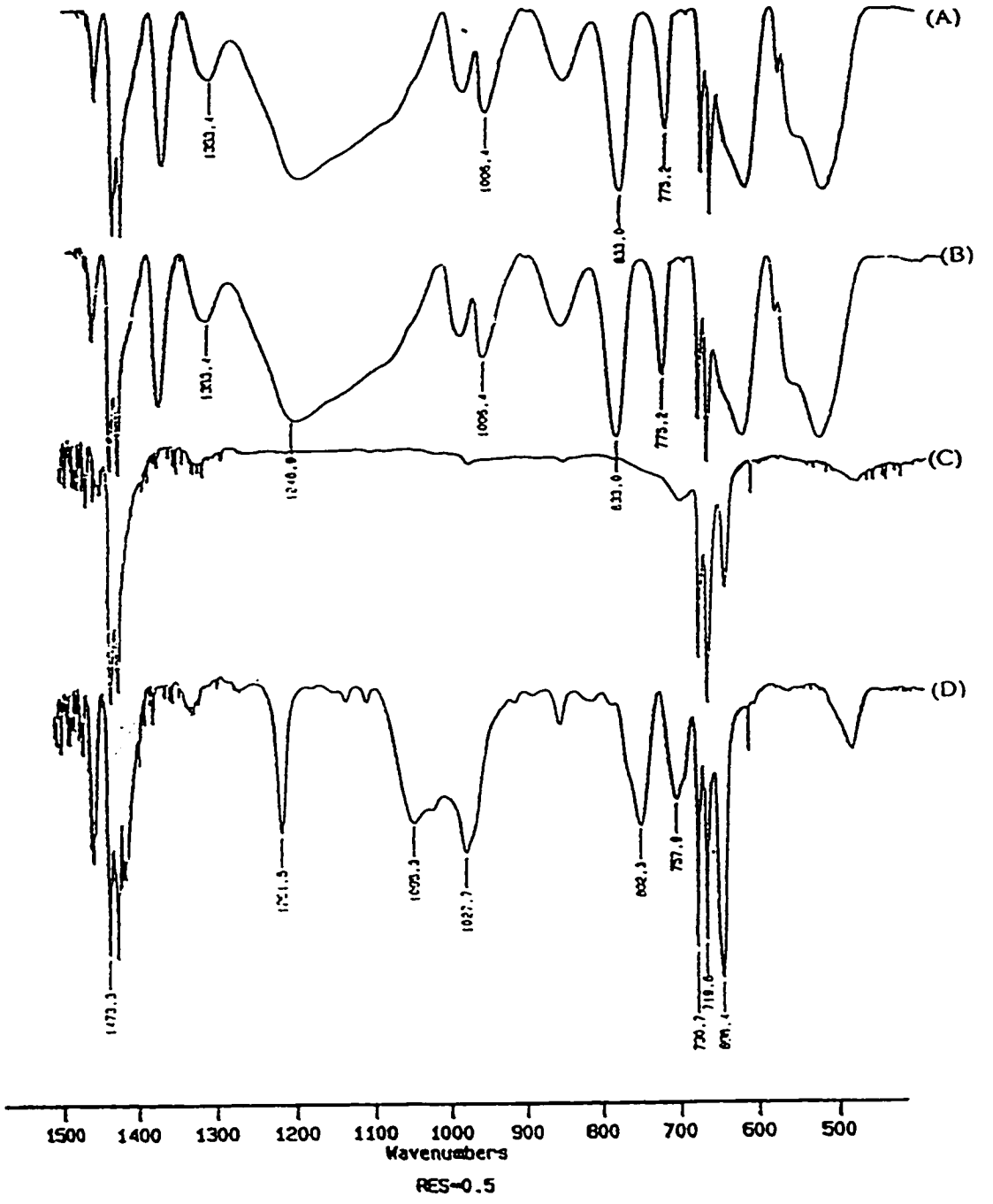

Fig. 2.15. FTIR spectra of (A) membrane #73, (B) membrane #83, (C) the PE substrate membrane, and (D) a poly(styrene-DVB) incorporated membrane.

a control, the PE substrate membrane and a poly(styrene-DVB)-filled membrane were also examined, Fig. 2.15 (C) and (D).

The peak at 698 cm^{-1}, Fig. 2.15(D), verifies that the poly(styrene-DVB)-filled membrane (before sulfonation) is mainly mono-substituted on the aromatic rings. As can be seen from Fig. 2.15(A) and (B), the intensity absorbance of this peak (at 698 cm^{-1}) decreases dramatically due to introduction of sulfonic acid groups. From Fig. 2.15(A) and (B), the intensity of the peak at 333 cm^{-1} (strong) compared to that at 775 cm^{-1} suggests that the substitution on the benzene ring is mainly in the *para* position [79]. The wide absorption between 1300 and 1080 cm^{-1} is due to absorption of $-SO_3^-Na^+$ [97]. The peaks at 1353 and 1006 cm^{-1}, Fig. 2.15(A) and (B), likely can be attributed to the diaryl sulfone absorptions [79,104,105]. These bands are due to the symmetric and anti-symmetric vibrations of a diaryl sulfone (the "sulfone bridge"), respectively. This suggests that sulfones are formed in membranes #73 (0°C sulfonation) and #83 (40°C sulfonation). For these two membranes, the relative intensity absorbances at 1353 and 1006 cm^{-1} are similar indicating that the amount of sulfone formed is similar at 0°C and 40°C.

Byun et al. [79], found that the "sulfone bridges" were formed in the sulfonation of poly(styrene-DVB) asymmetric membranes using concentrated sulfuric acid as the sulfonating reagent at 30°C. The amount of sulfone increased with increasing sulfonation time. Theodoropoulos et al. [106], crosslinked polystyrene *via* sulfone using chlorosulfonic acid as the sulfonating reagent at 50°C for 3 h. Indeed, chlorosulfonic acid was found to be the best reagent to form sulfone crosslinks. However, the degree of sulfone was not reported in that work. Pozniak and Trochimczuk [91] found that the

maximum sulfonation yield of poly(styrene-DVB) (23°C, 6 h) using chlorosulfonic acid was 82%, which is slightly lower than the maximum sulfonation yield (84%) in this work (chlorosulfonation, 40°C, 4 h).

The mechanism of sulfone formation is outlined in Fig. 2.16. Sulfonyl chloride (12) can lose a chloride ion to produce (11). This cation (11) can be attacked by an aromatic ring to form (14) *via* an electrophilic substitution mechanism. Finally, a "sulfone bridge" (15) is formed when (14) loses a proton.

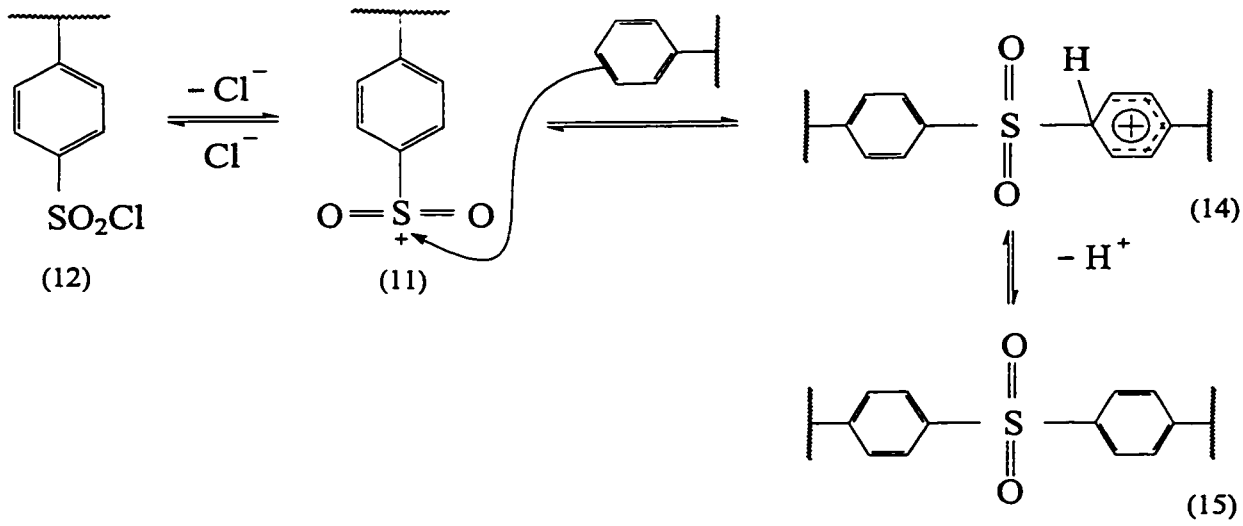

Fig. 2.16. Mechanism of sulfone formation.

In the literature, a number of papers confirmed the formation of "sulfone bridges" (product 15), but none of the papers examined the temperature effect on the degree of sulfone formation in the reaction of chlorosulfonation of polystyrene. In order to measure the degree of sulfone and find out the temperature effect on formation of sulfones, elemental analyses for sulfur (S), hydrogen (H) and carbon (C), of the membranes were

carried out. The total amount of S will include the sulfonate S and the sulfone S. The total amount of S is given by the elemental analysis and the amount of the sulfonate S can be calculated from the IEC. Thus, the degree of sulfone can be calculated.

A pore-filled membrane containing 135% of poly(styrene-DVB) with 1.0% of crosslinking, was cut into two rectangular pieces of the same size. One was sulfonated at 0°C for 4 h and the other at 40°C for 4 h. These membranes were cut in half and the elemental analyses carried out. The results of elemental analyses are given in Table 2.3. The mass increase and IEC were measured in separate experiments. Sodium (Na) and oxygen (O) contents were calculated based on IEC's of the membranes.

The results for the same membranes, ie., # 116 and #118 (40°C), #117 and #119 (0°C), were found to be identical. This means that the elemental analyses are reproducible. It was also found that the sum of all the elements was approximately 100%. The number of S atoms per ring was found to be greater than 1.0 in all the cases. This means that, on average, each aromatic ring has more than one sulfur. This result is consistent with the findings of Pepper et al. [77] with sulfonation of poly(styrene-DVB) resins where sulfonation yields of more than 100% were achieved using concentrated sulfuric acid.

It can be seen from the data shown in Table 2.3 that the difference of sulfone formation between 0°C and 40°C sulfonations was found to be small, ie., approximately ± 10%. This result is consistent with the FTIR results. The results indicate that the temperature effect on sulfone formation is small.

Table 2.3. Elemental analyses of sulfur, carbon and hydrogen.

Membrane Number	116	118	117	119
Mass increase (%)	135	135	135	135
DVB (%)	1.0	1.0	1.0	1.0
Sulfonation temperature (°C)	40	40	0	0
IEC (meq/g)	4.64	4.64	3.59	3.59
Sulfonation yield (%)	83.5	83.5	64.6	64.6
Elemental analysis (%, mol/mol)				
Carbon (C)	25.28	25.41	27.57	27.78
Hydrogen (H)	51.98	52.96	53.51	51.33
Sulfur (S)	2.35	2.39	2.27	2.35
Oxygen (O) [a]	*16.56*	*17.44*	*16.08*	*15.18*
Sodium (Na) [a]	*1.57*	*1.57*	*1.32*	*1.33*
Total:	98.04	99.76	100.75	97.97
Results of calculations				
Number of S atoms per ring	1.25	1.27	1.11	1.14
Yield of sulfonates [a] *(%)*	*83.5*	*83.5*	*64.6*	*64.6*
Yield of sulfones [a,b] (%)	42.0	43.3	46.3	49.2

a. Numbers in italic were calculated based on IEC.
b. Yield of sulfone was the difference between total sulfur and sulfonate sulfur.

However, the amount of sulfone present seems to be surprisingly high (approximately 45%). The calculations are based on the values of the IEC's and the results of the elemental analyses. Since membranes #116 and #118 are the same and membranes #117 and #119 are the same. Thus, the error of elemental analyses (Table 2.3) can be estimated to be less than 3.5%, eg., for sulfur (S). Therefore, the major error source of the yield of sulfone is likely due to the measurement of the total sulfonic acid content. It should be noted that polyethylene can be sulfonated but the sulfonation yield is low [107]. However, even the poly(ethylene-sulfonic acid) produced can also be titrated. It can be speculated that the measured IEC may not reflect the amount of the sulfonic acid groups. In other words, the key question is what fraction of ion-exchangeable groups can be measured by titration. Since the oxygen (O) content is calculated based on the measured IEC, a small error in IEC may lead to a big error in amount of sulfone. For example, if 10% of sulfonic acid formed cannot be measured, the yield of sulfone would be reduced to approximately 15%. At McMaster University, for the PVP-filled membranes, The McMaster Membrane Research Group [16] has found that, for PVP salt filled membranes, approximately 80% of the incorporated PVP salts was ion-exchangeable. This means that 20% of the PVP does not contribute to the measured IEC.

2.4. SUMMARY

This chapter has demonstrated the preparation of the pore-filled cation-exchange membranes by copolymerization of styrene and DVB within the pores of a PE substrate membrane followed by the sulfonation of the incorporated poly(styrene-DVB).

Styrene-DVB copolymers were incorporated into the substrate membrane using a thermally-induced polymerization method followed by extraction of non-anchored polymers. The incorporated poly(styrene-DVB) was evenly distributed across the substrate membrane. The morphology of the resulting membranes was examined using scanning electron microscope. The micro-structure of the substrate did not appear to change significantly as a result of this polymerization. The SEMs showed that the resulting cation-exchange membranes were porous.

The ion-exchange capacities of the resulting membranes measured by ion chromatography and titration methods gave identical results. The IEC increases as the mass increases. Sulfonation at 40°C led to higher sulfonation yields than at 0°C. The sulfonation yields for 40°C sulfonations appeared to approach a maximum value, approximately 85% of theoretical sulfonation yield. The results of elemental analyses suggested that each aromatic ring had more than one sulfur. The formation of sulfones in the chlorosulfonation reactions was observed by FTIR, indicating that sulfone formation gave an additional degree of crosslinking in the poly(styrene-DVB).

CHAPTER THREE

MEMBRANE CHARACTERIZATION

Ion-exchange membranes have been used in various applications, such as electrodialysis, diffusion dialysis, membrane electrolysis and membrane fuel cells. In order to understand the separation behavior of the membranes made in this work, it is necessary to fully characterize them. This chapter consists of two major sections which describe: (1) the swelling properties of the membranes, including thickness, water content, and factors affecting membrane dimension and charge density, and (2) the electrical and transport properties of the membranes, including membrane electrical resistance and transport numbers.

3.1. EXPERIMENTAL

3.1.1. Materials

The membranes used in this chapter were the poly(styrene-DVB sulfonic acid) pore-filled cation-exchange membranes described in Chapter 2. Inorganic reagents, NaCl, NaOH, Na_2SO_4, and $MgCl_2$ were all AR grades (Aldrich). Chloroform (Aldrich)

and deionized using the Barnstead/Thermolyne system (D 8904 and D 8901). The conductivity of the deionized water was approximately 2.0 μs/cm.

3.1.2. Swelling properties

3.1.2.1. Membrane Dimensions

The length and width of each membrane were measured using a scaled ruler with accuracy of 0.05 cm. The thicknesses of all wet membranes were measured using a calibrated pyconometer, according to the method described by Mika et al. [16].

The membrane to be measured was cut into a rectangular piece (5 cm × 5 cm) and soaked in deionized water at room temperature for 16 h. The membrane was placed between two pieces of wet filter paper, gently pressed to remove surface water and weighed. The membrane was transferred into the pyconometer whose mass and volume were known. A pyconometer, Fig. 3.1, containing the membrane was filled with distilled water, stoppered and placed in a thermostatted water bath (25.0 ± 0.1°C) for 30 min to allow the temperature to equilibrate. The pyconometer was removed from the water bath, dried and weighed. The thickness of membrane, d_m, was calculated using the following equation:

$$\text{Membrane thickness } (d_m, \text{cm}) = \frac{V_{pyc} - (m_{total} - m_{pyc} - m_{wet}) / 0.9970}{A_m} \qquad (3.1)$$

where A_m is the membrane area (approximately 25 cm^2), V_{pyc} is and calibrated volume of the pyconometer, and m_{pyc}, m_{wet}, and m_{total} are the masses of the pyconometer containing

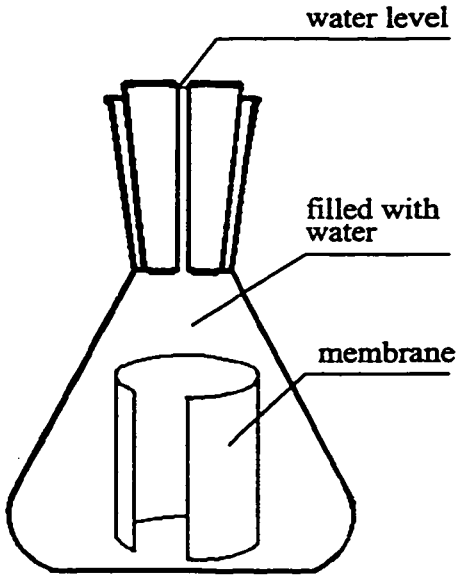

Fig. 3.1. Pyconometer used to measure membrane thickness.

distilled water, wet membrane, and pyconometer with distilled water and membrane, respectively. The constant 0.9970 (g/cm^2) is the density of pure water at 25.0°C [108].

The thickness of the dry membranes was measured using a digital micrometer (Mitutoyo, Model MDC-1P) with an accuracy of ± 1 μm. The membrane thickness was taken as the average of value from at least five measurements at various points on the membrane.

3.1.2.2. Water Content

The experimental procedure for measuring the water content of the membranes has been described by Mika et al. [16]. A wet membrane (Na^+-salt form) was placed

between two pieces of wet filter paper, gently pressed to remove surface water weighed. Then, this membrane was vacuum dried at room temperature until no further change in mass of the membrane (approximately 72 h). The membrane was weighed. The water content of the membrane was calculated using the following equation:

$$\text{Water content (\%)} = \frac{m_{wet} - m_{dry}}{m_{wet}} \times 100\% \qquad \textbf{(3. 2)}$$

where m_{wet} and m_{dry} are the masses of the wet and vacuum-dried membranes, respectively.

3.1.2.3. Ion-Exchange Concentration

The procedure of measuring and calculating ion-exchange concentration has been described by Stachera et al. [54]. The ion-exchange concentration (the fixed charge concentration) is the concentration of ion-exchange sites in the water of the membrane and can be expressed in unit of equivalents of ion-exchange sites per kilogram of water in the membrane. Ion-exchange concentration depends on the ion-exchange capacity (determined in Chapter 2) and the water content (measured above) of the membrane. Thus, the ion-exchange concentration was calculated using the following equation:

$$\text{Ion exchange concentration (eq / kg)} = \frac{\text{IEC}}{\text{Water content}} \qquad \textbf{(3. 3)}$$

where IEC was the ion-exchange capacity of the membrane.

3.1.3. Transport Number and Electrical Characterization

3.1.3.1. Transport Numbers

Membrane transport numbers were measured according to the method described by Kontturi et al. [119], using the apparatus shown in Fig. 3.2. The apparatus contained two cylinders, a stationary cylinder and a rotating cell. An ion-exchange membrane was tightly mounted at the bottom of the rotating cell cylinder. The exposed area of the membrane was 3.14 cm^2. The volume of the chamber between the rotating cell and the stationary cylinder is 30.0 mL (at the level of dotted line). Two Ag/AgCl electrodes were separated by the membrane and placed close to the membrane surfaces.

The membrane to be tested was equilibrated in a 1.00 M NaCl solution at 25°C for at least 8 h. The temperature of the thermostatted water bath was maintained at 25.0 ± 0.1°C. Thirty (30.00) mL of a 1.00 M NaCl solution was added to the chamber from the top of the stationary cylinder using a syringe with 6-inch needle. Approximately 300 mL of a standard NaCl solution (0.50 M) was added to the thermostatted container (outside the rotating cell). The level of the solutions in the chamber and in the thermostatted container were adjusted to be equal so as to eliminate a pressure difference. The cell potential, *E*, of the rotating cell was measured by a pH/microvoltmeter (Orion Model 720A) with an accuracy of ± 0.1 mV while the spinning cell is spinning. A magnetic stir bar in the thermostatted container was used to remove air bubbles beneath the rotating cell cylinder and stopped during the measurement. The cell potential was measured as a function of the rotation rate of the rotating cell, from 600 to 150 rpm in steps of 50 rpm.

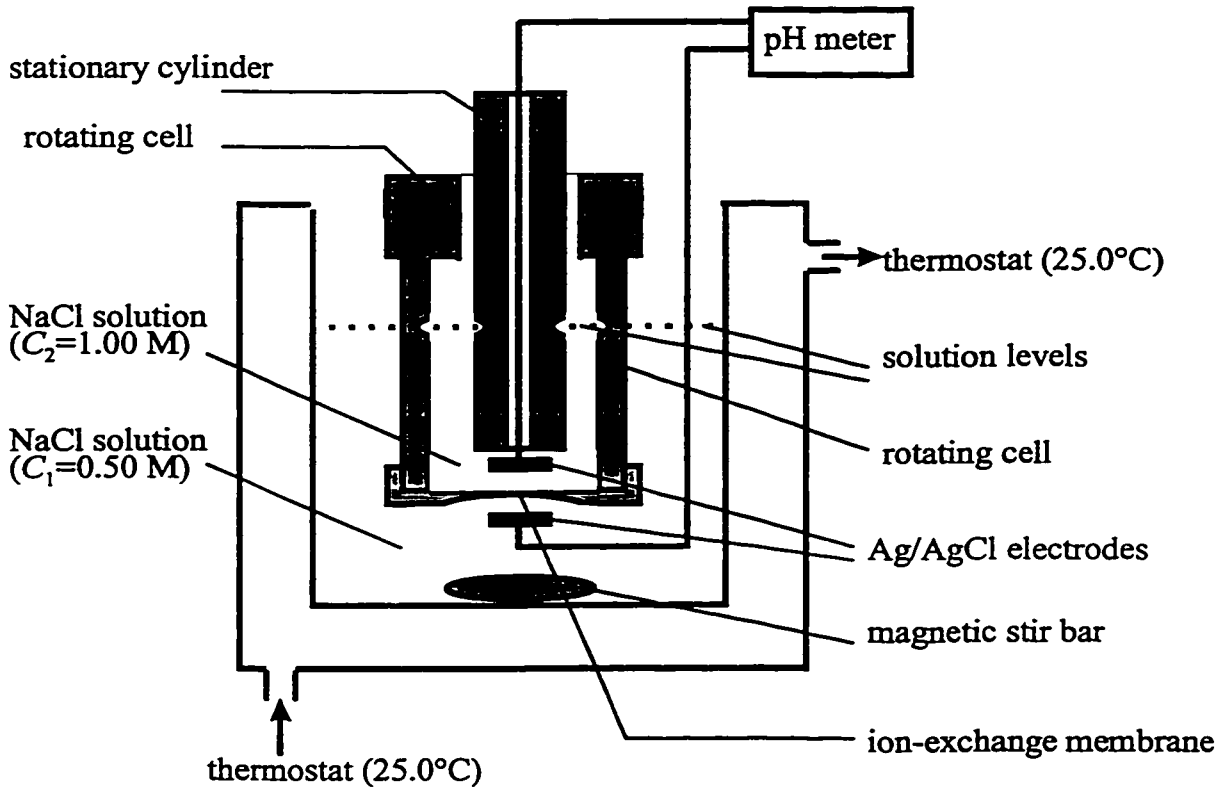

Fig. 3.2. Rotating cell used to measure membrane transport numbers [119].

The value of membrane potential, E_{mem} was calculated using a spreadsheet (Microsoft Excel, as shown in Appendix A). The membrane transport number of the sodium ion, $t^{M}_{+(Na)}$, was calculated using the following equation:

$$E_{mem} = \frac{2\, t^{M}_{+(Na)}\, RT}{F} \ln\left(\frac{C_2}{C_1}\right) \qquad (3.4)$$

where C_1 and C_2 were the concentrations of the NaCl solutions inside and outside the rotating cell, and R, T and F are the gas constant, absolute temperature and Faraday constant, respectively.

3.1.3.2. Electrical Resistance

There are several membrane resistance units that have been used in the literature. In this work, the electrical resistance membrane refers to "the area resistance of the membrane" (ohm·cm^2) which was determined according to the method described by Strathmann and co-workers [110]. The electrical resistance of a membrane was the difference between the resistance values measured with membrane and without the membrane [110-114]. In this work, the membrane electrical conductance was measured at 1000 Hz using a conductivity cell (Fig. 3.3) that consisted of two compartments of

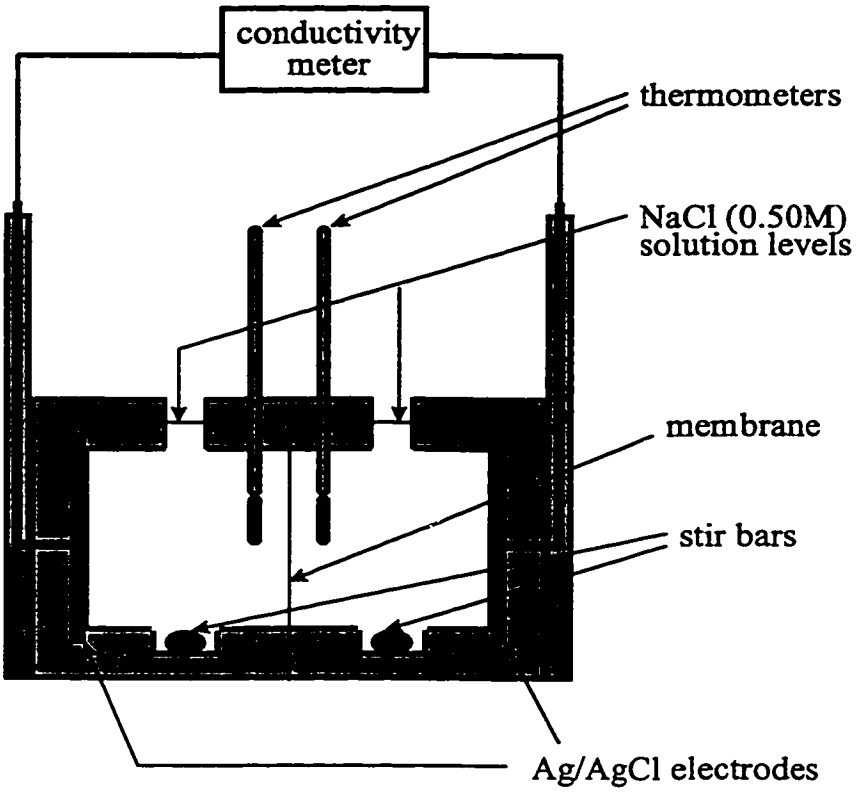

Fig. 3.3. Conductivity cell used to measure membrane electrical resistance.

equal volume (15.62 cm^3) separated by a membrane. The temperature of the thermostatted water bath was maintained at 25.0 ± 0.1 °C. The membrane was equilibrated with a standard solution (0.50 M, NaCl) at 25°C for at least 8 h prior to the measurements. The NaCl solution used was temperature equilibrated at 25°C for 1 h before the measurement of electrical resistance.

Fifteen (15.00) mL of a 0.50 M NaCl solution was added to the two compartments of the conductivity cell simultaneously and the system was allowed to equilibrate at 25°C for 30 min. Both chambers were stirred at identical rates of 25 revolutions per second in order to minimize concentration polarization effects. The conductivity was determined using a conductivity meter (YSI, Model 31). The membrane electrical resistance was calculated from the area and the conductance of the membrane according to the following formula [110]:

$$R_m = A_m \left(\frac{1}{\kappa^{0+m}} - \frac{1}{\kappa^{0}} \right) \qquad (3.5)$$

where R_m, A_m and κ were the (area) electrical resistance (ohm·cm^2), effective area (cm^2) of the membrane and the electrical conductances, respectively. The terms (κ) with superscripts 0+m and 0 referred to the electrical resistances with membrane and without membrane, respectively. The effective membrane area was 6.25 cm^2.

3.2. RESULTS AND DISCUSSION

3.2.1. Substrate Membrane Control

In order to examine the factors affecting membrane dimensions (length, width and thickness), it was necessary as a control experiment to investigate the effects of the membrane preparation processes on the substrate membrane, including thermal treatment (80°C) and treatments with organic solvents (chloroform or 1,2-dichloroethane). The control of the PE substrate membrane is important since any change in dimension of the substrate membrane will significantly affect the properties of the resulting membranes.

It should be noted that membrane lengths and widths used in this thesis are defined as shown in Fig. 3.4. The PE substrate microfiltration membrane was supplied by 3M Canada Company as a rolled flat sheet of 45.7 m (*150 feet*) × 25.4 cm (*10 inches*), Fig. 3.4. Small pieces, 10.5 cm (along the rolling direction) × 12.7 cm (roll width) were cut. As can be seen, the length and width of the membranes is different from those of the membrane roll.

As a control, the PE substrate membrane was treated under the identical experimental conditions but without styrene/DVB mixtures. These treatments included the thermal treatment (at 80°C) and the solvent extractions (Soxhlet and at room temperature). The thermal treatment tests were carried out by heating the PE substrate membrane at 80°C for 1 min in the reaction vessel (Fig. 2.1). The solvent extraction tests were carried out by either soaking the membrane in chloroform (or acetone) at room temperature or Soxhlet extracting for 30 min. The measurements were

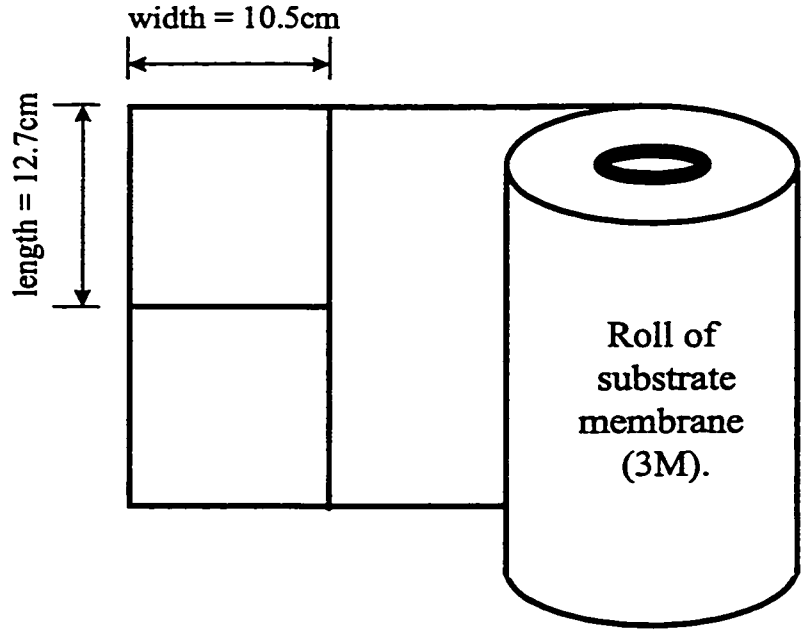

Fig. 3.4. Roll of substrate polyethylene membrane (3M).

repeated at least three times. The error was ± 0.1 cm (less than 1%)* in length and width measurements and ± 1 μm (2%)** in thickness measurement. The porosity of the substrate membrane before treatment was 78%***. The membrane porosity after treatment was calculated based on the changes in length, width and thickness of the membrane resulting from the treatments.

---

* The length was 12.7 cm and the width was 10.5 cm. The error was ± 0.5 cm.

** The thickness was 45 μm (3M) and 43 μm (this work). The error of thickness measurement was 1 μm.

*** The porosity was 78% (3M) and 76% (this work). The porosity of the membrane was calculated by $\text{Porosity (\%)} = \left(1 - \frac{\text{mass of membrane}}{\text{length} \times \text{width} \times \text{thickness} \times \text{PE density}}\right) \times 100\%$, where the density of linear, high density PE is between 0.92 and 0.96 g/cm^3. An average value (0.94 g/cm^3) was used in the calculations.

The results of thermal treatment and solvent extractions are given in Table 3.1. It was found that extraction with acetone at room temperature did not change membrane dimensions dramatically, ie., a decrease of less than 5%. However, chloroform extractions or a 1-minute thermal treatment (80°C) led to substantial decreases in membrane length and width. Our value of the porosity of an untreated membrane (76%, in brackets) was identical to the 3M value (78%). However, after thermal treatment, the porosity (60%) was found to be the same as the calculated porosity (61%) based on the original 3M porosity value and taking into account the dimension changes.

It can be seen from Table 3.1 that the thermal treatment (1 min at 80°C) and Soxhlet extraction (30 min with chloroform) had identical effects on membrane dimensions leading to porosity decreases from 78% to 61%. Room temperature extractions with acetone or chloroform had similar but smaller effects than the thermal treatment or the Soxhlet extraction. The membrane porosities following these extractions were approximately 71% (with acetone) and 68% (with chloroform).

These reductions in macroscopic dimensions mean a reduction in average pore size. The pore contraction should be considered in the characterization and evaluation of the cation-exchange membranes. For example, if the pores of the substrate membrane were to be fully filled with polystyrene, then the maximum mass that could be incorporated would be approximately 350%, based on a porosity of 78%. In the case of heat-treated membrane with a porosity of 61%, the maximum mass loading could only be approximately 155%. As discussed in Chapter 1, a decrease in porosity of the substrate

Table 3.1. Changes in dimensions and porosity of the substrate PE membrane[a].

Treatment				Before				After			
Process	Solvent	T (°C)	Time (min)	Length (cm)	Width (cm)	Thickness (μm)	Porosity (%)	Length (cm)	Width (cm)	Thickness (μm)	porosity (%)
Solvent extraction	Acetone	RT[b]	30	12.7	10.5	43	78	12.0	10.0	43	71
	$CHCl_3$	RT[b]	30	12.7	10.5	43	78	12.0	9.5	44	68
	$CHCl_3$	SE[c]	30	12.7	10.5	43	78	10.9	9.3	44	61
Thermal treatment		80	1	12.7	10.5	43	78 (76)[d]	10.8	9.4	44	61 (60)[d]

a. Each measurement was repeated at least 3 times. The error was less than 1% in length and width measurements and 2% in thickness measurement. The porosity of the substrate membrane before treatments was 78%. The porosity after treatment was calculated based on the changes in length, width and thickness assuming the polyethylene density (d = 0.94) and mass were not changed significantly.

b. RT stands for room temperature.

c. SE stands for Soxhlet extraction.

d. Numbers in brackets were single measurements.

membrane will increase the gel polymer concentration in the pore-filled membrane and thus, the pressure-driven permeability of the resulting membranes is expected to be low.

These changes in dimensions of the PE substrate membrane can be understood in terms of re-organization of the entangled polymer chains [105]. The substrate membrane was produced by thermally induced phase separation (TIPS) [106], followed by a bi-axial stretching of the film. As a result, internal forces are built during these membrane fabrication processes [106]. The temperature for the 1-min thermal treatment was 80°C, which is higher than the T_g but lower than the T_m for linear, high density polyethylene (PE) [107]. It would appear that at this temperature the PE chain movement can occur in order to relieve at least partially the internal forces of entangled polymer chains.

The effect of the organic solvents on membrane dimension changes is likely swelling of the polymer. Swelling of PE in the presence of an organic solvent will also allow the chain movement (chain re-organization). From Table 3.1, the dimensional changes of the substrate membrane are larger at higher temperatures. Thus, the Soxhlet extraction had a greater effect than the room temperature extraction.

3.2.2. Dimension Changes in Cation-Exchange Membranes

3.2.2.1. Factors Affecting Membrane Dimensions

The polyelectrolyte-filled ion-exchange membranes discussed in this work are hydrophilic materials which may swell in aqueous solutions. Thus, changes in dimensions of the ion-exchange membranes can also occur when the membranes absorb water. This

section reports measurements of the swelling of the polyelectrolyte-filled membranes and the resulting effects on water content and ion-exchange concentration.

Thicknesses of the wet cation-exchange membranes prepared in Chapter 2 were determined using a calibrated pyconometer. The major source of error in the thickness measurement appears to come from water on the membrane surfaces. The membrane thicknesses were based on the measured volumes of the membranes coupled with length and width measurements obtained in separate experiments. The total volume of the membrane can be obtained by multiplying length by width and by thickness. Although the errors in thickness measurements are quite large, within ± 10%*; the advantage of the pyconometer approach measurement is that it gives the average value of the thickness of a water swollen membrane. The data obtained in these measurements are given in Table 3.2.

As a control experiment, a substrate membrane was heated with a initiator and styrene but no DVB, in the same manner as used in the *in situ* polymerization used with the rest of membranes; no polystyrene was incorporated into the substrate membrane in the absence of DVB (Table 3.2, membrane #7). However, this treatment did lead to a contraction of the membrane dimensions.

This membrane (#7) was also subjected to the sulfonation conditions (15% chlorosulfonic acid in 1,2-dichloroethane, V/V, at 0°C) used to make cation-exchange

---

* The error in thickness was between 1 and 2% for dry membranes using micrometer and less than 10 % for wet membranes using pycnometer.

Table 3.2. Changes in length, width and thickness of the membranes in copolymerization and sulfonation.

Membrane #	Starting membrane[a]		Pore-filled membranes[b] (after copolymerization)					Ion-exchange membranes[c] (After sulfonation)					
	Length (cm)	Width (cm)	DVB (%)	Mass increase (%)	Length (cm)	Width (cm)	Thick-ness (μm)	Sulf. temp. (°C)	IEC (meq/g)	Length (cm)	Width (cm)	Thick-ness (μm)	Total Volume (cm^3)
Substrate membrane (control experiments)[a]													
Before thermal treatment (#0)	12.7	10.5	0	0									0.58
After styrene treatment (#7)[d]	12.7	10.5	0	0	10.8	9.4	44 ± 1						0.45
After Sulfona-on (#7)	12.7	10.5	0	0	10.7	9.3	45 ± 1	0	<0.1	10.7	9.5	45	0.46
Pore-Filled Cation-Exchange Membranes													
#69	12.7	10.5	1.0	64				0	2.25			65	
#75	12.7	10.5	1.0	80				0	2.12			65	
#117	12.7	10.5	1.0	135				0	3.59			78	
#70	12.5	10.5	1.0	150				0	3.49			85	
#34	12.7	10.5	2.5	33	10.5	8.6	33 ± 2	0	1.25	11.3	9.6	65	0.71
#15	12.7	10.5	2.5	65	10.5	8.8	-	0	1.86	13.8	11.6		

Table 3.2. Changes in length, width and thickness of the membranes in copolymerization and sulfonation. (Continued)

Membrane #	Starting membrane[a]		Pore-filled membranes[b] (after copolymerization)					Ion-exchange membranes[c] (After sulfonation)					
	Length (cm)	Width (cm)	DVB (%)	Mass increase (%)	Length (cm)	Width (cm)	Thick-ness (μm)	Sulf. temp. (°C)	IEC (meq/g)	Length (cm)	Width (cm)	Thick-ness (μm)	Total Volume (cm^3)
#47	12.7	10.5	2.5	65				0	1.95			63	
#73	12.7	10.5	2.5	78				0	2.05			63	
#67	12.7	10.5	2.5	83	10.5	8.7	35 ± 2	0	2.23	13.7	12.3	67	1.13
#68	12.7	10.5	2.5	80				0	1.92				
#91	12.7	10.5	2.5	128				0	2.53			76	
#43	12.7	10.5	2.5	143	11.0	8.5	38 ± 2	0	2.65	14.0	12.5		
#24	12.7	10.5	2.5	150				0	3.01	13.9	12.6	83	1.45
#65	12.7	10.5	2.5	180	10.2	8.5	37 ± 2	0	3.23	15.3	12.8	86	1.68
#74	12.7	10.5	2.5	192	10.1	8.2		0	3.55			86	
#64	12.7	10.5	2.5	256	12.2	9.8		0	3.85	17.3	14.5	89	2.23
#57	12.7	10.5	2.5	295				0	4.16			88	
#48	12.7	10.5	2.5	338	12.8	10.2	40 ± 2	0	4.35	18.5	14.7		
#118	12.7	10.5	1.0	135				40	4.64			81	

Table 3.2. Changes in length, width and thickness of the membranes in copolymerization and sulfonation. (Continued)

Membrane #	Starting membrane[a]		Pore-filled membranes[b] (after copolymerization)					Ion-exchange membranes[c] (After sulfonation)					
	Length (cm)	Width (cm)	DVB (%)	Mass increase (%)	Length (cm)	Width (cm)	Thick-ness (μm)	Sulf. temp. (°C)	IEC (meq/g)	Length (cm)	Width (cm)	Thick-ness (μm)	Total Volume (cm^3)
#92	12.7	10.5	2.5	72				40	3.28			72	
#101	12.7	10.5	1.0	115				40	4.05				
#135	12.7	10.5	2.5	117				40	4.01				
#95	12.7	10.5	2.5	142				40	4.50			82	
#97	12.7	10.5	1.0	190				40	5.23			83	

a. PE substrate membrane (before the thermal treatment): thickness = 45 μm, porosity = 78%, average pore diameter = 0.19 μm. The data were provided by the membrane supplier (3M).

b. Copolymerization carried out at 80°C, with 1.0% of benzoyl peroxide and various divinylbenzene; the dimensions of these membranes were measured when the membranes were vacuum dried.

c. Sulf. temp. stands for sulfonation temperature; sulfonation carried out in 15% (V/V) 1,2-dichloroethane at 0°C for 4 hours; the thicknesses of the sulfonated membranes were measured by a pycnometer; IEC stands for ion-exchange capacity; the error in thickness is less than 10%.

d. Styrene treatment refers to the thermal treatment with styrene but no divinylbenzene (no initiator) under the same conditions used in polymerization for the rest of membranes.

membranes. The resulting membrane had an ion-exchange capacity of less than 0.1 meq/g. After the treatment, the membrane was found to have a thickness of 46 μm, which was identical to the substrate membrane (45 μm) after the thermal treatment. These control experiments indicate that contraction of the PE substrate membrane occurs as a result of thermal treatments.

Incorporation of poly(styrene-DVB) leads to a further contraction in membrane dimensions. The data in Table 3.2 show that the length, width and thickness all decreased with increasing the incorporated poly(styrene-DVB). For example, membrane #67 decreased in length (from 12.7 to 10.5 cm), width (from 10.5 to 8.7 cm) and thickness (from 43 to 35 μm). The dimensional decreases in the poly(styrene-DVB)-filled membranes were somewhat larger than those seen with the control experiments (#7). The reduction in membrane dimension appears to depend on the mass loading of the incorporated poly(styrene-DVB). For example, membrane #34 with the lowest mass increase (33%) had the largest changes in dimensions while #48 with a 10-fold larger mass increase (338%) showed almost no change in its dimensions. These changes in dimensions (mostly contractions) are due to two possible reasons. One reason is because of the thermal shrinkage of the substrate membrane as discussed above. Another possible reason is that the incorporated poly(styrene-DVB) shrinks as unreacted monomer is removed.

The membranes containing poly(styrene-sulfonic acid) swell in water and increase their dimensions dramatically. For example, membrane #67 with a water content of 67%

increases its length (from 10.5 to 13.7 cm), width (from 8.7 to 12.3 cm), and thickness (from 35 to 67 μm). In fact, the thickness of membrane #67 almost doubles after sulfonation. The effect of sulfonation on the length and width is much smaller than on thickness of the membrane. Other membranes followed similar patterns.

3.2.2.2. Thickness Break Point

The McMaster Membrane Research Group has investigated the factors which affect the thickness of pore-filled ion-exchange membranes extensively [16,37,44,47,48]. In order to examine the effect of mass increase on thickness, a series of membranes with increasing mass gains and an identical degree of crosslinking (DVB = 2.5%) were prepared and their thicknesses were determined. The relationship between membrane thickness and mass increase is shown in Fig. 3.5. Membrane thicknesses increased uniformly up to mass increase of approximately 150%. However, membranes with mass increase greater than 150% showed no significant increase in membrane thickness. These two trend lines intersect at a mass increase of approximately 150%. The intersection point is defined as the thickness break point, Fig. 5.3.

The porosity of the substrate membrane after thermal treatment is approximately 61% (Table 3.1) suggesting that a mass increase of about 150% could be expected if the space in the pores were filled. Any additional incorporated poly(styrene-DVB) would have to be different from the incorporation before the thickness break point with all the pore space filled by the styrene-DVB copolymers, the incorporation could continue by

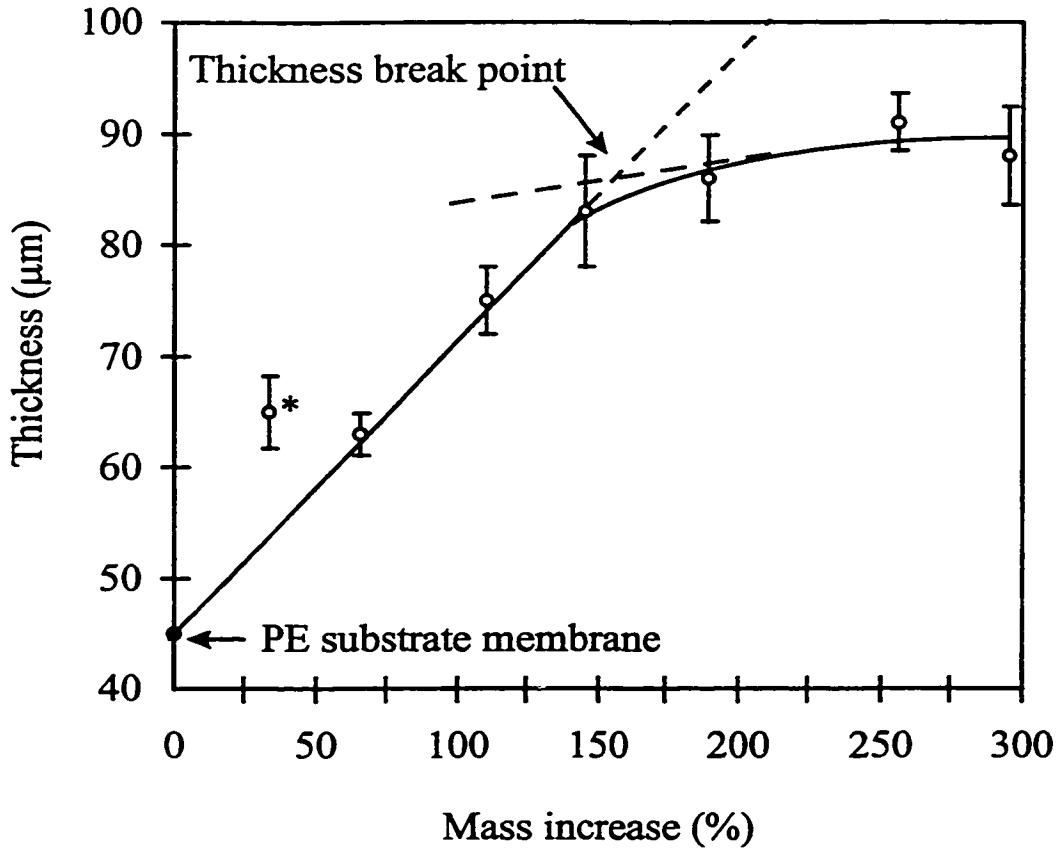

Fig. 3.5. Thickness of cation-exchange membranes as a function of mass increase of poly(styrene-DVB); • PE substrate membrane after the thermal treatment, and ◦ cation-exchange membranes.

polymerizing styrene/DVB which swells and diffuses into the incorporated copolymers. Such differences should dramatically change the dimensions of the resulting membranes at the thickness break point (~ 150% of mass increase).

3.2.2.3. Thickness Control for Pore-Filled Membranes

The increase in thickness versus mass increase (ie., up to the thickness break point) is consistent with the findings of Mika et al. [16,52] with the poly(4-vinylpyridinium salt) (PVP salt)-filled membranes prepared by *in situ* polymerization, but is inconsistent with the findings reported by Pandey et al. [44] with poly(vinylbenzyl ammonium salt)-filled membranes prepared by *in situ* crosslinking (for details see Section 1.3 in Chapter 1).

Typically, it was found by Mika et al. [16] that, for pore-filled membranes produced by *in situ* polymerization, the thickness was proportional to the mass gain, and that the thickness depended on ionization and nature of counter-ions. Same observations were obtained for different pore size and the starting substrate membranes [47,48]. No thickness break points were found in that work; however, it should be noted that the mass gains were less than 160%. The absence of discontinuity in thickness increase with mass gain in this work of Mika et al. is not surprising.

However, for the pore-filled membranes prepared by *in situ* crosslinking [44,46,50] the membrane thickness did **not** change significantly with an increase in mass gain. Further studies showed that, for membranes made by *in situ* crosslinking, the ionization of the incorporated polyelectrolytes had little effect on membrane dimension with a strong substrate membrane (with low porosity). For example, Pandey et al. [44] found that, for poly(vinylbenzyl ammonium salts)-filled membranes made by *in situ* crosslinkingt, no change in membrane dimension was observed with a strong PP substrate membrane of 60% porosity while with the higher porosity PP substrate membrane (80%

porosity), the thickness of pore-filled membranes started to increase when the mass loading was greater than 150%.

The basis of this difference may be rationalized by arguing the difference between *in situ* polymerization and crosslinking. As discussed in Chapter 1, it is generally assumed that, during *in situ* polymerization, a interpenetrating network could be formed with the membrane material and the incorporated polymer [118]. This would lead to an irreversible increase in the host membrane matrix and result in an increase in membrane thickness with mass gain. However, for the membranes made by *in situ* crosslinking, no interpenetration of the two polymer materials occurred.

Since PE is known to swell in the presence of styrene, interpenetrating network with the PE membrane is formed [118], it is not surprising that during formation of an interpenetration network within the PE substrate membrane that membrane thickness would increase with increasing the mass of the incorporated poly(styrene-DVB).

It is assumed that swelling of polyelectrolytes should lead to an expansion in all three dimensions. The total volume of the membranes as a function of mass increase is compared in Fig. 3.6. It is interesting to observe that in contrast to the changes in thickness there is, as expected, a linear relationship between total volume and mass increase of the incorporated poly(styrene-DVB) over the entire range of mass increase. In this work, it was found that the length and width started to increase when the mass increase is greater than 150%. Thus, the thickness did not increase significantly after 150% of mass increase.

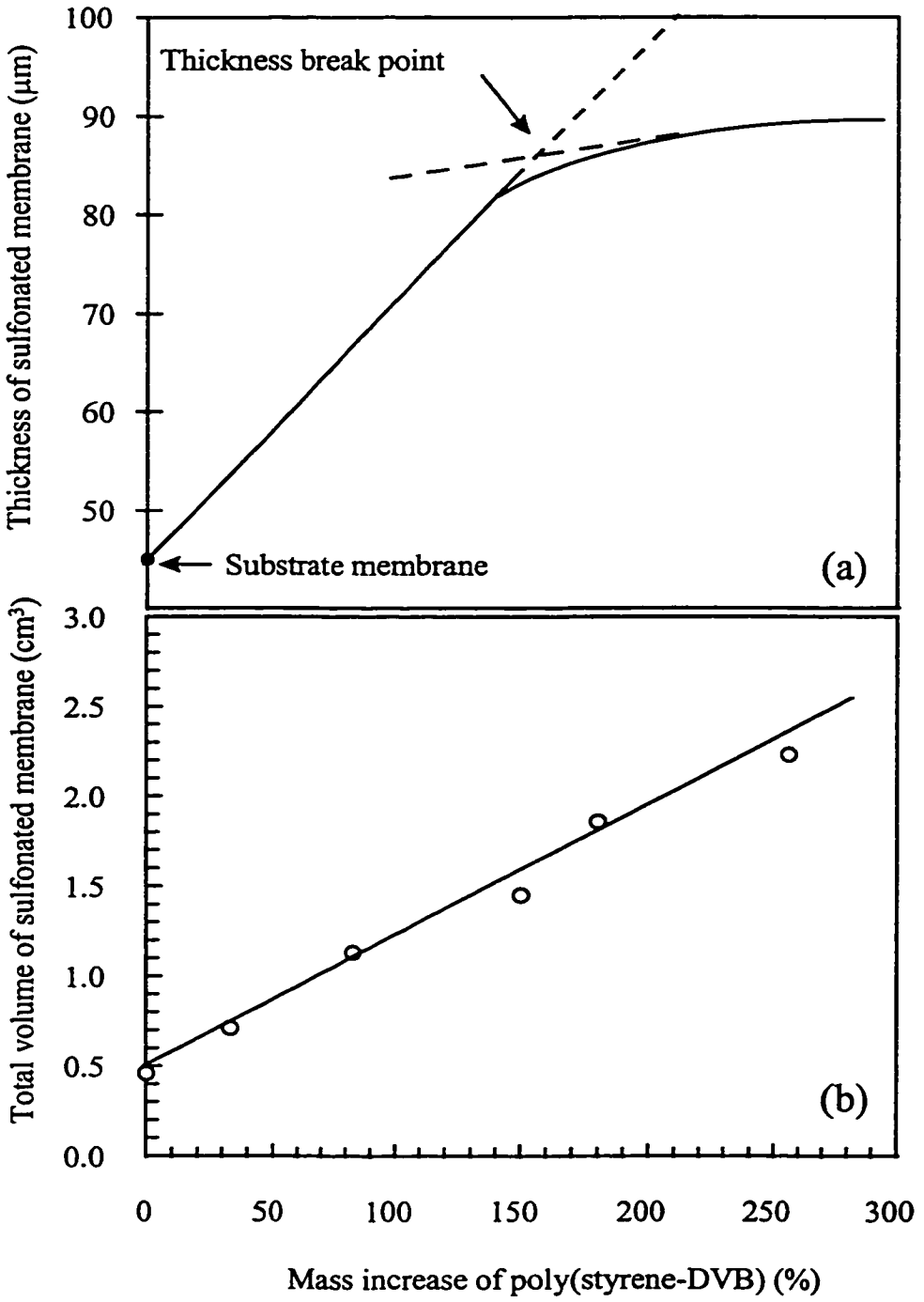

Fig. 3.6. Thickness and total volume as a function of mass increase of incorporated poly(styrene-DVB). (a) Fig. 3.6(a) is a reproduction of the plot of Fig. 3.5, (b) Data are taken from Table 3.2. Sulfonation temperature: 0°C. Size of starting membrane: 12.7 cm × 10.5 cm × 43 μm (length × width × thickness).

3.2.3. Water Content and Ion-Exchange Concentration

3.2.3.1. Water Content

Water contents of the pore-filled cation-exchange membranes were measured with the membranes in the Na^+-form. It was not possible to measure the water contents of the membranes in their H^+-forms as these membranes were difficult to dry completely. Ion-exchange concentration refers to the concentration of ion-exchange sites per kilogram of water in the membrane. The results of these measurements are given in Fig. 3.7 and Table 3.3. The error in water content measurement was estimated to be approximately ± 5%.

The membranes have water contents ranging from 60 to 75% (Fig. 3.7). The porosity of the substrate membrane (after the thermal treatment) was 61%. Since the error of the measurement is larger (approximately ± 5%), the water contents seem to be identical. The water contents of membranes with different degrees of crosslinking and derived from sulfonations at different temperatures are not significantly different at any mass increase and follow the same trend with increasing mass increase. For example, within experimental error, the points marked with • (1.0% of DVB and 0°C sulfonation), were found to be identical to those) marked with ○ (2.5% of DVB, 0°C sulfonation). Similarly, the points (2.5% of DVB and 40°C sulfonation) marked with (△) were the same as the points (2.5% of DVB and 0°C sulfonation) marked with (○). The results indicate that the effects of degree of crosslinking and sulfonation temperature on water content are small. The point marked with * (membrane #34) which is out the range of 60 - 75% is possible due to an experimental error.

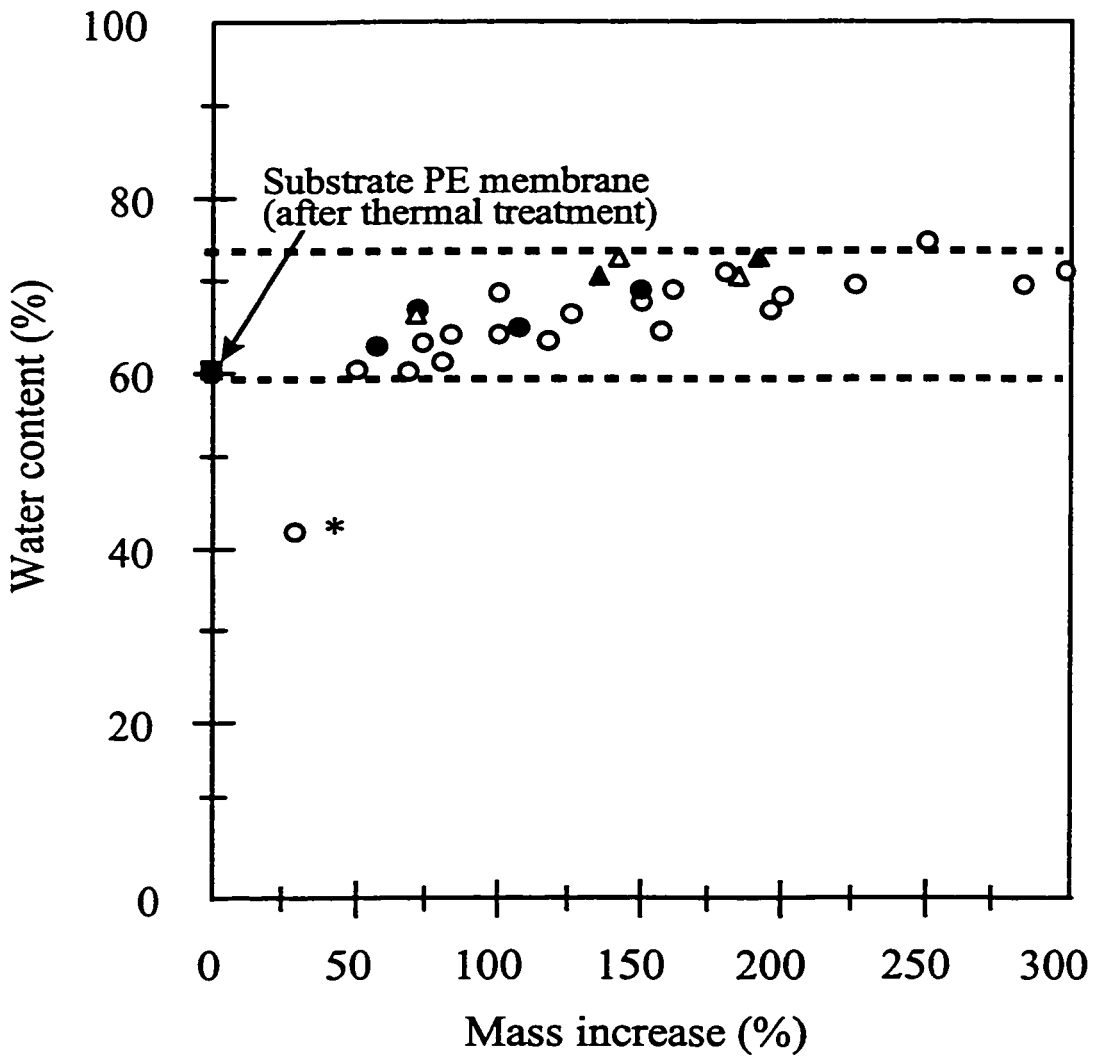

Fig. 3.7. Water content as a function of mass increase; the error of water content is approximately ± 5%.

■ void volume of the substrate polyethylene membrane,

● DVB = 1.0%, 0°C sulfonation, ○ DVB = 2.5%, 0°C sulfonation,

▲DVB = 1.0%, 40°C sulfonation, △ DVB = 2.5%, 40°C sulfonation.

Table 3.3. Water contents and ion-exchange concentrations of the cation-exchange membranes.

Membrane #	Sulfonation temperature (°C)	DVB (%)	Mass increase (%)	IEC[a] (meq/g)	Thickness[b] (μm)	Water content[c] (%)	# of water molecules (per fixed charge)	Ion-exchange concentration (eq/kg water)
#69	0	1.0	64	2.25	65	65	16	3.5
#75	0	1.0	80	2.12	65	63	17	3.4
#117	0	1.0	135	3.59	78	65	10	5.5
#70	0	1.0	150	3.50	85	68	12	5.1
#34	0	2.5	33	1.25	65	43	19	2.9
#47	0	2.5	65	1.95	63	60	17	3.3
#73	0	2.5	78	2.05	63	68	18	3.0
#67	0	2.5	83	2.23	67	67	17	3.3
#68	0	2.5	80	1.92	-	59	17	3.3
#91	0	2.5	128	2.53	76	69	15	3.7
#24	0	2.5	150	3.01	83	65	12	4.6
#65	0	2.5	180	3.23	86	69	12	4.7
#74	0	2.5	192	3.55	86	71	11	5.0
#64	0	2.5	256	3.85	89	71	10	5.4
#57	0	2.5	295	4.16	88	73	10	5.7

Table 3.3. Water contents and ion-exchange concentrations of the cation-exchange membranes. (continued)

Membrane #	Sulfonation temperature (°C)	DVB (%)	Mass increase (%)	IEC [a] (meq/g)	Thickness [b] (μm)	Water content [c] (%)	# of water molecules (per fixed charge)	Ion-exchange concentration (eq/kg water)
#92	40	2.5	72	3.28	72	67	11	4.9
#101	40	1.0	115	4.05	-	78	11	5.2
#135	40	2.5	117	4.01	-	71	10	5.7
#118	40	1.0	135	4.64	81	70	8	6.6
#95	40	2.5	142	4.50	82	71	9	6.3
#97	40	1.0	190	5.23	83	72	8	7.3

a. The error in ion-exchange capacity measurement is ± 1%.
b. The error in thickness measurement is ± 10%.
c. The error in water content measurement is ± 5%.

It can be seen in Fig. 3.7 that the trend of water content increases slightly as the mass of incorporated poly(styrene-DVB) increases. For example, the water contents were found to increase from approximately 60 to 75% as the mass of poly(styrene-DVB) incorporated increases from 50% to nearly 300%. The results are consistent with the results of Mika et al. [16] for the PVP salt-filled membranes prepared by *in situ* polymerization.

The increase in water content as mass increase is due to the swelling of the polyelectrolytes anchored in the membrane. As the polyelectrolytes swell, the dimensions increase in order to take up more water. The trend in water content is determined by the ratio of the water taken up to the total mass of membrane as a function of mass increase. The numbers of water molecules per fixed charge site are high, between 8 and 17 (Table 3.3) and the amount of water increases dramatically with the mass increases.

3.2.3.2. Ion-Exchange Concentration (Fixed Charged Concentration)

The ion-exchange concentrations of a series of membranes prepared with various degrees of crosslinking and sulfonation are given in Table 3.3. Ion-exchange concentration increased as the mass of poly(styrene-DVB) increased. Since the water content changed very little as a function of mass of poly(styrene-DVB) but the number of ion-exchange sites increased almost linearly with mass of the incorporated poly(styrene-DVB), ion-exchange concentration of the membranes increased with increasing the poly(styrene-DVB) mass.

The effect of the sulfonation temperature on ion-exchange concentration is significant. Sulfonation at 40°C afforded significantly higher ion-exchange concentrations than the reactions carried out at 0°C. For example, the ion-exchange concentration of membrane #118 (DVB = 1.0%, 40°C sulfonation) and membrane #117 (DVB = 1.0%, 0°C sulfonation) were 6.6 and 5.5 eq/kg, respectively. Similarly, membranes #95 (DVB = 2.5%, 142% of mass increase, 40°C sulfonation) and membrane #24 (DVB = 2.5%, 150% of mass increase, 0°C sulfonation) had ion-exchange concentrations of 6.3 and 4.6 eq/kg, respectively. Higher sulfonation temperatures led to an increase in degrees of sulfonation (Fig. 2.11) and ion-exchange capacity (Fig. 2.10); however, water contents (Fig. 3.7) were not significantly affected.

The relationship between ion-exchange concentration and mass increase of poly(styrene-DVB) for 0°C and 40°C sulfonations is shown in Fig. 3.8. A linear relationship between ion-exchange concentration and IEC is shown in Fig. 3.9. Since the water contents of these membranes are similar, it is not surprising to see a linear relationship between ion-exchange concentration and ion-exchange capacity.

3.2.3.3. Comparison with Commercial Cation-Exchange Membranes

The properties of the cation-exchange membranes prepared in this study have been compared with those of some commercial cation-exchange membranes (Table 3.4). When the properties of the membranes described in this thesis are compared with the commercial cation-exchange membranes, several key points stand out. The pore-filled

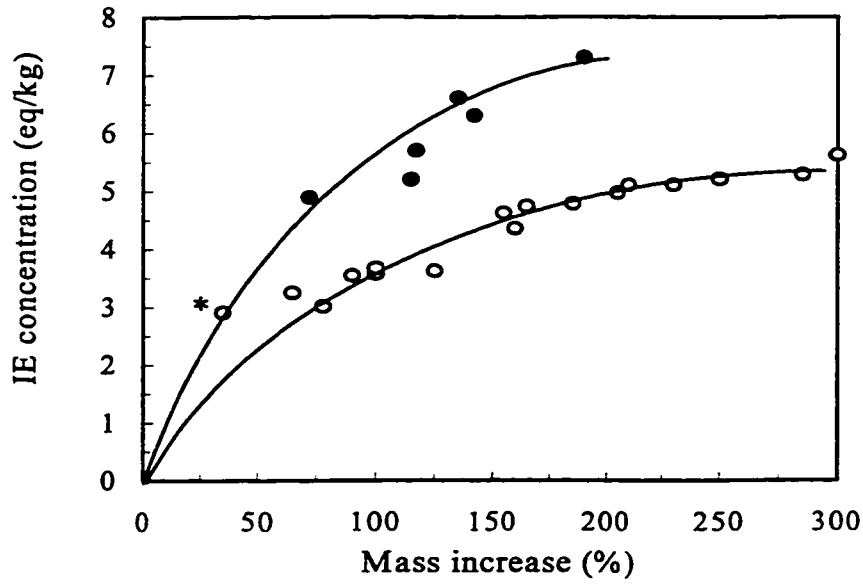

Fig. 3.8. Ion-exchange concentration as a function of mass increase;
• 40°C sulfonation, ○ 0°C sulfonation.

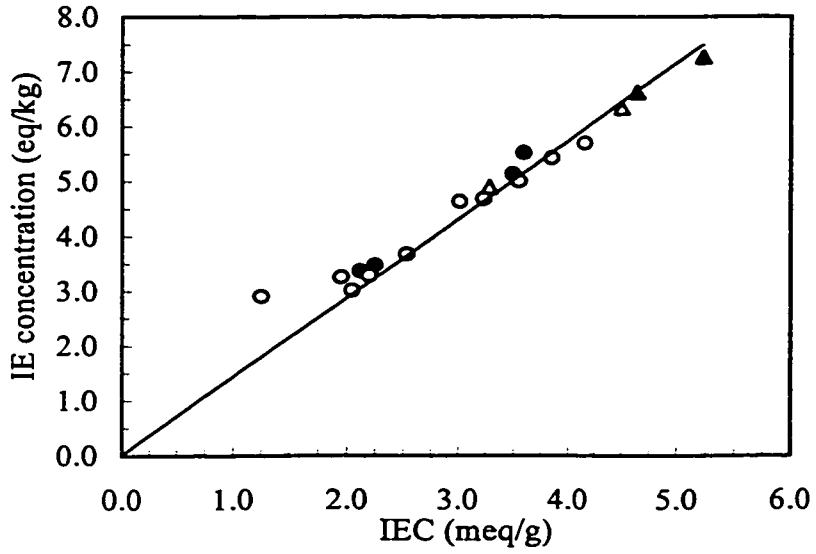

Fig. 3.9. Ion-exchange concentration as a function of ion-exchange capacity.
• DVB = 1.0%, 0°C sulfonation, ○ DVB = 2.5%, 0°C sulfonation,
▲DVB = 1.0%, 40°C sulfonation, △ DVB = 2.5%, 40°C sulfonation.

Table 3.4. Comparison of properties of the commercial cation-exchange membranes with the McMaster pore-filled membranes prepared in this study.

Membrane	Water content (%)	IEC (meq/g)	Thick-ness (μm)	Resis-tance (Ω cm^2)	Ion-Exch. Conc. (eq/kg)	Counterion transport number
61 AZL 183 [a]	29	2.0	600	4.5	5.0	0.81
61 CZL 183 [a]	25	2.6	700	7.2	7.65	0.95
AFM-C311 [a]	14	0.6	300	-	3.75	0.92
AMF-C100 [a]	18	1.1	220	4.8	5.0	0.88
C66-5T [a]	25	3.3	160	1.5	9.71	0.94
CH-45T [a]	21	2.3	170	2.1	8.52	0.96
CH-2T [a]	24	2.4	170	2.2	7.50	0.93
CL-25T [a]	24	2.0	180	2.9	6.45	0.90
CM1 [b]	32	2.57	150	-	5.68	-
CM2 [b]	27	2.02	120	-	5.50	-
CMV [a]	20	2.4	150	2.9	9.6	0.98
CR61 AZL389 [c]	48	2.6	1200	30	5.4	-
CRP [a]	29	2.6	600	6.3	6.50	0.82
K 101 [a]	19	1.4	240	2.1	5.83	0.95
MC 3142 [d]	20	1.3	220	20-30	5.2	0.82
MC 3470 [d]	26	1.5	600	6-10	4.29	0.83
Nafion 125 [e]	15	<1.0	130	20	< 5	-
Neosepta CMX-SR [c]	26	1.80	180	1.80	5.14	-
Neosepta CMA-21 [c]	35	1.90	150	0.50	3.45	-
NPES C/2 [g]	13-17	1.9	400	3-7	9.5-12.6	0.96
Selemion CMV [h]	-	1~2	~130	2.0~3.5	-	0.92
This study	60~70	up to 5.6	60~89	< 1.0	3.0~7.5	0.80~0.96

a. Reference [119].
b. References [120,121].
c. Manufacturer: Ionics, Watertown, Massachusetts (Reference [122]).
d. Manufacturer: Ionac Chemical, Birmingham, New Jersey (References [123,124]).
e. Manufacturer: Du Pont, Wilmington, Delaware (Reference [125]).
f. Manufacturer: Asahi Chemical, Japan (Reference [119]).
g. Manufacturer: Forschungsinstitut, Israel.
h. Manufacturer: Asahi Glass, Chiyoda, Japan. Data provided by the manufacturer.

membranes prepared in this work have (1) significantly higher water contents than commercial membranes; (2) thicknesses that are considerably smaller than those of commercial membranes; (3) ion-exchange capacities that are higher than those of commercial cation-exchange membranes.

3.2.4. Membrane Electrical Resistance

Electrical resistances of the cation-exchange membranes prepared in this study were measured at 25°C using an A/C conductivity cell, a conductivity meter, and a standard solution (0.50 M, NaCl) as the electrolyte. The difference in electrical resistance with and without membrane is the electrical resistance of the membrane (Table 3.5). The electrical resistance of the conductivity cell filled with the standard solution (0.50 M, NaCl) was found to be 27.0 ohms and the addition of a increased this value by only a very small amount. The membrane electrical resistance was below the sensitivity of the method (~1.0 ohm·cm2). While this method is not good enough to determine accurate membrane electrical resistances, these cation-exchange membranes were very conductive to ionic species.

The electrical properties of ion-exchange membranes are affected by both the ion-exchange concentration and water content. Table 3.4 lists some commercial cation-exchange membranes and their electrical resistance and counter-ion transport numbers, together with some other properties of the membranes, such as water content, ion-exchange concentration and thickness. The electrical resistances of most of the

Table 3.5. Transport numbers[a] and electrical resistances[b] of cation-exchange membranes, for NaCl solutions.

Membrane #	Sulfonation Temperature (°C)	Mass increase (%)	DVB (%)	IEC (meq/g)	Ion-exchange concentration (eq/kg)	# of water molecules (per site)	Transport number[a] $t^{M}_{+(Na)}$	Electrical resistance[b] (ohm·cm^2)
Substrate Membrane[c]	N.A.	0	0	0	0	N.A.	0.45	N.A.
#68	0	80	2.5	1.92	3.3	17	0.80	< 1.0
#69	0	68	1.0	2.10	3.3	16	0.80	< 1.0
#75	0	78	1.0	2.12	3.0	17	0.80	< 1.0
#67	0	83	2.5	2.23	3.3	17	0.82	< 1.0
#70	0	150	1.0	3.50	4.6	12	0.85	<1.0
#57	0	295	2.5	4.16	5.7	10	0.96	< 1.0
#101	40	115	1.0	4.05	5.2	11	0.92	< 1.0
#135	40	117	2.5	4.01	5.7	10	0.96	< 1.0
#118	40	135	1.0	4.64	5.3	8	0.94	< 1.0

a. Error less than ±0.01.
b. Sensitivity of approximately 1.0 ohm·cm^2.
c. Substrate membrane used after the thermal treatment.

commercial cation-exchange membranes typically lie between 2 and 8 ohm·cm^2 and the electrical resistances of the membranes prepared in this study are even lower, indicating that the membranes are more conductive to ionic species than the commercial cation-exchange membranes.

Electrical conductance through a membrane can be achieved by the transport of either a counter-ion or a co-ion or both. If the counter-ion is the major contribution to the high conductance (low resistance), the membranes are expected to have good performance in separating ionic species. However, if the co-ion is mainly responsible for the low resistance, the membranes are "leaky" to co-ions. Thus, transport of co-ions will lead to a poor performance in ion separations.

The low electrical resistance for these cation-exchange membranes is probably due to their high ion-exchange capacity and high water content. High water contents mean that the membranes prepared in this work are highly porous (ie., they have high void volumes).

A typical model for the migration of ionic species through charged, porous membranes is described in Fig. 3.10 [10]. Ions move freely (without effects of pore size and pore charge) in bulk solution driven by the current (I), Fig. 1.10(a). When the pore size of the cation-exchange membrane is small, the migration of ions are strongly affected by pore size and the fixed charges. The transport of co-ions is restricted due to the Donnan exclusion but co-ions can be transported through the membrane by a convective

flow which results in the convective current (i_c), Fig. 3.10(c). However, the migration of

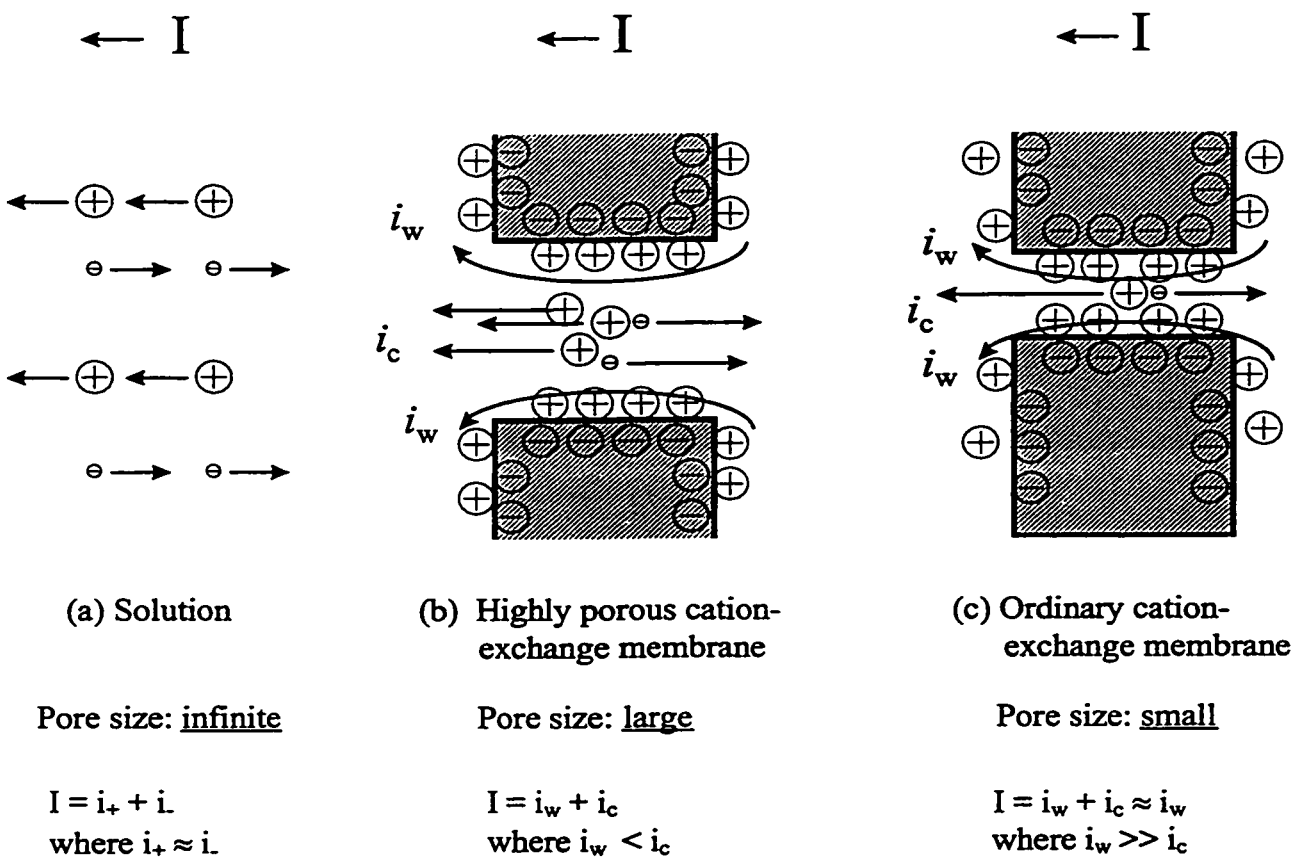

(a) Solution	(b) Highly porous cation-exchange membrane	(c) Ordinary cation-exchange membrane
Pore size: infinite	Pore size: large	Pore size: small
$I = i_+ + i_-$ where $i_+ \approx i_-$	$I = i_w + i_c$ where $i_w < i_c$	$I = i_w + i_c \approx i_w$ where $i_w >> i_c$

Fig. 3.10. Models for migration of ions in (a) solution, (b) highly porous cation-exchange membrane, and (c) ordinary porous cation-exchange membrane, in an electrical filed. I is electrical current, i_w is pore wall current, i_c is convection current.

cations is accelerated by fixed charges. The transport of counter-ions along the pore wall (due to the electrostatic interactions of the fixed charges) leads to pore wall flow, resulting in pore wall current (i_w), Fig. 3.10(c). In this case, the conductance primarily depends on the pore wall current (i_w), ie., $I \approx i_w >> i_c$.

The pore-filled cation-exchange membranes are highly porous and fit the case in Fig. 3.10(b). In this case, the transport of co-ions is enhanced dramatically by convective flow [126]. Thus, the current (I), including pore wall current (i_w) and convective current (i_c) is increased. Hence, the electrical resistance of the pore-filled membrane is expected to be lower than commercially available cation-exchange membranes.

3.2.5. Transport Numbers

3.2.5.1. Principle and Approach

The transport number of a membrane describes the mobility of an ionic species across a membrane driven by either electrical potential or chemical potential between the solutions separated by the membrane [114,127,128]. The net transport of ionic species cross the membrane results in an electrical current through the membrane. For ion-exchange membranes, counter-ions can migrate across the membranes but co-ions will be rejected by the membranes due to Donnan Exclusion. If, ideally, no co-ions are transported across the ion-exchange membrane, the transport numbers must be 1.00 for the counter-ion and 0 for co-ion. In practice, small amounts of co-ions associated with counter-ions can be transported through the membrane. Thus, the transport number for counter-ion can be calculated as the ratio of the measured electrical potential to the theoretical chemical potential of the membrane.

The transport number in the membrane was determined by the electromotive force (EMF) method reported by Kontturi et al. [109]. The measurement was performed by measuring the EMF of the following cell:

$$\text{Ag, AgCl} \mid \text{Aq. electrolyte } (C_1) \parallel \text{Aq. electrolyte } (C_2) \mid \text{AgCl, Ag} \qquad \textbf{(3. 6)}$$

where the symbol ‖ denotes the ion-exchange membrane between two aqueous electrolyte solutions with different concentrations [129], ie., $C_1 \neq C_2$. The chemical potential between the solutions, E_{max}, can be calculated from the Nernst equation:

$$E_{max} = \frac{2RT}{F} \ln \left(\frac{C_2}{C_1} \right)^n \qquad \textbf{(3. 7)}$$

where F, R, n, and T, are the Faraday constant, gas constant, valence of the counter-ion, and absolute temperature, respectively, and C_1 and C_2 are the activities of electrolyte solutions separated by the membrane.

Thus, for cation-exchange membranes, if n = 1 (ie., a mono-valent counter-ion, such as Na^+), is used, the membrane transport number for the cation, t_+^M, can be calculated using the following equation:

$$E_{mem} = t_+^M E_{max} = \frac{2\, t_+^M RT}{F} \ln \left(\frac{C_2}{C_1} \right) \qquad \textbf{(3. 8)}$$

where E_{mem} is the potential of the membrane without polarization layers. The detailed calculation of E_{mem} values is described in Appendix A.

3.2.5.2. Results of Transport Number Measurements

The transport numbers for the cation-exchange membranes were measured in a rotating cell filled with the standard NaCl solutions using the electromotive force (EMF) method [109]. In order to examine the effects of mass increase, degree of crosslinking

and sulfonation temperature, the transport numbers of a series of membranes were determined. The results are given in Table 3.5.

The transport number t_+^M, for the counter-ion (Na^+) for the PE substrate membrane was 0.45 (Table 3.5, first entry), reflecting the portion of the current through the membrane due to the net movement of this ionic species; this means that the fraction of the current carried by Cl^- is 0.55 (= 1.00 - 0.45). Since the PE substrate membrane is not charged, it will have little affect on the diffusion of ionic species through the membrane by electrostatic interactions and the transport of these ionic species will depend on their mobilities in solution which are related to their diffusion coefficients. The diffusion coefficients for Na^+ and Cl^- are 1.334×10^{-9} and 2.032×10^{-9} m^2/s, respectively [130]. Based on these diffusion coefficient values, the fraction of the current carried by Cl^- migration though the membrane would be approximately 0.6, a value fairly close to the experimental value of 0.55 for the PE substrate membrane.

Transport numbers reflect the magnitude of the electrostatic interactions between the fixed charge on the membrane and the mobile ions in solution. Thus, transport numbers should vary with the fixed charge concentrations (ion-exchange concentrations) of the membranes. The transport numbers for Na^+ for a series of poly(syrene-DVB sulfonic acid) membranes were determined (Table 3.5) and are plotted as a function of ion-exchange concentration (Fig. 3.11). The solid line shows the trend of the relationship with transport number and ion-exchange concentration. As can be seen, the transport number increased as the membrane ion-exchange concentration of increased. For example

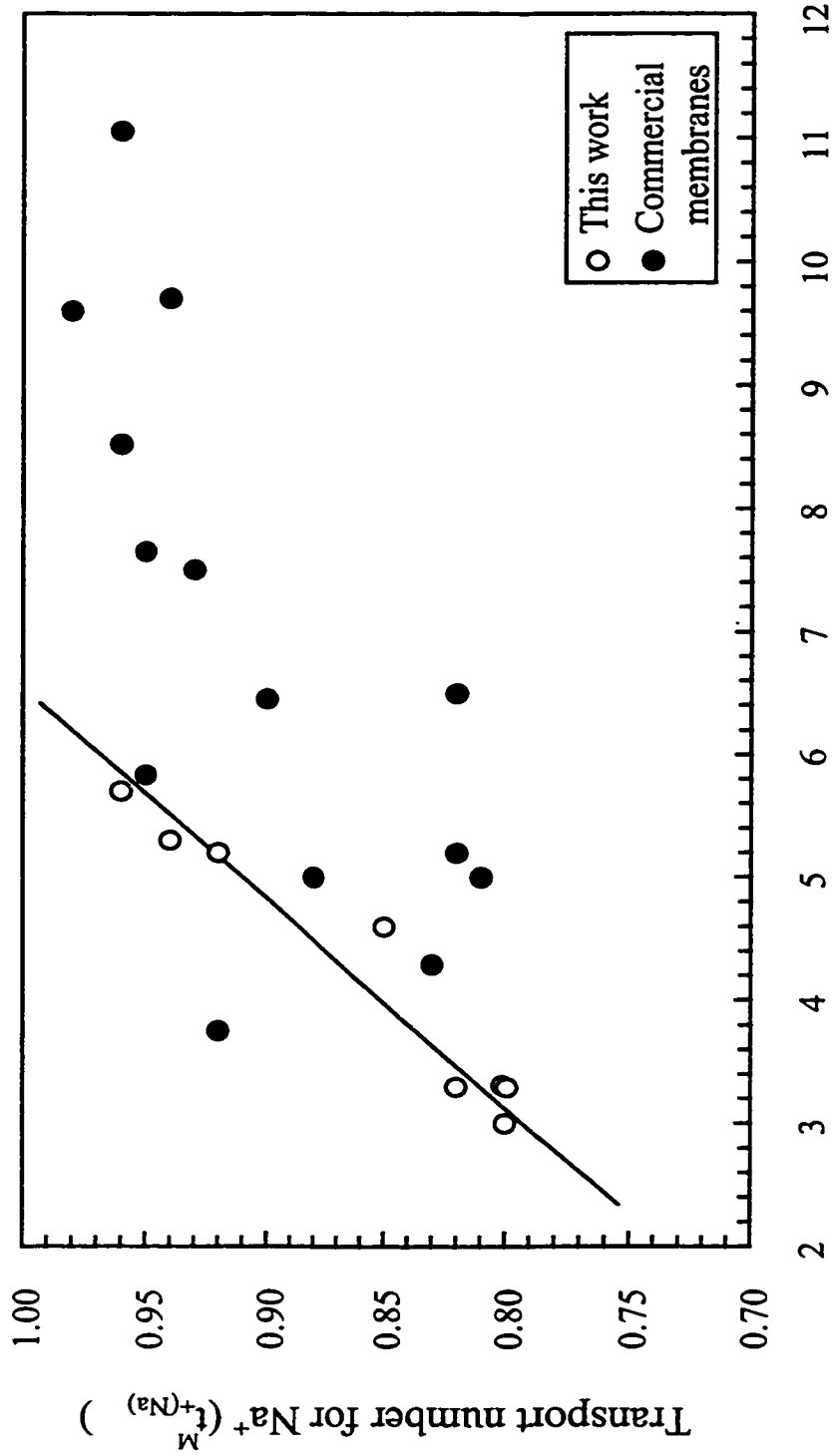

Fig. 3.11. Transport numbers as a function of ion-exchange concentration; the data for commercial membranes taken from Table 3.4.

the transport numbers for Na^+ increases increase from 0.80 to 0.96 when the ion-exchange concentrations increases from 3.3 eq/kg to 5.7 eq/kg.

This trend (Fig. 3.11) can be understood in terms of the Donnan Exclusion [16,19,131]. A higher ion-exchange concentration (fixed charge concentration) leads to a higher Donnan potential which results in greater electrostatic interactions between the fixed charges on membrane and the mobile ionic species in solution; counter-ions (Na^+) will be transported more readily through the charged membrane but co-ions (Cl^-) will be rejected.

The models discussed in Fig. 3.10 are useful in understanding counter-ions (Na^+) transport numbers. The membranes prepared in this work are highly porous membranes and are best reflected by Fig. 3.10(b). One explanation for the increase in ion-exchange concentration as a function of increasing ion-exchange concentration may be that as ion-exchange concentration increases there is a greater flow of counter-ions (Na^+) along the pore wall and a less transport of co-ions (Cl^-) by a convective flow due to the larger Donnan exclusion.

A comparison of transport and electrical properties to the commercially available cation-exchange membranes that were reported in the literature with the cation-exchange membranes prepared in this study is also listed in Table 3.4 and plotted in Fig. 3.11. First, the transport properties of the membranes made in this study are similar to those of commercial cation-exchange membranes; for example, transport numbers (marked as •) for the commercial membranes are ranged between 0.8 to 0.98 while the correponding values for the membranes prepared in this work ranged from 0.80 to 0.96. Other

properties of the commercial membranes, such as ion-exchange capacity, water content and thickness, are quite different from our membranes, reflecting differences in ion-exchange groups, manufacture and materials. In general, the commercial membranes with the higher ion-exchange concentrations have higher transport numbers. However, there does not appear to be a linear relationship between transport number and the ion-exchange concentration for the commercial membranes as shown in Fig. 3.11. A linear relationship between transport number and ion-exchange concentration has been observed in this work. This figure is instructive because, comparing to the commercial membranes, our membranes achieved relative high transport numbers at lower ion-exchange concentrations.

3.3. CONCLUSION

This chapter has discussed the control of changes in dimensions of the polyethylene substrate membrane. Pore contraction has been observed in the thermal treatment and solvent extraction used in membrane preparation. The length, width and porosity of the substrate membrane were found to be reduced during the membrane-making processes.

The PE substrate membrane was treated with styrene/DVB and resulting poly(styrene-DVB) was sulfonated at either 0 or 40°C to yield cation-exchange membranes. The swelling properties of these cation-exchange membranes, including

water content, thickness and ion-exchange concentration, were characterized and the effects of mass increase and sulfonation temperature on the swelling properties investigated. The water contents of all membranes are high, approximately 70%. The change in membrane thickness during poly(styrene-DVB) reactions depended on the formation of an interpenetrating polymer network with the polyethylene nodules of the substrate membrane. The membrane thickness increased as a function of mass of incorporated poly(styrene-DVB) until a thickness break point at approximately 150% of mass gain of poly(styrene-DVB). This break point was found to be related to the porosity of the PE substrate membrane. The ion-exchange concentrations of the membranes are high.

The electrical resistance and transport number of these cation-exchange membranes were characterized. The electrical resistances of these membranes were found to be less than 1.0 ohm·cm^2, significantly lower than those of many commercial membranes. The transport numbers for Na^+ ranged from 0.80 to 0.96 with higher transport numbers observed for membrane with higher ion-exchange concentrations. These transport numbers were in the same range of commercial cation-exchange membranes. however, the membranes made in this work achieved high transport numbers at lower ion-exchange concentration, suggesting that these membranes could be substitute for commercial cation-exchange membranes. Models of porous membranes were used to explain the electrical resistance and transport numbers of these membranes.

CHAPTER FOUR

MEMBRANE EVALUATION I

USING DIFFUSION DIALYSIS TO SEPARATE BASE AND SALT

Membrane separation processes which make use of a concentration difference as the driving force include gas separation, vapour permeation, pervaporation (PV), dialysis, diffusion dialysis (DD), carrier mediated processes and membrane contactors [132]. Some of the processes combine with other driving forces. For example, a pressure difference is also a driving force in gas separation, vapor permeation, and pervaporation. Depending on the selectivity and fixed charge concentration in ion-exchange membranes, diffusion dialysis can be an energy-efficient separation technique since the only force acting in the system is the concentration difference of the permeants between the feed and the permeate [133].

4.1. PRINCIPLE OF DIFFUSION DIALYSIS

4.1.1. Process of Diffusion Dialysis

The principle of DD is illustrated in Fig. 4.1. Proton and hydroxide ions are the most permeable ions in ion-exchange membranes while co-ions are rejected due to the

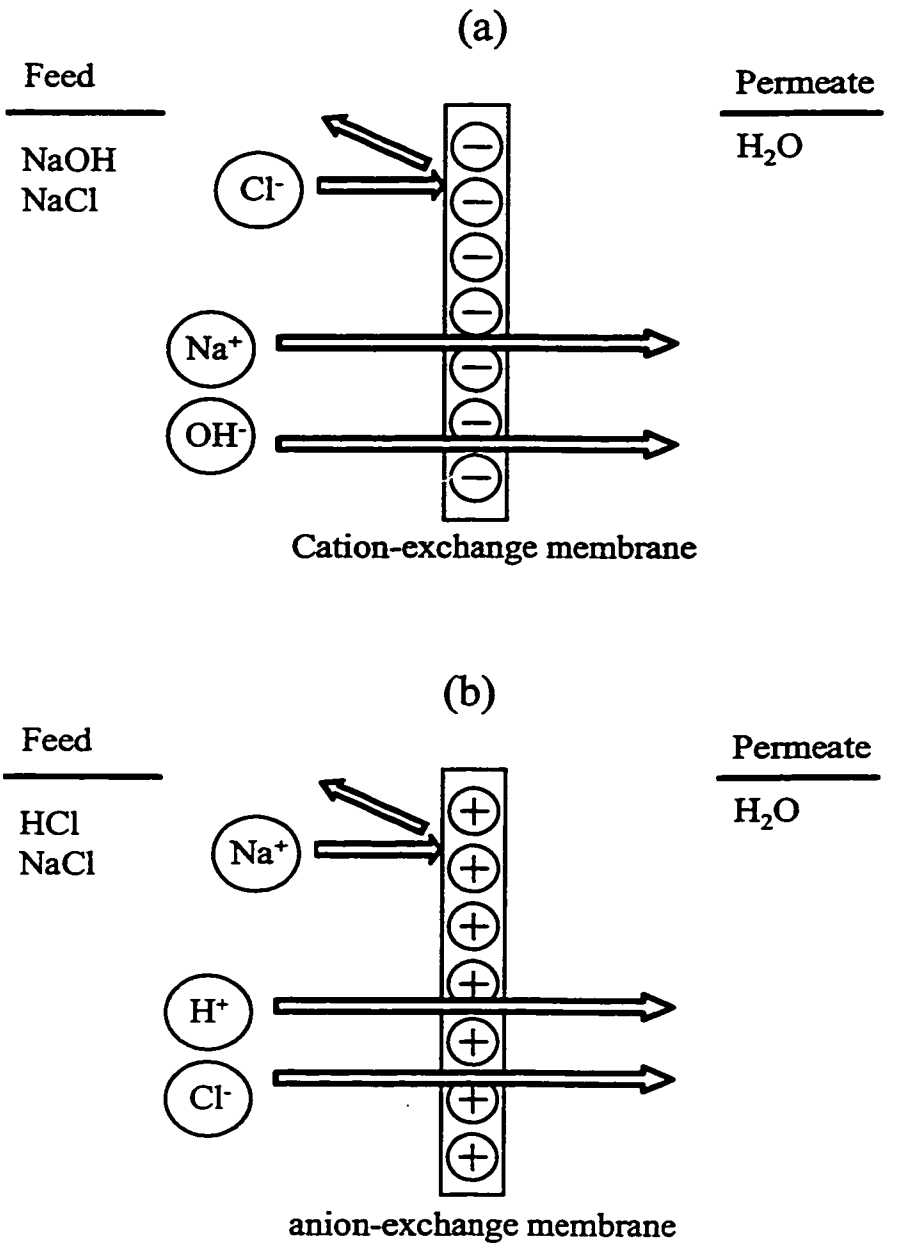

Fig. 4.1. Processes of diffusion dialysis with (a) cation-, (b) anion-exchange membranes.

Donnan exclusion. For example, in Fig. 4.1, a cation-exchange membrane rejects Cl^- but allows OH^- and the counter-ion (Na^+) to permeate through the membrane. As a result, NaCl is retained while NaOH permeates across the membrane, Fig. 4.1(a). Similarly for anion-exchange membranes, the NaCl from NaCl/HCl is retained while HCl permeates across the membranes, Fig. 4.1 (b).

The process of DD using an anion-exchange membrane has been shown to be effective for the separation and recovery of sulfuric and other acids from waste solutions being generated in the electroplating and steel industry [120,134]. Recently, Stachera et al. [54] reported acid recovery from the acid-metal ions mixed solutions using diffusion methods with pore-filled anion-exchange membranes containing poly(4-vinylpyridium salts).

A counter-current DD process for recovery (or removal) of acid from an acid/salt solution is, from an engineering point of view, rather simple and energy efficient, Fig. 4.2. The transport of H^+ is relatively fast due to high diffusivity and the possibility of water splitting in anion-exchange membranes which are leaky to H^+ ions [135].

A similar process can be used to separate base and salt by DD using a cation-exchange membrane. That is based on the differences in mobility of hydroxide ion and other anions. However, the separation ratio of base to salt is smaller [132,133]. There are only a small number of reports of the use of diffusion dialysis to separate the mixtures of base and salt. For example, Sata proposed that the recovery of base from base and aluminium salt mixtures was a new application for cation-exchange membranes [125].

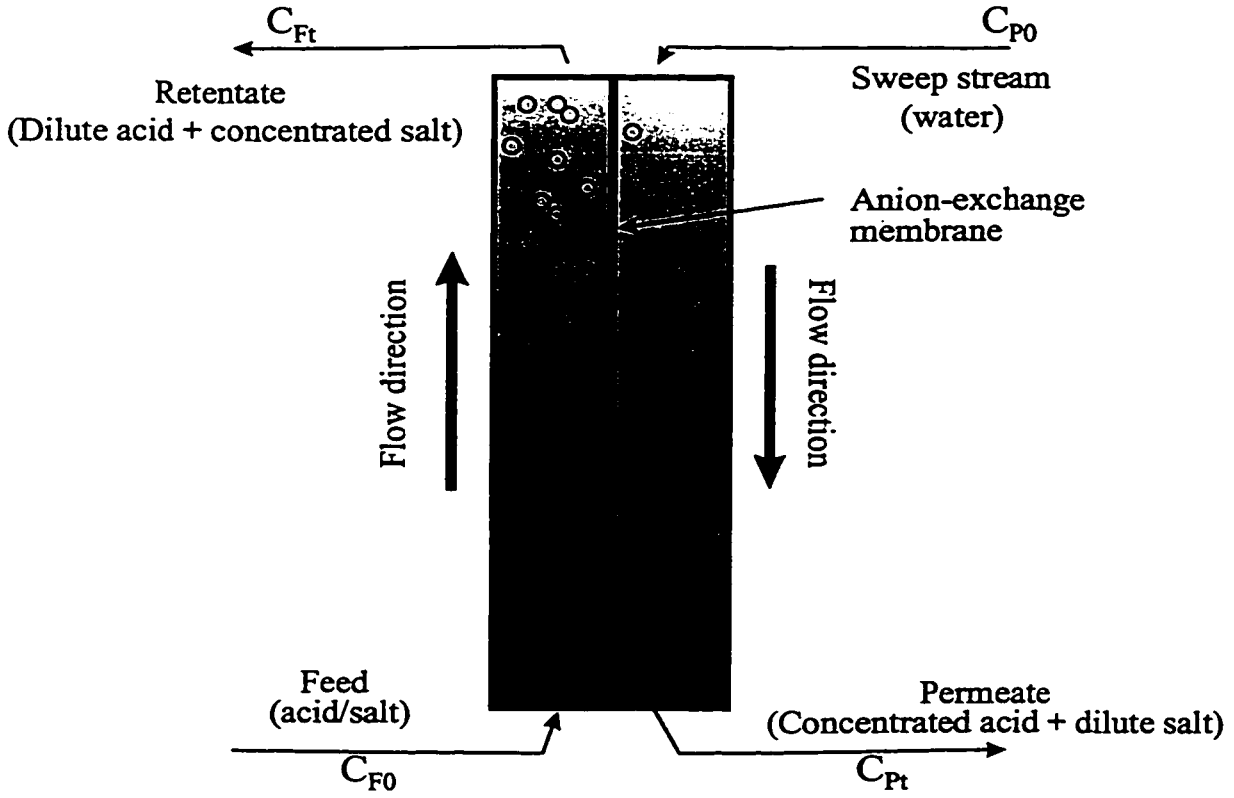

Fig. 4.2. A counter-current DD process for recovery of acid from an acid/salt solution; the grey color shows the concentration profile of acid, and the points (o) show the concentration profile of metal ions schematically.

Wycist and Trochimczuk reported the results of salt and base separation using a weak acid cation-exchange membrane [136].

The properties of the pore-filled cation-exchange membranes prepared in this work, such as high ion-exchange capacities and concentrations, and transport numbers (for details, see Chapters 2 and 3), suggested that the membranes would perform well in diffusion dialysis applications. Thus, the separation performance of NaOH from mixtures containing NaOH and a salt (NaCl or Na_2SO_4) using diffusion dialysis is investigated and reported in this Chapter.

4.1.2. Transport of Proton and Hydroxyl Ion

4.1.2.1. Proton Transport

The migration of a proton in water occurs by two different processes. The first is a free solution diffusion process, Fig. 4.3(a), in which the proton and associated water of hydration diffuse through the water phase. The second is a "proton-hopping" process in which the proton moves by a sequence of steps involving formation and breakage of hydrogen bonding of a series of water molecules. This second mechanism, involving a "proton hop" process, is so-called the Grothus mechanism, Fig. 4.3 (b) [137]. This mechanism involves a proton hopping from H_3O^+ to a neighboring H_2O molecule which, in turn, ejects one of the protons which is to form hydrogen bonding with a neighboring proton. Thus, a proton "hops" (is transported) from one water molecule to another. As a result, a succession of proton-hopping steps lead effectively to proton transport through the water. In the Grothus mechanism, the original proton entering the membrane is not the proton transported.

The free solution diffusion rate of a hydrated proton is much slower than the rate of the proton-hopping process [138]. The free solution diffusion coefficient of a proton is 2.30×10^{-9} m^2/s while the overall diffusion coefficient of a proton is 9.31×10^{-9} m^2/s. The overall diffusion includes both the proton-hopping and free solution diffusion processes.

The transport of proton through a hydrated ion-exchange membrane can, in principle, occur *via* both of the two processes which occur in water. One approach to explain transport in ion-exchange membrane is that the water in an ion-exchange material

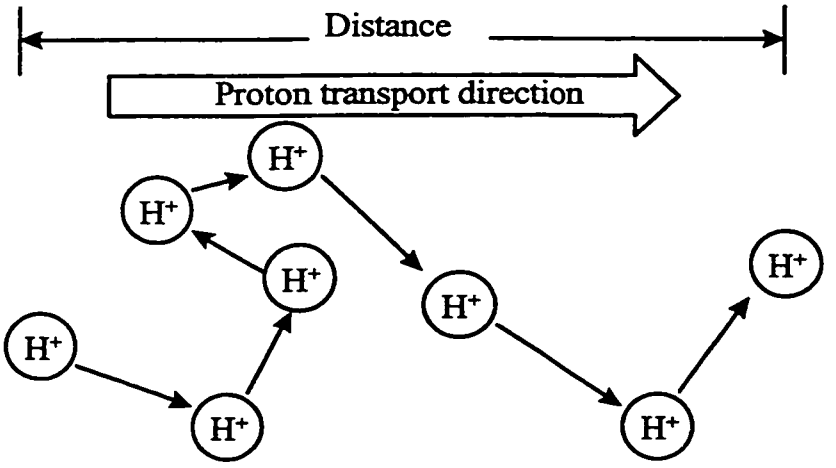

(a) Free solution diffusion . (H+) : hydrated proton.

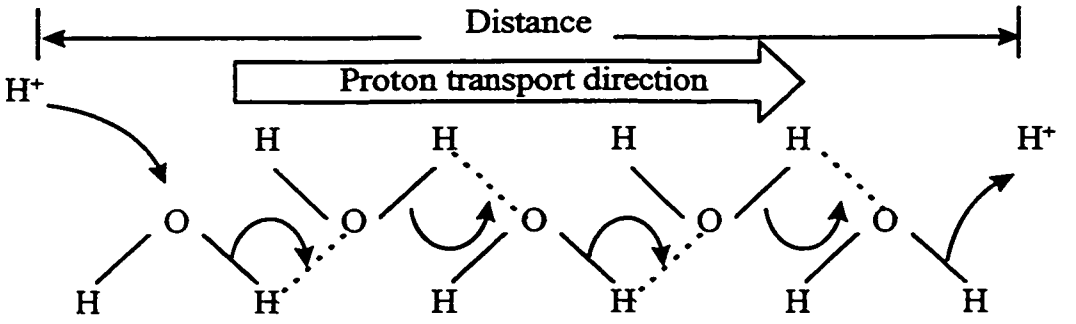

(b) Proton hop mechanism (Grothus mechanism).

Fig. 4.3. Proton transport *via* (a) free solution diffusion, and (b) proton hop (the Grothus mechanism, [137]).

can be understood as bound (or "non-freezable", "associated") water* and free (or "freezable", "bulk-like") water [55,56]. The free water resembles bulk water with the major interactions being hydrogen bonds. The bound water molecules, however, are in the vicinity of the materials while the free water is further away from them. The strength of the bonding between the bound water molecule and the material is greater than that of hydrogen bonding in the free water. Thus, the free water is bulk-like but the bound water is assumed to be a part of structure of the materials. The relative proportions of the different water types can be determined by differential scanning calorimeter (DSC), NMR, infrared, and other methods [55-57].

The free solution diffusion of a proton through a hydrated membrane can, in principle, involve both the free and bound water. However, the "free" diffusion is expected to be much slower in bound water. On the other hand, the proton-hopping (Grothus mechanism) can occur in both free and bound water.

4.1.1.2. Hydroxide Ion Transport

The transport of a hydroxide ion in an aqueous solution can be assumed to involve the free solution diffusion and a form of the Grothus' proton hop mechanism. In this proton hop mechanism, protons effectively move in the opposite direction to hydroxide

---

* Strictly speaking, the concept of bound and unbound water is accepted as a model of water in electrolyte solutions.

ions, Fig. 4.4 [138]. The process involves that a hydroxide ion removes one of the protons from a neighboring water molecule (site 1). Thus, water is produced and the negative charge is transferred to the oxygen at site 1. This negative charge then takes one of the protons from its neighboring water molecule and thus the negative charge is transferred to that oxygen (site 2). This process repeats and the negative charge is transferred to site 3, site 4, and so on. Therefore, a succession of this type of proton-hopping leads to a rapid transport of hydroxide ions in water.

Based on the proton-hop mechanism, the proton-hopping diffusion rate of transport of a hydroxide ion should be approximately equal to that of a proton. The overall diffusion rate of hydroxide ion (diffusion coefficient 5.27×10^{-9} m^2/s) is smaller than that of proton (9.31×10^{-9} m^2/s). This is due to the fact that the free solution diffusion rate of hydroxide ion is lower than that of proton.

4.1.1.3. Diffusion Dialysis with Base and Salt

The diffusion dialysis process using ion-exchange membranes has been studied for acid/salt [54,137,139-143] and base/salt systems [125,133,136,144,145]. The models of the diffusion processes are based on the ideal situation, ie., only counter-ions can go across ion-exchange membranes but the transport of co-ions is restricted by Donnan exclusion.

The DD process with NaOH/NaCl is illustrated in Fig. 4.5. Donnan exclusion effectively draws counter-ions (Na^+) into the membrane but rejects anions (Cl^- and OH^-).

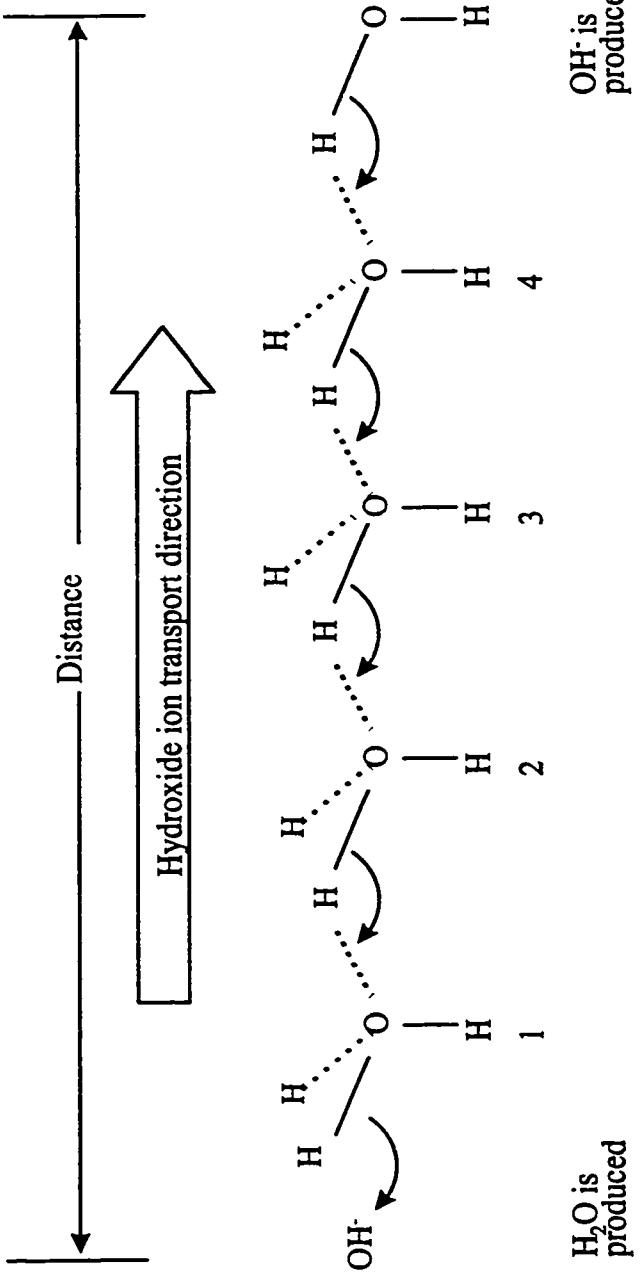

Fig. 4.4. Transport of hydroxide by the proton hop mechanism [10].

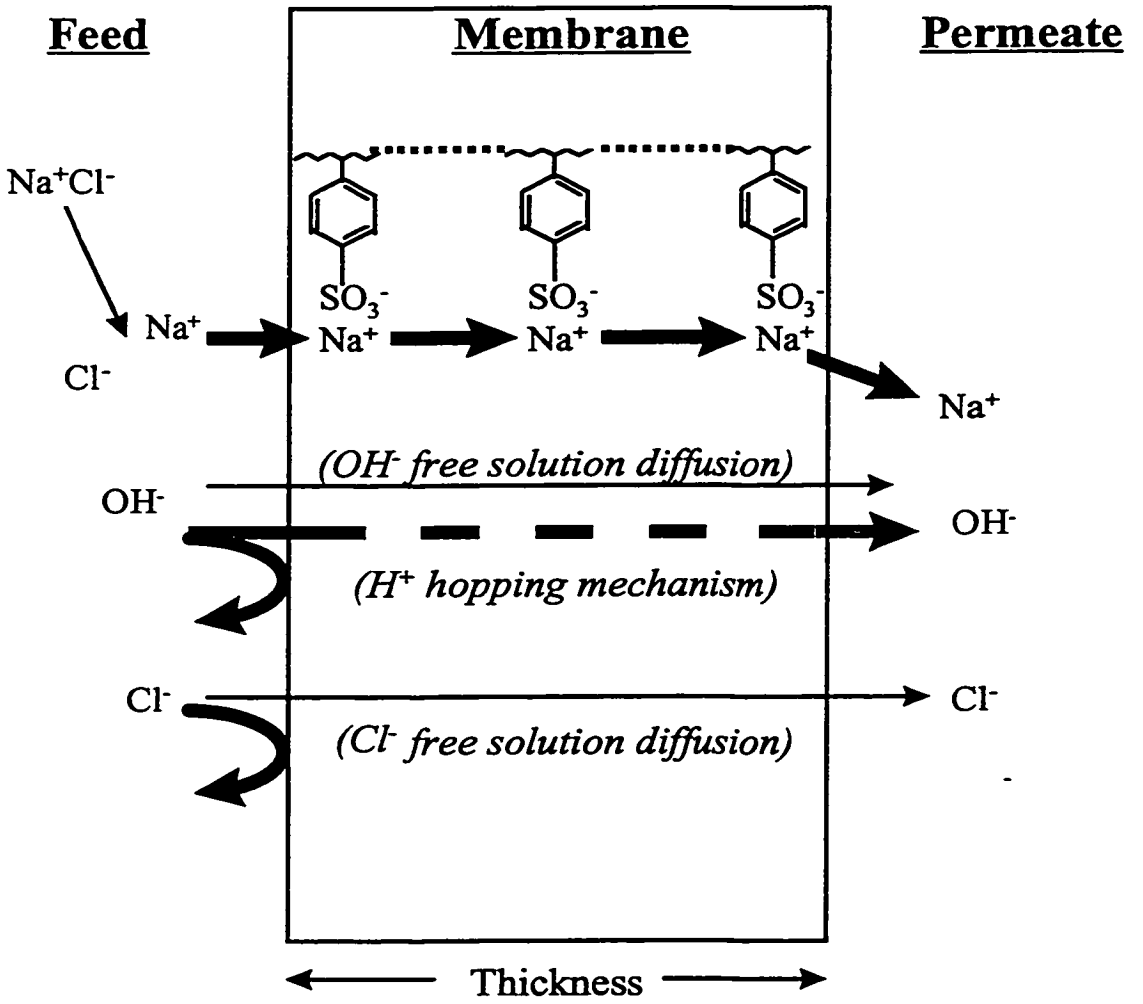

Fig. 4.5. Process of diffusion dialysis with NaOH/NaCl. Primarily NaOH is transported but some NaCl may "leak" across the membrane.

The driving force (the concentration difference) drives the counter-ion (Na^+) to transport across membrane *via* the association with the fixed charges ($-SO_3^-$). In order to maintain charge neutrality, the transport of the counter-ion (Na^+) cannot occur without the migration of an anion. Thus, the diffusion rate of the anions, such as Cl^-, through the membrane is affected by the diffusion of Na^+. The use of a cation-exchange membrane to recover NaOH then comes down to the relative differences in rate of transport of OH^- and other anions present in the feed solutions.

The ideal situation is that only counter-ion (Na^+) can enter a cation-exchange membrane but co-ions (Cl^- and OH^-) are totally rejected due to Donnan exclusion. The reality is that co-ions (Cl^- and OH^-) are not totally excluded. The degree of exclusion of the co-ions transported *via* free solution diffusion is related to the Donnan potential and concentration of the ions in the contacting solution. The rate of free solution diffusion of Cl^- and OH^- depends on the content of free water, eg., these rates are substantially decreased with reduced free water content. However, the transport of OH^- *via* proton hopping depends on the water in the membrane but is not controlled by Donnan exclusion. The OH^- ions transported includes the OH^- ions transported *via* free solution diffusion and proton-hopping. Thus, the discrimination between Cl^- and OH^- depends practically on the content of free water. A higher ion-exchange concentration in the membrane leads to a lower content of free water which is expected to lead to higher separation ratio (the rate of OH^- to Cl^-).

4.2. EXPERIMENTAL

4.2.1. Materials

The membranes used in this chapter were a substrate PE membrane supplied by the 3M Company and a cation-exchange membrane (#67) containing poly(styrene-DVB sulfonic acid). The preparation and characterization of membrane #67 have been described in Chapters 2 and 3, respectively.

Inorganic reagents used, NaOH, NaCl, and Na_2SO_4 (Aldrich), were all AR grade. The water was deionized and carbon filtered.

4.2.2. Permeability Measurements

The experiments were carried out in a diffusion cell, Fig. 4.6, constructed from Lucite®, which was described elsewhere [54]. Briefly, the cell consisted of two compartments of equal volume separated by the membrane. The active membrane area was 3.14 cm^2. The diffusion cell and the solutions to be used were placed in a water temperature-controlled bath (at 25.0 ± 0.1°C) for temperature equilibration for 45 min. Twenty-five (25.00) mL of a feed solution containing 1.0 M NaOH and 0.5 M salt (NaCl or Na_2SO_4), was added to one compartment and simultaneously 25.00 mL of water was added to the other compartment. The solutions in both compartments were stirred at an identical rate of 25 revolution per second. Approximately 5 mL of the feed and permeate solutions were withdrawn by two syringes simultaneously and rapidly from both compartments after a given period of time. The concentrations of the ionic components

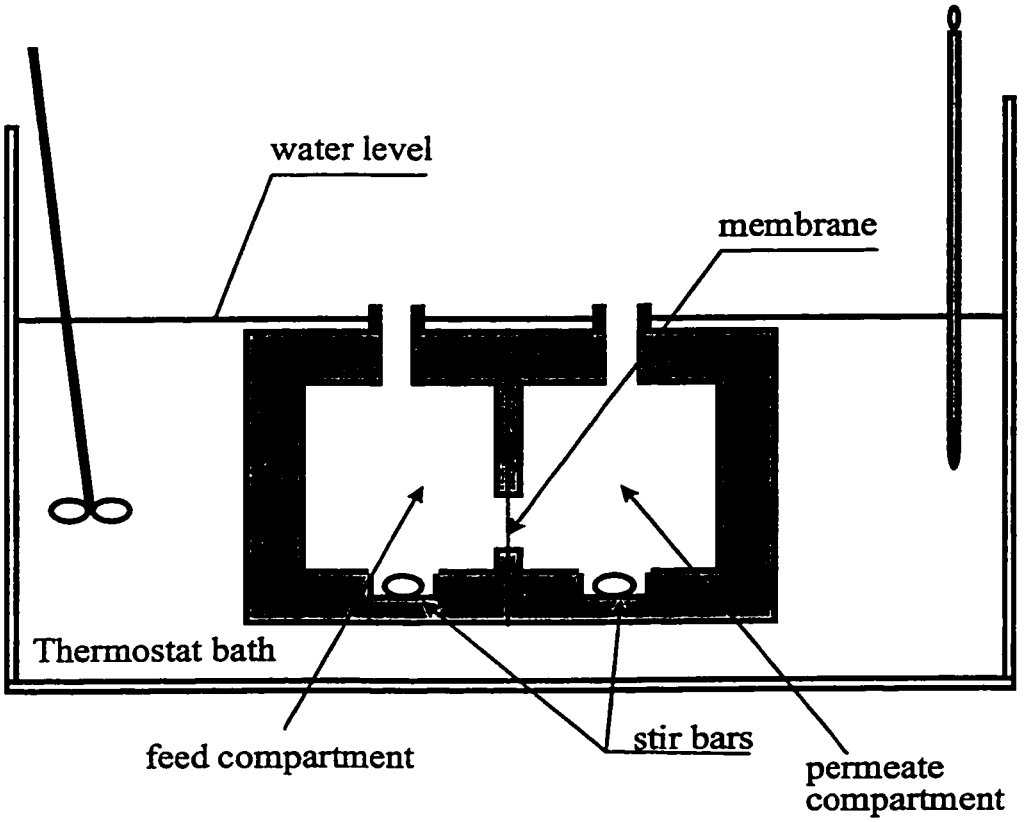

Fig. 4.6. Diffusion cell with thermostat water bath.

were determined by ion chromatography, (DIONEX, DX-100). The concentration of the base (NaOH) was determined by titration with a standard HCl solution. Water transport was calculated from a mass balance on the base (NaOH). Water transport was also verified by measuring the volume difference between the feed and the permeate using the syringes to quickly withdraw the feed and the permeate solutions simultaneously. The error in water transport between the calculated method and the measurement with syringe was approximately 10%.

At any time, the flux (J_i) of an ionic species across membrane is given by:

$$J_i = \frac{P_i}{d} \Delta C_i \qquad (4.1)$$

where P_i and ΔC_i are the permeability coefficient and concentration difference (mol/L) of the ionic species i, respectively, and d is the thickness of the membrane.

In this work, the dialysis coefficient (U) of the membrane for each component was calculated by the following equation:

$$U = \frac{W}{A \cdot t \cdot \Delta C} \qquad (4.2)$$

where W was the amount (mole) of component transported, A the active membrane area (m^2), and t the diffusion time (h). The logarithm concentration difference, ΔC, was calculated from the following equation [146]:

$$\Delta C = \frac{C_{F0} - \left(C_{Ft} - C_{Pt}\right)}{\ln\left[\frac{C_{F0}}{C_{Ft} - C_{Pt}}\right]} \qquad (4.3)$$

where C was the concentration of the ionic species, F and P denoted the feed and the permeate, respectively, and 0 and t denote the time 0 and time t, respectively (and illustrated in Fig. 4.2).

The separation ratio for the membrane was calculated by:

$$\text{Separation ratio} = U_{base} / U_{salt} \qquad (4.4)$$

4.3. RESULTS AND DISCUSSION

Membrane #67 was selected for the diffusion test since the properties of this membrane, such as water content, thickness, ion-exchange capacity/concentration, electrical resistant, and transport numbers have been determined. These properties of this membrane are listed in Table 4.1. These parameters were close to the average values of the pore-filled cation-exchange membranes prepared in this work (see Chapter 2 and 3 for detail). The separation results in this diffusion test for membrane #67 would be expected to reflect the representative performance of these pore-filled cation-exchange membranes.

4.3.1. Concentration Profile and Water Transport

4.3.1.1. Concentration Profile

In order to monitor the changes in ion concentrations in the feed and permeate solutions during the diffusion dialysis process, the ion concentrations of OH^- and Cl^- were determined at various periods of time. The raw data for calculations of dialysis coefficients, separation ratios and water transport are given in Appendix B. The concentration profiles for NaCl and NaOH presented in this case are plotted as a function of time, Fig. 4.7(a). Water transport through membrane was determined. The trend of water transport is shown in Fig. 4.7(b).

Table 4.1. Properties of membrane #67 used for diffusion dialysis.

Mass increase (%)	DVB (%)	Sulfonation temperature (°C)	Thickness (μm)	Water content (%)	# of water molecules (per fixed charge)	IEC[a] (meq/g)	IE conc.[b] (eq/kg)	Electrical resistance (ohm.cm^2)	Transport number ($t_{(Na^+)}$)
83	2.5	0	67	67	17	2.23	3.3	< 1.0	0.82

a. IEC: ion-exchange capacity.

b. IE conc.: ion-exchange concentration.

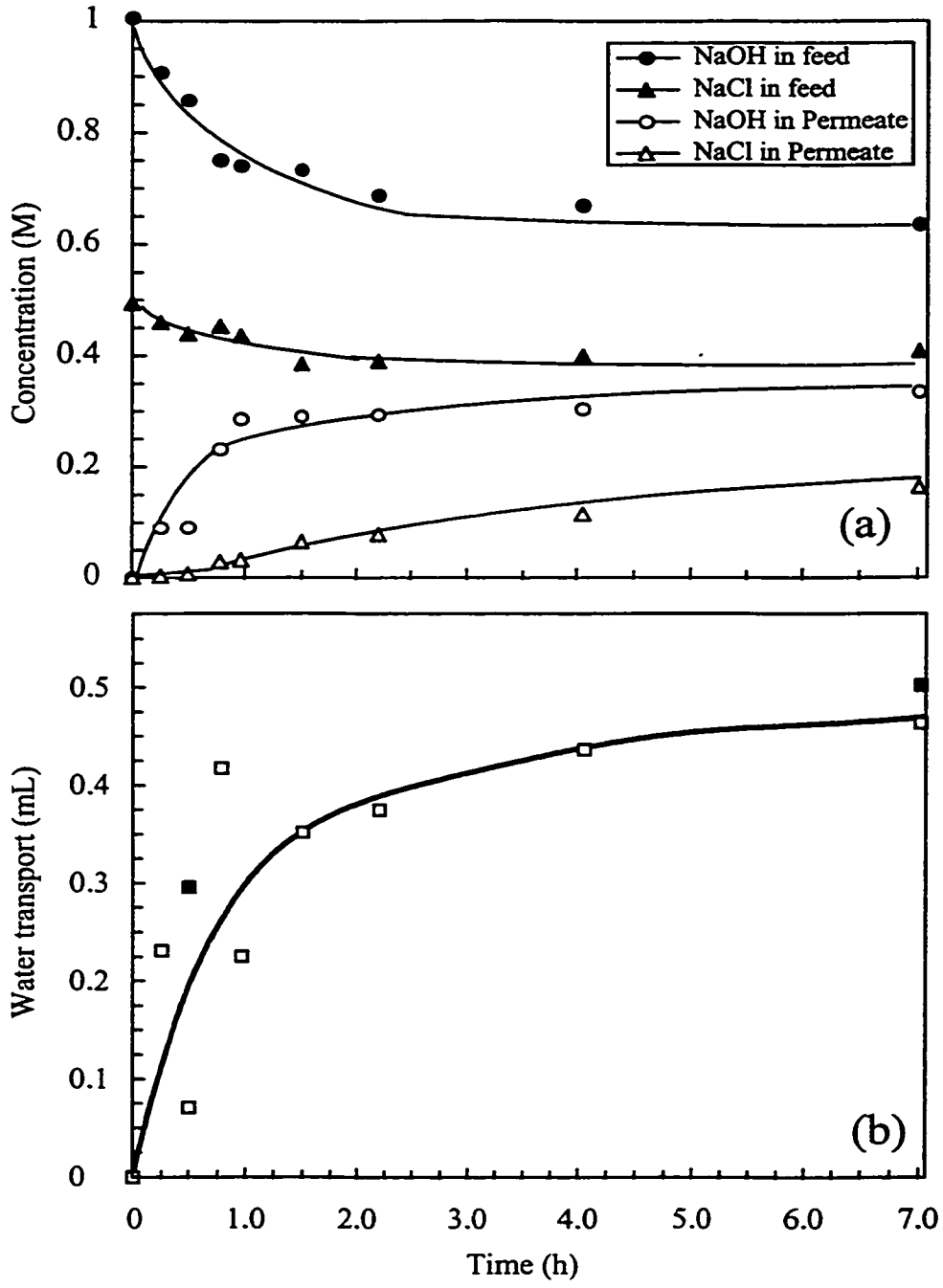

Fig. 4.7. (a) Concentration profiles of NaCl and NaOH as a function of time; the data are based on single measurements;
(b) Water transport from the permeate to the feed as a function of time; The membrane area is 3.14 cm^2; ■ measured using syringes; □ calculated based on mass balance.

From Fig. 4.7(a), the concentrations of the species in the feed decrease while the concentrations of the species in the permeate increase as the time increases. As expected, the concentration of NaOH in both the feed and permeate changes more significantly than that of NaCl. For example, in the feed, at the time of 1 h, the concentration of NaOH decreases 26% (from 1.0 to 0.74M) while the concentration of NaCl decreases only 8% (from 0.5 to 0.46 M). Similarly, in the permeate, the concentration of NaOH increases from 0 to 0.29 M while the concentration of NaCl increases from 0 to approximately 0.03 M. The explanation of this phenomenon of separation of NaOH and NaCl has been described in Section 4.1 of this chapter.

4.3.1.2. Water Transport

From Fig. 4.7(b), as the time increases, the volume of water transport across the membrane increases but the rate of water transport decreases. Water transport obtained by mass balance on NaOH and measured by syringe give similar trends. Approximately 0.26 mL of water transports from the permeate to the feed at 0.5 h (average rate $\approx$ 0.52 mL/h) and 0.48 mL at 7 h (average rate $\approx$ 0.07 mL/h). This is due to reduction of the driving force (concentration difference). The data in Fig. 4.7 are single measurements. The error in calculated water transport is even larger due the errors in the measurement of concentrations.

Water transport includes the water associated with the ionic species which diffuses from the feed to the permeate due to the concentration difference (electrical

effect) and the water which is transported from the permeate solution to the feed side due to the osmotic pressure (pressure effect) [10]. The net water transport was found to be against the direction of migration of the electrolytes (NaOH and NaCl). This result is because the pressure effect is greater than the electrical effect. Thus, the water diffusion process would not stop until the two effects are balanced.

Water transport is often disregarded in the studies of diffusion dialysis. This does not mean no water transport across the membrane but that the amount of water transport is small and that the error of measurement of water transport is large. Stachera et al. [54] found that water transport was less than 0.50 mL using the same test cell and negligible in acid recovery from acid/salts using diffusion dialysis with PVP salt-filled anion-exchange membranes. Elmidoui et al.[6], Sata [125], Wycist and co-worker [136] and Mika [145] disregarded the water transport in their diffusion dialysis studies.

4.3.2. Dialysis Coefficient

4.3.2.1. Determination of Transport Theory

It is usually assumed in the membrane transport theory that, for a single solute system, the dialysis coefficient is constant, independent of time [132]. In diffusion dialysis, according to Eq. 4.2, the relationship between $W/\Delta C$ and $A \cdot t$ should be linear. Recently, Stachera [147] observed that, for a single solute HCl system using positively charged pore-filled ion-exchange membranes, the dialysis coefficients did not change significantly with time. However, no work has been reported on the variation of dialysis coefficient for a mixed solute system using pore-filled ion-exchange membranes.

In this work, the dialysis coefficients and the separation ratios were determined for the diffusion dialysis of mixed solute systems (NaOH and salts) using the pore-filled cation-exchange membranes prepared in the previous chapter. This work also provides a test for the transport theory on the variation of the dialysis coefficient for a mixed solute system. The values of W and ΔC were determined at various times (t) in separate experiments and the raw data are given in Appendix B. The relationship of $W/\Delta C$ versus A·t is plotted in Fig. 4.7.

As can be seen, a non-linearity of the results of the dialysis coefficient over the time range (7 h) is obtained (the solid line in the best fit line, through the origin, of all the data). The dialysis coefficient (U) decreases with increasing the time, instead of being constant as expected for single solute systems. The deviation from linear behavior is because the transport theory was not solved for the mixed solute systems. There are two factors neglected. One is that the water transport is ignored in the calculation of the dialysis coefficient (U). As water is transported from the permeate to the feed, the osmotic pressure decreases. The second is that the concentration ratio of the competing ions changes with increasing time, ie., the concentration ratio of the faster ion to the slower ion decreases. This leads to a change in difference of the driving forces between the competing ions. Thus, with increasing time, a smaller dialysis coefficient (U) for the faster ion and a smaller ratio ($U_{faster\ ion}/U_{slower\ ion}$) are expected. This trend was observed for the data in Appendix B.

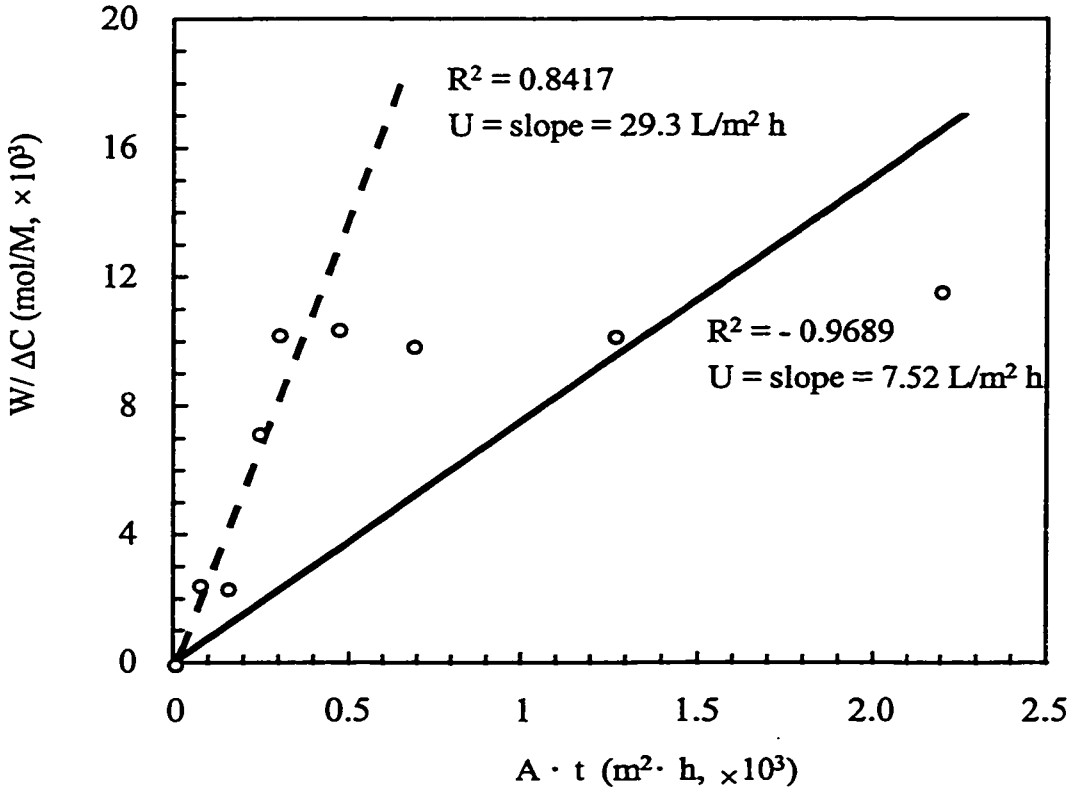

Fig. 4.8. Plot of rate of NaOH transported per unit log mean driving force (W/ΔC) as a function of area times time (A·t) for the mixed solute system containing 1.0 M NaOH and 0.5 M NaCl at 25°C; the solid and dashed lines are the trend lines calculated by the model (Eq. 4.2) based on the points obtained for 7 h (full time range) and 1 h, respectively; U (slope of the line) is the dialysis coefficient of NaOH.

However, a roughly linear relationship can be obtained (the dashed line in Fig. 4.7) in a shorter period of time (< 1 h). This indicates that the results obtained after a short, fixed time range give a relative dialysis coefficient with a less error, eg., the error in U_{NaOH} is 25% and 12% for over the time range (7 h) and for 1 h, respectively. This is because, in a short, fixed length of time, the amount of transported water and the change in concentration of the competing ions are relatively small. Comparing U for all the data (7 h) *versus* U for 1 h of operation only, the value of U increases from 7.5 ± 1.9 to 29.3 ± 3.6 L/m^2h. Simultaneously, the R^2 increases from – 0.97 (for 7 h) to 0.84 (for 1 h). These results suggest that the transport theory would be reasonably applicable for the mixed system under these conditions. It should be noted that the error in dialysis coefficient becomes larger at shorter times due to the low concentration of the ion in the permeate solution. In this study, for the remaining experiments, a time of 30 min was chosen for convenience (fewer experiments), and the dialysis coefficients obtained were, at least, reasonably accurate and comparable between membranes.

4.3.2.2. Determination of Dialysis Coefficient (U)

The dialysis coefficients for NaOH and salts (NaCl and Na_2SO_4) were measured. As a control experiment, an unmodified substrate membrane was also examined. The feed solutions used in the tests contained a mixture of the base and salt, ie., 1.00 M NaOH and 0.50 M NaCl, or 1.00 M NaOH and 0.50 M Na_2SO_4. The permeate compartment initially contained only deionized water. The experiments were carried out at 25°C for 30 min. The concentrations of the ionic species in both compartments were determined. The

dialysis coefficients of the base and salts and the ratios of their dialysis coefficients were calculated using Eqs. 2 and 3. The dialysis coefficients (U) are given in Table 4.2.

Table 4.2. Dialysis coefficients of NaOH, NaCl and Na_2SO_4 using the PE substrate membrane and membrane #67 at 25°C [a].

Feed Solution	1.0 M NaOH / 0.5M NaCl		1.0 M NaOH / 0.5 M Na_2SO_4	
Dialysis Coefficient	U_{NaOH} (L/m^2 h)	U_{NaCl} (L/m^2 h)	U_{NaOH} (L/m^2 h)	U_{Na2SO4} (L/m^2 h)
		PE membrane		
1	33.40	19.72	27.45	10.11
2	28.18	17.42	27.71	10.20
3	27.68	16.23	28.47	10.20
Average	29.75 ± 3.17[b]	17.79 ± 1.77[b]	27.87 ± 0.53[b]	10.17 ± 0.05[b]
		Membrane #67		
1	17.38	2.357	13.83	0.858
2	20.94	2.849	13.74	0.868
3	16.54	2.393	13.12	0.783
Average	18.29 ± 2.34[b]	2.533 ± 0.274[b]	13.56 ± 0.39[b]	0.836 ± 0.046[b]

a. The raw data and calculations are given in Appendix B.
b. Standard deviation of three measurements.

From Table 4.2, in six of eight cases, the standard deviation in dialysis coefficient (U) is approximately 2% when the time is set at approximately 30 min. This is significantly smaller than the error (up to 25%) in the measurement of U by changing the time. This suggests that the data obtained are reproducible and comparable. For both of the membranes, U_{NaOH} is greater than U_{NaCl}, and greater than U_{Na2SO4}. This is because hydroxide ions are the fastest anion with the largest diffusion coefficient [130]. Due to the higher Donnan exclusion of the bivalent co-ion (SO_4^{2-}), U_{NaCl} is greater than U_{Na2SO4}. As expected, for all the solutes (NaOH, NaCl, and Na_2SO_4), the dialysis coefficients for the substrate PE membrane are greater than those for membrane #67. This is due to the fixed charges in membrane #67 which restrict the transport of the co-ions. This leads to a difference in U of the ions transported. The separation ratios are discussed as follows (Section 4.3.2.3).

4.3.2.3. Calculation of Separation Ratio (U_{base}/U_{salt})

The separation ratios were calculated and are given in Table 4.3. For the uncharged substrate membrane, this separation ratio, as expected, is small. When the feed solution changes from NaOH/NaCl to NaOH/Na_2SO_4, the separation ratio (U_{NaOH}/U_{salt}) increases, ie., from 1.67 to 2.74 for the PE substrate membrane, since there is no charge (no Donnan exclusion). The separation ratio primarily depends on the diffusivity of the ionic species involved. The results suggested the separation in DD using the substrate membrane was poor.

Table 4.3. Dialysis coefficients, separation ratios and water transport for the systems of NaOH/NaCl and NaOH/Na_2SO_4 at 25°C [a].

Feed solution	U (L/m^2 h)		U_{NaOH}/U_{salt}	Water transport [b] (mL)
	U_{NaOH}	U_{salt}		
	PE substrate membrane			
1.00M NaOH + 0.50M NaCl	27.73	16.59	1.67	0.3
1.00M NaOH+0.50M Na_2SO_4	25.99	9.49	2.74	0.3
	Cation-exchange membrane #67			
1.00M NaOH + 0.50M NaCl	17.65	2.44	7.21	0.26 (*0.30*)
1.00M NaOH+0.50M Na_2SO_4	12.66	0.78	16.23	0.22 (*0.23*)

a. The raw data and calculations are given in Appendix B.
b. Calculated by a balance on NaOH; the values in bracket and italic obtained by single measurements were measured by syringes.

For membrane #67, U_{NaOH}, U_{NaCl} and U_{Na2SO4} are smaller than those for the PE substrate membrane. As can be seen from Table 4.3, the decrease in U_{NaCl} or U_{Na2SO4} is much larger than that in U_{NaOH}. This leads to an increase in the separation ratio. For example, when the feed solution is NaOH/NaCl, U_{NaOH}/U_{NaCl} is 7.21, and when the feed is NaOH/Na_2SO_4, U_{NaOH}/U_{Na2SO4} is 16.23. This can be also understood in terms of Donnan exclusion which discriminates on the base of the transport of co-ions across a charged membrane.

From Table 4.3, an increase in co-ion valency leads to an increase in the separation ratio. For membrane #67, when the salt changes from NaCl to Na_2SO_4, the

separation ratio increases from 7.21 to 16.23. The bivalent co-ion (SO_4^{2-}) is more excluded than the monovalent co-ion (Cl^-) by the Donnan effect due to the larger electrostatic interactions between the fixed charges and the bivalent co-ions. The effect of diffusivity in the membrane is less than the Donnan exclusion, though diffusion enhances the difference, ie., the diffusivity of SO_4^{2-} is lower than that of Cl^-. The results are consistent with the diffusion separation process discussed in Fig. 4.3.

The results suggest that NaOH and salts can be separated effectively by a cation-exchange membrane, such as #67, in a diffusion dialysis process.

4.3.3. Comparison with Results of Other Studies

A comparison is made, Table 4.4 which lists the diffusion dialysis results with various systems using cation-exchange membranes reported by Sata [125], Mika [145], and Wycisk et al. [136].

Sata [125] reported the performance with DD to separate NaOH and aluminate salt (AL), Table 4.4. In this case, AL in an alkaline solution should be a complex AlO_2^- rather than Al^{3+}. Thus, the system contains NaOH and $NaAlO_2$ and AlO_2^- while OH^- would act as the co-ions. As a result, OH^- is expected to go through while AlO_2^- is greatly restricted by the commercial cation-exchange membranes, CMX-SR and CMA-21. These membranes have similar ion-exchange capacities but different water contents. As can be seen in Table 4.4, U_{NaOH} is 1.63 $L/m^2 \cdot h$ for CMX-SR and 3.19 $L/m^2 \cdot h$ for CMA-21 while U_{salt} is 0.043 $L/m^2 \cdot h$ for CMX-SR and 0.112 $L/m^2 \cdot h$ for CMA-21. As

Table 4.4. Results of diffusion dialysis of separating alkaline and salts using cation-exchange membranes .

Membrane	Sata's results		Mika's results		Wycisk's results	
	NEOSEPTA CMX-SR	NEOSEPTA CMA-21	Poly(acrylic acid) cation-exchange membrane		Poly(mathacrylic acid-co-DVB) cation-exchange membrane	
Membrane properties:						
Resistance ($\Omega \cdot cm^2$)	1.80	0.50	-		0.91	
IEC (meq/g)	1.80	1.90	4.3		2.9	
Water content (%)	35	55	51		50	
Thickness (μm)	180	150	-		270	
Feed solution	5.0M NaOH 4.0 M AL	5.0M NaOH 4.0 M AL	1.0M NaOH 0.5M NaCl	1.0M NaOH 0.5M Na_2SO_4	1.0M NaOH 0.5M NaCl	1.0M NaOH 0.5M Na_2SO_4
U_{NaOH} (L/m^2h)	1.63	3.19	13.6	12.86	*12.23* [a]	*12.35* [a]
U_{salt} (L/m^2h)	0.043	0.112	11.6	0.77	*3.36* [a]	*1.08* [a]
$\frac{U_{NaOH}}{U_{salt}}$	38	28	4.9	15	*3.6* [b]	*11* [b]

a. Permeability coefficient, kg m^{-1} s^{-1} kPa^{-1}.

b. Permeability coefficient ratio.

discussed in Section 4.1, decreasing water content decreases the diffusion rate (dialysis coefficient) but increases the separation ratio. As expected, CMA-21 with a higher water content (55%) has a higher U_{NaOH} but a smaller separation ratio (U_{NaOH}/U_{salt} = 28) than CMX-SR.

Membrane #67 prepared in this work has a higher water content (67%) and a similar ion-exchange capacity (IEC = 2.23 meq/g). Comparing with Sata's work, although co-ions are monovalent, the larger AlO_2^- is expected to be more excluded than the smaller Cl^-. Thus, it is not surprising to observe in this work a much higher dialysis coefficient (U_{NaOH} = 12.66 -17.65 L/m^2·h) and a slightly lower separation ratio (U_{NaOH}/U_{NaCl} = 7.21-16.23 L/m^2·h). These results are consistent with the findings of Stachera et al. [54] who concluded that an increase in ion-exchange concentration of the membrane increased the separation ratios but reduced the diffusion coefficient for each ion.

Wycisk and Trochimczuk [136] reported their DD results with the same systems (NaOH/NaCl and NaOH/Na_2SO_4) using a cation-exchange membrane containing poly(methacrylic acid-co-DVB). They gave no information on water transport. However, in their paper, the permeability coefficient (P) was calculated by an equation derived from Eq. 4.1, assuming no water transport [135]. The permeability coefficient ratio (P_{NaOH}/P_{Salt}) was found to be between 3.3 and 3.6 for the NaOH/NaCl system and between 11 and 15 for the NaOH/Na_2SO_4 system, Table 4.4. These results are consistent with the results of dialysis coefficients obtained in this work. Permeability coefficients (P) are different from dialysis coefficients (U) since the membrane thicknesses are taken into account in permeability coefficients. Since both of the permeability coefficient (P)

and dialysis coefficient (U) are the measurement of ion permeability through membrane, comparable results for the separation ratio are tabulated.

Recently, Mika [145] studied diffusion dialysis of separation of NaOH and salts using a pore-filled cation-exchange membrane containing weak poly(acrylic acid) (PAA). That membrane was prepared by UV-initiated copolymerization of acrylic acid and the crosslinker, tetra(ethylene glycol) diacrylate (TTEGDA) using benzoin ethyl ether (BEE) as the photoinitiator. Comparing to the properties of membrane #67, Mika's membrane has a lower degree of crosslinking (TTEGDA = 1.5%), a much higher ion-exchange capacity (4.3 meq/g), and a lower water content (51%). The DD experiments were carried out under the same conditions of this work. Mika found that the dialysis coefficients (U_{NaOH} = 12-13 $L/m^2 \cdot h$) were similar to that of this work but separation ratios (U_{NaOH}/U_{NaCl} = 4.9 and U_{NaOH}/U_{Na2SO4} = 15) were smaller. As can be seen, the trend for changing the feed from NaOH/NaCl to NaOH/Na_2SO_4 is identical to that found by Wycist and this work. It should be noted that in Mika's work, besides the difference in functionality, the substrate membrane was different, a PP microporous membrane [145]. Hence, the difference in dialysis coefficients (U) and separation ratios (U_{NaOH}/U_{Na2SO4}) between Mika's work and this work are probably due to the differences in functionality and the properties of the membranes.

4.3. Summary

This chapter has discussed the evaluation of the cation-exchange membranes prepared in this work using diffusion dialysis with NaOH/NaCl and NaOH/Na_2SO_4. It was found that the cation-exchange membranes were capable of separating base and salt in DD applications.

Water transport was examined. Water transport depended on the net effect of the pressure and the electrical effects. The concentration of the ionic species across the membrane versus time was monitored. The diffusion coefficient and separation ratio were measured. The separation ratio of NaOH/Na_2SO_4 was found to be larger than that of NaOH/NaCl due to larger Donnan exclusion of the bivalent SO_4^{2-}.

The results obtained in this work were compared with the reported results of the DD using different cation-exchange membranes.

CHAPTER FIVE

MEMBRANE EVALUATION II

SEPARATION PERFORMANCE IN PRESSURE-DRIVEN PROCESSES

One of the most important industrial applications of membranes is pressure-driven separation of solutes and other species from water [148-150]. These processes include reverse osmosis (RO), nanofiltration (NF), ultrafiltration (UF), and microfiltration (MF).

Most membranes used in pressure-driven processes are non-charged or partially charged, such as thin film composite membranes with a charged skin layer. Due to the Donnan exclusion mechanism, the use of ion-exchange membranes in pressure-driven processes has interested membrane researchers for many years. Hoffer and Kedem in the 1960s investigated the separation of salts using charged membranes prepared by crosslinking albumin in a collodion matrix [151-154]. These workers developed mathematical models for separation performance of ion-exchange membranes under pressure-driven conditions. They reported negative rejections of the acid (HCl) for a mixture of salts/HCl under reverse osmosis condition [153-155]. Lonsdale et al., studied ion separation under pressure-driven conditions using commercial ion-exchange membranes [156]. Ceynowa reported the transport of electrolyte across a Nafion-120 cation-exchange membrane [157].

Recently, there has been renewed interest in using ion-exchange membranes in pressure-driven processes. Simons reported trace element removal from ash dam waters by nanofiltration [158]. Strathmann and co-workers have reported the retention measurements of charged membranes with electrolyte solutions in nanofiltration [159]. However, in spite of high solute rejections, low permeability and high cost of membranes have limited the application of ion-exchange membranes in pressure-driven processes.

Some nanofiltration thin-film-composite (TFC) membranes with charged skin layers (lower charge density than the pore-filled membranes and greater than conventional RO membranes), such as NF-45 (FilmTec Corporation) and Desal-5 (Osmonics), are commercially available and inexpensive. As non-commercialized membranes, McMaster pore-filled ion-exchange membranes are an alternative new approach. Poly(4-vinylpyridine salt) (PVP salt)-filled anion-exchange membranes have demonstrated superior performance for water softening and ion separation in extra-low-pressure nanofiltration [16,47,48]. The pore-filled membranes prepared in this work have high water contents and fixed charged concentrations which are expected to result in high fluxes and good rejection in pressure-driven processes.

One of the objectives of this thesis is to evaluate the membranes prepared in this work under pressure-driven conditions. This work will help gain an understanding of the mechanism of transport through examining separation performance of single and mixed ion systems. This understanding will help evaluate the performance of these membranes to NF applications such as water softening. The factors affecting pure water flux, separation of NaCl solutions, negative cation rejections are presented.

5.1. EXPERIMENTAL

5.1.1. Materials

The membranes used in this chapter were cation-exchange membranes containing poly(styrene-DVB sulfonic acid)-filled in a polyethylene membrane. The preparation and characterization of membranes have been described in Chapters 2 and 3, respectively.

Inorganic reagents used, NaOH, NaCl, HCl, $MgCl_2$, and Na_2SO_4 (Aldrich), were all AR grades. Pure water used in this study was RO permeate water that were further deionized and carbon filtered.

5.1.2. Pressure-Driven NF/RO System

The pressure-driven system used in this study was a 6-cell nanofiltration/reverse osmosis (NF/RO) testing system [160]. The system consists of: an 8-liter feed tank (1) and a magnetic stirrer (1'), a water-cooled heat exchanger (2), a high pressure pump (3) connected with an accumulator (4) pre-charged with nitrogen gas and a pressure-protector (5) which is a security system used to shut off the system power when the pressure is higher or lower than the pre-set maximum or minimum pressure, a sieve filter (6), six cross flow cells (7), a pressure gauge (8), a check valve (9) to protect the gauge from over pressurizing of the system, and a back pressure regulator (10). Three thermocouples, which were used to measure the temperature during the experiments, were installed in cells #2, #4, and #6.

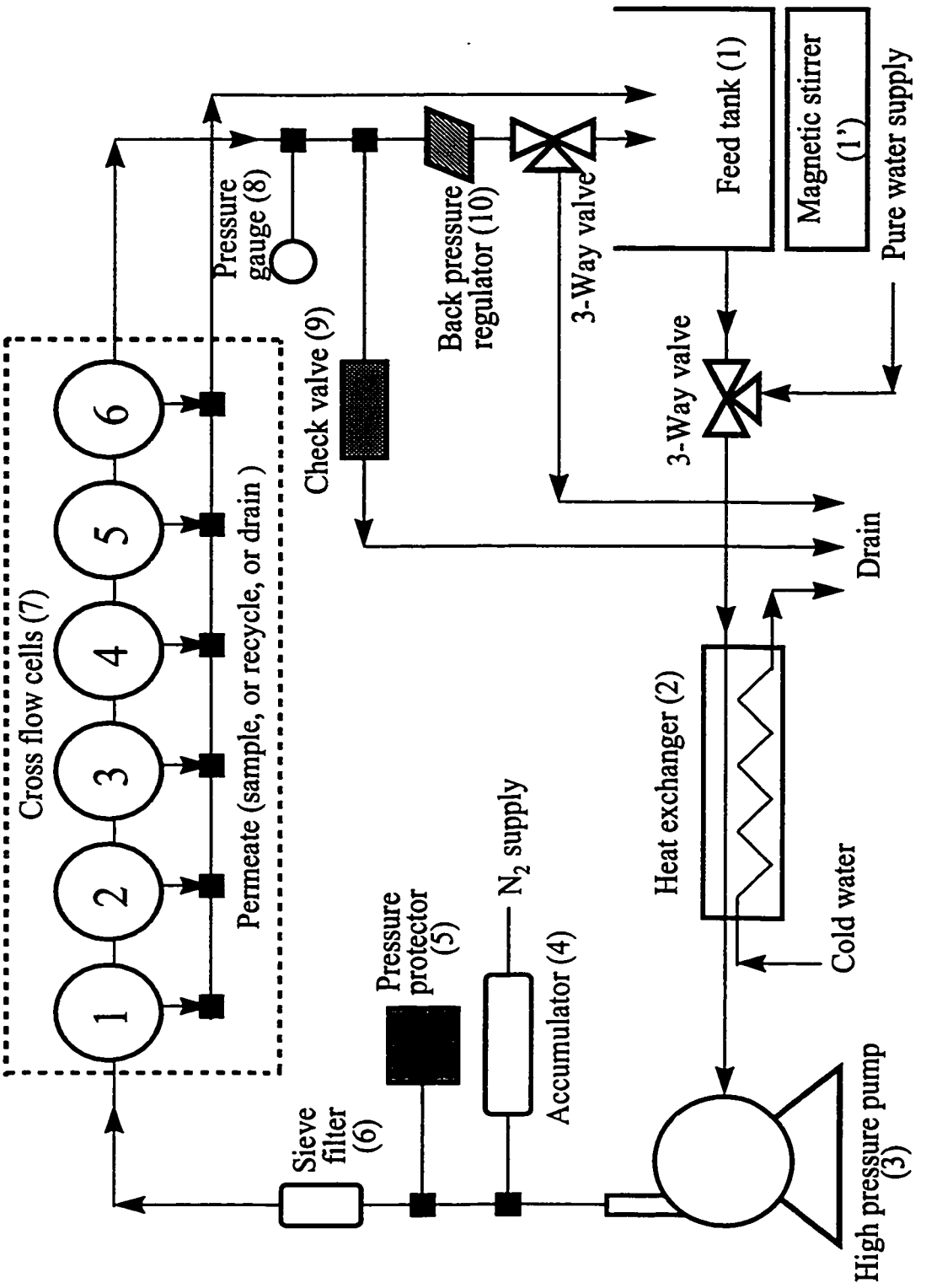

Fig. 5.1. Nanofiltration/reverse osmosis (NF/RO) system [160].

Each cross flow cell contained a flat sheet membrane sample which was placed on a porous support disk. The effective membrane area was 15.08 cm^2. The flow rate of the feed solution was controlled at 1.00 ± 0.05 L/min throughout the experiments. The temperature of the NF/RO system was controlled between 22 and 26 °C and the results of fluxes were corrected to 25 °C [16,47]. This system was kept running 24 hours a day, 7 days a week.

5.1.3. Permeability and Separation Measurements

Two sets of membranes prepared in this work were evaluated. The NF/RO system was run continuously for seven months with the first set of membranes. At this point, the membranes were replaced by the second set which was tested for a six-month period. Pure water was used as the initial feed until the flux was stabilized. Following stabilization, various solute solutions were used as the feed with pure water permeability measurements tested between the salt solution experiments.

Flux measurements were carried out by collecting and weighing the permeate sample for a given period of time. The concentrations of the feed and the permeate were determined by the conductivity meter (YSI, Model 31) for single solutes or by ion exchange chromatography (Dionex, DX-100) for the mixed solutes. The flux was calculated from the following equation:

$$\text{Flux } (kg/m^2s) = \frac{\alpha_T m}{\tau A_m} \qquad (5.3)$$

where m was the mass of permeate collected over the time τ, A_m was the active membrane area, and α_T was the temperature correction factor calculated by the following empirical equation [161]:

$$\alpha_T = - 0.575 \ln T + 2.85 \quad \textbf{(5. 4)}$$

where T was the temperature in Celsius.

The rejection of inorganic solutes or ionic species were calculated by the following equation:

$$\text{Rejection (\%)} = \left(1 - \frac{C_P}{C_F} \right) \times 100\% \quad \textbf{(5. 3)}$$

where C_F and C_P were the concentrations of the species in the feed and the permeate, respectively.

5.2. RESULTS AND DISCUSSION

Two sets of the cation-exchange membranes with various characteristics were selected to test in the NF/RO system. The properties of the membranes are given in Tables 5.1 and 5.2.

As can be seen in Table 5.1, set 1 has membranes with various mass increases and degrees of crosslinking (DVB percent). In order to study the effects of sulfonation temperature, ion-exchange concentration and substrate membrane, set 1 was replaced by

Table 5.1. Properties of set 1 of membranes used in the NF/RO system.

NF/RO Cell number	1	2	3	4	5	6
Membrane number	#68	#67	#71	#72	#70	#69
DVB (%)	2.5	2.5	2.5	2.5	1.0	1.0
Mass increase (%)	80	83	86	74	150	64
Sulfonation Temp. (°C)	0	0	0	0	0	0
IE Capacity (meq/g)	1.92	2.23	2.20	2.17	3.50	2.25
Water content (%)	59	67	-	-	68	65
Thickness (μm)	-	67	-	-	85	65
IE concentration (eq/kg)	3.3	3.3	-	-	5.1	3.5
Water flux at 2000 kPa ($\times 10^3$, kg/m^{2}s)	0.67	0.66	0.67	0.69	0.85	0.87

Table 5.2. Properties of set 2 of membranes used in the NF/RO system.

NF/RO Cell number	1	2	3	4	5	6
Membrane number	#85	#97	#92	#74	#70	#69
DVB (%)	3.5	1.0	2.5	2.5	1.0	1.0
Mass increase (%)	60	190	72	192	150	64
Sulfonation Temp. (°C)	0	40	40	0	0	0
Sulfonation yield (%)	57	83	82	55	58	61
IE Capacity (meq/g)	2.07	5.23	3.28	3.60	3.50	2.25
Water content (%)	-	72	67	-	68	65
Thickness (μm)	-	83	72	-	85	65
IE concentration (eq/kg)	-	7.3	4.9	-	5.1	3.5
Water flux at 2000 kPa ($\times 10^3$, kg/m^{2}s)	0.32	0.23	0.29	0.38	0.85	0.87
Remark				Different substrate *		

* Membrane #74 uses a different PE substrate membrane (see Table 5.4 for detail).

set 2. Set 2 has membranes with two sulfonation temperatures and various ion-exchange capacities/concentrations, mass increases, degrees of crosslinking, and a different substrate membrane. It should be noted that sets 1 and 2 both have membranes #69 and #70.

The results of pressure-driven permeation testing are presented and discussed in the following three subsections using pure water, NaCl solutions, and NaCl/$MgCl_2$ solutions as the feed. In this work, it is assumed that fouling of the membranes is negligible and that the structure of the porous support of each cell does not interfere effectively with solute or solvent transport significantly. The ranges and experimental errors in operational variables and measurements are given in Table 5.3.

Table 5.3. The ranges and experimental errors in operational variables and measurements.

Variable	Range	Error *(%)*
Pressure (kPa)	500 - 3500	*(± 2.5%)*
Temperature (°C)	23 - 26	± 0.1
Feed flow rate (L/min)	1.00	0.05
Flux ($\times 10^3$, kg/m^{2}s)	0.1 - 5	*(< 1%)*
Concentration (ppm)	0 - 12,000	*(± 2.5%)*
Mass (g)	5 - 15	± 0.01

5.2.1. Performance with Pure Water

5.2.1.1. Pure Water Flux

The results of pure water fluxes as a function of time for set 1 are shown in Fig. 5.2 and for set 2 in Fig. 5.3.

The stabilization time, from Fig. 5.2, for set 1 membranes at 2000 kPa at 25°C was approximately 150 h. This long stabilization time is likely due to the reorganization of the polyelectrolyte chains occurring under pressure. After stabilization (~ 180 h), NaCl solutions were tested and pure water fluxes were measured between NaCl solutions. The water fluxes, from Fig. 5.2, for the membranes do not change significantly after stabilization. It is known that fluxes for electrolyte solutions can be different from the pure water flux due to the electrostatic interactions between the ionic species and the fixed charges on the membranes. However, it was found that the pure water fluxes recovered when the electrolyte solutions were replaced by pure water. This suggests that a change in membrane structure occurs when an electrolyte is used but this change is reversible.

The results of pure water experiments for set 2 membranes, Fig. 5.3, have shown similar phenomena. Thus, the pore-filled cation-exchange membranes used in the NF/RO system are stable in separating salt solutions.

5.2.1.2. Effect of Degree of Crosslinking

The degree of crosslinking, Table 5.1, mainly affects the pure water flux, Fig. 5.2. For example, #69 and #70 (DVB = 1.0%) have identical water flux, 0.86×10^{-3} kg/m^{2}s,

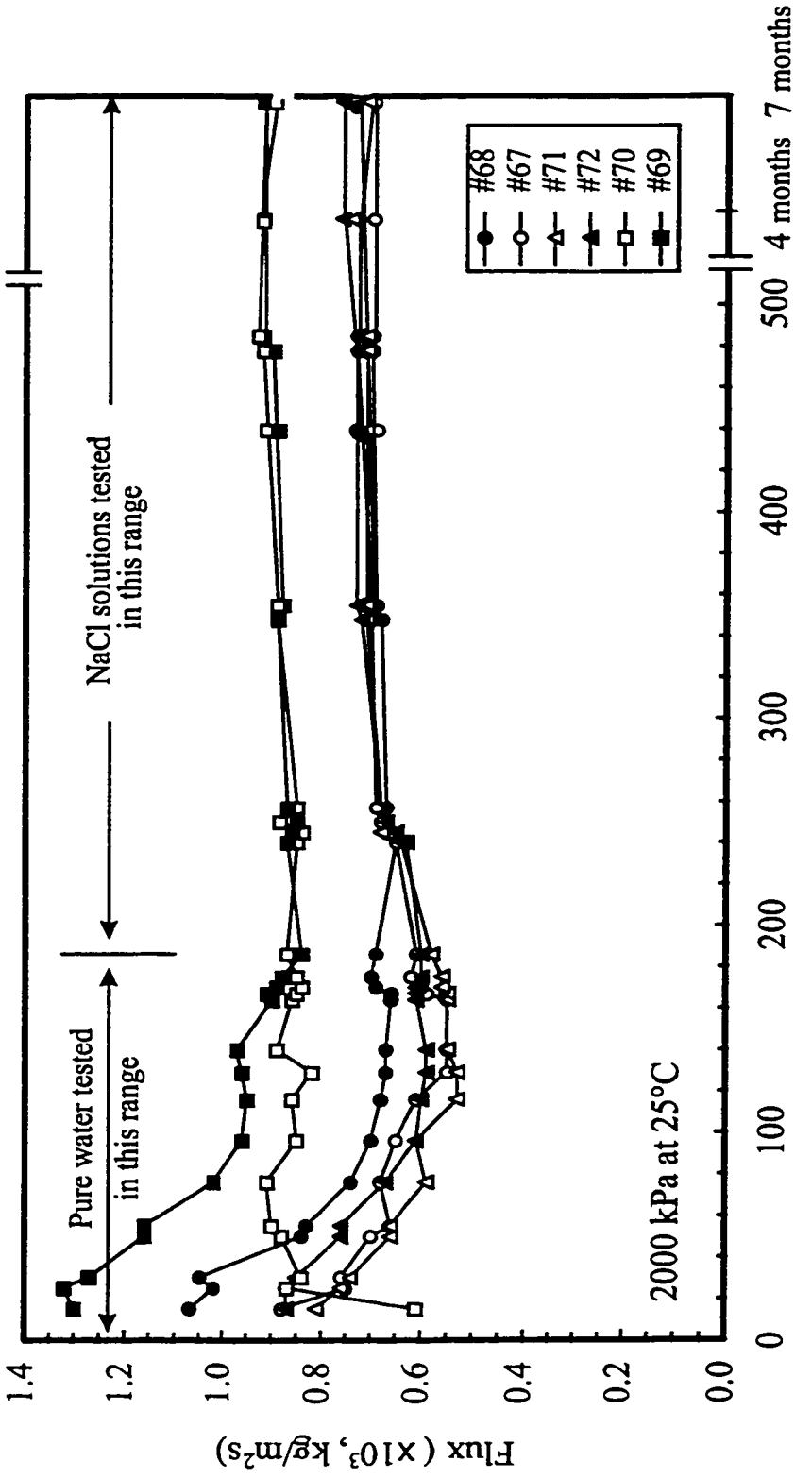

Fig. 5.2. Pure water flux of set 1 membranes versus time in NF/RO system; NaCl solutions were tested after 180 h; the error in flux is given in Table 5.4; 2000 kPa pressure at 25°C

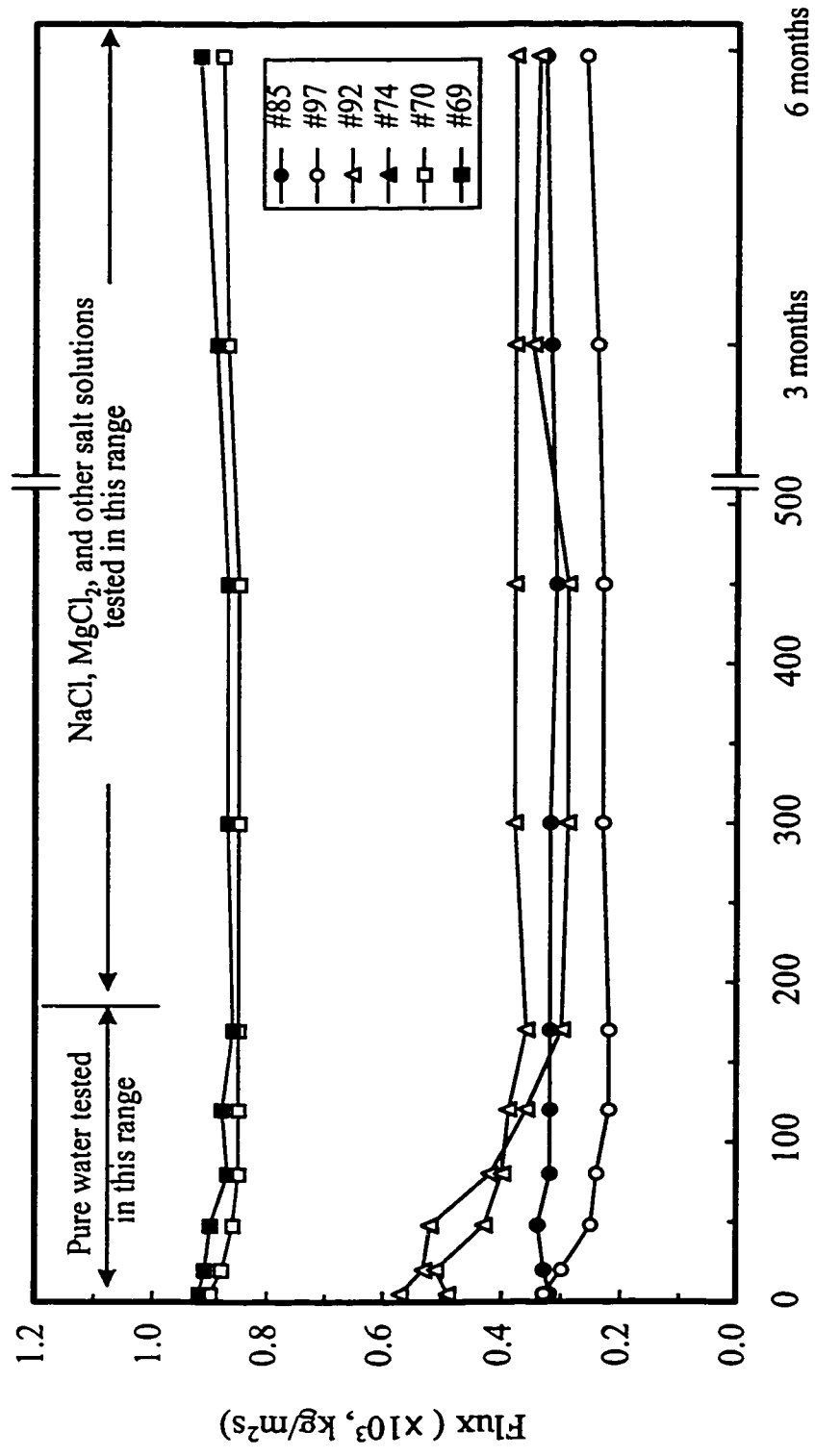

Fig. 5.3. Pure water flux of set 2 membranes versus time in NF/RO system; various salt solutions were tested after 180 h; membranes #69 and #70 were used in set 1; the error in flux is given in Table 5.4; 3000 kPa pressure at 25°C.

which is approximately 30% greater than for the other four membranes (DVB = 2.5%), 0.66×10^{-3} kg/m^{2}s. These results are consistent with the findings reported by Mika et al. for PVP-filled anion-exchange membranes [160].

5.2.1.3. Effect of Mass Increase

The mass increase does not affect pure water flux significantly, Table 5.1. Membranes #67, #68, #71, and #72 (DVB = 2.5%, 0°C sulfonation) have mass increase ranging from 74% to 86% (approximately 16% of difference) but nearly identical pure water fluxes. Membranes #69 and #70 (DVB = 1.0%, 0°C sulfonation) have identical pure water flux although membrane #70 had more than 2.5 times the mass increase of poly(styrene-DVB) incorporated than membrane #69. It is concluded that the mass increase does not affect pure water flux significantly.

5.2.1.4. Effect of Substrate Membrane

The substrate membrane of sample #74 is different from those of other membranes used in this study. A comparison of properties of the two substrate membranes is given in Table 5.4. As can be seen, the properties of the two substrate polyethylene membranes are similar. The water flux for membrane #74 (DVB = 2.5%) is 0.38×10^{-3} kg/m^{2}s, which is less than those for membranes #67 and #71, 0.66×10^{-3} kg/m^{2}s, even though #67 and #71 have different mass increases. The difference in pure water flux is likely due to the differences in pore size and thickness between the two substrate membranes. For example, the pore size of the substrate for membrane #74 is

Table 5.4. Comparison of two polyethylene substrate membranes [a] (3M).

Resulting membrane #	ID # [b]	Material	Thickness (μm, *mil*)	Pore size (μm)	Porosity (%)
Membranes except #74	PE-1 533-10	polyethylene	45, *1.8*	0.196	78
#74	PE-1 X1270-14	polyethylene	55, *2.2*	0.178	79

a. Data provided by the 3M Company.
b. Manufacturer's ID numbers.

0.178 μm, which is smaller than 0.196 μm for the rest of the membranes, while the thickness of the substrate for membrane #74 is approximately 20% thicker than that for the other membranes. Both the factors, pore size and thickness, are consistent with the observed reduced flux for membrane #74.

5.2.1.5. Effect of Sulfonation Temperature and Ion-Exchange Concentration

The effect of sulfonation temperature on pure water flux, Tables 5.1 and 5.2, is significant. For example, increasing the sulfonation temperature from 0°C to 40°C leads to a decrease of 73% in pure water flux, ie., from 0.85×10^{-3} kg/m^{2}s for membrane #70 (0°C sulfonation, DVB = 1.0%) to 0.23×10^{-3} kg/m^{2}s for membrane #97 (40°C sulfonation, DVB = 1.0%). For the membranes with identical degrees of crosslinking (DVB = 2.5%), an increase in sulfonation temperature from 0°C (#67) to 40°C (#92) leads to a 57% decrease in pure water flux, ie., from 0.29 ($\times 10^3$, kg/m^{2}s) for membrane #92 (40°C) to 0.67 ($\times 10^3$, kg/m^{2}s) of membrane #67 (0°C).

The mechanism of sulfonation and the effect of sulfonation temperature on ion-exchange capacity/concentration are discussed in Chapters 2 and 3. It was found that an increase in sulfonation temperature, ie., from 0°C to 40°C, led to an increase in ion-exchange capacity/concentrations. Thus, it is concluded that the 40°C sulfonation leads to a higher ion-exchange concentration but a lower pure water flux than the 0°C sulfonation.

The effects of sulfonation temperature and ion-exchange concentration on pure water flux are possibly due to the following reason. The 40°C sulfonation membranes have higher ion-exchange concentrations and the highly charged polyelectrolyte chains repel each other. These electrostatic interactions force the polyelectrolyte chains to extend into the pores. This resulted in an increase in excluded volume which will lead to a lower solution flux [34,60,62]. Thus, the pure water flux through the 40°C sulfonation membranes is expected to be lower than that through the 0°C sulfonation membranes.

5.2.2. Performance with NaCl Feed Solutions

Both sets of membranes were evaluated in the NF/RO system with inorganic solutes, such as NaCl, under various feed conditions. This section discusses fluxes and rejections of separating NaCl using the pore-filled cation-exchange membranes.

5.2.2.1. Flux of NaCl Solution

The conformation of polyelectrolytes affects the membrane performance. It is known that the conformation of polyelectrolytes changes according to the changes in the external solution, such as the ionic strength (salt concentration), the nature of ionic

species or the pH. For example, Mika et al. [16,47,48], reported the pH valve effect for PVP-filled membranes due to conformational changes with the pH of the contacting solutions.

The flux of NaCl solutions through both sets 1 and 2 membranes as a function of the concentration of NaCl was determined. The experiments with set 1 of membranes were carried out at 2000 kPa and with set 2 at 3000 kPa and 25°C using various concentrations of NaCl solutions as the feed. The flux results of sets 1 and 2 membranes are shown in Figs. 5.4 and 5.5, respectively.

The experiments for testing set 1 membranes were performed in the order of increasing concentration of NaCl, while set 2 membranes were performed in random order of concentration of NaCl. Similar trends of flux *versus* salt concentration were found. For both sets of membranes, the pure water flux was recovered when NaCl solutions were replaced by pure water.

The data shown in Fig. 5.4 and Fig. 5.5 illustrate that flux changes as a function of concentration of NaCl solution. The relationship between flux and concentration of NaCl is similar for sets 1 and 2. First, the flux increased by approximately 40-60% when the concentration of the NaCl solution increases from 0 to approximately 200 ppm. For example, for membrane #69, the flux increases approximately 60% (from 0.87×10^{-3} kg/m^2s to 1.38×10^{-3} kg/m^2s) when the feed is changed from pure water to an NaCl solution of 180 ppm. Secondly, after this increase in flux, the flux does not change significantly as the concentration of NaCl. For example, for set 1 membranes, the flux

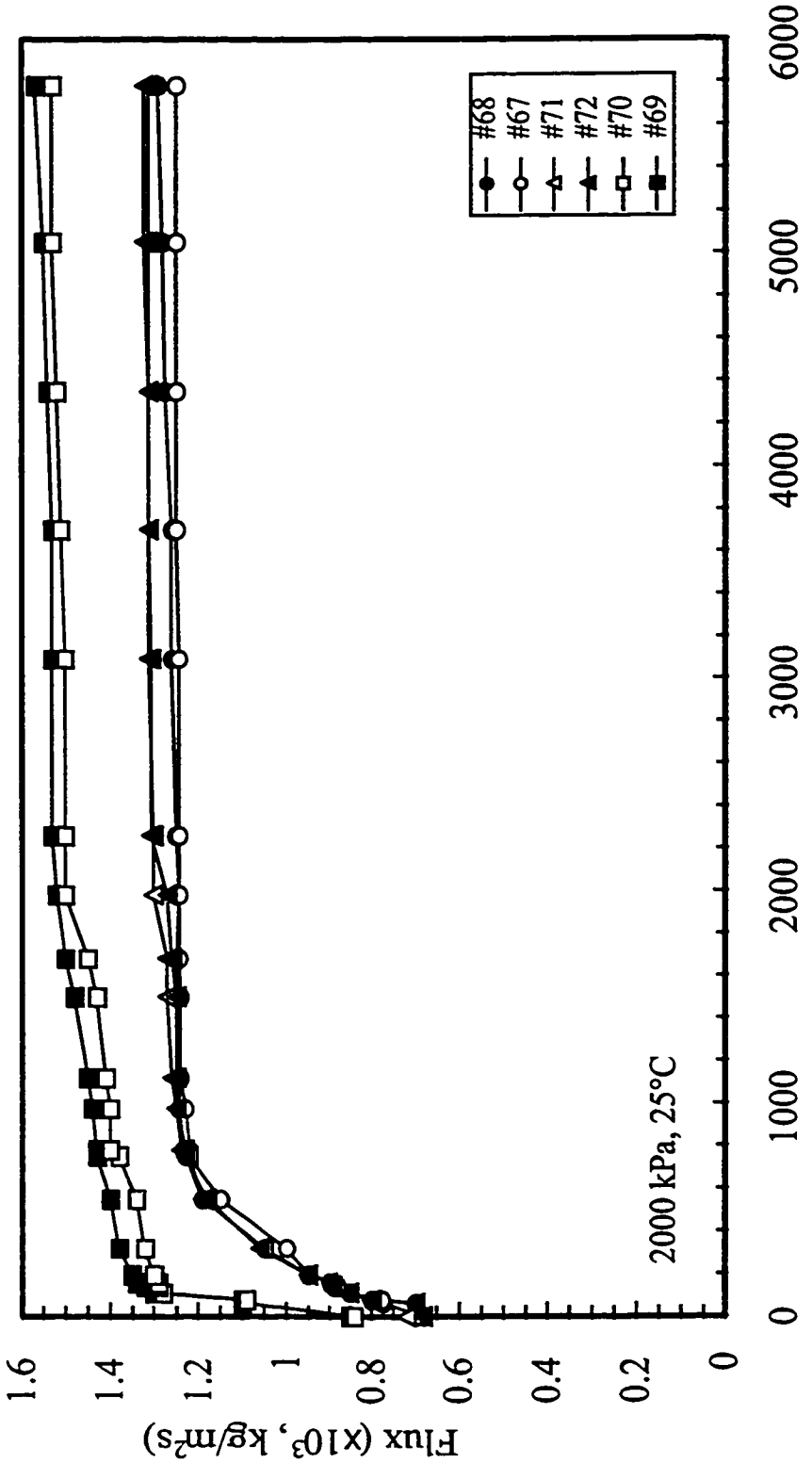

Fig. 5.4. Solution fluxes of set 1 membranes as a function of concentration of NaCl; the error in flux is given in Table 5.3; 2000 kPa pressure at 25°C.

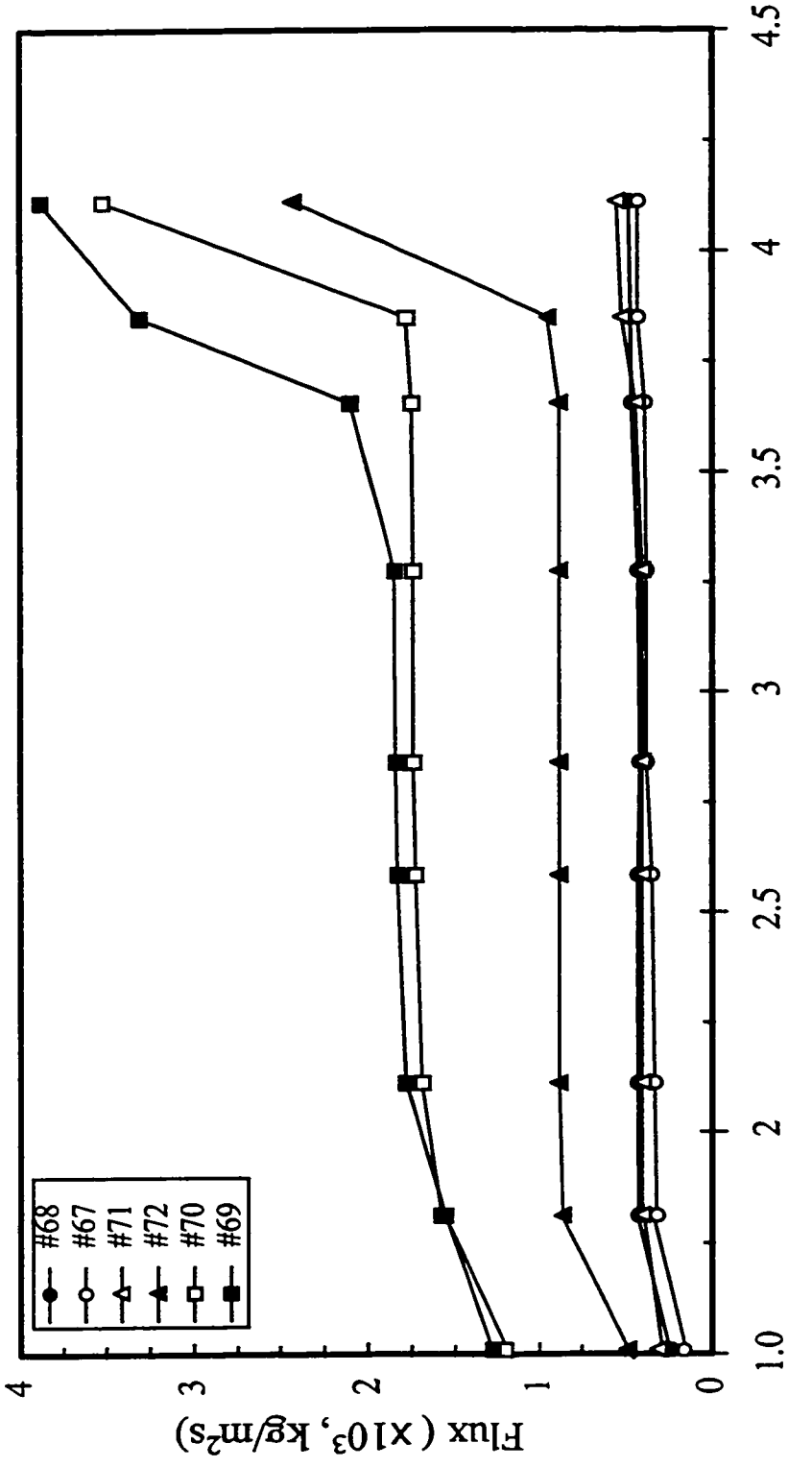

Fig. 5.5. Solution flux of set 2 membranes as a function of concentration of NaCl; the error in flux is given in Table 5.3; 3000 kPa pressure at 25°C.

increases less than 10% when the concentration of NaCl is increased from 500 ppm to nearly 6000 ppm. Thirdly, the flux of some membranes increases dramatically, ie., up to 3-5 times, when the concentration of NaCl is very high. For example, in Fig. 5.5, the flux of membrane #69 increases from 1.25×10^{-3} kg/m^{2}s to 3.88×10^{-3} kg/m^{2}s when the concentration of NaCl is increased from 4,460 ppm (log[NaCl] = 3.65]) to 13,590 ppm (log[NaCl] = 4.13). Set 1 membranes were never tested at such a high concentration and hence such an increase in flux was not observed. Mika et al. [16,48,160] have reported similar observations of the effect of high salt concentration on flux for PVP-filled anion-exchange membranes.

The flux of NaCl solutions, Figs. 5.4 and 5.5, was found to mainly depend on the degree of crosslinking. The fluxes for membranes #69 and #70 (DVB = 1.0%) are approximately 25% higher than those of the other four membranes (DVB = 2.5%). It was observed that the mass increase did not affect the fluxes of NaCl solutions significantly and that the effect of sulfonation was obvious. For example, from Fig. 5.5, the flux for membrane #70 (0°C sulfonation) is approximately 3 times higher than that for membrane #97 (40°C sulfonation) when the concentration of NaCl is between 200 and 5000 ppm.

Such behavior, ie., the increase in flux as the concentration of NaCl increase, is different from that of commercial TFC membranes where it is found that a higher feed concentration of salt solutions often leads to a lower flux due to osmotic pressure effects [161]. In this work, the increase in flux of NaCl solutions through the membrane is probably due to the change in the conformation of the polyelectrolytes in the membranes with salt concentration.

When pure water is used, the interactions between the charged polyelectrolyte segments repel each other and the polymer chains are forced to extend into the pores of the membranes. When pure water is replaced by a solution containing ionic species, the fixed charges are partially neutralized by the counter-ions (Na^+), known as charge screening (or charge shielding). This reduces the repelling forces between the charged polymer chains allowing the segment of the polymer chain to segregate on a micro level, effectively increasing the pathways available for solutions permeation and hence a higher flux is obtained. One model of this phenomenon is the ionic cluster model which is discussed next.

The effect of salt on polyelectrolyte structure can also be understood in terms of an ionic cluster model. The cluster models of polyelectrolytes proposed by Eisenberg [163,164] were based on linear ionomers and could be applied to slightly crosslinked polyelectrolytes. In salt solutions, the structure of the polyelectrolyte chains are not linear but assumed to form ionic clusters (coiling structure) by aggregating ion pairs. Ionic clusters contained fixed ion, counter-ions and the solvent (water). As a result, with increasing the concentration of counter-ions, the ionic clusters are re-organizing their conformation *via* breaking the old equilibrium and forming a new equilibrium of the ionic clusters in order to increase their entropy, resulting in reduction in repulsion between the charged polyelectrolyte chains. Hence, a higher flux is observed.

With the non-crosslinked polyelectrolyte gels, the effect of charge screening leads to collapse of the polyelectrolyte chains to the pore wall [165,166]. However, polyelectrolyte gel collapse is unlikely to occur in this work due to the following two

reasons. Firstly, the polyelectrolyte gels in the membrane is crosslinked by DVB as well as sulfone formation (Chapter 2). These crosslinks prevent collapse of the polyelectrolyte chains. Secondly, the concentration of the external NaCl used in this study does not seem to be high, ie., up to approximately 13,000 ppm (0.22 M) which is significantly lower than the ion-exchange concentrations (between 3.3 and 7.3 eq/kg) in this study. It is known that the concentration of the counter-ions (Na^+) is higher in the membrane than in the solution due to charge neutrality [167]. This suggests that the counter-ions in the membrane affect dramatically the polyelectrolyte gels which are "deformable". The charge screening leads to a significant increase in flux by increasing the ionic strength of the solution.

5.2.2.2. Rejection of NaCl

The results of salt rejections of membranes of set 1 and 2 as a function of concentration of NaCl are shown in Figs. 5.6 and 5.7.

For both sets of membranes, the rejection of NaCl decreases as the concentration of NaCl increased. For example, from Fig. 5.6, the rejection for membrane #70 decreases from greater than 99% to approximately 80% when the concentration of NaCl is changed from 300 ppm to nearly 6,000 ppm.

Comparing the salt rejection with flux in Fig. 5.4 and Fig. 5.5, for each membrane, generally, an increase in flux accompanies a decrease in rejection. For example, for membrane #69, an increase in concentration of NaCl by 600 ppm, from 0 to approximately 600 ppm, leads to an increase in flux by 60% (from 0.87×10^{-3} kg/m^{2}s to

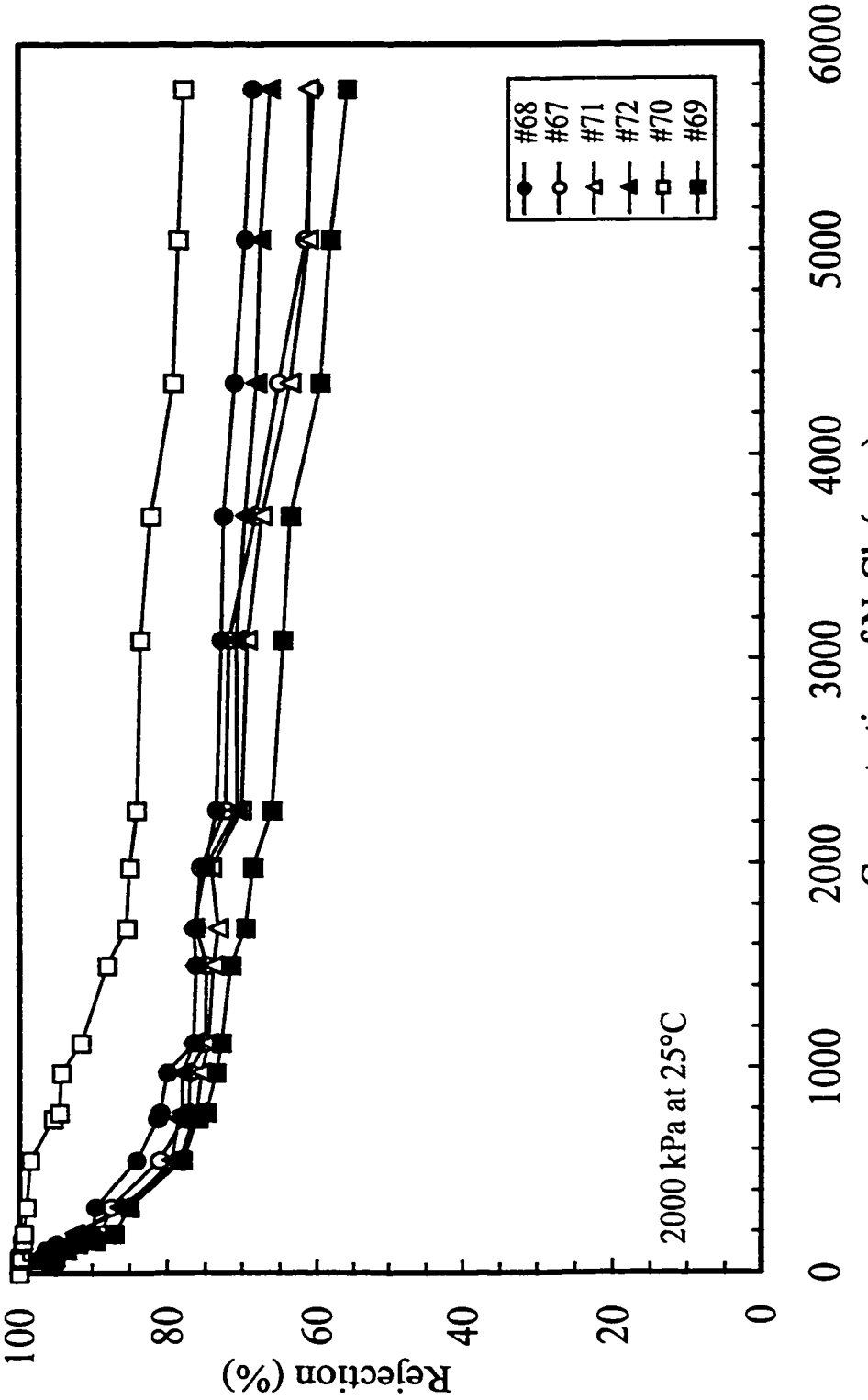

Fig. 5.6. Rejection of set 1 membranes as a function of concentration of NaCl; the error in rejection was less than 2.5%; 2000 kPa pressure at 25°C.

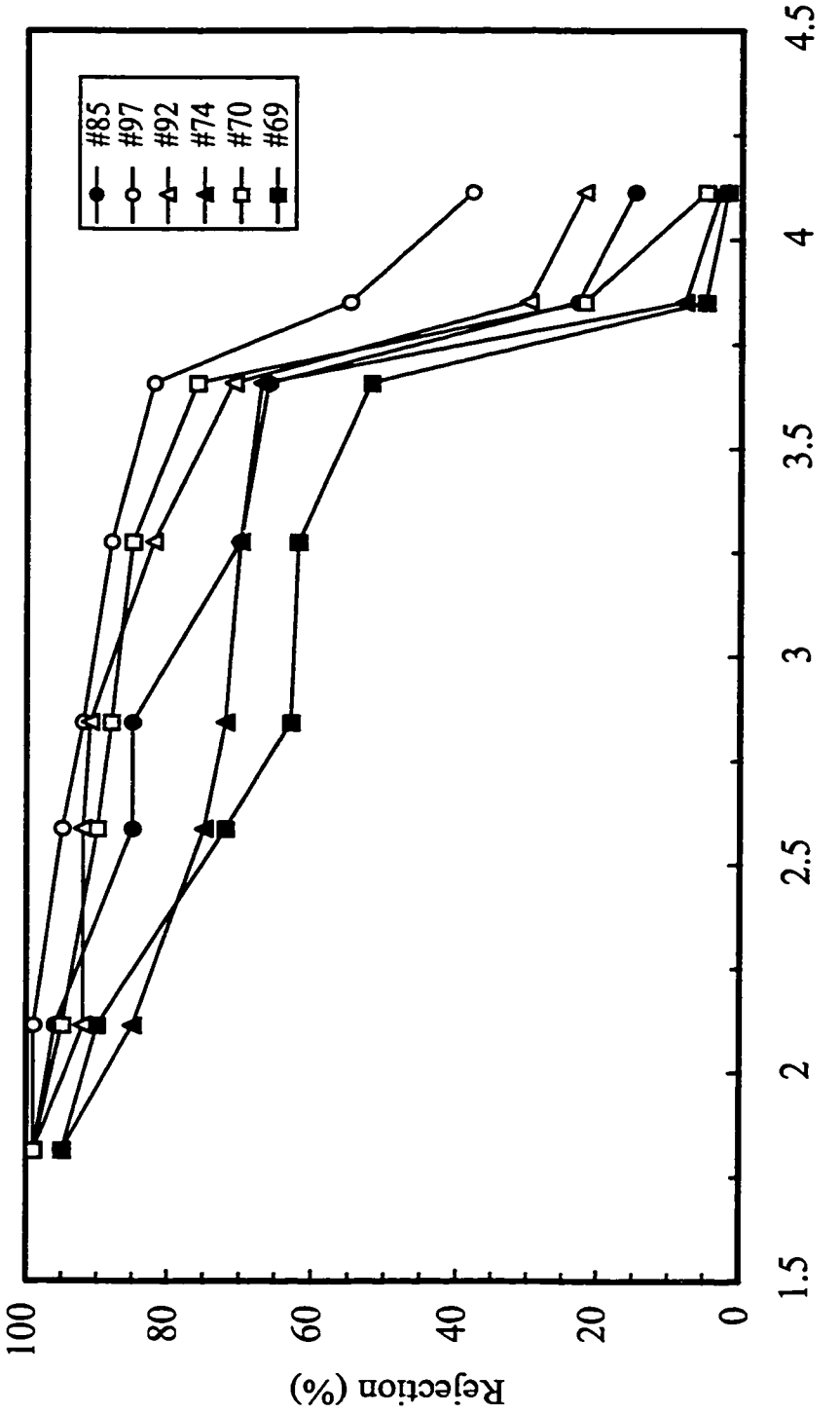

Fig. 5.7. Rejection of set 2 membranes as a function of concentration of NaCl; the error in rejection was less than 2.5%; 3000 kPa pressure at 25°C.

1.38×10^{-3} kg/m^{2}s) and a reduction in rejection of approximately 24% (from 99% to 76%). When the feed concentration is very high and the flux is further enhanced, the rejection decreases even more. For example, for membrane #69, an increase in concentration of NaCl by 35%, ie., from 4,500 ppm (log[NaCl] = 3.66) to 7,100 ppm (log[NaCl] = 3.85), leads to a decrease in rejection by over 80%, ie., from 52% to less than 10%, Fig. 5.7.

From Fig. 5.6, membrane #70 with the highest ion-exchange concentration (fixed charge concentration) has the highest rejection. The other five membranes with nearly identical ion-exchange concentrations appear to have lower and similar rejections. This is because the Donnan exclusion is higher for membranes with higher ion-exchange concentration. Similarly, for set 2 membranes, the rejection depends on ion-exchange concentration. For example, membrane #97 with the highest ion-exchange concentration was found to have the highest salt rejection, Fig. 5.7.

5.2.3. Performance with NaCl-$MgCl_2$ Feed Solution

The flux and rejection of the membranes for separating single solute (NaCl) solutions have been presented. The pore-filled membranes were tested also with $MgCl_2$ and mixed salt solutions (NaCl/$MgCl_2$). This section presents the separation performance of the single and mixed solute solutions using a typical pore-filled cation-exchange membrane (#67), also reported in sections 5.2.1 and 5.2.2. The other membranes were found to behave similarly. First, the major results are presented followed by a discussion of these results.

5.2.3.1. Results of Flux and Rejection of Single and Mixed Salt Solutions

The results of flux and rejection for membrane #67 as a function of salt concentration are shown in Fig. 5.8 for single solute solutions (NaCl or $MgCl_2$) and in Figs. 5.9 and 5.10 for mixed solute solutions (mixtures of NaCl/$MgCl_2$).

From Fig. 5.8, the flux of both single NaCl and single $MgCl_2$ solutions increases with increasing the feed concentration, similar to the results shown in Fig. 5.4. The solution flux of single NaCl was found to be higher than that of single $MgCl_2$ when the concentrations of NaCl and $MgCl_2$ were the same. The rejection of both single NaCl and single $MgCl_2$ decreases with increasing the feed concentration, similar to the results shown in Fig. 5.5. The rejection of single NaCl was found to be higher than that of single $MgCl_2$ when the concentrations of NaCl and $MgCl_2$ were the same.

From Fig. 5.9, the solution flux of mixed NaCl-$MgCl_2$ increases at the beginning but does not change significantly afterwards with increasing feed concentration of $MgCl_2$ when the concentration of NaCl is kept constant at 150 ppm. In this mixed system (NaCl-$MgCl_2$), the rejection of both NaCl and $MgCl_2$ decreases with increasing the feed concentration of $MgCl_2$ (while [NaCl] was kept constant). The rejection of NaCl was found to be lower than that of $MgCl_2$, opposite of the trend with single solute.

The pressure effect on flux and rejections is shown in Fig. 5.10. For the mixed salt system containing NaCl (110 ppm) and $MgCl_2$ (55 ppm), a non-linear relationship of flux *versus* pressure was observed, ie., flux increased as increasing the applied pressure.

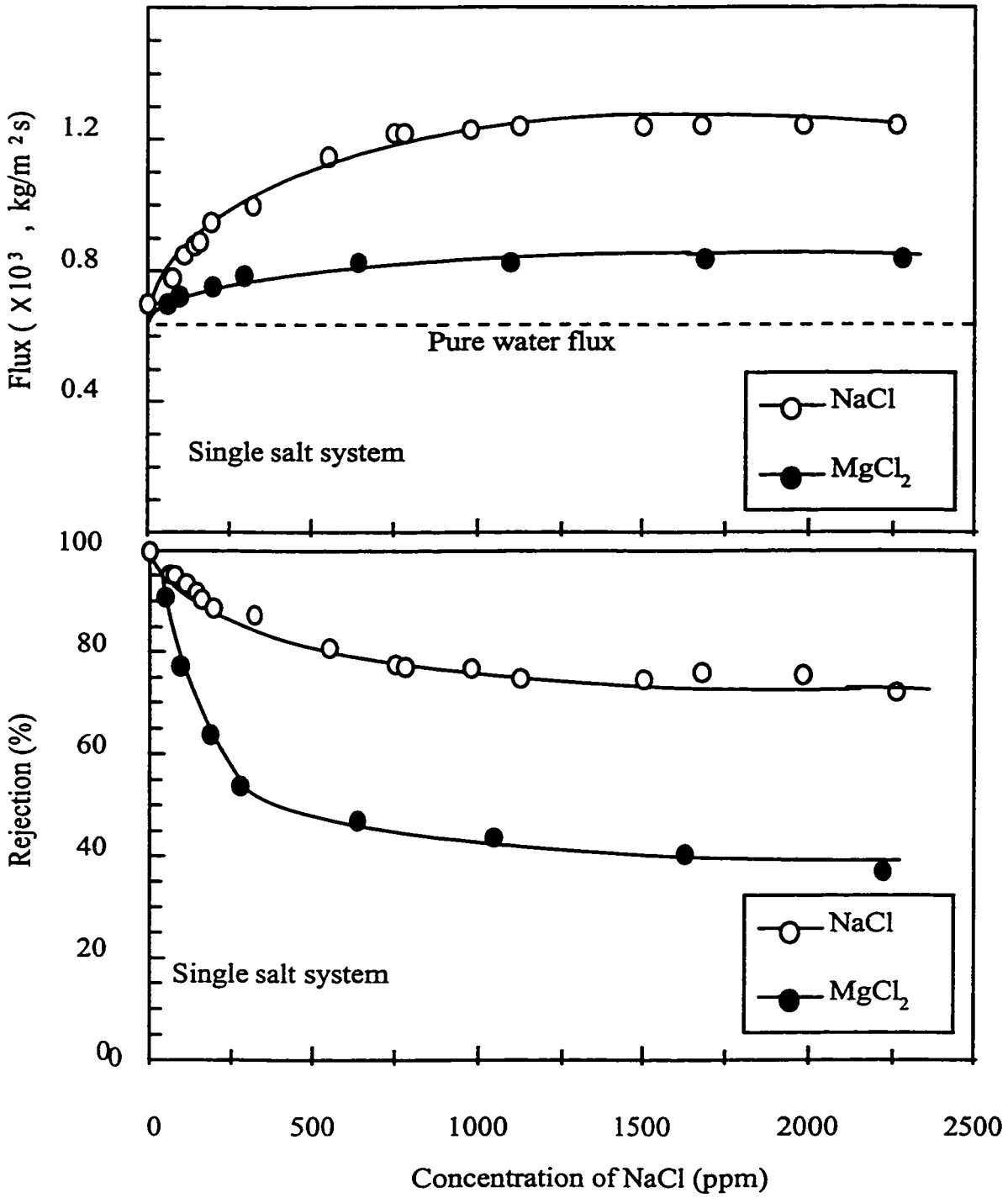

Fig. 5.8. Rejection and flux as a function of concentration for single solutes with membrane #67; the single salt systems were NaCl and $MgCl_2$; 2000 kPa pressure at 25°C.

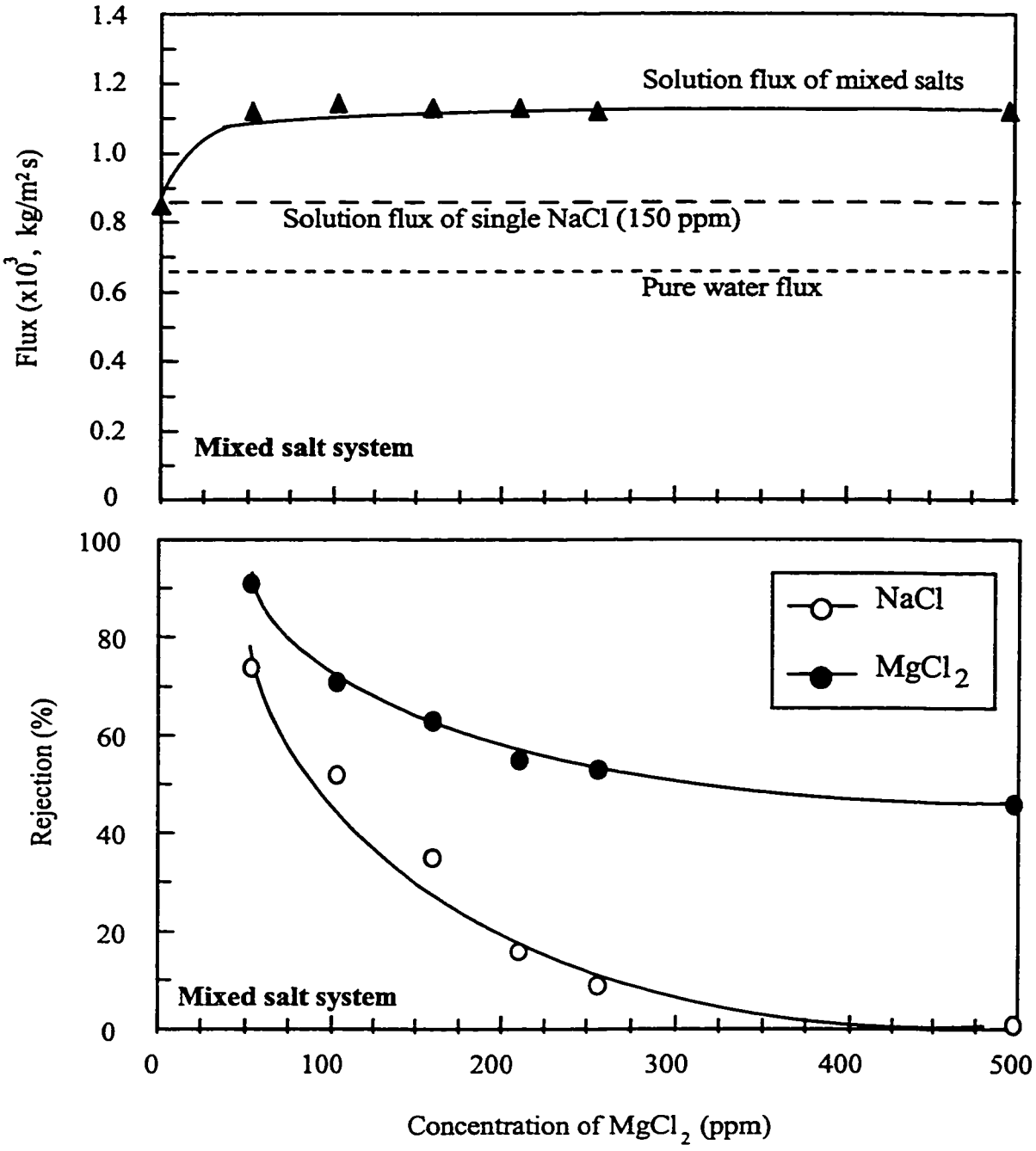

Fig. 5.9. Flux and rejection as a function of concentration of $MgCl_2$ with membrane #67; the mixed salt system was NaCl/$MgCl_2$; the concentration of NaCl was kept at 150 ppm; 2000 kPa pressure at 25°C.

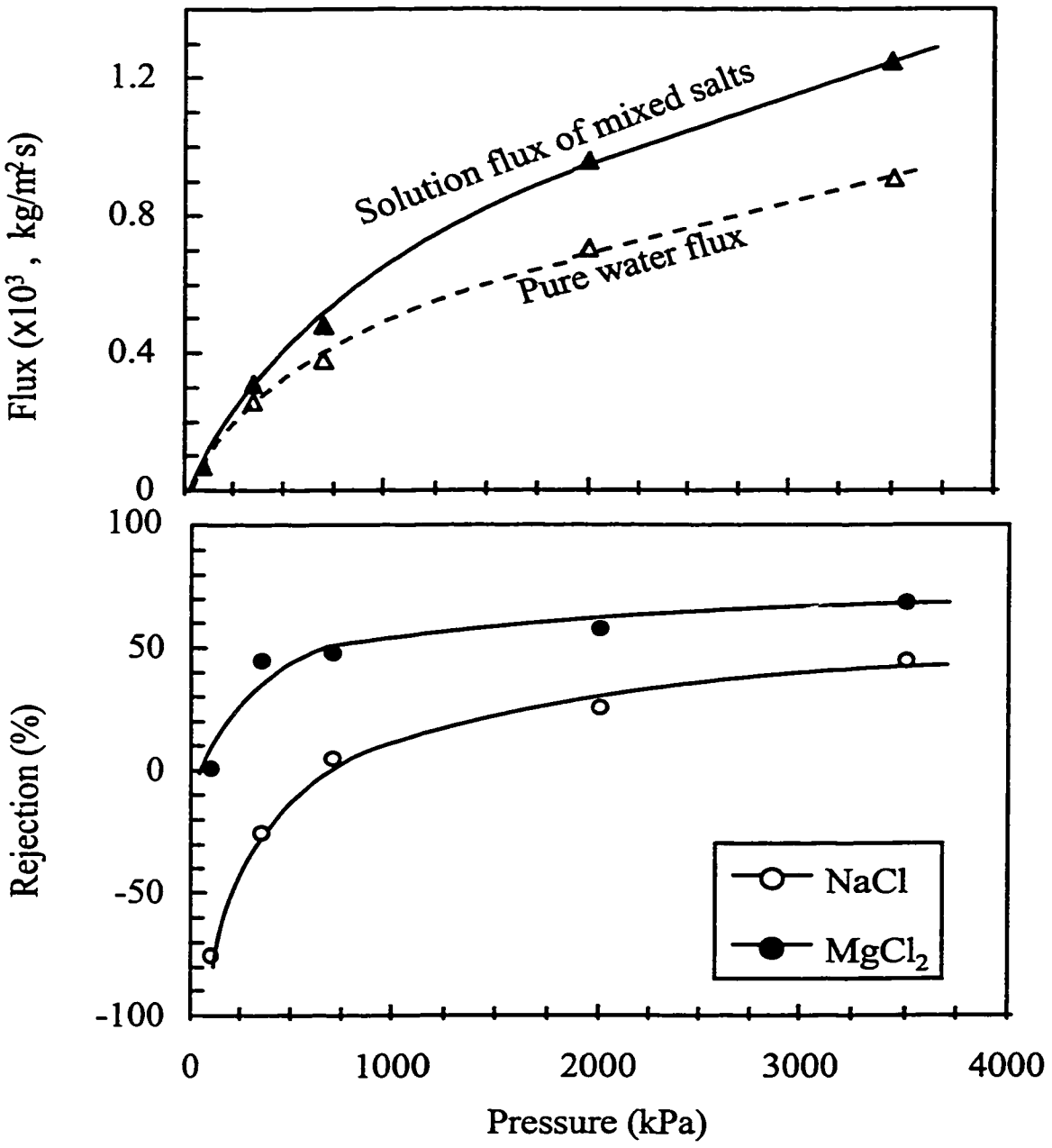

Fig. 5.10. Flux and rejection as a function of pressure for a mixed solute system; the feed contains 110 ppm of NaCl and 55 ppm of $MgCl_2$.

Fig. 5.10 shows that an increase in pressure leads to an increase in rejection of both cations. It was observed that decreasing the pressure increased the difference between of NaCl and $MgCl_2$ rejections, which increased the fractionation between NaCl and $MgCl_2$ cations, however at lower productivity. For example, at the pressure of 100 kPa, the rejection of $MgCl_2$ was nearly zero while the rejection of NaCl was found to be -75%.

5.2.3.2. Discussion of flux and rejection of single and mixed salt solutions

Usually Donnan exclusion, size exclusion, and the requirement of charge neutrality all contribute to the mechanism of the salt rejection in NF/RO processes. From Donnan exclusion considerations, the co-ions dominate the rejection of salts. However, size exclusion is of minor importance for these pore-filled membranes as evidenced by the reported low rejections of sucrose by Mika et al. [168]. Strathmann and co-workers [159] pointed out that the permeation of ions through charged membranes in NF processes depended primarily on the Donnan exclusion but the size effect also played an important role. For single salts, the rejection was observed to decrease with increasing valency of the counter-ion. Similar to the concentration effect presented in Section 5.2.2, bivalent ions (Mg^{2+}), compared to monovalent ions (Na^{+}), provides higher shielding to the fixed negative charges on the membrane and make it easier for co-ions (Cl^{-}) to pass through the membrane. As a result, the rejection of Mg^{2+} is expected to be lower than that of Na^{+}.

The solution flux, for single salt, decreases with increasing valency of the counter-ion, Fig. 5.8. This is not often seen for RO/NF TFC membranes. The confirmation of the

crosslinked polyelectrolyte gels of the pore-filled membrane strongly depends on ionic strength of the contacting solution and the nature of the salt. For example, besides higher effect of charge screening than the monovalent counter-ions (Na^+), the bivalent counter-ions (Mg^{2+}) in the membrane interact with two fixed charges, resulting in "ionic crosslinking". This kind of "ionic crosslinking" leads to a decrease in pore size. Hence, the flux of single $MgCl_2$ is lower than that of single NaCl. Another effect (steric effect) may add to the ionic crosslinking effect. It is known that the ion size of the hydrated, bivalent Mg^{2+} is larger than that of Na^+. Thus, a hydrated bivalent Mg^{2+} ion is more difficult to go through pores of the membrane than a monovalent Na^+ ion.

In the mixed salt system, NaCl and $MgCl_2$, with a co-ion in common, the difference in separation performance between Na^+ and Mg^{2+} is related to the change in valence of the competing cations, ie., the selectivity of one ion is affected by the presence of the other competing ion [169]. The rejection results with mixed solutes stand in marked contrast to the behavior of these membranes with single salts, Fig. 5.8. For the mixed salt solutions containing Na^+ and Mg^{2+}, the rejection of Na^+ is lower than that of Mg^{2+}, Fig. 5.9. The permeability of the monovalent ions (Na^+) through the cation-exchange membrane is higher than Mg^{2+}. This can be understood in terms of the charge neutrality and Donnan exclusion. Because of the higher interactions between the bivalent ions (Mg^{2+}) and fixed charges, the Donnan exclusion prefers to attract Mg^{2+} into the membrane from solution but to repel the co-ions (Cl^-). Due to the charge neutrality, the transport of counter-ions through the membrane must be accompanied by co-ions (Cl^-). The transport of the bivalent Mg^{2+} requires twice amount of the co-ions (Cl^-) than the

monovalent Na^+. However, the Donnan exclusion restricts the transport of Cl^-. Thus, the monovalent counter-ions (Na^+) are forced to permeate preferentially comparing to the bivalent counter-ions (Mg^{2+}). Hence, a lower rejection is observed for monovalent Na^+ than bivalent Mg^{2+} in the mixed salt system.

The difference in free solution diffusivity between Na^+ and Mg^{2+} could be a factor affecting their rejections. The diffusion coefficient is 1.33×10^{-9} m^2/s for Na^+ and 0.71×10^{-9} m^2/s for Mg^{2+} [130]. These numbers are applicable in free solution. The ion diffusivity in a membrane is generally different due to hindrance and electrostatic interactions between the mobile ions and the fixed charges of the membrane. The difference in diffusion coefficient suggests that Na^+ diffuses faster than Mg^{2+} in dilute solution. However, for the polyelectrolyte highly filled membranes in this work, this effect should be smaller than the Donnan exclusion effect. For example, if the difference in diffusivity were the main effect, the net effect should have led to a lower rejection of single NaCl than single $MgCl_2$. This is not observed in Fig. 5.8.

From Fig. 5.10, the observed relationship of flux *versus* pressure was not linear through the origin. A linear relationship is common in RO/NF membranes. This result is similar to the finding of Mika et al. [16,64,68,168], who reported the results of pressure effect on separating salts in NF using PVP-filled membranes. The non-linear relationship is likely due to that the highly swollen polyelectrolyte gels are deformable by the flow through the membrane. When a solution flows through pores filled with swollen polyelectrolyte gels, the solution penetrates into a certain depth limit of the gel and perturbs the equilibrium. An increase in solution flow forces the polyelectrolyte chains to

realign along the flow field. This alignment forces charged neighboring chains closer together resulting in an increase in excluded volume interactions and a lower solution flux [34,62]. Recently, Levie [62] used a simplified polyelectrolyte-grafted brush model to developed mathematical equations which were in good agreement with the experimental NF data obtained by Mika et al. [16].

5.2.4. Interpretation and Tap water Results

From Fig. 5.9, the rejection of Na^+ was found to decrease with increasing the concentration ratio of Mg^{2+}/Na^+. Negative rejections of Na^+ were found in the mixed $NaCl/MgCl_2$ system, Fig. 5.10. A negative rejection, calculated by Eq. 5.3, means that the ion is more concentrated in the permeate than in the feed. In the literature, negative rejections were observed and various reasonable explanations had been used to understand this phenomenon.

Kimura [171] had similar findings to the results shown in Fig. 5.8 and Fig. 5.9 for the same system of mixed salts using a sulfonated poly(2,6-dimethylphenylene ether) ion-exchange membrane. His explanation was based on partial association of the counter-ion (Mg^{2+}) of the higher valency within the fixed charges in the membrane. Tsuru et al. [172] and Bardot et al. [173] also had similar findings using negatively charged, commercial membranes. They interpreted ion separation by the convective and diffusive fluxes caused by the addition of counter-ions of different mobilities.

The McMaster Membrane Research Group [16] has reported the negative rejection of acids for HCl/NaCl system using PVP-filled anion-exchange membranes in

NF. A number of papers [16,150-155,161,174,175] have reported and attempted to understand negative rejection. For example, Hoffer and Kedem's early papers reported negative rejection of acid using a negatively charged membrane [150-154]. Negative rejections for anions and anion complexes [176] have also been observed experimentally in multi-anion systems in nanofiltration and reverse osmosis. Recently, Nielsen and Jonsson [170] have reported experimental data and modelling studies of negative rejections in multi-anion solutions.

In this study, negative cation rejection has been observed with multi-cationic solutions using the pore-filled cation-exchange membranes. For instance, for in the mixed ion system, Fig. 5.10, when the pressure was decreased from 3500 kPa to 100 kPa, the rejection of decreased from 43% to -75% for Na^+. But at the time, the rejection of Mg^{2+} did not go negative, ie., from 70% to nearly 0%.

Tap water and a synthetic mixed solute solution containing 2.0×10^{-3} M of NaCl and 1.0×10^{-3} M of $MgCl_2$ were used as the feed with membranes #67 and #68 under the conditions (350 kPa, 25°C). The results are presented in Table 5.5.

From Table 5.5, negative rejections were observed with both tap water and the synthetic solution. For instance, with tap water, the rejection of Na^+ was negative (-29%) while the rejections for Mg^{2+} and Ca^{2+} were positive, Table 5.5. Tap water is a complex system and concentration of all ionic species present was not measured. Thus, a simple synthetic mixture ($NaCl/MgCl_2$) was also examined and again the rejection was negative for Na^+ (-25%) and positive for Mg^{2+}. When a single cationic solution was used in the

Table 5.5. Rejection of inorganic ions using pore-filled cation-exchange membranes [a].

Ion	Na^+	Mg^{2+}	Ca^{2+}	Cl^-	SO_4^{2-}
			Tap water [b]		
Ion concentration in feed (ppm)	23	7	30	21	30
Rejection (%)	-29	21	23	16	26
			Synthetic solution [c]		
Ion concentration in feed, ppm ($\times 10^3$, *M*)	42 (*2.0*)	23 (*1.0*)	-	140 (*4.0*)	-
Rejection (%)	-25	45	-	58	-

a. The error in concentration measurement is given in Table 5.3; 350 kPa pressure at 25°C.
b. Using #67: IEC = 2.23 meq/g, mass increase = 83%, DVB = 2.5%, ion-exchange concentration = 3.3 eq/kg, flux = 0.31×10^{-3} kg/m^{2}s.
c. Using #68: IEC = 1.92 meq/g, mass increase = 80%, DVB = 2.5%, ion-exchange concentration = 3.3 eq/kg, flux = 0.33×10^{-3} kg/m^{2}s.

experiments, only positive rejections for the cation were observed irrespective of the charge of the cation due to electroneutrality. The rejection of a monovalent cation (Na^+) could be negative only in the presence of ions with competing ions, such as multi-valent cations (Mg^{2+} or Ca^{2+}). This is good for water softening, eg., Na^+ is concentrated in the permeate while most of hard Mg^{2+} and Ca^{2+} ions are removed.

The pressure affected the negative rejection significantly in pressure-driven separation processes. As can be seen in Fig. 5.10, negative rejections of Na^+ were

observed when the pressure was low (low flux), ie., at 100 kPa and 350 kPa. This was discussed in the previous section (5.2.3.2) (due to the Donnan exclusion and charge neutrality).

Modelling studies are helpful to understand the performance of the membranes. For example, Nielson and Jonson [170] found in their data that negative rejections up to 1000% were obtained at low pressures. The results of the reductions in negative rejections (more negative) obtained from modelling studies were consistent with the experimental results. However, the model developed by Yaroshchuk [174] based on irreversible thermodynamics had failed to analyze the transport properties of macroscopically homogeneous gels.

Garcia-Aleman [175] recently calculated and modelled the performance of the commercial NF membranes and membranes used in this work. The model developed by Garcia-Aleman had ten adjustable parameters which were determined based on the data obtained in the experimental work [175]. The model successfully fitted the performance of the commercial NF membranes but this model failed to fit the performance of the pore-filled cation-exchange membranes prepared in this study. The model could qualitatively but not quantitatively describe the salt rejections as a function of the salt concentrations, based on the data shown in Figs. 5.8, 5.9 and 5.10. For example, the model could satisfactorily predict the rejection of Mg^{2+} but over-predict the rejection of Na^{+}. The author concluded that the performance of the pore-filled cation-exchange membranes depended on the charge interactions (charge screening) and changes in conformation of the polyelectrolyte gels which were not included in the model.

5.3. CONCLUSION

This chapter has presented the results of evaluation of pore-filled cation-exchange membranes using a pressure-driven separation process.

These membranes were found to be capable of rejecting single and mixed, monovalent and bivalent inorganic ions, such as Na^+ and Mg^{2+}, in pressure-driven processes. The difference in flux mainly depends on the degree of crosslinking but the difference in rejection primarily depends on membrane ion-exchange concentration (Donnan exclusion). The effect of the feed concentration on permeability and separation is significant. The effect of mass increase of poly(styrene-DVB) on flux is small.

Transport mechanisms are discussed to understand the performance of the pore-filled membranes. For example, charge screening (shielding), the coiling ionic cluster — model, and the exclusion mechanism are described. The conformation of the polyelectrolyte gel changes in the presence of the electrolyte solutions.

Negative rejections for cations were observed in mixed salt solutions in this study. The degree of negative rejection is affected by the solution flux (and pressure) and concentration ratio of the competing mobile ions.

CHAPTER SIX

CONCLUSIONS AND FUTURE WORK

This chapter summarizes the work described in this thesis and then seeks to compare the membrane nanofiltration performance with other pore-filled membranes that have occurred at McMaster University, In doing this, references will be made to the recent development on pore-filled membranes.

6.1. Summary

The key findings in this thesis are:

- A new method of incorporating poly(styrene-DVB) in the PE substrate membrane by *in situ* polymerization has been developed. The mass loading of the incorporated poly(styrene-DVB) can be controlled up to approximately 600% by adjusting the degree of crosslinking and the polymerization time. Pore-filled cation-exchange membranes can be made by chlorosulfonation of the incorporated poly(styrene-DVB). The effect of sulfonation temperature on the sulfonation yield has been determined.

- The pore-filled cation-exchange membranes made in this work are robust, being stable under test conditions, relatively easy to made and potential cost effective.
- The incorporated polyelectrolyte, poly(styrene-sulfonic acid) was found to be evenly distributed in the PE substrate membrane.
- The membranes have been shown to have high ion-exchange capacities and water contents. The electrical resistance of the pore-filled membranes was found to be low. The counter-ion transport numbers are high.
- The pore-filled membranes are capable of separating inorganic salts in diffusion dialysis and pressure-driven processes. The transport of ionic species through these membranes has been discussed.
- A contraction of the PE substrate membrane ("pore contraction") was observed during the thermally initiated polymerization step. The membrane thickness changed with the mass loading. The thermal contraction has the effect of reducing the pore size and porosity of the base membrane. As will be shown in this chapter, this is an important factor in determined the performance of the membranes.

6.2. Recent Development on Pore-Filled Membranes at McMaster University

At the last stage of writing this thesis, Mika and other members of Dr. Childs'

group [65] have compared the properties of several series of polyelectrolyte-filled membranes in terms of nanofiltration applications. Out of this work, there has a rapid increase in understanding of the pore-filled class of membranes. As a result, it is interesting to compare the nanofiltration performance of the membranes prepared in this work with other systems recently studied in the McMaster laboratory to see whether they fit into the pattern and overall picture which has recently been developed.

The approach taken by the McMaster Membrane Group was to prepared several series of pore-filled membranes in which the chemical structure, concentration and charge density of the incorporated polyelectrolyte gels were systematically varied. These well characterized membranes were then examined in terms of their hydrodynamic (Darcy) permeability and separation of a standard NaCl solution of (300 ppm). The pressure regime used in this study was between 100 and 500 kPa.

The polyelectrolyte gels selected in the work of these very recent studies include quaternized and partially quaternized poly(4-vinylpyridinium salts) (PVP salts), poly(vinylbenzyl ammonium salts) (PVBA salts) with different crosslinking agents, and crosslinked poly(acrylic acid) (PAA). The chemical structures of these polyelectrolyte gels are shown in Fig. 6.1. The results of the study are summarized in two key figures, Fig. 6.2 (permeability *vs* volume fraction) and Fig. 6.3 (rejection *vs* permeability). It should be noted that the PAA-filled membranes are negatively charged, weak acid cation-exchange membranes and it is of considerable interest to compare their behavior with the membranes made in this work.

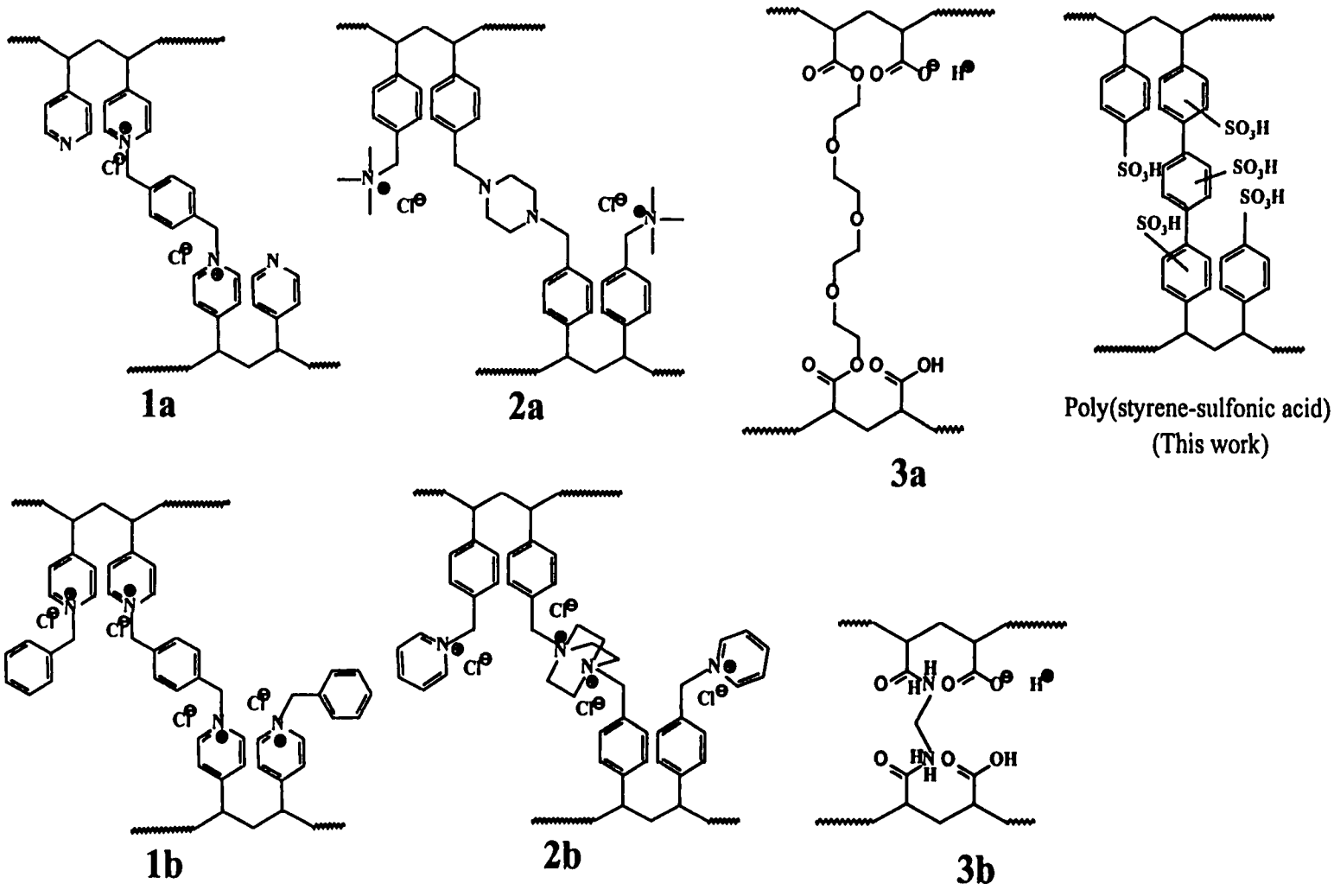

Fig. 6.1. Chemical structures of pore-filling gels.

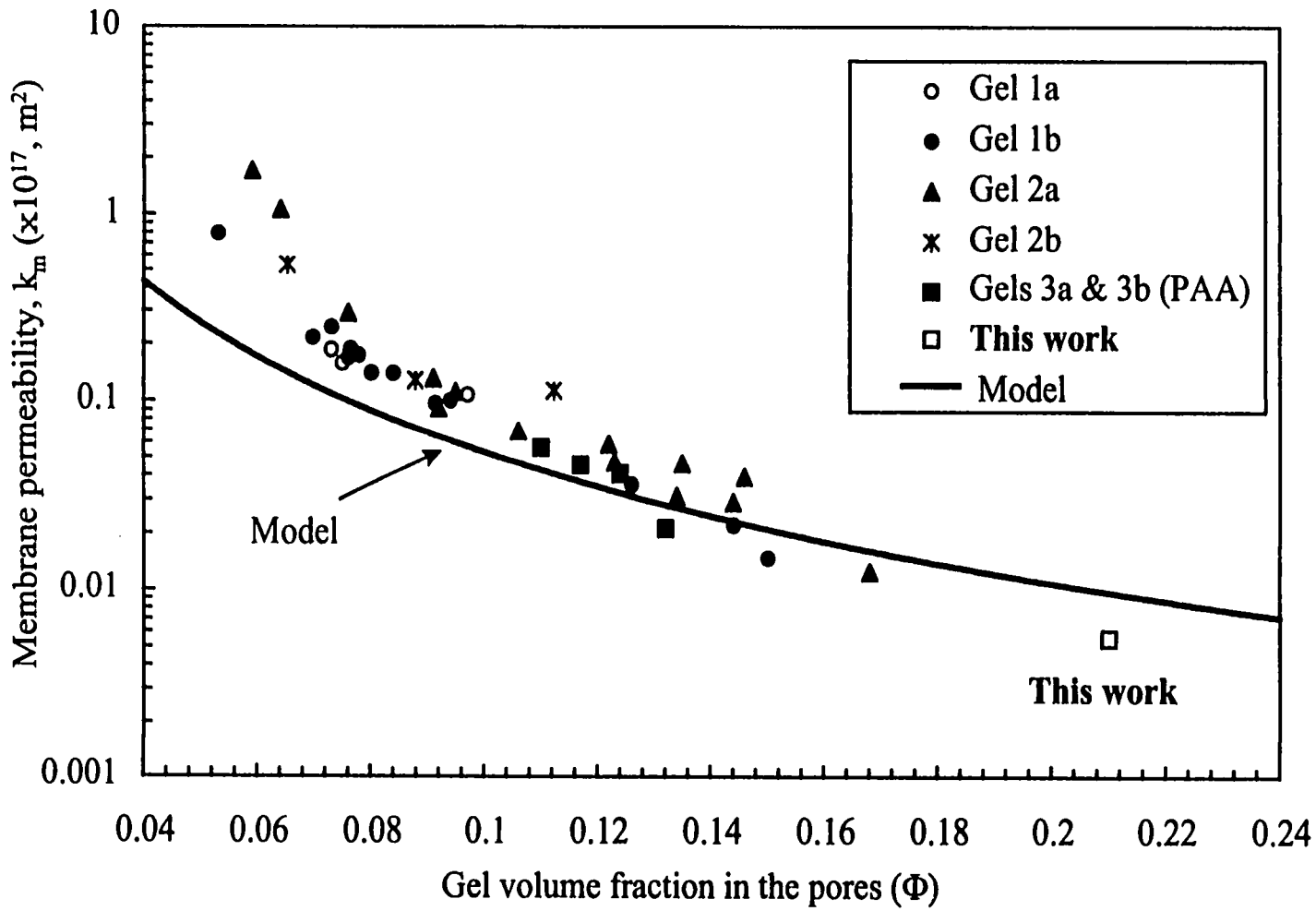

Fig. 6.2. Membrane hydrodynamic permeability as a function of gel volume fraction.

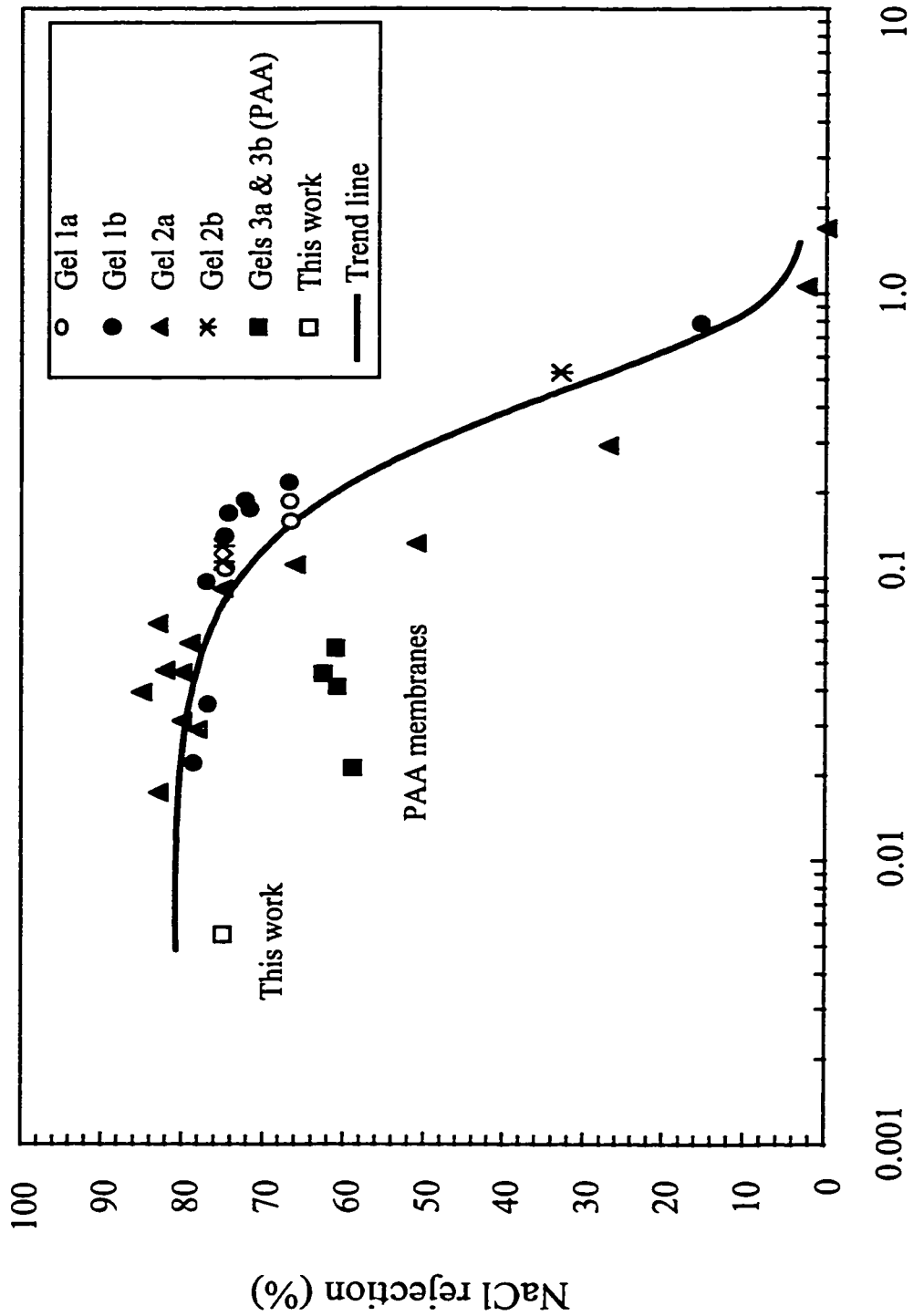

Fig. 6.3. Rejection of NaCl as a function of membrane permeability; 300 kPa pressure, 300 ppm NaCl.

As can been from the data shown in Fig. 6.2, there is a good correlation between hydrodynamic (Darcy) permeability and gel volume fraction in the pores. The Darcy permeability is inversely related to the gel volume fraction in the membrane pores, ie., decreasing with increasing the gel polymer concentration. The solid curve (Fig. 6.2) is calculated from the model developed Childs and co-workers [47,64] which assumes that the polyelectrolyte gel homogeneously fills the pores of the host membrane. It can also be seen that the model reproduces the trends in the experimental data, practically at the higher gel polymer concentrations. It is important to note that the relationship between hydrodynamic permeability and gel volume fraction holds irrespective of the gel polymer type and gel polymer charge. In the other words, the negatively charged PAA-filled membranes (points marked as ■ in Fig. 6.2) have the same permeabilities as the positively charged PVP salt- and PVBA salt-filled membranes of the same gel polymer volume fraction. When the polymer volume fraction is lower than approximately 0.07, the hydrodynamic permeabilities becomes scattered possibly due to heterogeneity in the gels at low concentrations.

The separation of a standard NaCl solution (300 ppm) of all the membranes is shown in Fig. 6.3. It can be seen that for the positively charged membranes, there is a single correlation which holds. The data for these membranes fall into two regions with a break point at of hydrodynamic permeability of *ca.* 2×10^{-18} m^2, corresponding to a gel volume fraction of *ca.* 0.08. When the membrane permeability (k_m) is less than 2×10^{-18} m^2, the rejection of the standard NaCl (300 ppm) solution is nearly constant at a value of approximately 80%. When the hydrodynamic permeability exceeds the break point (2 ×

10^{-18} m^2), the rejection decreases dramatically. The results clearly suggest that, in the region ($k_m < 2 \times 10^{-18}$ m^2, or $\Phi < 0.08$), there is no advantage in increasing the gel polymer fraction in terms of improving separation.

The effect of nominal charge density on membrane performance is evident with gels **1a** and **1b**. The charge density of gel in the partially charged PVP salt-filled membranes (**1b**) have the very similar NaCl rejections to the fully quaternized PVP salts-filled membranes (**1a**) whose nominal charge density is over 10 times higher (Fig. 6.3). This means that the nominal charge density is poor indicator of the effective charge density. It is known that the presence of counter-ions significantly affects the gel conformation of the polyelectrolytes. The charged polyelectrolyte chains can form ionic clusters with counter-ions [163,164], the so-called charge condensation) [177].

This means that gels with different nominal charge densities can have similar effective charge density. It can be assumed that the gel structure (average mesh radius) will be similar for different gels at the identical gel polymer concentration. Thus, the similar salt rejections for gels with various nominal charge densities can be expected.

It should be noted that the limiting rejections of the negatively charged PAA-filled membranes (marked as ■) are significantly lower than the positively charged membranes. This is not a fact of the charge density but seems to be due to the presence of the negatively charged gel. As discussed in Chapters 1, 4 and 5, the transport of salts depends upon the transport of the co-ions across the membrane. When the permeability is low, the convective flow is slow but the diffusive flow does not change significantly and becomes more important. The diffusion coefficient is 1.33×10^{-9} m^2/s for Na^+ and 2.03×10^{-9} m^2/s

for Cl^- [130]. This difference in diffusivity will lead to the difference in ion transport through the membrane of different charge type. Thus, NaCl will diffuse more readily through negatively charged membranes where Cl^- is the co-ion than positively charged membranes where Na^+ is the co-ion.

Poly(styrene sulfonic acid) gels are negatively charged. The obvious question is whether the poly(styrene-sulfonic acid)-filled membranes prepared in this work follow the same permeability pattern observed in the recent work discussed above. It also of interest to see whether the negatively charged poly(styrene-sulfonic acid)-filled membranes also have lower rejections of NaCl as was observed for the PAA-filled membranes.

6.3. Comparison of Performance of Other Pore-Filled Membranes

In order to compare permeability of the poly(styrene-sulfonic acid)-filled membranes described in this thesis with the results discussed above, it is necessary to calculate the hydrodynamic (Darcy) permeability of these membranes and examine the separation of a standard NaCl solution (300 ppm). Unfortunately, most of the data obtained in this work were obtained at much higher pressures (2000 and 3000 kPa) than 300 kPa selected in the study as a standard. However, one membrane (membrane #69) was tested in the same pressure range (100 - 3000 kPa). The performance of this membrane can be compared with the results discussed above.

The relationship between flux and pressure is shown Fig. 6.4. It was found that the water flux-pressure was not a linear relationship over the whole pressure range.

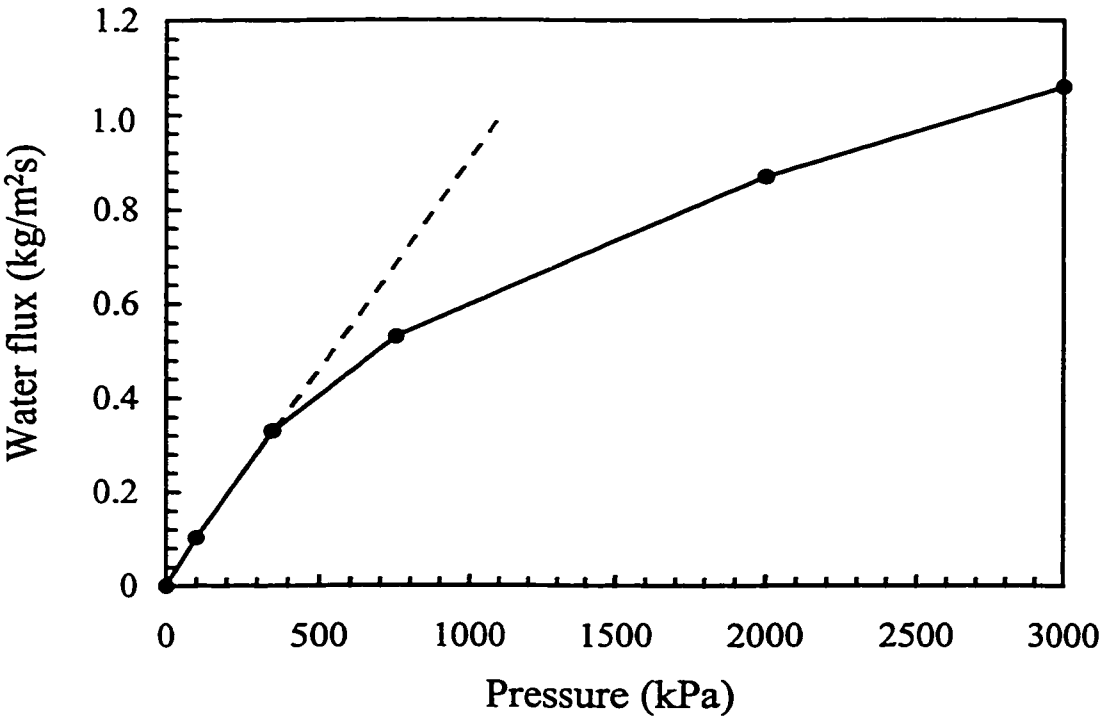

Fig. 6.4. Water flux as a function of pressure for membrane #69.

However, a linear relationship through the origin was found when the pressure was less than 500 kPa. The slope of the line at the pressure below 500 kPa was used to calculate the hydrodynamic (Darcy) permeability (k_m) using the following empirical equation:

$$k_m = \frac{Q\, d\, \eta}{A_m\, \Delta P} \qquad \textbf{(6. 1)}$$

where Q is the volume flow across the membrane (m^3/s), d is the membrane thickness (m), η is the permeate viscosity (Pa·s), A_m is the membrane area (m^2), and ΔP is the

applied pressure (Pa). The permeability was derived from the slope of the straight line obtained by plotting $Q\eta/A_m$ as a function of ΔP. The non-linearity of the pressure-flux relation with membrane #69 means that it is not possible to use other membrane tested only at 2000 kPa or 3000 kPa in the comparisons.

The polymer volume fraction (ϕ) was calculated from:

$$\phi = \frac{(m_{m,dry} - m_s)\,\upsilon_2}{V_m - \frac{m_s}{d_{PE}}} \qquad \textbf{(6. 2)}$$

where $m_{m,dry}$ is the mass (kg) of a pore-filled sample (in a dry state), m_s is the mass (kg) of the substrate in the sample, υ_2 is the partial specific volume (m^3/kg) of the gel polymer, V_m is the volume (m^3) of the swollen sample, and d_{PE} is the density of the high density polyethylene (kg/m^3) and ε is the substrate porosity.

The hydrodynamic permeability obtained for membrane #69 is shown in Fig. 6.2 as a function of gel volume fraction (marked as open square □) where the hydrodynamic permeability of this membrane was much lower than those of the recently tested membranes [65]. As can be seen, this membrane still behaved in a similar manner to other pore-filled membranes and fitted the permeability model that has been recently developed.

The rejection of NaCl (300 ppm) is also included in Fig. 6.3 (marked as □). The rejection was found to be 75% which appeared to be in the same range of most of the positively charged membranes studied (Fig. 6.3). However, again it should be noted that the poly(styrene-sulfonic acid)-filled membrane has a much lower permeability. It is

interesting to compare the rejection with PAA-filled membrane (negatively charged). As can be seen, the rejection of membrane #69 appeared to be higher than that of the PAA-filled membranes (marked as ■ in Fig 6.3). The difference in NaCl rejection result from PAA-filled membranes studied might be meaningful but before a detailed comparison is made, more data are required.

It is unfortunate that the performance of only a single poly(styrene-sulfonic acid)-filled membrane can be estimated and that this membrane has a higher gel volume fraction (0.21) than other membranes. However, the hydrodynamic permeability lies on the line predicted by the model and the rejection of NaCl also falls in the range of other membranes studied. This strongly suggests that poly(styrene-sulfonic acid)-filled membranes with lower gel volume fractions would follow the same trend as the other pore-filled membranes and that high performance water softening membranes could be produced with poly(styrene-sulfonic acid).

The results discussed above also strongly suggest that in order to obtain high performance membrane, the gel volume fraction must be appropriate, ie., as low as *ca.* 0.08 - 0.10 (Fig. 6.2), and the nominal charge density is *ca.* 0.2 mmol/cm^3 [65]. If this could be achieved with poly(styrene-sulfonic acid), the resulting membrane should have a high salt rejection (approximately 80% for NaCl (300 ppm)) and a high hydrodynamic (Darcy) permeability (approximately 1×10^{-18} m^2).

In order to achieve gel volume fraction in the range between 0.08 and 0.10, a high porosity substrate membrane and relatively low mass loadings of poly(styrene sulfonic acid) are required. In the work described in Chapter 3 of this thesis, the observed "pore

contraction" during the fabrication steps unfortunately reduced the porosity and pore size of the substrate membrane.

6.3. Recommendations

The key focus of future work should be targeted at making poly(styrene sulfonic acid) based membranes with the gel volume fraction of approximately 0.08-0.10. these membranes should show excellent performance in ultra low pressure-driven water softening capability and because of their negative charges, be resistant to fouling by large, negatively charged materials (such as humic acids) in the treatment of natural water. In order to obtain these membranes, new membrane-making methods should be developed.

As the gel volume fraction substantially depends on the porosity of the host membrane, the pore contraction of the host membrane would be reduced if thermal treatment (high temperature) can be avoided. UV initiated polymerization methods can avoid high temperatures effectively. When the pore contraction is reduced, with the same mass loading, the gel volume fraction will be lower and the flux should be expected to be enhanced without decreasing the salt rejection. The mass load could also be better controlled if the styrene/DVB starting concentration were reduced using suitable solvents.

APPENDIX A

CALCULATION OF TRANSPORT NUMBER

The transport numbers were calculated using Eq. 3.3. The theoretical basis of the equation has been discussed by Lakshminarayanaiah [114]. The experiment was carried out at 25°C (T = 298 °K), and the ratio C_1 / C_2 = 2. Faraday constant F = 9.648 × 10^4 C mol^{-1}, ideal gas constant R = 8.314 J $mol^{-1}K^{-1}$. Simplification of Eq. 3.3 leads to,

$$t^{M}_{+(Na)} = - 28.09\ E_{mem} \qquad \textbf{(A. 1)}$$

where $t^{M}_{+(Na)}$ is the membrane transport number of the counter-ion (Na^+). Thus, the membrane transport number of co-ion (Cl^-) is

$$t^{M}_{-(Cl)} = 1 - t^{M}_{+(Na)} \qquad \textbf{(A. 2)}$$

The membrane potential E_{mem} is obtained when the polarization layers are removed. The potential is the intercept on the voltage axis which is obtained by plotting the voltage versus $1/\sqrt{\omega}$ (ω is the spinning rate of the rotating cell) and by extrapolating the curve to the vertical axis, Fig. A.1. The calculation of the electrical potential was done using Microsoft Excel. Print-outs samples of the work sheet, Table A.1, and cell formula, Table A.2, for the calculation of the transport number in Microsoft Excel 7.0.

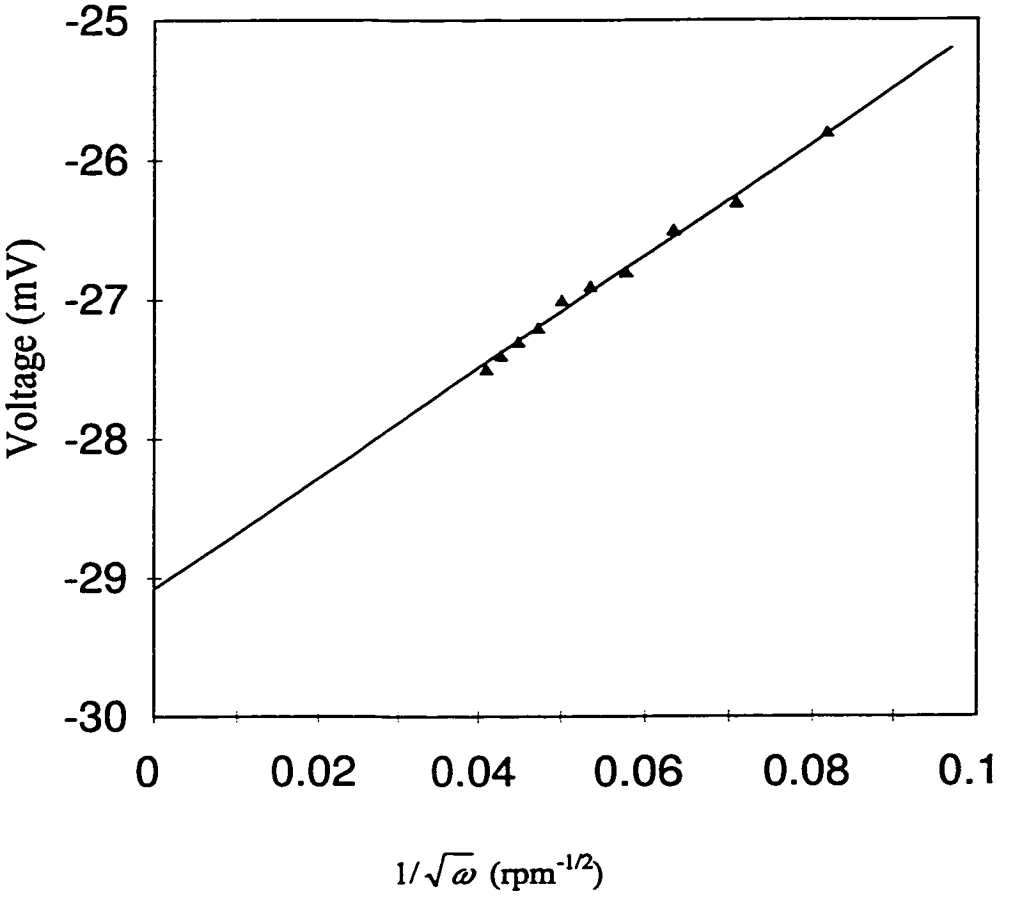

Fig. A.1. The electrical potential as a function of $1/\sqrt{\omega}$ (membrane #67).

The intercept (E_{exp}) is -29.1 mV and the transport number for the counter-ion, Na^+, was calculated 0.818.

Table A.1. Work sheet of calculation of transport numbers in Microsoft Excel 7.0.

A	A	B	C	D	E	F
1	Membrane		#67	#68	#69	#70
2	mass increase (%)		83	80	68	150
3	DVB (%)		2.5	2.5	1.0	1.0
4	IEC (meq/g)		2.23	1.92	2.10	3.50
5	DATA					
6	Rotating ω (rpm)	$1/\sqrt{\omega}$ ($rpm^{-1/2}$)	Voltage (mV)	Voltage (mV)	Voltage (mV)	Voltage (mV)
7	600	0.0408	-27.5	-27.1	-27.2	-28.4
8	550	0.0426	-27.4	-27.0	-27.0	-28.3
9	500	0.0447	-27.3	-26.9	-27.0	-28.2
10	450	0.0471	-27.2	-26.8	-26.8	-28.0
11	400	0.0500	-27.0	-26.6	-26.7	-27.9
12	350	0.0535	-26.9	-26.3	-26.7	-27.7
13	300	0.0577	-26.8	-26.3	-26.5	-27.6
14	250	0.0632	-26.5	-26.1	-26.4	-27.3
15	200	0.0707	-26.3	-25.9	-26.2	-27.0
16	150	0.0816	-25.8	-25.5	-25.9	-26.5
17	RESULTS					
18	Intercept (potential, mV)		-29.10	-28.62	-28.26	-30.21
19	Standard Error		0.047	0.058	0.073	0.044
20	MEMBRANE TRANSPORT NUMBERS					
21	$t^{M}_{+(Na)}$		0.818	0.804	0.795	0.849

Table A.2. Cell formula for calculation of transport numbers in Microsoft Excel 7.0.

A	A	B	C	D	E	F
1	Membrane		#67	#68	#69	#70
2	mass increase (%)		83	80	68	150
3	DVB (%)		2.5	2.5	1.0	1.0
4	IEC (meq/g)		2.23	1.92	2.10	3.50
5	DATA					
6	Rotating ω (rpm)	$1/\sqrt{\omega}$ ($rpm^{-1/2}$)	Voltage (mV)	Voltage (mV)	Voltage (mV)	Voltage (mV)
7	600	=1/SQRT(A7)	-27.5	-27.1	-27.2	-28.4
8	550	=1/SQRT(A8)	-27.4	-27.0	-27.0	-28.3
9	500	=1/SQRT(A9)	-27.3	-26.9	-27.0	-28.2
10	450	=1/SQRT(A10)	-27.2	-26.8	-26.8	-28.0
11	400	=1/SQRT(A11)	-27.0	-26.6	-26.7	-27.9
12	350	=1/SQRT(A12)	-26.9	-26.3	-26.7	-27.7
13	300	=1/SQRT(A13)	-26.8	-26.3	-26.5	-27.6
14	250	=1/SQRT(A14)	-26.5	-26.1	-26.4	-27.3
15	200	=1/SQRT(A15)	-26.3	-25.9	-26.2	-27.0
16	150	=1/SQRT(A16)	-25.8	-25.5	-25.9	-26.5
17	RESULTS					
18	Intercept (potential, mV)		=INTERCEPT(C7:C15,$B$7:$B$15)	=INTERCEPT(D7:D15,$B$7:$B$15)	=INTERCEPT(E7:E15,$B$7:$B$15)	=INTERCEPT(F7:F15,$B$7:$B$15)
19	Standard Error		=STEYX(C7:C15,$B7:$B15)	=STEYX(D7:D15,$B7:$B15)	=STEYX(E7:E15,$B7:$B15)	=STEYX(F7:F15,$B7:$B15)
20	MEMBRANE TRANSPORT NUMBERS					
21	$t^{M}_{+(Na)}$		=-0.0281*C18	=0.0281*D18	=0.0281*E18	=-0.0281*F18

APPENDIX B

CALCULATION OF DIALYSIS COEFFICIENT

In diffusion dialysis, the amount (W, mol) of the component transported across the membrane can be expressed as:

$$W = U \cdot A \cdot t \cdot \Delta C \qquad \textbf{(B. 1)}$$

where U is the dialysis coefficient ($L/m^2 \cdot hr$), A the effective membrane area (m^2), t the time (hr), and ΔC the logarithm mean concentration difference (mol/L). When $C_{p0} = 0$, the term ΔC is calculated by:

$$\Delta C = \frac{C_{F0} - \left(C_{Ft} - C_{Pt} \right)}{\ln \left(\frac{C_{F0}}{C_{Ft} - C_{Pt}} \right)} \qquad \textbf{(B. 2)}$$

where C is the concentration of the transported component, the subscripts F and P denote the feed and the permeate, respectively, and 0 and t the time 0 and time t, respectively.

The above assumes little or no water transport, $V_{Pt} \approx V_{P0}$. Thus, W can be calculated by:

$$W = C_{Pt} \cdot V_{Pt} \approx C_{Pt} \cdot V_{P0} \qquad \textbf{(B. 3)}$$

where V is the volume (L).

In this work, it was found that a small amount of water was transported across the membrane from the permeate to the feed. The water transport was determined from a mass balance on the base (NaOH):

$$C_{F0} \cdot V_{F0} = C_{Ft} \cdot V_{Ft} + C_{Pt} \cdot V_{Pt} \qquad \textbf{(B. 4)}$$

Define the volume of water transported as $V_{H2O,\,trans}$.

$$C_{F0} \cdot V_{F0} = C_{Ft} \cdot (V_{F0} + V_{H2O,\,trans}) + C_{Pt} \cdot (V_{P0} - V_{H2O,\,trans}) \qquad \textbf{(B. 5)}$$

In this study, $V_{F0} = V_{P0} = 0.02500$ L. Thus, Eq. B.5 leads to:

$$(C_{Ft} - C_{Pt}) \cdot V_{H2O,\,trans} = C_{F0} \cdot V_{F0} - C_{Ft} \cdot V_{F0} - C_{Pt} \cdot V_{P0} \qquad \textbf{(B. 6)}$$

and $$V_{H2O,trans} = \frac{C_{F0} \cdot V_{F0} - C_{Ft} \cdot V_{F0} - C_{Pt} \cdot V_{P0}}{C_{Ft} - C_{Pt}} = \frac{C_{F0} - C_{Ft} - C_{Pt}}{C_{Ft} - C_{Pt}} \cdot V_{F0} \qquad \textbf{(B. 7)}$$

The concentrations of NaOH and NaCl (or Na_2SO_4) in the feed and permeate were measured (see Chapter 4 for detail). The raw data and calculations of the dialysis coefficient (U), the separation ratio (U_{base}/U_{salt}), and the water transport ($V_{H2O,\,trans}$) are summarized in Tables B.1, B.2, B.3, B.4, and B.5.

Table B.1. Calculation of the dialysis coefficient and water transport for the substrate PE membrane with NaOH/NaCl.

Membrane #: PE-1
Feed: 1.0M NaOH + 0.5M NaCl Vol. of Feed (L): 0.02500
Permeate: Water (initial) Vol. of Permeate (L): 0.02500
Temp. (°C): 25.0 Membrane area (m^2): 0.000314

	Time	Feed		Water	Permeate		NaOH			NaCl			U(NaOH)
	(hr)	[NaOH] (M)	[NaCl] (M)	transport (L)	[NaOH] (M)	[NaCl] (M)	ΔC (M)	W (mol)	U (L/m^2hr)	ΔC (M)	W (mol)	U (L/m^2hr)	U(NaCl)
	0	0.9858	0.4642	0	0	0		0	0		0	0	
# 1	0.50	0.7817	0.4001	0.00158	0.1651	0.0501	0.7868	0.00413	33.40	0.4044	0.00125	19.72	1.694
# 2	0.57	0.7992	0.3981	0.00102	0.1605	0.0500	0.7997	0.00401	28.18	0.4034	0.00125	17.42	1.618
# 3	0.63	0.7569	0.4184	0.00253	0.1695	0.0533	0.7695	0.00424	27.68	0.4127	0.00133	16.23	1.706
											Average:		1.673
											Standard deviation:		0.048

Table B.2. Calculation of the dialysis coefficient and water transport for the substrate PE membrane with $NaOH/Na_2SO_4$.

Membrane #: PE-1
Feed: 1.0M NaOH + 0.5M Na_2SO_4 Vol. of Feed (L): 0.02500
Permeate: Water (initial) Vol. of Permeate (L): 0.02500
Temp. (°C): 25.0 Membrane area (m^2): 0.000314

	Time	Feed		Water	Permeate		NaOH			NaCl			U(NaOH)
	(hr)	[NaOH] (M)	[NaCl] (M)	transport (L)	[NaOH] (M)	[NaCl] (M)	ΔC (M)	W (mol)	U (L/m^2hr)	ΔC (M)	W (mol)	U (L/m^2hr)	U(NaCl)
	0	0.9858	0.4401	0	0	0		0	0		0	0	
# 4	0.500	0.8028	0.4038	0.001611	0.1403	0.02593	0.8135	0.00351	27.450	0.4082	0.00065	10.110	2.715
# 5	0.500	0.8062	0.4149	0.001422	0.1418	0.02651	0.8146	0.00355	27.706	0.4137	0.00066	10.199	2.717
# 6	0.500	0.7899	0.3963	0.002016	0.1438	0.02591	0.8040	0.00360	28.465	0.4042	0.00065	10.201	2.790
											Average:		2.741
											Standard deviation:		0.043

Table B.3. Calculation of the dialysis coefficient and water transport for membrane #67 with NaOH/NaCl.

Membrane #: #67
Feed: 1.0M NaOH + 0.5M NaCl Vol. of Feed (L): 0.02500
Permeate: Water (initial) Vol. of Permeate (L): 0.02500
Temp. (°C): 25.0 Membrane area (m^2): 0.000314

	Time	Feed		Water	Permeate		NaOH			NaCl			U(NaOH)
	(hr)	[NaOH] (M)	[NaCl] (M)	transport (L)	[NaOH] (M)	[NaCl] (M)	ΔC (M)	W (mol)	U (L/m^2hr)	ΔC (M)	W (mol)	U (L/m^2hr)	U(NaCl)
	0	0.9858	0.4642	0	0	0		0	0		0	0	
# 7	0.52	0.8541	0.4378	0.001121	0.0978	0.00685	0.8660	0.00245	17.38	0.4474	0.00017	2.357	7.376
# 8	0.58	0.8475	0.4388	0.000303	0.1296	0.00932	0.8448	0.00324	20.94	0.4466	0.00023	2.849	7.350
# 9	0.50	0.8547	0.4299	0.001330	0.0904	0.00667	0.8703	0.00226	16.54	0.4434	0.00017	2.393	6.911
											Average:		7.212
											Standard deviation:		0.261

Table B.4. Calculation of the dialysis coefficient and water transport for membrane #67 with NaOH/Na_2SO_4.

Membrane #: #67
Feed: 1.0M NaOH + 0.5M Na_2SO_4 Vol. of Feed (L): 0.02500
Permeate: Water (initial) Vol. of Permeate (L): 0.02500
Temp. (°C): 25.0 Membrane area (m^2): 0.000314

	Time	Feed		Water	Permeate		NaOH			NaCl			U(NaOH)
	(hr)	[NaOH] (M)	[NaCl] (M)	transport (L)	[NaOH] (M)	[NaCl] (M)	ΔC (M)	W (mol)	U (L/m^2hr)	ΔC (M)	W (mol)	U (L/m^2hr)	U(NaCl)
	0	0.9858	0.4401	0	0	0		0	0		0	0	
# 10	0.50	0.8662	0.4227	0.001355	0.0768	0.00232	0.8840	0.00192	13.83	0.4302	0.00006	0.858	16.109
# 11	0.58	0.8379	0.4151	0.002031	0.0869	0.00271	0.8631	0.00217	13.74	0.4261	0.00007	0.868	15.831
# 12	0.50	0.8631	0.4401	0.001576	0.0729	0.00216	0.8844	0.00182	13.12	0.4390	0.00005	0.783	16.754
											Average:		16.231
											Standard deviation:		0.473

Table B.5. Concentration profile, dialysis coefficient and water transport for membrane #67 with NaOH/NaCl.

Membrane #: #67
Feed: 1.0M NaOH + 0.5M NaCl Vol. of Feed (L): 0.02500
Permeate: Water (initial) Vol. of Permeat (L): 0.02500
Temp. (°C): 25.0 Membrane area (cm^2): 0.000314

#	Time (hr)	Feed		Water transport (L)	Permeate		NaOH			NaCl			U(NaOH) U(NaCl)
		[NaOH] (M)	[NaCl] (M)		[NaOH] (M)	[NaCl] (M)	ΔC (M)	W (mol)	U (L/m^2hr)	ΔC (M)	W (mol)	U (L/m^2hr)	
Initial	0	1.0270	0.4950	0	0	0		0	0		0	0	
# 1	0.25	0.9073	0.4594	0.00088	0.09081	0.0026	0.9177	0.00227	31.497	0.4757	0.00006	1.727	18.243
# 2	0.50	0.8575	0.4388	0.00257	0.09065	0.0069	0.8906	0.00227	16.200	0.4627	0.00017	2.380	6.806
# 3	0.78	0.7505	0.4748	0.00217	0.2315	0.0286	0.7443	0.00579	31.596	0.4702	0.00071	6.177	5.115
# 4	0.97	0.7404	0.4580	0.00002	0.2862	0.0320	0.7021	0.00716	33.558	0.4596	0.00080	5.731	5.855
# 5	1.50	0.7323	0.3850	0.00026	0.2901	0.0650	0.6940	0.00725	22.176	0.4011	0.00163	8.599	2.579
# 6	2.20	0.6874	0.3902	0.00293	0.2935	0.0780	0.6606	0.00734	16.070	0.3966	0.00195	7.114	2.259
# 7	4.05	0.6698	0.3988	0.00364	0.3039	0.1150	0.6406	0.00760	9.322	0.3797	0.00288	5.952	1.566
# 8	7.02	0.6355	0.4086	0.00469	0.3351	0.1638	0.5911	0.00838	6.430	0.3553	0.00410	5.228	1.230

APPENDIX C

NOMENCLATURE

ACRONYMS

4VP	4-Vinylpyridine
BEE	Benzoin ethyl ether
BPO	Benzoyl peroxide
DABCO	1,4-Diazabicyclo[2,2,2]octane
DD	Diffusion dialysis
DSC	Differential scanning calorimetry
DVB	Divinylbenzene
EDX	Energy dispersive X-ray spectroscopy
EMF	Electromotive force
FTIR	Fourier transform infrared
IE	Ion-exchange
IEC	Ion-exchange capacity
MF	Microfiltration
NF	Nanofiltration
PAA	Poly(acrylic acid)
PE	Polyethylene
PIP	Piperazine
PP	Polypropylene
PS	Polystyrene
PV	Pervaporation
PVA	polyvinyl alcohol
PVBA salt	poly(vinylbenzyl ammonium salt)
PVBCl	poly(vinylbenzyl chloride)
PVP	Poly(4-vinylpyridine)
PVP salt	Poly(4-vinylpyridinium salt)
RO	Reverse osmosis
SEM	Scanning electron microscope
TFC	Thin film composite
UF	Ultrafiltration
WC	Water content

SYMBOLS

A, A_m	Membrane area
a_i	Activity of ionic species I
C_F,	Feed concentration
C_P	Permeate concentration
D	Diffusion coefficient
d, d_m	Membrane thickness
d_{PE}	Density of polyethylene
E_i	Electrical potential of the ionic spices I
E_{mem}	Membrane chemical potential
F	Faraday constant, 9.648×10^4 C mol^{-1}
i_c , i_w	Currents of convection flow, and pore-wall flow
J_i	Flux of ionic species I
k_m	Hydrodynamic permeability
m, m_{wet}, m_{dry}	Masses of membrane, wet membrane, and dried membrane
P_i	Permeability coefficient of ionic species I
ΔP	Applied pressure
Q	Volume flow across the membrane (m^3/s)
R	Ideal gas constant, 8.314 J mol^{-1}K^{-1}
R_m	Area membrane electrical resistance
T	Absolute temperature (°K)
T_g	Glass transition temperature
T_m	Melting point
t^M, t_+^M	Membrane transport number, and cation transport number
U	Dialysis coefficient
u_i	Electrochemical mobility of ionic species i
x	Membrane thickness
z_i	Valence of ionic species I

GREEK

α_T	Experimental temperature correction factor
η	Viscosity
ϕ	Polymer volume fraction
κ	Conductivity
μ^o	Standard chemical potential
ψ	Electrical potential
τ	Time
υ_2	Partial specific volume

REFERENCES

[1] H. Strathmann, Synthetic Membranes and Their Preparation: Handbook of Industrial Membrane Technology, edited by M.C. Porter, Noyes Publications, Park Ridge, New Jersey (1990).

[2] R.F. Machacek and A.D. Little (Boston), Membrane markets - alive and growing, membrane technologies for process industries workshop, Sheridan Science and Technology Park, Mississauga, Ontario (Feb 26, 1998).

[3] M.C. Porter, Membrane Filtration: Handbook of Separation Techniques for Chemical Engineers, edited by P.A. Schweitzer, McGraw-Hill, New York (1979) p. 2.

[4] R. Baker, Controlled Release of Bioactive Materials, Academic Press, New York (1980).

[5] A.J. Appleby and F.R. Foulkes, Fuel Cell Handbook, van Nostrand Reinhold, New York (1990).

[6] D. Paul and K-V. Peinemann, Membranes (Overview), Polymeric Materials Encyclopedia, edited by J.C. Salamone, CRC Press, Inc., Boca Raton, Florida (1996) p. 4076.

[7] H.M. Cheung and W.R. P. Raj, Membranes, Porous (Synthesized from Microemulsions), Polymeric Materials Encyclopedia, edited by J.C. Salamone, CRC Press Inc., Boca Raton, Florida (1996) p. 4083.

[8] H. Strathmann, Membrane separation processes in the environmental protection industry, Membrane processes for acid/metal ion recovery, Ontario Centre for Materials Research (OCMR) Workshop, Days Inn, Mississauga, Ontario, Canada (October 21, 1997).

[9] J. Korkisch, Handbook of Ion Exchange Resins, Vol. I, CRC Press, Boca Raton, Florida (1989).

[10] F. Helfferich, Ion Exchange, McGraw-Hill Inc., New York (1962).

[11] H.P. Gregor, J.I. Breman, F. Gutoff, R.D. Broadley, D.E. Baldwin, and C.G. Overberger, Studies on ion-exchange resins, capacity of sulfonic acid cation-exchange resins, J. Colloid Sci., 6 (1951) 20.

[12] J.A. Greg, Ion-Exchange Developments and Applications: Proceeding of IEX '96, Royal Society of Chemistry Information Services, Cambridge, UK (1996).

[13] V. Freger, E. Korin, J. Wisniak, and E. Korngold, Preferential sorption in ion-exchange pervaporation membranes: sorption of water-ethanol mixture by sodium polyethylene sulphonate, J. Membrane Sci., 128 (1997) 151.

[14] D.S. Flett, Ion Exchange Membranes, Ellis Howood Limited, Chichester, West Sussex, UK (1983). M.C. Porter, Handbook of Industrial Membrane Technology, Noyes Publications, Park Ridge, New Jersey (1990).

[15] A. Eisenberge and H.L. Yeager, Perfluorinated Ionomer Membranes, ACS Symposium Series 180, Washington, D.C. (1982)

[16] A.M. Mika, R.F. Childs, J.M. Dickson, B.E. McCarry, and D.R. Gagnon, A new class of polyelectrolyte-filled microfiltration membranes with environmentally controlled porosity, J. Membrane Sci., 108 (1995) 37.

[17] F.G. Donnan, Theorie der membtrangleichgewichte und membranpotentiale bei vorhandensein von nicht dialysierenden elektrolyten. Ein beitrag zu physikalisch - chemischen physiologie, Zeitschrift fur Elektrochemie, 17 (1911) 572.

[18] F.G. Donnan, The theory of membrane equilibria, Chem. Rev., 1 (1925) 73.

[19] F. Donnan, Z. Phys. Chem., A162 (1932) 346.

[20] M.C. Porter, Ultrafiltration, Handbook of Industrial Membrane Technology, Noyes Publications, Park Ridge, New Jersey (1990) p. 161.

[21] R. Schlögl, Stofftransport durch membranen, Steinkopf Verlag, Darmstadt (1964).

[22] R.E. Kesting, Synthetic Polymeric Membranes, A Structural Perspective, 2nd edition, Irvine, California, John Wiley & Sons, New York (1985) p. 157.

[23] E.L Cussler, Diffusion: Mass Transfer in Fluid System, Cambridge University Press, Cambridge, UK (1985).

[24] C.C. Gryte and H.P. Gregor, Poly(styrene sulfonic acid)-poly(vinyl fluoride) interpolymer ion-exchange membranes. I. Preparation and characterization, J. Polym. Sci.: Polym. Phys. Ed., 14 (1976) 1839.

[25] R. Wycist and P.N. Pintauro, Sulfonated polyphosphazene ion-exchange membranes, J. Membrane Sci., 119 (1996) 155.

[26] M.C. Wijers, M. Jin, M. Wessling, and H. Strathmann, Supported liquid membranes modification with sulfonated poly(ether ether ketone): Permeability, Selectivity and Stability, J. Membrane Sci., 147 (1998) 117.

[27] H.C. Visser, F. de Jong, and D.N. Reinhoudt, Kinetics of carrier-mediated alkali cation transport through supported liquid membranes: Effect of membrane solvent, co-transported anions, and support, J. Membrane Sci., 107 (1995) 267.

[28] I.J. Youn, Y. Lee, and W.H. Lee, Analysis of Co-Ni separation by a supported liquid membrane containing HEH(EHP), J. Membrane Sci., 125 (1997) 231.

[29] G.Akau and R.T. Wakeman, Electric field enhanced crossflow of hydrophobically modified water soluble polymer, J. Membrane Sci., 131 (1997) 229.

[30] M.G. Kodzwa, M.E. Staben, and D.G. Rethwisch, Photoresponsive control of ion-exchange in leucohydroxide containing hydrogel membranes, J. Membrane Sci., 158 (1999) 89.

[31] H.C. Visser, Supported liquid membranes with improved stability; kinetics and mechanism of carrier mediated salt transport, Ph.D. Thesis, University of Twente, Enschede, The Netherlands (1995).

[32] R.W. Baker, M.E. Tuttle, D.J. Kelly, and H.K., Lonsdale, Coupled transport membranes, I. Copper separation, J. Membrane Sci., 2 (1999) 213.

[33] N. Hiratsuka and N. Yaginuma, Support for electrophoretic analysis, US Patent 4,006,069 (1977).

[34] J.T. Kim and J.L. Anderson, Diffusion and flow through polymer-lined micropores, Ind. Eng. Chem. Res., 30 (1991) 1008.

[35] G.E. Gillberg-LaForce and E.M. Gabriel, Modified microporous structures, US Patent 5,049,275 (1991).

[36] T. Yamaguchi, S.-I. Nakao, and S. Kimura, Design of pervaporation membrane for organic-liquid separation based on solubility control by plasma-graft filling polymerization technique, Ind. Eng. Chem. Res., 32 (1993) 848.

[37] F.M. Winnik, A. Morneau, A.M. Mika, R.F. Childs, A. Roig, E. Molins, and R.F. Ziolo, Polyacrylic acid pore-filled microporous membrane and their use in membrane-mediated synthesis of nanocrystalline ferrihydrite, J. Can. Chem., 76 (1998) 10.

[38] M. Ulbricht, Photograft-polymer-modified microporous membranes with environment-sensitive permeabilities, Reactive Polymer, 31 (1996) 165.

M. Ulbrich and H.H. Schwarz, Novel high performance photo-graft composite membranes for separation of organic liquids by pervaporation, J. Membrane Sci., 136 (1997) 25.

[39] K.L. Thunhorst, R.D. Noble and C.N. Bownman, Transport of ionic species through functionalized poly(vinylbenzyl chloride) membranes, J. Membrane Sci., 128 (1998) 183.

[40] H. Yamagishi, K. Saito, S. Furusaki, and J. Amoto, Molecular weight distribution of methyl methacrylate grafted onto a microfiltration membrane by radiation induced graft polymerization, J. Membrane Sci., 85 (1993) 71.

[41] R. Simons and M.R. Dickson, Characterization of pall rail charged microporous membranes, J. Membrane Sci., 76 (1993) 75.

[42] V. Kapur, J.C. Charkoudian, S.B. Kessler, and J.L. Anderson, Hydrodynamic permeability of hydrogels stabilized within porous membranes, Ind. Eng. Chem. Res., 35 (1996) 3179.

[43] E.L. Cussler, G.E. Gillberge-LaForce, M.J. Sansone, and D.K. Schisla, Process for making microporous membranes having gel-filled pores, and separations methods using such membranes, US Patent 5,160,627 (1992).

[44] A.K. Pandey, R.F. Childs, M.West, J.N. Lott, B.E. McCarry, and J.M. Dickson, Formation of pore-filled ion-exchange membranes using *in situ* crosslinking poly(vinylbenzyl ammonium salt) filled membranes, Submitted to J. Membrane Sci. (1999).

[45] U. Micka, C. Jolm, and K. Kremer, Strongly charged flexible polyelectrolytes in poor solvents, Langmuir, 15 (1999) 4033.

[46] Private communication with A.M. Mika (1999).

[47] A.M. Mika, R.F. Childs, and J.M. Dickson, Chemical valves based on poly(4-vinylpyridine)-filled microfiltration membranes, J. Membrane Sci., 153 (1999) 45.

[48] A.M. Mika and R.F. Childs, Acid/base properties of poly(4-vinylpyridine) anchored within microporous membranes, J. Membrane Sci., 152 (1999) 129.

[49] Private communication with A.M. Mika (1998).

[50] M. Kim, R.F. Childs, A.M. Mika, and J.-F. Weng, PEI-filled membranes for water softening, Manuscript in preparation (1999).

[51] R.F. Childs, A.K. Pandey, J.M. Dickson, B.E. McCarry, M. West, and J.N.A. Lott, A Simple and Effective Way of Making Pore-Filled Anion-Exchange Membranes - Poly(vinylbenzyl Ammonium Salts), The 1999 International Congress on Membranes & Membrane Process (ICOM'99), Toronto, Ontario, June 12-18, 1999.

[52] A.M. Mika, R.F. Childs, M. West, and J.N. Lott, Poly(4-vinylpyridine)-filled microfiltration membranes: Physiochemical properties and morphology, J. Membrane Sci., 136 (1997) 221.

[53] A.M. Mika, R.F. Childs, J.M. Dickson, B.E. McCarry, and D.R. Gagnon, Porous, polyelectrolyte-filled membranes: effect of crosslinking on flux and separation, J. Membrane Sci., 135 (1998) 81.

[54] D.M. Stachera, R.F. Childs, A.M. Mika, and J.M. Dickson, Acid Recovery using diffusion dialysis with poly(4-vinylpyridine)-filled microporous membranes, J. Membrane Sci., 148 (1998) 119.

[55] F.X. Quinn, E. Kampff, G. Smyth, and V.J. McBierty, Water in hydrogels. 1. Study of water in poly(N-vinyl-2-pyrrolidone/methyl methacrylate) copolymer, Macromolecules, 21 (1988) 3191.

[56] G. Smyth, F.X. Quinn, and V.J. McBierty, Water in hydrogels. 2. Study of water in poly(hydroxyethyl methacrylate), Macromolecules, 21 (1988) 3198.

[57] S.P. Rowland (editor), Water in Polymers, ACS Symposium Series 127, American Chemical Society, Washington, D. C. (1980).

[58] J.L. Anderson, P.F. McKenzie, and R.M. Webber, Model for hydrodynamic thickness of thin polymer layers at solid/liquid interfaces, Langmuir, 7 (1991) 162.

[59] J.L. Harden, O.V. Borsov, and M.E. Cates, Deformation of polyelectrolyte brushes in strong flows: good solvent regime, Macromoleculars, 30 (1997) 1179.

[60] J.T. Kim and J.L. Anderson, Hindered transport through micropores with adsorbed polyelectrolytes, J. Membrane Sci., 47 (1989) 163.

[61] W.K. Idol and J.L. Anderson, Effects of adsorbed polyelectrolytes on convective flow and diffusion in porous membranes, J. Membrane Sci., 28 (1986) 269.

[62] C.J. Levie, Investigation into the permeation behavior of filled-pore membranes: Modelling the transport of solvent in chemical valve membranes, M. Eng. Thesis, McMaster University, Hamilton, Ontario (1996).

[63] V. Kapur, J.C. Charkoudian, S.B. Kessler, J.L. Anderson, Hydrodynamic permeability of hydrogels stabilized with porous membrane, Ind. Eng. Chem. Res., 35 (1996) 3179.

[64] A.M. Mika, R.F. Childs, and J. Garcia-Aleman, and J.M. Dickson, Theoretical design and physical modelling of charged "gel in shell" nanofiltration membranes, The 1999 International Congress on Membranes & Membrane Process (ICOM'99), Toronto, Ontario, June 12-18, 1999.

[65] R.F. Childs, A.M. Alicja, A.K. Padey, C.McCrory, S. Mouton, and J.M. Dickson, Nanofiltration using pore-filled membranes: effect of polyelectrolyte composition on performance, Submitted to J. Membrane Sci., (1999).

[66] G. Schmid and H. Schwarz, Z. Electrochemie, 56 (1952) 35.

[67] A. Yaroshchuk and E. Staude, Charge membranes for low pressure reverse osmosis properties and applications, Desalination, 86 (1992) 115.

[68] A.M. Mika, R.F. Childs, and J.M. Dickson, Ultra-low pressure water softening: a new approach too membrane construction, Desalination, 121 (1999) 149.

[69] C. Combe, E. Molis, P. Lucas, R. Riley, and M.M. Clark, The effect of CA membrane properties on adsorptive fouling by humic acid, J. Membrane Sci., 154 (1999) 73.

[70] M. der Nobili, E. Gjessing, and P. Sequi, Size and Shapes of Humic Substances by Gel Chromatography, Humic Substances II, edited by M.H.B. Hayes, P. MacCarthy, R.L. Malcolm, and R.S. Swift, John-Wiley & Sons, New York (1989) p. 561.

[71] R.L. Albright and P.A. Yarnell, Encyclopedia of polymer science and engineering, Wiley-InterScience Publications, John Wiley & Sons, New York (1987) Vol. 8.

[72] Private communication with A.M. Mika (1995).

[73] J.C. Bevington, S.W. Breuer, T.N. Huckerby, B.J. Hunt, and R. Jones, Further study of fluorinated derivatives of benzoyl peroxides initiators of radical polymerizations - kinetic chain lengths and related quantities, European Polymer J., 34 91998) 539.

[74] S.H. Ibbotson, C.R. Lambertt, M.C. Lynch, M.N. Moran, and I.E. Kochevar, Enhanced UV-induced plasma-membrane damage in the presence of benzoyl peroxide, J. Investgating Dermatology, 108 (1997) 762.

H.I. Unal and O. Sanli, Swelling-assisted copolymerization of 4-vinyl pyridine on poly(ethylene-terephthalate) films using a benzoyl peroxide initiator, J. Applied Polymer Sci., 62 (1996) 1161.

[75] J.O. Morley and D.W. Roberts, Molecular modeling studies on aromatic sulfonation. 1. Intermediates formed in the sulfonation of toluene, J. Org. Chem., 62 (1997) 7358.

[76] H. Cerfontain, Mechanistic Aspects in Aromatic Sulfonation and Desulfonation, InterScience, New York (1968).

[77] K.W. Pepper, Sulphonated crosslinked polystyrene: a monofunctional cation-exchange resin, J. Applied Chem., I, March (1951) 124.

[78] K.W. Pepper, D. Raichenberg, and D.K. Hale, Properties of ion-exchange resins in relation to their structures, Part IV. Swelling and shrinkage of sulfonated polystyrene, J. Chem. Soc., (1952) 3129.

[79] H.S. Byun, R.P. Burford, and A.G. Fane, Sulfonation of cross-linked asymmetric membranes based on polystyrene and divinylbenzene, J. Applied Polym. Soc., 52 (1994) 825.

[80] J.C. Salamone, editor, Polymeric Materials Encyclopedia, Reactions of Polymers, Vol. 14, CRC Press, Inc., Boca Raton, Florida (1988) p. 131.

[81] D.W. Emerson, D.T. Shea, and E.M. Sorensen, Functionally modified poly(styrene-divinylbenzene). Preparation, characterization, and bactericidal action, Ind. Eng. Chem. Prod. Res. Dev., 17 (1978) 269.

[82] W.R. Bussing and N.A. Peppas, Friedel-Crafts crosslinking methods for polystyrene modification: 1. Preparation and kinetics, Polymer, 24 (1983) 209.

[83] L.T.C. Lee and K.-J. Lie, Preparation of high performance polyelectrolyte membrane, US Patent, 4,083,768 (1978).

[84] D.B. Ehrlinger, Strongly acidic microporous membranes for cationic exchange, World Intellectual Property Organization, WO (1991) 91/10498.

[85] H.S. Makowski, R.D. Lundberg, and G.H. Singhal, Flexible polymeric compositions comprising a normally plastic polymer sulfonated to about 0.2 to about 10 mole % sulfonate, US Patent 3,870,841 (1975).

[86] L.T.C. Lee and K.-J. Lie, Preparation of high performance polyelectrolyte membrane, US Patent, 4,083,768 (1978).

[87] C.C. Gryte and H.P. Gregor, Poly(styrene-sulfonic acid)-poly(vinylidene fluoride) interpolymer ion-exchange membranes. I. Preparation and characterization, J. Polym. Sci., Polym. Phys. Ed., 14 (1976) 1839.

[88] I.L. Finar, Organic Chemistry, Longmans, London, UK (1993) Chapter 25.

[89] D.G. Barar, K.P. Staller, and N.A. Peppas, Friedel-Crafts crosslinking methods for polystyrene modification: 3. Preparation and swelling characteristics of cross-linked particles, Ind. Eng. Chem. Prod. Res. Dev., 22 (1983) 161.

[90] P. Molyneux, Water-Soluble Synthetic Polymers: Properties and Behavior, Vol. II, CRC Press, Boca Raton, Florida (1983) p. 37.

[91] G. Pozniak and W. Trochimczuk, Tubular interpolymer ion-exchange membranes 1. Cation-exchange membranes based on polyethylene modified with styrene-divinylbenzene copolymers, Angew. Makromol. Chem., 127 (1984) 171.

[92] H.C. Cheek, C. Tibberts, and E.M Zippi, Sulfonation methods for poly(styrene/divinylbenzene), Abstracts of Papers of the American Chemical Society, 211 (1996) ORGN 329.

[93] E. Erbay and O. Okay, Macroporous styrene-divinylbenzene copolymers - formation of stable porous structures during the copolymerzation, Polymer Bulletin, 4 (1998) 379.

[94] P. Rempp and E.W. Merrill, Polymer Synthesis, Hiithing and Wept Press (1996) p. 85.

[95] E. Trommsdorff, H. Kohle, and P. Lagally, Macromol. Chem., 1 (1949) 169.

[96] H.F. Mark, N.M. Bikales, C.G. Overberger, G. Menges, and J.I. Kroschwig (editors), Encyclopedia of Polymer Science and Engineering, Vol. 4, John Wiley & Sons, Inc., New York (1986) p. 192.

[97] C.-D. Ihm and S.-K. Ihm, Pervaporation of water-ethanol mixtures through sulfonated polystyrene membranes prepared by plasma graft-polymerization, J. Membrane Sci., 98 (1995) 89.

[98] N.B. Colthup, L.H. Daly, and S.E. Wiberley, Introduction to Infrared and Raman Spectroscopy, 2nd edition, Academic Press, New York (1975) p. 206.

[99] T. Momose, T. Kitazumi, and I. Ishigaki, Radiation grafting of α,β,β-trifluorostyrene onto poly(ethylene-tetrafluoroethylene) film by preirradiation method. III. Properties of anion-exchange membrane obtained by chloromethylation and quaternization of grafted film, J. Applied Polym. Sci., 39 (1990) 1221.

[100] A.S. Gozdz and W. Trochimczuk, Continuous modification of polyethylene with styrene and divinylbenzene in melt, J. Applied Polym. Sci., 25 (1980) 947.

[101] M. Struck and H. Widdecke, Surface fuctionalization of polymer network, Die Angew. Makromol. Chem., 235 (1996) 131.

[102] F. Kucera and J. Jancar, Homogeneous and heterogeneous sulfonation of polymers: a review, Polym. Eng. Sci., 38 (1998) 783.

[103] T.W.G. Solomons, Fundamentals of Organic Chemistry, John Wiley & Sons, Inc., New York (1994) Chapter 15.

[104] L.J. Bellamy, Advances in Infrared Group Frequencies, Methuen & Co. Ltd., (1968) Chapter 7, p. 219.

[105] I. Rabia, J. Zerouk, M. Kerkouche, and M. Belkhodja, Chemical and textural characteristics of porous styrene-divinylbenzene copolymers as a function of chlorosulfunation reaction parameters, React. Func. Polym., 28 (1996) 279.

[106] A.G. Theodoropouulos, V.T. Tsakalos, and G.N. Valkanas, Sulfone-type crosslinks in sulfonation of macronet polystyrene backbone, Polymer, 34 (1993) 3905.

[107] S.B. Idage, S. Barrinarayanan, S.P. Vernerkar, and Sivaram, X-ray photoelectro spectroscopy study of sulfonated polyethylene, Langmuir, 12 (1996) 1018.

[108] D.R. Lide and H.P.R. Frederikse, editors, CRC Handbook of Chemistry and Physics, 77th Ed., CRC Press, New York (1996) Chapter 6, p. 10.

[109] K. Kontturi, A. Savonen, and M. Vuoristo, Study of adsorption and ion-exchange properties of some porous membrane, Acta Chemica Scandinavica, 48 (1994) 1.

[110] B. Bauer, H. Strathmann, and F. Effenberger, Anion-exchange membranes with improved alkaline stability, Desalination, 79 (1990) 125.

[111] J. Benavente and G. Jonsson, Transport of Na_2SO_4 and $MgSO_4$ solutions through a composite membrane, J. Membrane Sci., 80 (1993) 275.

[112] Y. Hirata, Y. Yamamoto, M. Date, A. Yamauchi and H. Kimizuka, Electrokinetic phenomena in amphoteric membranes, J. Membrane Sci., 41 (1989) 177.

[113] A. Yamauchi, Y. Okazaki, R. Kurosaki, Y. Hirata, and H. Kimizuka, Effect of ionic charge on the electrical properties of an amphoteric ion exchange membranes, J. Membrane Sci., 32 (1987) 281.

[114] N. Lakshminarayanaiah, Counter-ion transference in ion-exchange membranes, J. Phys. Chem., 73 (1969) 97.

[115] M. Trznadel and M. Kryszewski, Thermal shrinkage of oriented polymers, J. Macromol. Sci. - Rev. Macromol. Chem. Phys., C32(3&4) (1992) 259.

[116] D.R. Lloyd, K.E. Kiner, and H.S. Tseng, Microporous membrane formation via thermally induced phase separation. I. Solid-liquid phase separation, J. Membrane Sci., 52 (1990) 239.

[117] J. Brandrup and E.H. Immergut, Polymer Handbook, Interscience Publishers, Jon Wiley & Sons, New York (1966) Chapter 6, p. 44.

[118] D. Fisher and H.H. Eysel, Analysis of polyethylene surface sulfonation, J. Appl. Polym. Sci., 52 (1994) 545.

[119] K. Kneofel and K. Hattenbach, Properties and long-term behavior of ion exchange membranes, Desalination, 34 (1980) 77.

[120] A. Narebska and A. Warzawski, Diffusion dialysis, Effect of membrane composition on acid/salt separation, Separation Sci. Tech., 27 (1992) 703.

[121] Y. Kobuch, H. Motomura, Y. Noma, and F. Hanada, Application of ion exchange membranes to the recovery of acids by diffusion dialysis, J. Membrane Sci., 27 (1986) 173.

[122] T. Okada, S. Kjelstrup-Ratje, S. Moller-Holst, L.O. Jerdal, K. Friestad, G. Xie, and R. Holmen, Water and ion transport in the cation exchange membrane systems NaCl-$SrCl_2$ and KCl-$SrCl_2$, J. Membrane Sci., 111 (1996) 159.

[123] G. Scibona, C. Fabiani and B. Scuppa, Electrochemical behavior of Nafion type membrane, J. Membrane Sci., 16 (1983) 37.

[124] A. Lindheinmer, J. Molenat and C. Gavach, A study of the superselectivity of Nafion perfluorosulfonic membranes, J. Electroanal. Chem., 216 (1987) 71.

[125] T. Sata, New applications of ion exchange membranes. Macromolecules 1992, Invited lectures of the 3th IUPAC international symposium on macromolecules, Prague, Czechoslovakia (1992) (Edited by J. Kahovec), VSP, Utrecht, The Netherlands (1993) p. 451.

[126] K.S. Spiegler and C.D. Coryell, J. Phys. Chem., 57 (1953) 687.

[127] C. Gavach, A. Lindheimer, D. Cros, and B. Brun, Selectivity of ion transfer in carboxylic ion exchange membranes. Part I. Transport numbers of K^+, Na^+ and Cl^- in the S18 SAFT membrane, J. Electroanal. Chem., 190 (1985) 33.

[128] S. Atieh and H.Y. Cheh, Transport properties of Permion TM membranes in concentrated alkaline solutions. I. Potassium hydroxide solution, J. Membrane Sci., 42 (1989) 243.

[129] D.K. Hale and D.J. McCauley, Trans. Faraday Soc., 57 (1961) 135.

[130] D.R. Lide, editor, CRC Handbook of chemistry and physics, 77th edition (1996-1997), CRC Press, Boca Raton, Florida (1996) Chapter 5, p.98.

[131] A. Narebska and A. Warszawski, Diffusion dialysis, transport phenomena by irreversible thermodynamics, J. Membrane Sci., 88 (1994) 167.

[132] M. Mulder, Basic Principles of Membrane Technology, 2nd edition, Chapter VI. Membrane Processes, Kluwer Academic Publishers, Norwell, Massachusetts (1996).

[133] T. Sata, Recent trends in ion exchange membrane research, Pure Appl. Chem, 58 (1986) 1613.

[134] Y. Kobuchi, H. Motomura, Y. Noma, and F. Hanada, Application of ion exchange membranes to the recovery of acids by diffusion dialysis, J. Membrane Sci., 27 (1986) 173.

[135] A. Elmidoui, J. Molenate, and C. Gavach, Competitive diffusion of hydrochloric acid and sodium chloride through an acid dialysis membrane, J. Membrane Sci., 55 (1991) 79.

[136] R. Wycist and W.M. Trochimczuk, Salt and base separation with interpolymer type carboxylic ion-exchange membrane, J. Membrane Sci., 65 (1992) 141.

[137] Y. Lorrain, G. Pourcelly, and C. Gavach, Influence of cations on the proton leakage through anion-exchange membranes, J. Membrane Sci., 110 (1996) 181.

[138] H.G. Hertz, Diffusion and conductance in ionic liquids, A linear response treatment, Zeitschrift Fur Physikalisch Chemie, Supplementheft 1 (1982) Akademische Verlagsgesellshaft, Wiesbaden, Germany (1982).

[139] D.K. Shiffer, E.M. Choy, D.F. Evans, and E.L. Cussler, More Membrane Pumps, AIChE J., 70 (1974) 150.

[140] W.C. Babcock, R.W. Baker, E.D. Lachapelle, and K.L. Smith, Coupled transport membranes, II. The mechanism of uranium transport with tertiary amine, J. Membrane Sci., 7 (1980) 71.

[141] W.C. Babcock, R.W. Baker, E.D. Lachapelle, and K.L. Smith, Coupled transport membranes, III. The rate-limiting step in uranium transport with tertiary amine, J. Membrane Sci., 7 (1980) 89.

[142] T. Imato, H.-I. Yabu, S. Morooka and Y. Kato, Evaluation of permselectivity of a liquid anion-exchange membrane by diffusion dialysis, J. Membrane Sci., 10 (1982) 21.

[143] P.R. Danesi, R. Chiariza and M. Muhammed, Mass transfer rate in liquid anion-exchange process, I. Kinetics of the two-phase acid extraction in system trilaurylamine-toluene-HCl-water, J. Inorg. Nucl. Chem., 40 (1978) 1581.

[144] M. Ersoz, A. Keles and S. Yildiz, Diffusion of amines through polysulfonated ion-exchange membranes, Sep. Sci. Tech., 32(11) (1997) 1851.

[145] Private communication with A. M. Mika (1997).

[146] P. Sridhar and G. Subramaniam, Recovery of acid from cation-exchange resin regeneration waste by diffusion dialysis, J. Membrane Sci., 45 (1989) 280.

[147] Private communication with D. M. Stachera (1999).

[148] W. Ho and K. Sirkar, Membrane Handbook, Van Nostrand Reinhold, New York, (1992).

[149] R. Rautenbach,, K. Vossenkaul, T. Linn, and T. Katz, Waste water treatment by membrane processes-new development in ultrafiltration, nanofiltration and reverse osmosis, Desalination, 108 (1996) 247.

[150] K. Linde and A. Jonsson, Nanofiltration of salt solutions and landfill leachate, Desalination, 103 (1995) 223.

[151] E. Hoffer and O. Kedem, Hyperfiltration in charged membranes: The fixed charged model, Desalination, 2 (1967) 25.

[152] E. Hoffer and O. Kedem, ibid, 5 (1968) 167.

[153] E. Hoffer and O. Kedem, Ion separation by hyperfiltration through charged membranes. I. Calculation based on TMS model, Ind. Eng. Chem., Process Des. Develop., 11 (1972) 221.

[154] E. Hoffer and O. Kedem, Ion separation by hyperfiltration through charged membranes. II. Separation performance of collodion-polybase membrane, Ind. Eng. Chem., Process Des. Develop., 11 (1972) 226.

[155] E. Hoffer and O. Kedem, Negative rejection of acids and separation of ions by hyperfiltration, Desalination, 5 (1969) 167.

[156] H.K. Lonsdale, W. Pusch, and A. Walch, Donnan-membrane effects in hyper-filtration of ternary systems, J. Chem. Soc., Faraday Trans. I, 71 (1975) 501.

[157] J. Ceynowa, Osmotic flow across ion exchange membranes in sulfuric acid solutions, Die Angewan. Makcomol. Chem., 127 (1984) 187.

[158] R. Simons, Trace element removal from ash dam waters by nanofiltration and diffusion dialysis, Desalination, 89 (1993) 325.

[159] J.M.M. Peeters, J.P. Boom, M.H.V. Mulder, and H. Strathmann, Retention measurements of nanofiltration membranes with electrolyte solutions, J. Membrane Sci., 145 (1998) 199.

[160] H. Mehdizadeh, Modelling of transport phenomena in reverse osmosis membranes, Ph. D. Thesis, McMaster University, Hamilton, Ontario (1990).

[161] S. Sourirajan, Reverse Osmosis, Academic Press, New York (1970).

[162] R.F. Childs, A.M. Mika, A.K. Pandey, M. Kim, C. McCrory, S. Mounton and J.M. Dickson, Nanofiltration using pore-filled membranes, Euromembrane 99, Leuven, Belgium (September 19-22, 1999).

[163] A. Eisenberg, Ion-Containing Polymers, Academic, New York (1977).

[164] K.A. Mauritz, Review and critical analyses of theories of aggregation in ionomers, J. Mol. Sci., Macromol., Chem. Phys., C28(1) (1988) 65.

[165] E. Vesterinen, A. Dobrodumov, and H. Tenhu, Spin-labeled polyelectrolyte gels based on poly(N-isopropylacrylamide). Effects of the network structure and the gel collapse on the ESR spectra, Macromolecules, 30 (1997) 1311.

[166] S.G. Starodoubtsev, A.R. Khokhlov, E.L. Sokolov, and B. Chu, Evidence for polyelectrolyte/ionomer behavior in the collapse of polycationic gels, Macromolecules, 28 (1995) 3930.

[167] J. Xu, X. Xing, S. Yamamoto, Y. Tanji, and H. Unno, Effect of ion adsorption on its permeation through nanofiltration membranes, J. Chem. Eng. Japan, 30 (5) (1997) 806.

[168] A.M. Mika, R.F. Childs, M. Armstrong, and J.M. Dickson, Novel water softening membranes with tunable properties, North America Membrane Society (NAMS '98) Cleveland, Ohio (May 18-20, 1998).

[169] G. Jonsson and C. Boesen, Water and solute transport through cellulose acetate reverse osmosis membranes, Desalination, 17 (1975) 145.

[170] D.W. Nielsen and G. Jonsson, Bulk-phase criteria for negative ion rejection in nanofiltration of multicomponent salt solutions, Sep. Sci. Tech. 29 (1994) 1165.

[171] S. Kimura, Reverse osmosis performance of sulfonated poly(2,6-dimethyl-phenylene ether) ion-exchange membranes, Ind. Eng. Chem., Prod. Res. Develop., 10 (1971) 335.

[172] T. Tsuru, S. Nakao, and S. Kimura, Calculation of ion rejection by extended Nernst-Planck equation with charged reverse osmosis membranes for single and mixed electrolyte solutions, J. Chem. Eng. Japan, 24(4) (1991) 511.

[173] C. Bardot, E. Gaubert, and A. Yaroshuk, Unusual mutual influence of electrolytes during pressure-driven transport of their mixtures across charged porous membranes, J. Membrane Sci., 103 (1995) 11.

[174] A. Yaroshchuk, Osmosis and reverse osmosis in fine-porous charged diaphragms and membranes, Adv. Colloid Interface Sci., 60 (1995) 1.

[175] J. Garcia-Aleman, Mathematical modeling of the pressure-driven performance of nanofiltration membranes; mixed electrolyte systems, M. Eng. Thesis, McMaster University, Hamilton, Ontario (1998).

[176] T. Hayashita, M. Takagi, and K. Ueno, Negative rejection of group IB metal cyanide complexes in the hyperfiltration by cellulose acetate membranes. Donnan membrane effect, Sep. Sci. Tech., 18 (1983) 461.

[177] G.S. Manning, Counter-ion binding in polyelectrolyte theory, Acc. Chem. Res., 12 (1979) 443.

[178] R.M. Nyquist, B.Y. Ha, and A.J. Liu, Counterion condensation in solutions of rigid polyelectrolytes, Macromolecules, 32 (1999) 3481.